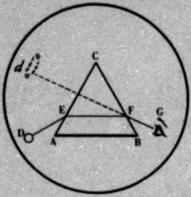

optics and spectroscopy

volume viii
number 6
june 1960

OPTICAL SOCIETY OF AMERICA

USSR ACADEMY OF SCIENCES

RUSSIAN EDITORIAL STAFF FOR
OPTIKA I SPEKTROSKOPIYA sponsored by
USSR ACADEMY OF SCIENCES

Editor: S. E. FRISH

Assistant Editor: P. P. FEOFILOV
Corresponding Secretary: L. S. SAZONOV

Associate Editors:

M. M. GUREVICH M. A. EL'IASHEVICH A. A. LEBEDEV V. P. LINNIK
S. L. MANDEL'SHTAM I. V. OBREIMOV V. K. PROKOF'EV
N. N. SOBOLEV A. N. TERENIN A. I. TUDOROVSKII

Translated from *OPTIKA I SPEKTROSKOPIYA* on the initiative of
THE OPTICAL SOCIETY OF AMERICA, INC.
with a grant-in-aid from
THE NATIONAL SCIENCE FOUNDATION

TRANSLATION EDITORIAL STAFF

Scientific Editors

CYRUS FELDMAN, *Oak Ridge National Laboratory*

CARL W. GARLAND, *Massachusetts Institute of Technology*

MATHEW G. GIBBONS, *Oakland, California*

Administrative Editor: PATRICIA R. WAKELING, *OSA*

Published monthly by the Optical Society of America, Inc. Executive office: 1155 Sixteenth Street, N.W., Washington, D.C. Subscriptions for one year to members of the Society: Associates $13.00; Regular members and Fellows $17.00. Subscriptions for non-members of the Society: One year U. S. and Possessions, $25.00; Foreign $28.00. Back numbers: $3.00 per copy. Subscriptions, changes of address and undeliverable copies should be referred to the Executive offices in Washington, D.C. The office of publication is 2500 South State Street, Ann Arbor, Michigan. Second class postage paid at Ann Arbor, Michigan.

Printed in the U.S.A. by Edwards Brothers, Inc., Ann Arbor, Michigan.

ISOTOPE SHIFT IN THE SPECTRUM OF NEODYMIUM

Yu. P. Dontsov, V. A. Morozov, and A. R. Striganov

Received 5 November 1959

New results in the investigation of the isotope shift in the spectrum of neodymium are presented. Separated isotopes were investigated in this work whereas in other investigations natural neodymium was used. A Fabry-Perot interferometer and a hollow cathode discharge tube were employed. The isotope shift was measured between the components of even-even isotopes for 16 lines. No basic difference was seen between the relative shifts of lines Nd I and Nd II, nor was any change of relative anomalous shift with wavelength observed. The differences in separation among the line components due to neodymium isotopes whose nuclei do not show static deformation can be partially explained as an irregular change in the amplitude of zero vibrations of the nucleus' quadrupole moment.

INTRODUCTION

A number of publications have been dedicated to the problem of the isotope effect in the atomic spectra of neodymium.[1-5] In these investigations the isotope shift between the line components of five even-even isotopes of neodymium has been measured for 30 lines. In the spectrum of neodymium, as in the spectrum of samarium, an anomalous shift was observed between the line components of Nd^{148} and Nd^{150} at the entry of the 45th pair of neutrons into the nucleus.

A most complete investigation was made by Nöldeke and Steudel,[3, 4] who determined the relative positions of the line components of the even-even isotopes of neodymium. According to their data, the relative shifts between the isotopes Nd^{142}, Nd^{144}, Nd^{146}, Nd^{148}, and Nd^{150} for lines of Nd I and Nd II are those given in Table 1.

Table 1

Spectral assignment of lines	Relative shift				$\frac{\Delta\nu\,(148-150)}{\frac{1}{3}\,\Delta\nu\,(142-148)}$
	$\Delta\nu$ (142—144)	$\Delta\nu$ (144—146)	$\Delta\nu$ (146—148)	$\Delta\nu$ (148—150)	
Nd I	1.00	0.90	1.07	1.50	1.52
Nd II	1.00	0.90	0.91	1.39	1.48

Since samples of natural neodymium containing even-odd isotopes were used in both of the above investigations, there remains some uncertainty in the accuracy of the observed isotope structural intervals. In order to obtain a more reliable determination of the isotope shift between all the components of even-even neodymium isotopes, the distances were remeasured using enriched isotopes. Improvement in accuracy is important in establishing the trend of the isotope shift beyond the components of Nd^{142} which occurs with the addition of more neutrons following completion of the $2d_{3/2}$ shell.

EXPERIMENTAL PART

A high resolution Fabry-Perot (IZS-9) interferometer with silvered glass plates was used. At 5600 A, its coefficient of reflection was 90% and its coefficient of transmission 4%. The interferometer was crossed externally with a three-prism spectrograph (ISP-51) having a UF-84 camera.

A hollow cathode discharge tube served as the light source. The power was provided by a high voltage rectifier which furnished a potential of 1500 volts. The discharge current for the majority of experiments was kept at 80 ma. The carrier gas was argon which circulated in the vacuum system and was purified by a potash trap. The cathode was cooled with liquid nitrogen.

The even isotopes of neodymium were separated electromagnetically,[6] and used in this investigation in the form of the oxide (Nd_2O_3). The isotopic composition of the samples is given in Table 2. From these samples two 18 mg specimen were prepared by mixing equal parts of the three isotopes. Specimen I was composed of Nd^{142}, Nd^{146}, and Nd^{150}, and specimen II of Nd^{144}, Nd^{148}, and Nd^{150} The isotopic composition of these specimens is given in Table 2. The three-isotope specimen of neodymium oxide was converted into the chloride ($NdCl_3$), and then dissolved in distilled water. This aqueous solution was introduced into the cavity of the aluminum cathode and evaporated.

Table 2

Designation of samples	Isotopic composition (%)						
	Nd^{142}	Nd^{143}	Nd^{144}	Nd^{145}	Nd^{146}	Nd^{148}	Nd^{150}
142	98.5	1.0	0.5	< 0.1	< 0.1	< 0.1	< 0.1
144	0.4	1.5	96.6	1.5	< 0.1	< 0.1	< 0.1
146	< 0.1	0.2	0.5	1.1	97.8	0.3	< 0.1
148	0.8	0.7	1.0	0.5	3.1	92.8	1.1
150	0.5	0.4	1.1	0.4	0.9	2.1	94.6
Specimen I . .	33.0	0.5	0.7	0.5	32.9	0.8	31.5
Specimen II . .	0.6	0.9	32.9	0.8	1.3	31.6	31.9

The spectrum of each specimen was photographed using various interferometer spacings. The spacings were 6, 8, 10, 15, and 20 mm, depending on the width of the line's isotope structure. Kodak II-F plates and isopanchromatic film (speed: 130 GOST units) were used. The exposure time varied from 5 to 90 min, depending on the intensity of spectral lines and the quantity of the sample.

The isotope structure was measured with an IZA-2 comparator on two or three plates which were obtained with various interferometer spacings. The root mean square error of the directly measured distances $\Delta\nu$)142-146), $\Delta\nu$(146-150), $\Delta\nu$(144-148), and $\Delta\nu$(148-150) was derived by the least squares method. Since the shift between the components of neighboring isotopes was found by deduction from directly measured distances, the errors in the intervals $\Delta\nu$(142-144), $\Delta\nu$(146-148), and $\Delta\nu$(146-148) were approximately 2, 3, and 4 times greater.

RESULTS AND DISCUSSION

The measured distances between the components of even-even isotopes and their root mean square errors are given in Table 3. The table contains 16 spectral lines; three belong to the Nd II[7] spectrum and 10 to Nd I.[8] Fourteen lines have negative shifts which are characteristic of the volume effect (the component of a heavier isotope is shifted toward the longer wavelengths). Two lines (5273.4 and 5319.8 A) have positive shifts, showing that the transition occurs from a higher term which has a greater isotope shift than a lower term. Comparing the data from Table 3 with the results of other authors,[1-5] it can be seen that the measurements of the majority of spectral lines by various authors are in fairly good agreement within the limits of accuracy. However, an important difference was observed between our data and those of the other investigators for the lines 4688.6, 4966.7, 5291.7, 5653.6, 6310.5, and 6485.7 A. It can be assumed that these discrepancies are due to measuring errors caused by the superposed hyperfine structure of samples of natural neodymium.

Table 3

Wavelength (A)	Shift (10^{-3} cm^{-1})			
	$\Delta\nu$ (142–144)	$\Delta\nu$ (144–146)	$\Delta\nu$ (146–148)	$\Delta\nu$ (148–150)
4688.6 I	−96.0 ± 7.2	−95.0 ± 6.0	−103.5 ± 4.5	−149.5 ± 3.0
4966.7 I	−81.0 ± 8.0	−64.0 ± 6.0	−81.0 ± 4.0	−104.0 ± 1.0
5022.6 I	−81.2 ± 8.5	−70.3 ± 7.0	−83.7 ± 6.0	−114.0 ± 2.5
5273.4 II	+53.9 ± 2.2	+44.2 ± 1.7	+55.1 ± 1.2	+ 79.7 ± 0.7
5291.7	−70.0 ± 2.9	−63.2 ± 1.6	−80.3 ± 1.1	−103.3 ± 0.5
5319.8 II	+41.8 ± 4.0	+33.6 ± 2.6	+42.5 ± 1.8	+ 59.2 ± 1.5
5575.5 I	−96.1 ± 2.7	−79.0 ± 2.0	−98.0 ± 1.0	−128.0 ± 0.5
5653.6 I	−56.1 ± 3.5	−52.0 ± 3.0	−60.9 ± 2.9	− 84.9 ± 1.9
5813.9 I	−47.2 ± 3.2	−43.2 ± 2.7	−48.4 ± 2.2	− 71.6 ± 1.7
6007.7 I	−38.8 ± 4.9	−30.7 ± 4.4	−39.3 ± 3.3	− 54.6 ± 3.0
6178.6 I	−47.6 ± 2.7	−38.1 ± 2.0	−48.8 ± 1.7	− 57.7 ± 0.8
6310.5 I	−36.9 ± 5.8	−38.9 ± 4.8	−39.2 ± 3.7	− 55.0 ± 2.6
6319.7	−59.6 ± 2.2	−49.5 ± 1.7	−62.3 ± 1.2	− 80.1 ± 0.5
6355.9	−74.8 ± 5.6	−58.9 ± 3.5	−74.1 ± 2.9	−101.0 ± 1.4
6394.8 II	−38.0 ± 7.5	−37.0 ± 6.5	−39.0 ± 5.0	− 56.0 ± 2.0
6485.7 I	−39.8 ± 2.0	−36.5 ± 1.5	−42.1 ± 1.0	− 55.8 ± 0.5

In Table 4 the relative isotope shifts are given for each line. The first distance, $\Delta\nu(142\text{-}144)$, is used as unity. The last column gives the relative anomalous shifts

$$\frac{\Delta\nu(148\text{-}150)}{\frac{1}{3}\Delta\nu(142\text{-}148)}$$

which characterize the change of the anomalous shift with wavelength. The mean values and their root square errors, as derived from 16 lines, are given at the end of the table. Comparison of the data in each column with the mean values shows fairly good agreement. Only in a few cases does the deviation from the mean exceed the limits of accidental error of individual measurement. One of the possible causes of these deviations could be the superposition of neighboring lines. This can be checked by a more careful investigation of the neodymium spectra.

From Table 4 it is seen that the magnitude of the relative isotope shift between the components of even isotopes does not exceed the root mean square error for the individual values of each interval. This means that we have not observed any important differences in the relative shifts of lines Nd I and Nd II. In this respect our data differ from those of Nöldeke and Steudel (Table 1). Comparing our mean values with the data in Table 1, we see that when natural neodymium is used for measuring the isotope shift of spectral lines, the hyperfine structure of even-odd isotopes Nd^{143} and Nd^{145} introduces a systematic error into the determination of the distances $\Delta\nu(146\text{-}148)$ for lines of Nd II and $\Delta\nu(148\text{-}150)$ for lines of Nd I.

Table 4

Wavelength (A)	Relative shift				$\frac{\Delta\nu\,(148-150)}{\frac{1}{3}\Delta\nu\,(142-148)}$
	$\Delta\nu$ (142–144)	$\Delta\nu$ (144–146)	$\Delta\nu$ (146–148)	$\Delta\nu$ (148–150)	
4688.6 I	1.00	0.99	1.08	1.56	1.52
4966.7 I	1.00	0.79	1.00	1.28	1.38
5022.6 I	1.00	0.87	1.03	1.40	1.45
5273.4 II	1.00	0.82	1.02	1.48	1.56
5291.7	1.00	0.90	1.15	1.48	1.45
5319.8 II	1.00	0.80	1.02	1.42	1.51
5575.5 I	1.00	0.82	1.02	1.33	1.40
5653.6 I	1.00	0.93	1.08	1.51	1.51
5813.9 I	1.00	0.91	1.03	1.52	1.55
6007.7 I	1.00	0.79	1.01	1.41	1.50
6178.6 I	1.00	0.80	1.02	1.21	1.29
6310.5 I	1.00	1.05	1.06	1.49	1.44
6319.7	1.00	0.83	1.05	1.34	1.40
6355.9	1.00	0.79	0.99	1.35	1.46
6394.8 II	1.00	0.97	1.03	1.47	1.47
6485.7 I	1.00	0.92	1.06	1.40	1.41
Mean . . .	1.00	0.87 ± 0.02	1.04 ± 0.01	1.42 ± 0.02	1.46 ± 0.02

Table 4 shows that the relative anomalous shift does not change with wavelength. At this point it should be mentioned that in the work of Korolev and Osipov,[5] in which natural neodymium was used, some inaccuracies are present in the determination of the shift of some lines (5291.7 A, 6310.5 A). As a result, the authors obtained a considerable difference in the magnitude of the relative anomalous shift. From this, they drew erroneous conclusions concerning the dependence of the relative anomalous shift on wavelength.

The Figure shows the isotope structure of neodymium lines, presented schematically by giving the relative shifts, the distance $\Delta\nu(142\text{-}144)$ being taken as unity. The results show that isotope drifts are not equidistant in the spectrum of Nd. Aside from the known "jump" at the entry of the 45th pair of neutrons, a variation in the isotope shift is observed starting with Nd^{142}, whose nucleus contains 82 neutrons and whose $2d_{3/2}$ shell is filled.

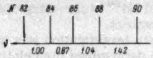

Isotope structure of neodymium spectral lines.

An anomalous shift between the line components of isotopes with N = 88 and N = 90 neutrons is observed in the spectra of neodymium, samarium, and gadolinium. This "jump" in the isotope shift is caused by a static deformation of the nucleus which appears when N = 90. Nuclei with a smaller number of neutrons do not show static deformation. However, these nuclei have variable quadrupole moments which on the average are equal to zero. The presence of the variable quadrupole moment, as was indicated by Dontsov,[9] must be revealed by the magnitude of the isotope shift. The unequal separation of the line components of neodymium isotopes, whose nuclei do not show static deformation, is apparently explained by a nonuniform change in the amplitude of zero vibrations of the quadrupole moment of the nucleus.

In conclusion, the authors express their gratitude to B. A. Alekseev, V. S. Zolotarev, G. Ya. Shchepkin, and their co-workers for the preparation of separated isotopes of neodymium, which made this work possible.

Comments added in proof: In reference 9, an incorrect value was used for the coefficient in expression (5). As a result, the calculated values of the relative "quadrupole", or better still, "vibrational" increments in isotope shifts for spherically symmetric nuclei turned out, as indicated in reference 9, to be approximately fifty times smaller than the experimental ones. D. P. Grechukhin commented that the same expression can be used for surface vibrations as is used for deformed nuclei:

$$Q_0^2 = \frac{16\pi}{5} B\,(E2,\, 0 \rightarrow 2).$$

The values of Q_0^2 obtained in this case are 16π times greater than those used in reference 9, and the calculated "vibrational" increments in the isotope shift are in good agreement with experiment.

REFERENCES

1. P. F. A. Klinkenberg. Physica 11, 327 (1945).
2. K. Murakawa. Phys. Rev. 96, 1543 (1954).
3. G. Nöldeke and A. Steudel. Z. Physik 137, 632 (1954).
4. G. Nöldeke and A. Steudel. Naturwissenschaften 41, 332 (1954); G. Nöldeke. Z. Physik 143, 274 (1955).
5. F. A. Korolev and Iu. P. Osipov. Doklady Akad. Nauk SSSR 110, 365 (1956).
6. B. A. Alekseev, S. F. Bulygin, V. S. Zolotarev, B. V. Panin, E. S. Chernorotov, and G. Ya. Shchepkin. Vtoraya mezhdunarodnaya konferentsiya po mirnomu ispol'zovaniiu atomnoi energii (doklady sovetskikh uchenykh) (Second Intern. Conf. on Peaceful uses of Atomic Energy (Reports by USSR Scientists)) 6, 102, Moscow (1959).
7. W. E. Albertson, G. R. Harrison, and J. R. McNally. Phys. Rev. 61, 167 (1942).
8. P. F. A. Klinkenberg. Physica 12, 33 (1946).
9. Yu. P. Dontsov. Opt. i Spektr. 8, 446 (1960), Optics and Spectroscopy 8, 236 (1960).

ANALYSIS OF THE FINE STRUCTURE IN THE BANDS OF THE SiCl MOLECULE

I. E. Ovcharenko, L. N. Tunitskii, and V. I. Yakutin

Received 20 July 1959

A rotational analysis of the (1,0), (0,0) and (0,1) bands of the $B^2\Sigma \rightarrow X^2\Pi$ transition in the SiCl molecule is carried out for the first time, and the rotational constants for the $B^2\Sigma$ and $X^2\Pi$ states are determined.

Four electronic states, $X^2\Pi$, $B^2\Sigma$, $C^2\Delta$, and $D^2\Sigma$ are known for the SiCl molecule.[1-4] Vibrational constants which have been determined for these states are given in Table 1, which is taken from the work of Jevons.[4] In the opinion of Jevons[4] the tabular values which are accompanied by a question mark could not be determined with complete certainty because of the experimental conditions used. A rotational analysis for the SiCl molecule is carried out for the first time in the present work.

EXPERIMENTAL METHOD

The SiCl spectrum was excited in a pulsed gas-discharge tube similar to the one we used earlier.[5] It is composed of a cylindrical quartz tube, 1 (see Figure), 12 cm in length and 6 mm in internal diameter, ending in a quartz window, 2. Two U-shaped quartz tubes, 3 and 4, are sealed into the cylindrical tube. Electrode tubes, 5 and 6, carrying wolfram rods 4 mm in diameter are sealed into the U-shaped tubes. The electrodes are welded to molybdenum foil, which in turn is sealed to the quartz. Leading from the middle of the cylindrical tube is a branch, 7, for the insertion of silicon tetrachloride. In preparing for the experiment the cylindrical tube was evacuated to a high vacuum and was heated to redness by means of a burner. Then it was opened to the atmosphere, and the branch, 7, was filled with silicon tetrachloride, after which the branch was placed in a dewar containing liquid nitrogen. Then the tube was evacuated again, filled with helium to a pressure of 2-3 mm of mercury and sealed off. During photographing of spectra the U-shaped tubes, 3 and 4, were immersed in liquid nitrogen in a dewar, and the branch containing the silicon tetrachloride was placed in a dewar above the level of the liquid nitrogen. During the process the silicon tetrachloride was driven from the branch, 7, into the U-shaped tubes, 3 and 4. The pressure of the fumes from the silicon tetrachloride in the tube was regulated by means of the position of the branch, 7, above the level of the liquid nitrogen. The tube was connected directly to the secondary winding of a 15 kw transformer. Secondary voltage was calculated as 15 kv. The primary winding of the transformer was connected into the line once per second for 0.02 sec by means of a special relay. The magnitude of the voltage supplied to the primary winding of the transformer was regulated by means of an input resonator. In the photographing of spectra a DFS-3 spectrograph was used in the third order (dispersion 0.57 A/mm, resolving power 432,000). Exposure durations were about 2-3 sec. The spectra were measured with the aid of an IZA-2 comparator, with the arc spectrum of iron serving as standard. The fine-structure wavelengths were determined according to the formula

$$\lambda = \lambda_0 + a\Delta x + b\Delta x^2. \qquad (1)$$

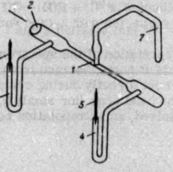

Table 1. Values of the Vibrational Constants of the SiCl Molecule (according to reference 4)

State	T_e (cm^{-1})	ω_e (cm^{-1})	ω_0 (cm^{-1})	$\omega_e x_e$ (cm^{-1})
$D^2\Sigma$	45005.9	—	663?	—
$C^2\Delta$	41247.8	674.2	669.8	2.20
$C^2\Delta$	41234.8			
$B^2\Sigma$	34186.0	701.5?	697.7	1.40?
$X^2\Pi_{\frac{3}{2}}$ . . .	207.9	535.4	531.0	2.20
$X^2\Pi_{\frac{1}{2}}$ . . .	0			

The constants λ_0, a, and b are determined from ten iron lines by the method of averages separately for each sub-band. The accuracy of our measurements is illustrated by the results given in Table 2. Column I of this table gives the accepted tabular values of the wavelengths of the iron lines, column II gives the wavelengths of the iron lines calculated according to the formula

$$\lambda = 2987.292 - 0.57546\ \Delta x - 0.0000432\ \Delta x^2, \qquad (1a)$$

which is valid for the $^2\Sigma \rightarrow {}^2\Pi_{3/2}$ sub-band of the (0,1) band, and column III gives the difference between the measured and tabular values. It follows from Table 2 that the maximum error in measurement does not exceed 0.007 A.

Table 2. Accuracy of the Wavelength Measurements (in A) of Lines in the Iron Spectrum

I	II	III
2987, 292	2987, 291	−0.001
2967, 460	2967, 466	+0.006
2985, 550	2985, 549	−0.001
2983, 572	2983, 570	−0.002
2981, 854	2981, 858	+0.004
2980, 539	2980, 534	−0.005
2976, 131	2976, 135	+0.004
2973, 237	2973, 238	+0.001
2973, 134	2973, 129	−0.005
2972, 279	2972, 286	+0.007

INTERPRETATION OF THE SPECTRUM

In the present work the interpretation of the fine structure of the three bands (1,0), (0,0) and (0,1) of the $B^2\Sigma - X^2\Pi$ transition of the SiCl molecule has been carried out. The magnitude of the splitting in the $X^2\Pi$ states ($^2\Pi_{1/2}$ and $^2\Pi_{3/2}$) of the SiCl molecule is $A \approx 207$ cm^{-1}. The rotational constant B of the ground state of the SiCl molecule may be taken as approximately equal to 0.24 cm^{-1}, by analogy with the AlCl molecule. This means that the magnitude of A/B is approximately equal to 862. This value, according to the Hill-Van Vleck criterion, corresponds to Hund's case "a." The rotational terms and formulas for the branches of the $^2\Pi - {}^2\Sigma$ and $^2\Sigma - {}^2\Pi$ transitions corresponding to Hund's case "a" are treated in the work of Mulliken.[6] For the $^2\Sigma - {}^2\Pi$ transitions the values of the rotational terms and the wave numbers of the branches are determined by the formulas

$$^2\Sigma:\; I = K + \frac{1}{2};\; F_1(I) = W + \frac{1}{2}\gamma\left(I - \frac{1}{2}\right) + B\left(I - \frac{1}{2}\right)\left(I + \frac{1}{2}\right) - D\left(I - \frac{1}{2}\right)^2\left(I + \frac{1}{2}\right)^2. \quad (2)$$

$$^2\Sigma:\; I = K - \frac{1}{2};\; F_2(I) = W - \frac{1}{2}\gamma\left(I - 1\frac{1}{2}\right) + B\left(I + \frac{1}{2}\right)\left(I + 1\frac{1}{2}\right) - D\left(I + \frac{1}{2}\right)^2\left(I + 1\frac{1}{2}\right)^2. \quad (3)$$

$$^2\Pi_{\frac{1}{2}};\; F_{1c} = W_1 + \frac{1}{2}a\left(I + \frac{1}{2}\right) + B_1 I(I+1) - D_1 I^2(I+1)^2, \quad (4)$$

$$^2\Pi_{\frac{1}{2}};\; F_{1d} = W_1 - \frac{1}{2}a\left(I + \frac{1}{2}\right) + B_1 I(I+1) - D_1 I^2(I+1)^2, \quad (5)$$

$$^2\Pi_{\frac{3}{2}};\; F_{1c} = F_{1d} = W_2 + B_2 I(I+1) - D_2 I^2(I+1)^2; \quad (6)$$

$$^{S}R_{21}(I) = \nu_1 - \frac{1}{4}(a + 5\gamma - 15B) + \left(4B - B_1 - \frac{1}{2}a - \frac{1}{2}\gamma\right)I + (B - B_1)I^2 + \ldots, \quad (7)$$

$$R_1(I) = \nu_1 + \frac{1}{4}(a + \gamma + 3B) + \left(2B - B_1 + \frac{1}{2}a + \frac{1}{2}\gamma\right)I + (B - B_1)I^2 + \ldots, \quad (8)$$

$$^{R}Q_{21}(I) = \nu_1 + \frac{1}{4}(a - 3\gamma + 3B) + \left(2B - B_1 + \frac{1}{2}a - \frac{1}{2}\gamma\right)I + (B - B_1)I^2 + \ldots, \quad (9)$$

$$Q_1(I) = \nu_1 - \frac{1}{4}(a + \gamma + B) - \left(B_1 + \frac{1}{2}a - \frac{1}{2}\gamma\right)I + (B - B_1)I^2 + \ldots, \quad (10)$$

$$^{Q}P_{21}(I) = \nu_1 - \frac{1}{4}(a + \gamma + B) - \left(B_1 + \frac{1}{2}a + \frac{1}{2}\gamma\right)I + (B - B_1)I^2 + \ldots, \quad (11)$$

$$P_1(I) = \nu_1 + \frac{1}{4}(a + \gamma + 3B) - \left(2B + B_1 - \frac{1}{2}a - \frac{1}{2}\gamma\right)I + (B - B_1)I^2 + \ldots, \quad (12)$$

$$R_2(I) = \nu_2 - \frac{1}{4}(5\gamma - 15B) + \left(4B - B_2 - \frac{1}{2}\gamma\right)I + (B - B_2)I^2 + \ldots, \quad (13)$$

$$^{Q}R_{12}(I) = \nu_2 + \frac{1}{4}(\gamma + 3B) + \left(2B - B_2 + \frac{1}{2}\gamma\right)I + (B - B_2)I^2 + \ldots, \quad (14)$$

$$Q_2(I) = \nu_2 + \frac{1}{4}(-3\gamma + 3B) + \left(2B - B_2 - \frac{1}{2}\gamma\right)I + (B - B_2)I^2 + \ldots, \quad (15)$$

$$^{P}Q_{12}(I) = \nu_2 - \frac{1}{4}(\gamma + B) - \left(B_2 - \frac{1}{2}\gamma\right)I + (B - B_2)I^2 + \ldots, \quad (16)$$

$$P_2(I) = \nu_2 - \frac{1}{4}(\gamma + B) - \left(B_2 + \frac{1}{2}\gamma\right)I + (B - B_2)I^2 + \ldots, \quad (17)$$

$$^{O}P_{12}(I) = \nu_2 + \frac{1}{4}(-3\gamma + 3B) - \left(2B + B_2 - \frac{1}{2}\gamma\right)I + (B - B_2)I^2 + \ldots, \quad (18)$$

where W, W_1, and W_2 are the values of the electronic and vibrational energies for the $^2\Sigma$, $^2\Pi_{1/2}$ and $^2\Pi_{3/2}$ states, respectively; $\nu_1 = W - W_1$ and $\nu_2 = W - W_2$; γ is the doublet splitting constant of the $^2\Sigma$ state, and a is the λ-type doubling constant of the $^2\Pi_{1/2}$ state. A number of conclusions follow from formulas (8)-(19).

1. The distances between fine-structure lines of the main branches R_1, Q_1, Q_2, and P_2 and the corresponding satellite branches $^{R}Q_{21}$, $^{Q}P_{21}$, $^{Q}R_{12}$, and $^{P}Q_{12}$ for the same I are equal to γI or $\gamma(I+1)$, respectively. In our case γ is small and the lines of the main branches and the corresponding satellite branches are not resolved even for large I. As a consequence, branches R_1 and $^{R}Q_{21}$, Q_1 and $^{Q}P_{21}$, Q_2 and $^{Q}R_{12}$, P_2 and $^{P}Q_{12}$ coincide.

2. Band edges were formed by the P_1, Q_1, $^{O}P_2$, and P_2-branches. In the work of Jevons[4] the observed edges were erroneously ascribed to the P_2, Q_2, P_1, and Q_1 branches, respectively.

3. In the $^2\Sigma - {}^2\Pi_{1/2}$ sub-bands for large I one should expect insignificant discrepancy between the first combination differences $\Delta_1F''(I) = R(I) - Q(I+1)$ and $\Delta_1F''(I) = Q(I) - P(I+1)$ connected with λ-type doubling in the $^2\Pi_{1/2}$ state.

In the interpretation of the spectrum the Q_1, R_1, Q_2, P_2, and R_2-bands at some distance from the band edge were separated out directly during comparator measurements. Near the band edge (for small I), where the lines were badly resolved, an extrapolation according to the formula

$$\nu_n = \nu_0 + (n-1)\Delta_1 + \frac{(n-1)(n-2)}{2}\Delta_2. \qquad (19)$$

was used to separate the bands.

The constants ν_0, Δ_1, and Δ_2 were determined from 30 equations composed in conformity with the frequency values of the separated lines of a branch. The enumeration of the lines in the branches is determined from the convergence condition of the corresponding first and second combination differences.

In the $^2\Sigma - {}^2\Pi_{1/2}$ sub-bands, where λ-type doubling occurs, the numeration in the Q_1- and R_1-branches stops at the first combination differences with small I values for which the combination defect is small. The P_1-branches are chosen in accordance with the already known second combination differences of the $^2\Sigma - {}^2\Pi_{3/2}$ sub-bands. According to formulas (7)-(18), the P_1- and R_2-branches are characterized by the presence of a linear term approximately equal to 3B, and hence often intersect the corresponding Q_1, R_1 and Q_2, P_2 branches, which have linear terms approximately equal to B, and run parallel, coinciding for small I values. The lines of the P_1- and R_2-branches are often superimposed on the more intense lines of the Q-branch. Consequently, there is less accuracy in the determination of the wave numbers of the lines of the former branches. As an additional check of the correctness of the rotational analysis carried out here, the lines of the $^0P_{12}$-branches, which form edges in the $^2\Sigma - {}^2\Pi_{3/2}$ sub-bands, were separated out with the aid of the relation

$$^0P_{12}(I) = P_2(I) - \Delta_1 F'(I-2) \qquad (20)$$

The fine-structure lines with I values up to I = 70.5 were separated out for all branches of the (0,1), (0,0) and (1,0) bands. Tabulated results of the fine structure analysis require considerable space and hence are not presented here. Comparison of the experimental values of the wave numbers of the fine-structure lines with values calculated according to the magnitudes of the rotational constants with the aid of formulas (7)-(18) shows that for most of the lines the discrepancy does not exceed 0.1 cm⁻¹. For the remaining lines (in those cases where a group of lines belonging to different branches is not resolved) this discrepancy is as much as 0.3 cm⁻¹. As a result of the rotational analysis it is established that the levels of the $^2\Pi_{3/2}$ state have higher energy than the levels of the $^2\Pi_{1/2}$ state, that is, the $^2\Pi$ electronic state of the SiCl molecule has normal term order, in agreement with the already known normal term order for isoelectronic molecules.

CALCULATION OF THE ROTATIONAL CONSTANTS

The rotational constants were calculated from the second combination differences with the aid of the following formulas

$$\Delta_2 F_1''(I) = 4B_1''\left(I+\frac{1}{2}\right) - 8D_1''\left(I+\frac{1}{2}\right)^3 + a, \qquad (21)$$

$$\Delta_2 F_2''(I) = 4B_2''\left(I+\frac{1}{2}\right) - 8D_2''\left(I+\frac{1}{2}\right)^3, \qquad (22)$$

$$\Delta_2 F_1'(I) = 4B'I - 8D'I^3, \qquad (23)$$

$$\Delta_2 F_2'(I) = 4B'(I+1) - 8D'(I+1)^3, \qquad (24)$$

where the indexes 1 and 2 indicate that the values refer to the sub-bands * $^2\Sigma - {}^2\Pi_{1/2}$ and $^2\Sigma - {}^2\Pi_{3/2}$, respectively.

---

*Translator's note: misprinted "3" in text.

In the calculations we initially neglected the terms containing D and determined the average values of the B's. We then calculated values for the D's by means of the relationship

$$D = \frac{4B^3}{\omega^2}, \qquad (25)$$

From the values found for the D's the magnitudes of the B's were then recalculated with the aid of formulas (21)-(24), taking into account terms involving D.

The calculation of the rotational constants was carried out with combination differences from I = 40.5 to I = 70.5. The λ-doubling constant a was determined from the combination defect with the aid of the relationship

$$\epsilon = 2a(I+1). \qquad (26)$$

In view of the smallness of a, it was not determined with great exactness. The wave numbers of the zeroth lines were calculated using the values of the rotational constants, and the wave numbers of the fine-structure lines were calculated with the aid of formulas (7)-(18). The values obtained for the rotational constants and the zeroth lines are given in Table 3. The root-mean-square error in the determination of the B's is 0.0001. It should be noted that the wave numbers which we obtained for band edges are larger by about 1.5 cm⁻¹ than those given in the works of Jevons and Datta. This discrepancy is connected with a slight displacement of the SiCl spectrum with respect to the spark spectrum of iron. The displacement was observed in all our photographs.

Table 3. (a) Values of the Rotational Constants of the SiCl Molecule

Electronic state	B_e (cm⁻¹)	α (cm⁻¹)	$D_e \cdot 10^{-7}$ (cm⁻¹)	a (cm⁻¹)
$X^2\Pi_{\frac{1}{2}}$ . . .	$B_1 = 0.2550$	0.0016	2.341	0.004 ± 0.001
$X^2\Pi_{\frac{3}{2}}$ . . .	$B_2 = 0.2556$	0.0016	2.355	—
$B^2\Sigma$	$B = 0.2782$	0.0015	1.752	—

(b) Values of the Wave Numbers of the Zeroth Lines (cm⁻¹)

Sub-band	Zeroth lines of the band		
	(0.1)	(0.0)	(1.0)
$^2\Sigma \to {}^2\Pi_{\frac{1}{2}}$	33662.0	34193.6	34892.2
$^2\Sigma \to {}^2\Pi_{\frac{3}{2}}$	33455.7	33987.1	34685.8

REFERENCES

1. W. Jevons. Proc. Roy. Soc. A89, 187 (1913).
2. W. Jevons. Proc. Roy. Soc. A106, 174 (1924).
3. A. C. Datta. Z. Physik 78, 486 (1932).
4. W. Jevons. Proc. Phys. Soc. (London) 48, 563 (1936).
5. V. M. Tatevskii, L. N. Tunitskii, and M. M. Novikov. Opt. i Spektr. 5, 520 (1958).
6. R. S. Mulliken. Revs. Modern Phys. 3, 89 (1931).

VIBRATIONAL CONSTANTS AND DISSOCIATION ENERGY OF THE BeCl MOLECULE

M. M. Novikov and L. N. Tunitskii

Received 21 September 1959

The vibrational structure of the bands of the BeCl molecule has been restudied. Thirty new heads of the Q_1-branches of the bands and 43 new heads of the R_1- and R_2-branches have been found. The values of the vibrational constants ω_0 and $\omega_0 x_0$ in the upper and lower states have been made more precise, and the second anharmonicity coefficients $\omega_0 y_0$ have been determined for the $A^2\Pi$ and $X^2\Sigma$ states. The value of the third anharmonicity coefficient for the $X^2\Sigma$ state has been estimated. A nonlinear extrapolation has been carried out and a new most probable value for the dissociation energy of the BeCl molecule is given: 5.9 ± 0.5 ev. In the 2620 A region, new bands have been discovered, which apparently are to be ascribed to a transition from a new, higher electronic state of the BeCl molecule.

For the BeCl molecule, two electronic states are known: $X^2\Sigma$ and $A^2\Pi$, for which the vibrational constants ω_e and $\omega_e x_e$ were determined (on the basis of the Q_1-band heads) by Fredrickson and Hogan.[1] The values of the rotational constants B_0' and B_0'' were also approximately estimated, on the basis of a series of resolved lines of the R_2- and R_1-branches and the magnitude of the isotopic shift. With the help of a linear extrapolation, the values 4.33 and 3.47 ev were obtained[1] for the dissociation energies of the $X^2\Sigma$ and $A^2\Pi$ states respectively. The same values were given in Rosen's handbook.[2] Gaydon,[3] revising the linear-extrapolation data, takes 3 ± 0.5 ev as the most probable value of the dissociative energy in the ground state.

The estimates just presented for the dissociation energy of the BeCl molecule cannot be considered as reliable, since they are based on the analysis of 10 bands altogether, with v' and $v'' \leqslant 3$. In the present work, the vibrational constants and dissociation energy for the BeCl molecule are made more precise on the basis of analysis of 39 bands with v' and $v'' \leqslant 10$.

EXPERIMENTAL PROCEDURE

The quartz gas-discharge pulse tube used by us in the investigation of the spectrum of BeF and described in the previous work[4] served as the source of excitation of the BeCl spectrum. Since overlapping of the bands is considerably more pronounced in the BeCl spectrum than in the BeF spectrum, the operating conditions of the tube were changed so as to obtain a considerably less-developed fine structure and to reduce the overlapping of the bands to an even greater extent. During the experiments, the spiral tube was heated to a temperature not higher than 300°C and an ohmic resistance was included in the high-voltage supply circuit of the tube, reducing the current in the pulse and the heating of the molecular gas at the time of the pulse. The procedures cited made it possible to reduce the relative intensity in the spectra of the R_1- and R_2-band heads, which are located at a relatively large distance from the band origin, and to obtain maximally intense Q_1-heads. The spectra were photographed with the help of a DFS-3 spectrograph (dispersion, 2 A/mm; resolving power, 144,000). Aerial photographic film, type 10, with a sensitivity 1000 at Sd 0.85 was used for the photographic record. The spectra were measured with the help of an IZA-2 comparator. The arc spectrum of iron served as comparison spectrum.

RESULTS OF THE MEASUREMENTS

In reference 1, 10 heads of the Q_1-branches of the bands and 32 heads of the R_1- and R_2- branches of the bands (for 16 bands altogether) were measured and interpreted in the $\Delta v = -1$, $\Delta v = 0$, and $\Delta v = +1$ sequences. The equations calculated on the basis of these data for the frequencies of the heads of the R_1-, R_2-, and Q_1-branches of the bands have the form

$$\nu_{R_1} = 28030.55 + 813.64\left(v' + \frac{1}{2}\right) - 1.96\left(v' + \frac{1}{2}\right)^2 - 839.38\left(v'' + \frac{1}{2}\right) + 7.78\left(v'' + \frac{1}{2}\right)^2 - 6.03\,{}'v' + \frac{1}{2}\Big)\left(v'' + \frac{1}{2}\right). \quad (1)$$

$$\nu_{R_2} = 28008.03 + 809.06\left(v' + \frac{1}{2}\right) - 2.33\left(v' + \frac{1}{2}\right)^2 - 831.14\left(v'' + \frac{1}{2}\right) + 6.52\left(v'' + \frac{1}{2}\right)^2 - 5.54\left(v' + \frac{1}{2}\right)\left(v'' + \frac{1}{2}\right). \quad (2)$$

$$\nu_{Q_1} = 27970.46 + 824.19\left(v' + \frac{1}{2}\right) - 6.03\left(v' + \frac{1}{2}\right)^2 - 846.58\left(v'' + \frac{1}{2}\right)^2 + 5.11\left(v'' + \frac{1}{2}\right)^2. \quad (3)$$

In the present work, thanks to the procedures described above, we succeeded in simplifying the structure of the observed spectrum and in establishing the most favorable conditions for the measurement of the heads

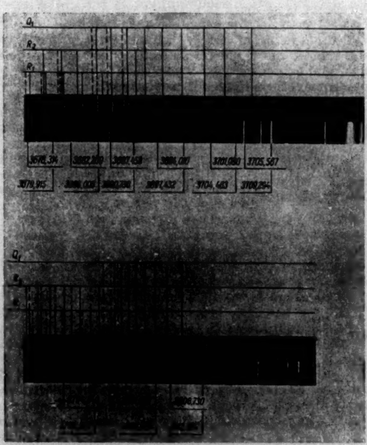

Table 1. Heads of the R_1-, R_2-, and Q_1-Branches of the Bands of the BeCl Molecule

$v'v''$	ν(cm^{-1})	$v'v''$	ν(cm^{-1})	$v'v''$	ν(cm^{-1})	$v'v''$	ν(cm^{-1})	$v'v''$	ν(cm^{-1})
0.0 R_1	28016.2	5.4$_i$	28668.5	6.4	29426.0	5.6$_i$ R_1	—	3.5$_i$	26363.9
R_2	27996.9		—		29404.0	R_2	—		26365.0
Q_1	27958.9		—		29382.9	Q_1	27045.2		26289.8
Q_1^*	27959.5		—		29380.8	Q_1^*	—		—
Q_1^{**}	27960.1		—		29381.2	Q_1^{**}	27046.2		26289.4
1.1 R_1	27991.0	6.5 R_1	28630.1	7.5	29372.0	6.7 R_1	27073.0	4.6	26340.6
R_2	27971.6	R_2	28611.2		29331.3	R_2	27061.2		26332.4
Q_1	27934.3	Q_1	28585.5		29332.1	Q_1	27019.6		26272.6
Q_1^*	27935.7	Q_1^*	28583.8		29329.6	Q_1^*	27018.8		26271.7
Q_1^{**}	27934.8	Q_1^{**}	28584.7		29330.2	Q_1^{**}	27020.2		26272.6
2.2 R_1	27964.4	6.5$_i$ R_1	—	8.6	29314.6	6.7$_i$ R_1	—	4.6$_i$	26348.7
R_2	27944.7	R_2	—		29296.5	R_2	—		26340.6
Q_1	27908.8	Q_1	28582.3		29278.6	Q_1	27024.8		26280.9
Q_1^*	27910.5	Q_1^*	—		29277.0	Q_1^*	—		—
Q_1^{**}	27909.2	Q_1^{**}	28582.1		29277.2	Q_1^{**}	27025.7		76281.6
3.3	27937.2	7.6 R_1	28585.5	0.1	27190.7	7.8	27046.4	5.7	26323.1
	27918.6	R_2	28568.0		27175.4		27034.7		26315.1
	27883.6	Q_1	28543.7		27123.2		26997.0		26263.3
	27884.0	Q_1^*	28542.2		27123.9		26996.6		26262.0
	27883.1	Q_1^{**}	28543.3		27123.9		26997.9		26263.4
4.4	27908.8	7.6$_i$ R_1	28582.3	0.1$_i$	27195.0	7.8$_i$	—	5.7$_i$	26331.4
	27890.5	R_2	28565.2		27179.2		—		26323.1
	27856.7	Q_1	—		27128.0		27002.0		26272.6
	27856.1	Q_1^*	—		—				—
	27856.0	Q_1	—		27128.6		27003.4		26272.7
1.0	28823.8	8.7 R_1	28537.2	1.2	27174.1	8.9	27016.9	6.8	26302.0
	28800.1	R_2	28520.9		27158.7		27005.3		26294.3
	28770.1	Q_1	28500.6		27108.3		26971.4		26252.0
	28771.3	Q_1^*	28499.4		27109.7		26973.1		26250.8
	28770.0	Q_1^{**}	28499.7		27108.7		26973.0		26252.1
1.0$_i$	28819.3	8.7$_i$	28533.9	1.2$_i$	27178.2	9.10	26987.9	6.8$_i$	26310.6
	28794.9		28518.7		27162.7		—		26302.7
	28765.5		—		27112.7		—		26261.5
	—		—		—		—		—
	28766.8		—		27113.4		—		26261.5
2.1	28787.3	9.8	28485.1	2.3	27156.6	0.2	26391.1	7.9	—
	28763.3		28427.7		27142.1		26382.2		—
	28735.1		28456.2		27092.6		26302.0		26238.3
	28736.4		28455.3		27094.2		26297.9		26238.3
	28735.4		28553.6		27093.1		26297.8		26238.9
2.1$_i$	28782.9	2.0	29622.0	2.3$_i$	27161.1	0.2$_i$	—	7.9$_i$	—
	28758.9		29595.1		27146.0		26391.1		—
	28731.1		29571.3		27097.0		26310.6		26247.6
	—		29572.1		—		—		—
	28731.4		29571.6		27097.9		26307.0		26247.9
3.2	28749.8	2.0$_i$	29613.2	3.4	27138.0	1.3	26380.7	8.10 R_1	—
	28726.9		29585.6		27123.8		26371.8	R_2	—
	28699.1		—		27076.3		26294.4	Q_1	26221.3
	28700.3		—		27077.3		26293.4	Q_1^*	26224.4
	28699.2		—		27076.8		26292.5	Q_1^{**}	26223.4
3.2$_i$	28745.8	3.1	29574.9	3.4$_i$	27143.1	1.3$_i$	26388.4	8.10$_i$	—
	28723.4		29549.0		—		26380.7		—
	28695.4		29527.0		27081.1		26302.7		26231.4
	—		29526.2		—		—		—
	28695.6		29525.4		27081.7		26301.7		26232.8
4.3	28711.4	3.1$_i$	29566.6	4.5	27118.3	2.4	26369.1		
	28689.6		29540.4		27104.9		26360.4		
	28662.5		—		27058.6		26287.6		
	28662.8		—		27059.1		26287.5		
	28662.3		—		27059.5		26286.8		
4.3$_i$	28708.0	4.2	29527.0	4.5$_i$ R_1	27123.2	2.4$_i$	26376.9		
	—		29502.0	R_2	—		26369.1		
	28758.0		29479.5	Q_1	27064.0		26296.9		
	—		29479.1	Q_1^*	—		—		
	28658.0		29478.5	Q_1^{**}	27064.6		26295.9		
5.4	28671.6	5.3	29577.4	5.6 R_1	27097.2	3.5	26356.0		
	28649.5		29453.9	R_2	27084.2		26346.6		
	28625.3		29430.2	Q_1	27040.1		26280.9		
	28623.9		29430.6	Q_1^*	27040.5		26280.3		
	28624.3		29430.5	Q_1^{**}	27040.5		26280.3		

Note: R_1, R_2, Q_1 – measured wave numbers of the band heads; Q_1^* – wave numbers of heads calculated without taking account of the second and third anharmonicity coefficients; Q_1^{**} – wave numbers of heads, taking account of the second and third anharmonicity coefficients. Bands of the isotopic molecule are designated by the index "i."

of the Q_1-branches, which lie near the band origin and may be used directly for determination of the vibrational constants with very high accuracy. We measured 39 heads of the Q_1-branches and 75 heads of the R_1- and R_2-branches for 40 bands altogether of the molecule $BeCl^{35}$, and 20 heads of the Q_1-branches and 32 heads of the R_1- and R_2-branches for 26 bands altogether of the isotopic molecule $BeCl^{37}$, in the $\Delta v = -2$, $\Delta v = -1$, $\Delta v = 0$, $\Delta v = +1$, and $\Delta v = +2$ sequences. Examples of the spectra obtained ($\Delta v = -1$ and $\Delta v = -2$ sequences) are presented in the Figure. The search for the heads of the Q_1-branches of the bands in these sequences, as can be seen from the spectra, presents no difficulty at all. The wave numbers of the band heads measured are given in Table 1.

VIBRATIONAL CONSTANTS AND EXTRAPOLATED VALUES OF THE DISSOCIATION ENERGY OF THE BeCl MOLECULE IN THE $X^2\Sigma$ AND $A^2\Pi$ STATES

The equation of Fredrickson and Hogan for the Q_1-band heads[3] does not satisfactorily describe the position of the Q_1-band heads with values of v′ and v″ > 3. For v′ = 8 in the $\Delta v = +2$ and $\Delta v =$ 1 sequences, the discrepancy between the calculated and experimental values of the wave numbers of the Q_1 heads reaches 24 cm^{-1}. Therefore, new equations describing the position of the Q heads have been found, on the basis of the values obtained by us for the wave numbers of the heads of the Q_1-bands. These equations were obtained by the following method. From the experimental values of the wave numbers of the heads of the Q_1-bands of adjacent sequences ($\Delta v = 2$ and $\Delta v = 1$; $\Delta v = 1$ and $\Delta v = 0$; $\Delta v = 0$ and $\Delta v = -1$; and $\Delta v = -1$ and $\Delta v = -2$), the values of $\Delta G_0'(v') = \nu_{Q_1}^{v'+1,\, v''} - \nu_{Q_1}^{v'v''}$ and $\Delta G_0''(v'') = \nu_{Q_1}^{v',\, v''+1} - \nu_{Q_1}^{v'v''}$ presented in Tables 2 and 3 have been calculated. From the values of $\Delta G_0'(v')$ and $\Delta G_0''(v'')$, the vibrational constants have been computed by the method of least squares.[5]

If we suppose that $\Delta G_0'(v')$ and $\Delta G_0''(v'')$ are determined by Eqs. (4) and (5),

$$\Delta G_0'(v') = \omega_0' - (2v' + 1)\,\omega_0'x_0'. \tag{4}$$

$$\Delta G_0''(v'') = \omega_0'' - (2v'' + 1)\,\omega_0''x_0''. \tag{5}$$

then the vibrational constants prove to be

$$\nu_0 = 27959.5,\quad \omega_0' = 817.28,\quad \omega_0'' = 840.46,$$

$$\omega_0'x_0' = 5.497,\quad \omega_0''x_0'' = 4.831\ (\text{cm}^{-1}). \tag{6}$$

The wave numbers of the Q_1 heads must satisfy the equation

$$\nu_{Q_1} = 27959.5 + (817.28v' - 5.497v'^2) - (840.46v'' - 4.831v''^2). \tag{7}$$

In Table 1 the values of the wave numbers of the heads calculated according to formula (7) are compared

Table 2. Values of $\Delta G_0'(v')$(in cm^{-1}), Computed From the Heads of the Q_1-Branches of Bands of Different Sequences

Sequences for which the computation was carried out	$\Delta G_0'(0)$	$\Delta G_0'(1)$	$\Delta G_0'(2)$	$\Delta G_0'(3)$	$\Delta G_0'(4)$	$\Delta G_0'(5)$	$\Delta G_0'(6)$	$\Delta G_0'(7)$
$\Delta v = 2$; $\Delta v = 1$		801.2	791.9	780.4	768.3	757.6	746.6	734.9
$\Delta v = 1$; $\Delta v = 0$	811.2	800.8	790.3	778.9	—	—	—	—
$\Delta v = 0$; $\Delta v = -1$	811.1	800.5	791.0	780.4	—	—	—	—
$\Delta v = -1$; $\Delta v = -2$	805.3	798.2	788.7	777.7	767.5	756.3	745.0	733.1

Table 3. Values of $\Delta G_0''(v'')$(in cm^{-1}), Computed From the Heads of the Q_1-Branches of Bands of Different Sequences

Sequences for which the computation was carried out.	$\Delta G_0''(0)$	$\Delta G_0''(1)$	$\Delta G_0''(2)$	$\Delta G_0''(3)$	$\Delta G_0''(4)$	$\Delta G_0''(5)$	$\Delta G_0''(6)$	$\Delta G_0''(7)$	$\Delta G_0''(8)$	$\Delta G_0''(9)$
$\Delta v = 2$; $\Delta v = 1$	836.2	827.9	817.0	804.9	797.4	788.4	778.0			
$\Delta v = 1$; $\Delta v = 0$	835.8	826.3	815.5	805.8						
$\Delta v = 0$; $\Delta v = -1$	835.7	826.0	818.2	807.3	798.1					
$\Delta v = -1$; $\Delta v = -2$		821.2	813.9	805.0	795.4	786.0	776.8	767.6	758.7	750.1

with those determined experimentally. As follows from the table, the discrepancy does not exceed 2.5 cm^{-1}. The values of the dissociation limits in the $X^2\Sigma$ and $A^2\Pi$ states obtained with the help of a linear extrapolation based on the vibrational constants[6] differ somewhat from the previously reported values[1] and are $D_0' = 30{,}390\ cm^{-1} = 3.76$ ev and $D_0'' = 36{,}555\ cm^{-1} = 4.53$ ev.

Table 4. Comparison of the Spectra of the Molecules BeF, BeCl, MgF, MgCl, and CaCl

Kind of molecule	Electronic transition	λ (A)	Note
BeF	$A^2\Pi \rightarrow X^2\Sigma^+$	3315—2815	
BeCl	$A^2\Pi \rightarrow X^2\Sigma^+$	3686—3468	
BeCl		2620 A region	Discovered by us
MgF	$A^2\Pi \rightarrow X^2\Sigma^+$	2686—3468	
MgF	$B^2\Sigma \rightarrow X^2\Sigma^+$	3742—2630	
MgCl	$A^2\Pi \rightarrow X^2\Sigma^+$	3950—3600	
MgCl		3865—3855	Transition not determined
CaCl	$A^2\Pi \rightarrow X^2\Sigma^+$	6370—7050	
CaCl	$B^2\Sigma \rightarrow X^2\Sigma^+$	6080—5820	
CaCl	$C^2\Pi \rightarrow X^2\Sigma^+$	3950—3640	

In Table 4 the spectrum and electronic states of the BeCl molecule are compared with the spectra and electronic states of the similar molecules BeF, MgF, MgCl, and CaCl. On the basis of this comparison, it appears reasonable to suppose that the $X^2\Sigma$ state of the BeCl molecule is the ground state $X^2\Sigma^+$. There are no direct experimental data which establish the ground state of the BeCl molecule. If the $X^2\Sigma$ state of the BeCl molecule is the ground state $X^2\Sigma^+$, then the correlation which was carried out for the BeF molecule[4] and was based on application of the noncrossing rule for potential curves remains true for BeCl also. According to this correlation, the $X^2\Sigma$ and $A^2\Pi$ states of the BeCl molecule must have a common dissociation limit and must correlate with the ground state of the separated atoms $Be(^1S) + Cl(^2P)$. With a common dissociation limit, the values D_0'', D_0', and ν_0 are connected by the relation

$$D_0'' - D_0' = \nu_0 = 27960\ cm^{-1}. \qquad (8)$$

The dissociation limits obtained by us on linear extrapolation do not satisfy Eq. (8) and consequently do not correspond to the assumed correlation.

In connection with the foregoing, an attempt was made to satisfy the requirements of the assumed correlation by introducing the second and third anharmonicity coefficients $\omega_0 y_0$ and $\omega_0 z_0$. From the values of $\Delta G_0'(v')$ and $\Delta G_0''(v'')$ presented in Tables 2 and 3, and with the help of the relations written below

$$\Delta G_0'(v') = \omega_0' - (2v' + 1)\,\omega_0' x_0' + \left(3v'^2 + 3v' + 1\right)\omega_0' y_0', \qquad (9)$$

$$\Delta G_0''(v'') = \omega_0'' - (2v' + 1)\,\omega_0'' x_0'' + \left(3v''^2 + 3v'' + 1\right)\omega_0'' y_0'' \qquad (10)$$

the most probable vibrational constants ω_0, $\omega_0 x_0$, and $\omega_0 y_0$ were computed and the average errors in their determination estimated. The vibrational constants obtained are

$$\left.\begin{aligned} \omega_0' &= 816.0 \pm 0.33, \\ \omega_0' x_0' &= 5.06 \pm 0.072, \\ \omega_0' y_0' &= -0.0368 \pm 0.0061\ (cm^{-1}). \end{aligned}\right\} \qquad (11)$$

$$\left.\begin{aligned} \omega_0'' &= 841.3 \pm 0.344, \\ \omega_0'' x_0'' &= 5.11 \pm 0.077, \\ \omega_0'' y_0'' &= 0.0205 \pm 0.0049\ (cm^{-1}). \end{aligned}\right\} \qquad (12)$$

The extrapolated value of the dissociation energy in the $A^2\Pi$ state was determined analytically from the values of the vibrational constants (11). With the help of the expression

$$\Delta G_0'(v') = 816.0v' - 5.06v'^2 - 0.0368v'^3 \qquad (13)$$

for the vibrational term, the maximum value of the vibrational quantum number, v'_{max}, and $G_0'(v'_{max})$, which equals the extrapolated value of the dissociation energy D_0', were calculated:

$$D_0' = G_0'\left(v'_{max.}\right) = G_0'(51) = 23500\ cm^{-1}. \qquad (14)$$

The dissociation limit D_0' was obtained by a relatively short extrapolation, and therefore is sufficiently accurate. We take it as $D_0' = 23{,}500 \pm 4000\ cm^{-1}$. The dissociation limit of the $X^2\Sigma$ state then, according to the equality (8), is given by

$$D_0'' = 23500 \pm 4000 + 27960 \approx 51500 \pm 4000\ cm^{-1}. \qquad (15)$$

It proved impossible to obtain the dissociation limit D_0'' from the vibrational constants in (12), since the curve of $\Delta G_0''(v'')$ computed from these vibrational constants has a minimum equal to 417 cm^{-1} at $v'' = 83$ and does not intersect the v'' axis.

Thus we take the dissociation limit D_0'' equal to $51{,}500 \pm 4000\ cm^{-1}$. It proved impossible to match the vibrational constants of the $X^2\Sigma$ state with the dissociation limit $D_0'' = 51{,}500\ cm^{-1}$ by adjustment of the values of the vibrational constants ω_0'', $\omega_0'' x_0''$, and $\omega_0'' y_0''$. The vibrational constants of the $X^2\Sigma$ state, computed according to the method of averages on the bases of the known values of $\Delta G''(v'')$ with the additional condition (15), are

$$\omega_0'' = 838.0,\quad \omega_0'' x_0'' = 4.59 \text{ and } \omega_0'' y_0'' = 0.00838\ (cm^{-1}). \qquad (16)$$

The values of $\Delta G_0''(v'')$ calculated from these vibrational constants when $v'' = 0\text{–}1$ differ from the experimental values by +3, and when $v'' = 8\text{–}9$ by $-3\ cm^{-1}$. The wave numbers of the band heads calculated from the vibrational constants (11) and (16) differ from the experimental values by 6–8 cm^{-1}.

From what has been said, in order to get agreement of the vibrational constants of the $X^2\Sigma$ state with the fixed dissociation limit $D_0'' = 51{,}500\ cm^{-1}$, it is necessary to introduce the third anharmonicity coefficient $\omega_0'' z_0''$ into the expression for the vibrational term. When this is done, naturally, all the vibrational constants change, but these changes are very small. Therefore, we have taken the values of ω_0'', $\omega_0'' x_0''$, and $\omega_0'' y_0''$ according to (12) and calculated v''_{max} and $\omega_0'' z_0''$ with the help of the equations

$$\begin{aligned} \left(\frac{\partial G''}{\partial v''}\right)_{max.} &= 841.3 - 10.22v''_{max.} \\ &+ 0.0615v''^2_{max.} + 4\omega_0'' Z_0'' v''^3_{max.} = 51500. \end{aligned} \qquad (17)$$

$$\begin{aligned} G''\left(v''_{max.}\right) &= 841.3v''_{max.} - 5.13v''^2_{max.} \\ &+ 0.0205v''^3_{max.} + \omega_0'' Z_0'' v''^4_{max.} = 51500. \end{aligned} \qquad (18)$$

The values found for the vibrational constants and the dissociation limit are

$$\begin{gathered} \omega_0'' = 841.3,\quad \omega_0'' x_0'' = 5.11,\quad \omega_0'' y_0'' = 0.0205, \\ \omega_0'' Z_0'' = -0.0000592\ (cm^{-1}). \end{gathered} \qquad (19)$$

$$D_0'' = G_0''\left(v''_{max.}\right) = G_0''(133) = 51500\ (cm^{-1}). \qquad (20)$$

The wave numbers of the band heads for the vibrational constants (11) and (19) are determined by Eq. (21) given below and, according to Table 1, agree well with experiment.

$$\begin{aligned} \nu_{Q_1} &= 27960.1 + (816.0v' - 5.06v'^2 - 0.0368v'^3) \\ &- (841.3v'' - 5.11v''^2 + 0.0205v''^3 - 0.0000582v''^4). \end{aligned} \qquad (21)$$

The values of v'_{max}, v''_{max}, D'_0, and D''_0 obtained by this present work are presented in Table 5, where they are compared with the values of the corresponding quantities obtained by linear extrapolation. The values for the dissociation energy presented in Table 5 are probably somewhat high, since one may expect, on the potential curves of the $X^2\Sigma$ and $A^2\Pi$ states, the presence of maxima associated with the interaction of these states and the $^2\Sigma$ and $^2\Pi$ states which correlate with the atomic states $Be(^3P) + Cl(^2P)$. Therefore, we have somewhat lowered the values obtained for the dissociation energy and have taken them to be equal to

$$D'_0 = 19500 \pm 4000 \text{ and } D''_0 = 47500 \pm 4000\ (\text{cm}^{-1}).$$

Table 5. Values of v'_{max}, v''_{max}, $G'_0(v'_{max})$, and $G''_0(v''_{max})$, Taking Account (I) and not Taking Account (II) of the Second and Third Anharmonicity Coefficients

v'_{max}		v''_{max}		$G'_0(v'_{max})$		$G''_0(v''_{max})$	
I	II	I	II	I	II	I	II
51	74	133	87	23500	30400	51500	36600

In Table 6 are presented the vibrational constants and the values of the dissociation energy of the $A^2\Pi$ and $X^2\Sigma$ states under consideration, assumed to be the most probable on the basis of the results set forth above, provided only that the correlation stated above between the molecular states $X^2\Sigma$ and $A^2\Pi$ and the atomic states does not require some kind of change.

Table 6. Vibrational Constants (in cm^{-1}) and Values of the Dissociation Energy (ev) of the $X^2\Sigma$ and $A^2\Pi$ States

Electronic state	ν_e	ω_e	$\omega_e x_e$	$\omega_e y_e$	$\omega_e z_e$	D_0
$X^2\Sigma^+$	—	841.3	5.11	0.0205	−0.0000582	5.9 ± 0.5
$A^2\Pi$	27960.1	816.0	5.06	−0.0368	—	2.4 ± 0.5

NEW BANDS OF THE BeCl MOLECULE

Parker[6] reported a band system of BeCl (the $^2\Pi \rightarrow {}^2\Sigma$ transition) lying in the yellow-green region of the spectrum, the Q_1-band heads of which are described by the equation

$$\nu_{Q_1} = 18685.6 + \{540.0\,(v' + 1/2) - 7.1\,(v' + 1/2)^2\} - \{551.1\,(v'' + 1/2) - 6.2\,(v'' + 1/2)^2\}. \qquad (22)$$

Under our experimental conditions, Parker's bands were not found. In the 2620 A region, we did find bands (one sequence), similar, from a superficial viewpoint, to the $A^2\Pi \rightarrow X^2\Sigma$ band system of the BeCl molecule. The wavelengths of the heads of these bands are presented in Table 7. It may be supposed that these bands belong to the BeCl molecule, since analogous bands are present in the spectra of similar molecules.

Table 7. Wavelengths of the Band Heads Located in the 2620 A Region

N	λ (A)	N	λ (A)	N	λ (A)
1	2610.213	10	2622.223	19	2632.160
2	11.855	11	22.377	20	32.741
3	14.170	12	23.403	21	37.593
4	14.420	13	23.524	22	38.083
5	16.936	14	26.722		
6	18.101	15	26.970		
7	18.186	16	27.583		
8	19.857	17	27.662		
9	19.967	18	31.778		

REFERENCES

1. W. R. Fredrickson and M. E. Hogan. Phys. Rev. 46, 454 (1934).
2. B. Rosen. Constantes selectionnées. Données spectroscopiques concernant les molécules diatomiques. Paris, 1951.
3. A. Gaydon. "Energiya dissotsiatsii i spektry dvukhatomnykh molekul" (Dissociation Energy and Spectra of Diatomic Molecules), Izd. Inostrannoi Lit., Moscow, 1959.
4. V. M. Tatevskii, L. N. Tunitskii, and M. M. Novikov. Opt. i Spektr. 5, 520 (1958).
5. A. N. Krylov. "Lektsii o priblizhennykh vychisleniyakh" (Lectures on Approximate Calculations), Gosudarst. Izd. Tekh.-Teoret. Lit., Moscow, 1950.
6. A. E. Parker. Phys. Rev. 45, 752 (1934).

SPECTROSCOPIC INVESTIGATION OF THE STATE OF THE GAS BEHIND A SHOCK WAVE. III

F. S. Faizullov, N. N. Sobolev, and E. M. Kudryavtsev

Received 28 September 1959

The generalized spectrum-line reversal method was used to measure the temperature of nitrogen and air behind a shock wave in the range of shock-wave velocities from 1.9 to 4.3 km/sec, and for gas pressures in the plug from 0.1 to 4 atm. It was established that there was satisfactory agreement between the experimental and the theoretical variation of the temperature of the plug with the shock-wave velocity. The distribution of temperature along the plug was studied for various shock-wave velocities.

The present communication presents the results obtained in a thermometric study of nitrogen, air, and argon behind a shock wave, using the generalized method of spectrum-line reversal. A description of the experimental arrangement, the equipment used, and the methods of measuring the temperature, the shock-wave velocity, and the length of the plug* has been given in previously published accounts of work carried out in our laboratory.[1-4]

Systematic measurements of the temperature of air and nitrogen by the method of spectrum-line reversal were made at a distance of 3.5 meters from the diaphragm separating the high and low pressure chambers; the diameter of the tube was 92 mm. For high shock-wave velocities ($U_s > 3.5$ km/sec) obtained by means of a two-diaphragm arrangement, measurements were carried out at a distance of 2.9 meters from the last diaphragm. The temperature was measured with the sodium D lines and with the resonance line of ionized barium, Ba II 4554 A. The effective brightness temperature of the comparison source in the region of these lines was 4750°K.

TEMPERATURE DISTRIBUTION ALONG THE PLUG

According to the most elementary principles of gas dynamics one would expect a constant temperature along the whole length of the plug. However, the first experiments in which temperature measurements were made on nitrogen and air with the sodium D lines showed that only for relatively small values of U_s was the recorded temperature constant along part of the theoretical length of the plug (Fig. 1). For $U_s > 3$-4 km/sec a sharp drop in temperature was observed immediately behind the shock-wave front. For the explanation of this effect two hypotheses were advanced: (1) the shock-wave velocity along the shock tube is not constant, and as a consequence, since each element of the length of the plug is formed in a definite region of the tube, a corresponding temperature change along the plug is possible; (2) the sodium emission is retarded with respect to the shockwave front, so that the temperatures measured are characteristic of the state of the gas at the end of the plug or even in the region of mixing of hydrogen and the gas under study.

A detailed study of the distribution of the velocity U_s along the shock tube, undertaken in connection with the first hypothesis, allowed us to make a decision as to its validity. As shown by the results in reference 4, the shock-wave velocity actually drops off from the point of observation in the direction of the diaphragm. If one assumes that the elements of the plug "remember" the conditions under which they were formed, and that temperature equalization along the plug does not occur, one would expect also a corresponding fall of the temperature along the plug. The dot-dash curve in Fig. 1 shows the distribution of temperature along the plug, calculated with the variation of the shock-wave velocity along the tube[4] taken into account. As is evident from the figure the experimentally determined temperature variation along the plug agrees with the calculated variation only for low velocities (curve a). For high velocities (curve c) the experimental value of the temperature falls off much more quickly than the calculated value. An experimental study of the retardation of the sodium emission[4] showed that the D line emission begins immediately behind the shock-wave front. Consequently, a temperature measured by the sodium emission represents the temperature of the main part of the plug and not of just its cold end bordering on the contact region.

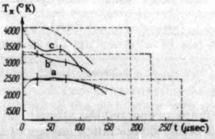

Fig. 1. Temperature distribution along the plug for nitrogen (p_1 = 10 mm Hg) for various shock-wave velocities U_s. Value of U_s (km/sec): curve a—2.32 ± 0.07; curve b—2.75 ± 0.05; curve c—3.14 ± 0.04. Each curve is the average of six experiments. The dashed curve is the temperature according to ideal theory, and the dot-dash curve the temperature calculated with the distribution of the shock-wave velocity along the tube taken into account. The abscissa scale gives the time of arrival of the element in question of the plug at the point of observation situated at a distance of 3.5 meters from the diaphragm.

Thus, neither of the working hypotheses was able to explain the temperature variation along the plug which was observed at high shock-wave velocities. This made it necessary to verify still another plausible hypothesis for the explanation of the observed phenomena. During the passage of the shock wave along the shock tube there is always a boundary layer formed near the walls of the tube, the temperature of which is lower than the temperature of the core of the plug. This layer contains a large amount of cold sodium vapor which comes from the walls and which absorbs strongly but emits only weakly. The presence of this vapor can lead to a significant lowering of the temperature as measured by the reversal method.[1, 2] Experiments showed that the strongest absorption is produced in the part of the boundary layer which is formed directly on the windows used for transmitting the radiation. If the windows are carefully washed with hot water before each experiment to remove traces of sodium chloride a satisfactory agreement between experiment and theory is obtained, that is, the temperature variation along the plug corresponds to the distribution of the shock-wave velocity along the tube (Fig. 2). A further significant step was taken when we changed from temperature measurements with the sodium D lines to measurements with the resonance line of ionized barium Ba II 4554 A (in these experiments the walls of the shock tube were lightly smeared with a solution of barium chloride). In this case barium ions were present only in the core of the plug, and consequently the cold boundary layer was transparent for the radiation of the Ba II line and could not affect the measured value of the temperature.

---

*Translator's note: the word "plug" is used as the translation of a Russian word designating the region of hot gas between the shock-wave front and the beginning of the contact region.

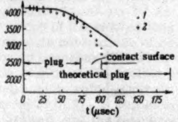

Fig. 2. Temperature distribution along the plug for nitrogen (p_1 = 10 mm Hg). The solid curve is the temperature calculated with the distribution of the shock-wave velocity along the tube taken into account. The points give the experimental data: 1—measured with the Na D lines; 2—measured with the Ba II line. The data on the length of the plug were obtained by the schlieren method.

In Fig. 2, along with data obtained with the sodium D lines, are given data obtained with the Ba II line. As is evident from the figure, in both cases the experimental results are in satisfactory agreement with the calculated results. The same conclusions were also reached with other shock-wave velocities. We have thus shown that it is possible to use the reversal method for measuring the temperature distribution along the plug. The agreement of the theoretical and experimental data on the value of the temperature and its distribution behind the shock wave indicates that the theory is valid. The fact that temperatures measured with the Na and the Ba II line are identical proves that thermodynamic equilibrium exists in nitrogen and air behind a shock wave. The observed distribution of temperature along the plug indicates that the plug "remembers" the conditions under which each of its individual elements was formed.

RESULTS OF AN INVESTIGATION OF THE TEMPERATURE BEHIND A SHOCK WAVE IN AIR

About a hundred experiments were carried out on the measurement of the temperature distribution in the air behind a shock wave with initial pressures of 2, 10, and 50 mm Hg. Hydrogen at pressures from 10 to 120 atm was used as the driver gas in all the experiments and shock-wave velocities from 1.9 to 4.3 km/sec were obtained. A typical form of the oscillograms obtained in these experiments is given in Fig. 3. The end of the homogeneous part of the gas flow (the plug), determined by means of the schlieren shadow method,[4] is designated by the letter K and in the case given coincides with the instant of extinction of the emission. Strong absorption is observed in the rather extended contact region behind the plug; this is due to the increased impurity concentration in the region of mixing.

In experiments with an initial air pressure of 50 mm Hg and U_s = 1.9-2.3 km/sec (Fig. 4) in contrast to other experimental conditions, a rise in temperature which could reach 600° was observed in the contact region. For these conditions a corresponding increase in the velocity was also observed in the velocity distribution along the tube. We ascribe this increase of temperature to a process of hydrogen combustion in the contact region. It should be noted that this process is more important in the initial stage when the hydrogen flows out unevenly through the shattered diaphragm and mixes with air. After the gas flow is established no great broadening of the region of combustion will occur, since the processes of diffusion are not rapid enough. Thus the shock wave has at first a tendency to move more quickly because of the energy contributed by the combustion process. The gas located at the beginning close to the diaphragm will be heated relatively more by the strong shock wave and will reach a higher temperature than the gas which at the beginning was at the window. In those cases in which combustion is observed in the contact region some rise in temperature can occur even in the region of the homogeneous flow; this is probably caused by the liberation of energy in the combustion region. A convincing proof of the combustion in air is furnished by experiments with nitrogen under the same initial conditions. In this case no anomaly is present, either in the variation of the temperature along the plug or in the distribution of the shock-wave velocity along the tube. When the initial pressure of the air is decreased to 10 mm Hg or lower, and also when the shock-wave velocity is increased, the effect of combustion is imperceptible.[4]

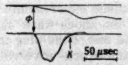

Fig. 3

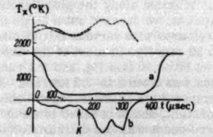

Fig. 4

Fig. 3. Typical form of oscillogram obtained for temperature measurements in air (p_1 = 2 mm Hg, U_s = 4.08 km/sec). Φ—shock wave front; K—beginning of the contact region. The upper curve gives the flux $\Phi_{x+1} - \Phi_1$, the lower curve the flux Φ_x (cf. reference 4).

Fig. 4. Form of the oscillograms (a,b) and temperature distribution along the plug for air when combustion occurs (p_1 = 50 mm Hg, U_s ≈ 2.20 km/sec). K is the beginning of the contact region; the dashed curve gives experimental values of the temperature, the dot-dash curve theoretical values of the temperature calculated with the distribution of the shock-wave velocity along the tube taken into account.

Figure 5 gives the results of our experiments on the measurement of the temperature of the air behind the shock wave as a function of the shock-wave velocity. The

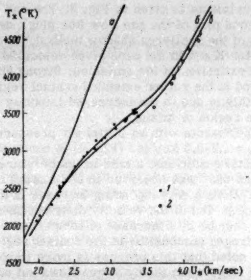

Fig. 5. Variation of the temperature of the air behind a shock wave with the shock-wave velocity. The curves represent calculated data for T_1 = 293°K: curve a—ideal gas; curve b—air (p_1 = 1 atm); curve c—air (p_2 = 0.5 atm). The points represent experimental data: 1—p_1 = 10 mm Hg; 2—p_1 = 2 mm Hg.

points on the graph refer to the temperature of the homogeneous part of the plug. The diagram also shows data on the calculated variation of the temperature with the shock-wave velocity for air (real gas) and for an ideal gas. As is evident from the figure, the temperature of the air behind the shock wave as measured by the reversal method agrees with the calculated value to within ±70°.

RESULTS OF AN INVESTIGATION OF THE TEMPERATURE BEHIND A SHOCK WAVE FOR NITROGEN

Since the experiments with nitrogen were considered to be much more reliable for studying the temperature distribution along the plug because of the absence of combustion, we carried out a large number of similar measurements with various initial nitrogen pressures from 1 to 50 mm Hg. In most of the experiments the pressure was 50 or 10 mm Hg, and the range of shock-wave velocities was from 2 to 3.2 km/sec. In these experiments the temperature of the nitrogen behind the shock wave was constant, and decreased towards the end of the plug in agreement with the distribution of the shock-wave velocity along the tube (Fig. 2).

On oscillograms corresponding to p_1 = 10 mm Hg and U_s = 2.0-2.3 km/sec, a narrow region of low temperature was observed immediately behind the shock-wave front (Fig. 1(a)); this may be related to the vibrational relaxation of the nitrogen molecules. This means that the reversal method can be used to determine the electron excitation temperature. At the same time it is well known from experiments on the quenching of resonance fluorescence[5, 6] that molecular gases (in contrast to monatomic gases) have large effective quenching cross sections. This fact suggests that the excitation temperature might be determined by the effective vibrational temperature rather than by the effective translational temperature[6] of the gas molecules. It is evident that if the vibrational relaxation time is large, measurements by the reversal method may give a much lower excitation temperature, although the translational temperature in this case may be higher than the equilibrium value. We wish to point out that we have not made any special study of this effect. However, the observed values of the relaxation times (~40 μsec) does not contradict data in the literature.[7, 8]

For $U_s > 3.2$ km/sec and expecially in work with the two diaphragm arrangement when the intermediate compartment was filled with hydrogen at a pressure of ~5 atm, a sharp temperature peak was observed near the end of the plug. The extreme regions of the two oscillograms in Fig. 6 correspond to this maximum. In the distribution of the shock-wave velocity along the tube there is also a maximum which corresponds approximately in position with the temperature maximum. Both of these maxima can probably be explained by NH formation reactions which can take place with the generation of heat, since under these conditions (T ~ 4000°K) the hydrogen is almost completely dissociated. It would be possible to confirm this hypothesis if, say, helium rather than hydrogen were used as the driver gas. However, this would give rise to a number of technical difficulties.

The results obtained for nitrogen are given in Fig. 7. In this case, just as for air, the points on the graph refer to the temperature of the homogeneous part of the plug. It is evident from the diagram that the experimental results agree satisfactorily (within ±70°) with the calculated data.

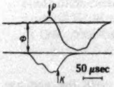

Fig. 6

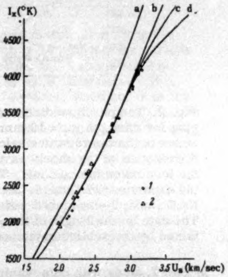

Fig. 7

Fig. 6. Form of oscillogram obtained for nitrogen with the two-diaphragm arrangement (p_1 = 10 mm Hg, $U_s > 3.2$ km/sec). Φ—shock wave front; P—region of increased temperature; K—beginning of the contact region.

Fig. 7. Variation of the temperature of nitrogen behind a shock wave with the shock-wave velocity. The lines represent calculated data for T_1 = 293°K; curve a—ideal gas; curve b—nitrogen (without dissociation); curve c—nitrogen (p_2 = 1 atm); curve d—nitrogen (p_2 = 0.5 atm). The points represent experimental data: 1—p_1 = 10 mm Hg; 2—p_1 = 50 mm Hg.

APPLICATION OF THE GENERALIZED REVERSAL METHOD TO THE STUDY OF THE STATE OF ARGON BEHIND A SHOCK WAVE

We also made an attempt to apply the reversal method (with Ba II 4554 A radiation) to the study of the state of argon behind a shock wave. A typical oscillogram for argon is given in Fig. 8. On the emission curve (the lower curve) a series of clearly defined maxima (peaks) are seen. The shape of a curve is repeated from one experiment to another for the same conditions and does not change very much when the initial pressure p_1 is varied. Oscillograms obtained using the sodium D lines have a similar form. Special experiments showed that the presence of these peaks cannot be caused by inhomogeneities occurring at the walls of the tube. The effect is probably related to processes taking place in the argon plug itself.

Experiments showed that the reversal method cannot be used for temperature measurements in argon with the same success as in the case of air and nitrogen. For pressures in the plug of about 0.5 atm the measured temperatures were more than 1000° lower, and for pressures of 4 atm approximately 400° lower (cf. Fig. 9) than the calculated values; only for pressures in the plug of 11-12 atm were the measured and calculated temperatures the same. It should be noted particularly that the difference between theory and experiment increases as the temperature being measured increases. We consider that in this case the discrepancy is due not to inaccuracy of the theory but to some property of the argon itself. The fact is that for argon the effective cross sections for collisions of the second kind with excited atoms and ions are extraordinarily small, much smaller than the corresponding effective cross sections for nitrogen and air.[5, 6] As a consequence, a considerable fraction of the excited ions make transitions to the ground state not because of collisions of the second kind but by spontaneous emission; this leads to a decrease in the population of the excited levels as compared with the equilibrium value. Only when the pressure in the plug is increased to 11-12 atm in argon are equilibrium conditions attained, and the temperature measured by the reversal method represents the kinetic temperature of the gas. The fact that for the same temperatures in the case of nitrogen and air equilibrium conditions in the plug are reached in air at pressures of the order of 0.1 atm, and in argon at 11-12 atm, is confirmation that for argon the effective cross section for collisions of the second kind with excited barium ions is approximately two orders of magnitude smaller than for nitrogen and air. This conclusion is in agreement with data in the literature.[5, 6] A development of this method of estimating or determining values of cross sections for collisions of the second kind seems to us promising, since in a shock-tube comparatively clear-cut experimental conditions can be realized.

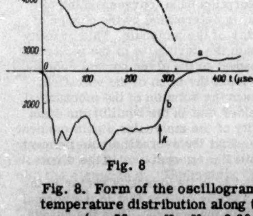

Fig. 8

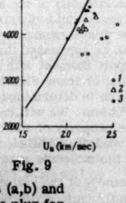

Fig. 9

Fig. 8. Form of the oscillograms (a,b) and temperature distribution along the plug for argon (p = 50 mm Hg, U_s = 2.20 km/sec). K is the beginning of the contact region. The dotted curve represents experimental values, the dot-dash curve theoretical values of the temperature.

Fig. 9. Variation of the temperature of argon behind a shock wave with the shock-wave velocity. The line represents calculated data, the points experimental data. Values of the pressure p_1 (mm Hg): 1—5, 2—50, 3—150.

In a recent investigation[9] dealing with temperature measurements of the gas behind a shock wave the reversal method suggested by us[1] was used. However, inaccuracies tolerated in the work did not allow the authors to observe the lowering of the experimental value of the temperature in argon as compared with the theoretical value, as has been established by us.

CONCLUSION

The results discussed show that the problem, which we formulated in the introduction in reference 2, can be considered to be solved. A spectroscopic method has been developed for the measurement of the gas temperature in a shock tube, which permits the temperature distribution along the plug to be studied. A thermometric investigation of the state of nitrogen and air behind the shock wave was carried out under a wide range of experimental conditions, and the experimental results were compared with the theory. The satisfactory agreement of the theoretical and experimental data indicate the admissibility beyond all doubt of the simplifying assumptions on which the calculations of the state of the gas behind a shock wave are based. From this it can be concluded that in the range of conditions studied thermal equilibrium is established in the space of a few microseconds after the passage of the shock wave through the gas. The length of the part of the plug which is homogeneous in temperature is approximately one-half as long as that predicted on the basis of the simplest gas-dynamical considerations.

For the study of the state of nitrogen and air behind the shock wave in the temperature range 1500-3000°K it is most expedient to carry out the measurements with the sodium D lines, and at temperatures higher than 3000° with a line of ionized barium, since in this case the effect of the cold boundary layer is eliminated. The method was tested up to 5000°K. Its use for measuring higher temperatures would require comparison sources of correspondingly higher temperature. It is probably necessary to go over to pulsed light sources; we intend to do this in the near future. As far as initial pressures are concerned the method was tested with air and nitrogen pressures down to ~1 mm Hg (the pressure in the plug was ~0.1 atm). In going to lower pressures, on the one hand the emission intensity of the lines used for the temperature measurements will drop, and this is undesirable; on the other hand, deviations from equilibrium between the emission and the kinematic degrees of freedom can be expected. We observed this effect in the case of argon even at comparatively high pressures. Investigations at low initial pressures are of interest not only from a practical point of view but also for elucidation of the question of the speed with which equilibrium is established. The generalized spectrum-line reversal method will undoubtedly find a wide application also in the study of vibrational and dissociational relaxation. Here also experiments at low initial pressures are of the greatest interest.

As is seen from the results of this investigation, the accuracy of the method is entirely adequate; under our conditions with temperatures up to 5000° errors of individual measurements, inclusive of systematic errors, did not exceed ±100°. With a standard tungsten lamp (in measuring temperatures of ~2500°) an accuracy of ±50° can be assured.

It should be noted that the method developed can be successfully applied in the study of the state of a gas not only behind a shock wave but also in a number of other cases. In particular it can probably be used with success for a study of the state of the explosion products in laboratory bombs in investigating gaseous reactions in explosions and combustion.

In conclusion the authors express their gratitude to A. V. Potapov and S. S. Semenov for discussion of the investigation and valuable advice, and also to E. T. Antropov and A. A. Sapronov for assistance in the preparation of the apparatus.

REFERENCES

1. N. N. Sobolev, A. V. Potapov, V. F. Kitaeva, F. S. Faizullov, V. N. Alyamovskii, E. T. Antropov, and I. L. Isaev. Izvest. Akad. Nauk SSSR, Ser. Fiz. **22**, 730 (1958).
2. N. N. Sobolev, A. V. Potapov, V. F. Kitaeva, F. S. Faizullov, V. N. Alyamovskii, E. T. Antropov, and I. L. Isaev. Opt. i Spektr. **6**, 284 (1959), Optics and Spectroscopy **6**, 185 (1959).
3. F. S. Faizullov, N. N. Sobolev, and E. M. Kudryavtsev. Doklady Akad. Nauk SSSR **127**, 541 (1959).
4. F. S. Faizullov, N. N. Sobolev, and E. M. Kudryavtsev. Opt. i Spektr. **8**, 585 (1960), Optics and Spectroscopy **8**, 311 (1960).
5. P. Prigsheim. "Fluorescence and Phosphorescence," Interscience, New York, 1949.
6. A. G. Gaydon. Energy transfer in hot gases. Natl. Bur. Standards, Circ. No. 523, 1 (1954).
7. V. Blackman. J. Fluid Mech. **1**, 61 (1956).
8. S. J. Lukasik and J. E. Young. J. Chem. Phys. **27**, 1149 (1957).
9. S. A. Losev and N. A. Generalov. Pribory i Tekh. Ekspt. No. 3, 108 (1959).
10. S. A. Losev and N. A. Generalov. Pribory i Tekh. Ekspt. No. 5, 150 (1959).

CALCULATION OF INTENSITIES AND POLARIZATIONS IN THE INFRARED SPECTRA OF POLYATOMIC MOLECULES. I

L. A. Gribov

Received 14 October 1959

A method is set forth for the calculation of intensities and polarizations in the infrared spectra of polyatomic molecules, based on the vector representation of the change of the dipole moment during the vibration of a given form. An example of the use of the method is presented.

In 1941 Vol'kenshtein[1, 2] proposed a semiclassical theory of intensities and polarizations in the vibrational spectra of polyatomic molecules, later developing it together with El'yashevich.[3-5] These authors[1-5] start from the assumption that the dipole moments of a whole series of polyatomic molecules can be considered in a sufficiently good approximation to be composed additively of the dipole moments of the separate chemical bonds in the molecule, and that this additivity is maintained for small deviations from the equilibrium position. With all of its inadequacies the Vol'kenshtein theory still appears to be the single real basis for practical applications. Using the method of Vol'kenshtein and El'yashevich, Sverdlov[6-8] has produced a series of calculations of intensities in the infrared spectra of polyatomic molecules in the zero and first approximations of the valence-optical scheme. The values of the electro-optical parameters of the chemical bonds obtained in this work correspond well with those calculated from the magnitudes of the static dipole moments of the molecules.

However, even taking account of simplification, the methods of calculation employed by many authors and introduced in a series of foreign papers[9-11] continue to remain somewhat cumbersome and less descriptive (particularly on transition to the first approximation). The basic shortcoming of these methods is the necessity to calculate the partial derivatives of the dipole moment of the molecule with respect to the normal coordinates in some Cartesian system of coordinates with the help of intermediate, so-called valence-optical coordinates.

The investigation in general form of the dependences of the intensities and polarizations on certain molecular parameters is also ah extremely difficult one.

In a development of the idea of Mayants[13] we[12] have proposed a simpler and more descriptive calculation scheme, which is not connected directly with the calculation of the derivatives of the dipole moment of the molecule. With the help of a quite simple formula, we were successful in expressing in an obvious form the absorption transition probability factor, using the parameters of the molecule and the form of the vibration; this provides the possibility of calculating the derivatives of the intensities and polarizations with respect to the electro-optical parameters and the parameters of the matrices T^{-1} and U. It is also true that the proposed calculation scheme is quite convenient for the use of electronic computers.

As is well known, in the semiclassical approximation the intensity of the absorption band, corresponding to a given normal vibration, is determined by the change of the dipole moment vector of the molecule. This quantity can be expressed through the derivative of the molecular dipole moment with respect to the given normal coordinate, or found directly from the form of the vibration, which is determined from the solution of the mechanical problem. We will consider that in the equilibrium state the property of additivity of the molecular dipole moment is strictly fulfilled, i.e., that the over-all dipole moment of the molecule μ equals $\sum_i \mu_i \mathbf{e}_i$, where μ_i is the dipole moment of the i bond and $\mathbf{e}_i$ is its direction vector in the equilibrium state. We assume further that in the normal vibrations the additivity is maintained. Then the change of the dipole moment vector in the m-th normal vibration is

$$\Delta\mu_m = \sum_i \Delta\mu_{im}\mathbf{e}_i + \sum_i \mu_i \Delta\mathbf{e}_{im}.$$

The dipole moment of the bond μ_i for all of the normal vibrations of the molecule has a single completely defined value. The magnitude of $\Delta\mu_{im}$, that is, the absolute change of the dipole moment of the i-th bond in the vibration, in the general case must depend on the form of the vibration. In the zero approximation of the valence-optical scheme we consider that the dipole moment of a bond is a function only of the length of the given bond, i.e.,

$$\Delta\mu_{im} = \left(\frac{\partial\mu_i}{\partial q_i}\right)_0 q_{im}.$$

In the first approximation we take into account the fact that the distribution of the electric charge, localized on the given bond, will change not only with changes of the bond length but also (probably to a lesser degree) with changes of the valence angles and lengths of the adjacent bonds. In other words

$$\Delta\mu_{im} = \sum_l \left(\frac{\partial\mu_i}{\partial q_l}\right)_0 q_{lm} + \sum_k \left(\frac{\partial\mu_i}{\partial\gamma_k}\right)_0 \gamma_{km}.$$

The symbol q designates the internal coordinates of change of the bond lengths, and the symbol γ the internal angular and nonplanar coordinates. In the transition to the first approximation of the valence-optical scheme the corresponding corrections are introduced only in the sum $\sum_l \Delta\mu_{1m}\mathbf{e}_1$, which is readily calculated since the equilibrium configuration is known.

For the determination of $\sum_l \mu_l \Delta\mathbf{e}_{lm}$ it is necessary to find $\Delta\mathbf{e}_{lm}$, that is, the bending of the bonds during the molecular vibrations. It was shown previously[12] that

$$\Delta\mathbf{e}_{im} = \sigma_i(\Delta\mathbf{r}_{im} - q_{im}\cdot\mathbf{e}_i). \tag{1}$$

Here and below, the quantities σ and ε, commonly used in the vibrational theory of polyatomic molecules, characterize the mass and the equilibrium distances ($\Delta\mathbf{r}_{im}$ is the displacement of the atoms forming the i-th bond from the equilibrium position). The displacements of the atoms from the equilibrium position during a vibration of given form can be found using the formula[9-11]

$$\|\mathbf{r}_i\|_m = \varepsilon\tilde{\mathbf{B}}T\left\|\begin{matrix} q \\ \gamma \end{matrix}\right\|_m, \tag{2}$$

where ε is a diagonal matrix of order N (the number of atoms in the molecule) with elements ε_i; **B** is the matrix relating the internal coordinates with the atomic displacements (the elements of this matrix are formed from the coordinates of the vectors $\mathbf{e}_i$, $\mathbf{f}_{ij}$, taken with the respective coefficients, and the vectors used to characterize the nonplanar vibrations); T is the inverse matrix of the kinematic coefficients.

In order to obtain the differences $\Delta\mathbf{r}_i$, required for the calculation of $\Delta\mathbf{e}_i$, it is necessary to subtract termwise the corresponding lines of the matrix ($\varepsilon\tilde{\mathbf{B}}$T) from each other. We will denote this operation by the symbol Δ. Then

$$\|\Delta\mathbf{e}_i\|_m = \sigma(\Delta\varepsilon\tilde{\mathbf{B}}T - \mathbf{E})\left\|\begin{matrix} q \\ \gamma \end{matrix}\right\|_m, \tag{3}$$

where σ is a diagonal matrix of the order N-1 with the elements σ_i, **E** is a diagonal matrix of the same order with the elements $\mathbf{e}_i$. The matrix ($\Delta\varepsilon\tilde{\mathbf{B}}$T − **E**) will be rectangular with the number of columns equal to the number of independent internal coordinates. The advantage of the use of formula (3) lies in the fact that for the bending of a bond $\Delta\mathbf{e}_i$ is found as a function of all internal coordinates; whereas usually the influence of all coordinates is taken into account only in the first approximation, and in the zeroth, for a simplification of the calculations of the partial derivatives, the bending of the bond is assumed to be independent of coordinates of the type q.

Replacing the sum by the product of a row matrix and a column matrix and normalizing (the normalizing factor equals

$$\left.\frac{\sqrt{h\nu_m}}{\sqrt{2(q,\gamma)_m U\left\|\begin{matrix} q \\ \gamma \end{matrix}\right\|_m}}\right),$$

we obtain for the zeroth approximation

$$\Delta\mu_m = \left[(\mathbf{e}_i)\left\|\begin{matrix} \left(\frac{\partial\mu_1}{\partial q_1}\right)_0 0\ldots 0 \\ \cdots\cdots\cdots \\ 0\ldots 0\left(\frac{\partial\mu_{N-1}}{\partial q_{N-1}}\right)_0 \end{matrix}\right\| + (\mu_i)\,\sigma\,(\Delta\varepsilon\tilde{\mathbf{B}}T - \mathbf{E})\right]$$

$$\cdot\left\|\begin{matrix} q \\ \gamma \end{matrix}\right\|_m \frac{\sqrt{h\nu_m}}{\sqrt{2(q,\gamma)_m U\cdot\left\|\begin{matrix} q \\ \gamma \end{matrix}\right\|_m}}, \tag{4}$$

where N is the number of atoms in the molecule.

For the first approximation $\sum_1^{N-1}\Delta\mu_{1m}\mathbf{e}_1$ takes the form

$$\sum_{i=1}^{N-1}\left\{\sum_{n=1}^{N-1}\left(\frac{\partial\mu_i}{\partial q_n}\right)_0 q_{nm} + \sum_{l=N}^{2N-5}\left(\frac{\partial\mu_i}{\partial\gamma_l}\right)_0 \gamma_{lm}\right\}\mathbf{e}_i.$$

In matrix form this expression can be written as

$$(\mathbf{e}_1,\ldots,\mathbf{e}_{N-1})\cdot$$

$$\left\|\begin{matrix} \left(\frac{\partial\mu_1}{\partial q_1}\right)_0\left(\frac{\partial\mu_1}{\partial q_2}\right)_0\cdots\left(\frac{\partial\mu_1}{\partial q_{N-1}}\right)_0\left(\frac{\partial\mu_1}{\partial\gamma_1}\right)_0\cdots\left(\frac{\partial\mu_1}{\partial\gamma_{2N-5}}\right)_0 \\ \cdots\cdots\cdots\cdots\cdots\cdots\cdots\cdots\cdots \\ \left(\frac{\partial\mu_{N-1}}{\partial q_1}\right)_0\left(\frac{\partial\mu_{N-1}}{\partial q_2}\right)_0\cdots\left(\frac{\partial\mu_{N-1}}{\partial q_{N-1}}\right)_0\left(\frac{\partial\mu_{N-1}}{\partial\gamma_1}\right)\cdots\left(\frac{\partial\mu_{N-1}}{\partial\gamma_{2N-5}}\right)_0 \end{matrix}\right\|\left\|\begin{matrix} q_1 \\ q_2 \\ \cdot \\ \cdot \\ \cdot \\ q_{N-1} \\ \gamma_1 \\ \cdot \\ \cdot \\ \cdot \\ \gamma_{2N-5} \end{matrix}\right\|_m$$

$$= (\mathbf{e}_1,\ldots,\mathbf{e}_{N-1})\left\|\left(\frac{\partial\mu}{\partial q}\right),\ \left(\frac{\partial\mu}{\partial\gamma}\right)\right\|\cdot\left\|\begin{matrix} q \\ \gamma \end{matrix}\right\|_m,$$

where $(\partial\mu/\partial q)$ is a square matrix of order N − 1 with elements $(\partial\mu_i/\partial q_1)_0$, and $(\partial\mu/\partial\gamma)$ is a rectangular matrix with elements $(\partial\mu_1/\partial\gamma_1)_0$.

Then the general expression for $\Delta\mu_m$ in the first approximation is written in the form

$$\Delta\mu_m = \left[(\mathbf{e}_1,\ldots,\mathbf{e}_{N-1})\left\|\left(\frac{\partial\mu}{\partial q}\right),\ \left(\frac{\partial\mu}{\partial\gamma}\right)\right\| + (\mu_1,\ldots,\mu_{N-1})\,\sigma\,(\Delta\varepsilon\tilde{\mathbf{B}}T - \mathbf{E})\right]$$

$$\times\left\|\begin{matrix} q \\ \gamma \end{matrix}\right\|_m \frac{\sqrt{h\nu_m}}{\sqrt{2(q,\gamma)_m U\left\|\begin{matrix} q \\ \gamma \end{matrix}\right\|_m}}. \tag{5}$$

In the zeroth approximation the nondiagonal elements of the matrix $(\partial\mu/\partial q)$ and the matrix $(\partial\mu/\partial\gamma)$ are assumed equal to zero, and formula (5) transforms into formula (4).

Both in the zeroth and first approximations the expression in square brackets remains unchanged for all normal vibrations of a given molecule. Only the form of the vibrations and the normalizing factor are changed. $\Delta\mu_m$ is expressed obviously through the mechanical and electro-optical parameters of the molecule in the coordinates $\mathbf{e}_i$ and $\mathbf{f}_{ij}$.

For practical calculations it is convenient from the very start to introduce, in the most profitable way, a threefold system of coordinates and to determine the projections of all unit vectors along the chosen axes. In this case the expression in square brackets is written in a scalar form and all of the computations can be carried out on machines. By using the rule of matrix differentiation, formulas (4) and (5) permit us to find the partial derivatives of $\Delta\mu_m$ (and this is significant for the intensities and polarizations) with respect to any parameters of the molecule. The derivatives of the frequencies and forms of vibrations necessary for this are calculated by Mayants' method,[14, 15] and the derivatives of the matrix T by the formula

$$\frac{\partial T}{\partial x} = -T\,\frac{\partial T^{-1}}{\partial x}\,T$$

(X is the differentiation parameter).

It should be noted that the calculation of the partial derivatives of $\Delta\mu_m$ with respect to the force constants, angles, and bond lengths of a molecule requires, in the general case, a knowledge of the derivatives of the electro-optical parameters with respect to these quantities. This question needs special clarification. However, if from certain considerations the dependence of the bond dipole moments and of their derivatives (with respect to the internal coordinates) on the force and geometrical constants of the molecule is known, or it is possible to neglect this dependence (this variation can be regarded as a sort of zero approximation), then the derivative of $\Delta\mu_m$ can be calculated easily if the derivatives of T, the forms of the vibrations, and of the normalizing factor are known. The general formula for the derivative of $\Delta\mu_m$ with respect to any parameter X will have the form

$$\frac{\partial(\Delta\mu_m)}{\partial x} = \Big[\Big\{\frac{\partial \mathbf{e}_i}{\partial x}\Big\}\Big\|\Big(\frac{\partial\mu}{\partial q}\Big),\ \Big(\frac{\partial\mu}{\partial\gamma}\Big)\Big\| + (\mathbf{e}_i)\Big\|\Big(\frac{\partial^2\mu}{\partial q\,\partial x}\Big),\ \Big(\frac{\partial^2\mu}{\partial\gamma\,\partial x}\Big)\Big\|$$

$$+ \Big\{\frac{\partial\mu_i}{\partial x}\Big\}\sigma(\Delta_i\tilde{\mathbf{B}}T - \mathbf{E}) + (\mu_i)\frac{\partial}{\partial x}\sigma(\Delta_i\tilde{\mathbf{B}}T - \mathbf{E})\Big]\cdot\left\|\begin{matrix} q \\ \gamma \end{matrix}\right\|_m$$

$$\cdot\frac{\sqrt{h\nu_m}}{\sqrt{(q,\gamma)_m U \left\|\begin{matrix} q \\ \gamma \end{matrix}\right\|_m}} + \Big[(\mathbf{e}_i)\Big\|\Big(\frac{\partial\mu}{\partial q}\Big),\ \Big(\frac{\partial\mu}{\partial\gamma}\Big)\Big\| + (\mu_i)\,\sigma(\Delta_i\tilde{\mathbf{B}}T - \mathbf{E})\Big]\frac{\partial}{\partial x}$$

$$\times\left(\left\|\begin{matrix} q \\ \gamma \end{matrix}\right\|_m \frac{\sqrt{h\nu_m}}{\sqrt{(q,\gamma)_m U \left\|\begin{matrix} q \\ \gamma \end{matrix}\right\|_m}}\right).$$

By far the most tedious part of the calculation of $\Delta\mu_m$ is the determination of the vectors $\Delta \mathbf{e}_{im}$. The problem is simplified substantially if the molecule has symmetry and a complete transition to symmetry coordinates is made. For symmetry coordinates formula (2) takes the form

$$\|\mathbf{r}_i\|_m = \varepsilon\tilde{\mathbf{B}}^s T^s \left\|\begin{matrix} q \\ \gamma \end{matrix}\right\|_m^s.$$

The normalizing factor equals

$$N_m^2 = \frac{h\nu_m}{(q,\gamma)_m^s\, U^s \left\|\begin{matrix} q \\ \gamma \end{matrix}\right\|_m^s}.$$

$\mathbf{B}^s$ is the matrix relating the symmetry coordinates to the atomic displacements in the vibrations. It is possible to obtain it by multiplication from the left by matrix **B** of the matrix of transition from the natural coordinates to the symmetry coordinates. The calculation of the atomic displacements in the vibrations is of paramount interest since it helps to depict more completely the picture of the normal vibration of the molecule. After calculation of $\|\mathbf{r}_i\|$ we find $\Delta\mathbf{e}_i$ for each group of equivalent bonds, for one representation of the vectors, and then, taking into consideration that the vector $\Delta\mathbf{e}_i$ is transformed by symmetry operations with the same rules as the internal coordinates, and that the electro-optical parameters of equivalent bonds are identical, we determine the entire sum

$$\sum_i \mu_i \Delta\mathbf{e}_{im}.$$

Since all atomic displacements leading to changes of the equilibrium configuration of the molecule, i.e., to vibrations, must be completely described by 3N − 6 independent internal coordinates, then in the presence of complementary relations among the internal coordinates they must be taken into account before formation of the matrix T^{-1}, and in the matrix **B** the lines corresponding to the dependent coordinates must be eliminated.

We will dwell briefly on the calculation of the intensities and polarizations of the characteristic vibrations. From formula (5) it is seen that the vibration can be characterized for polarization when it is characterized in its form, and for intensity only then when it is characterized both in frequency and in form simultaneously. However, this conclusion is of an approximate nature. Indeed, consider in the molecule a group of atoms, the vibrations of which are completely characterized both in frequency and form. If this group is carried over without change into another molecule, the corresponding frequencies and forms of the vibrations will be maintained. This phenomenon is connected with the specificity of chemical forces, which manifests itself in the smallness of the nondiagonal force constants, in particular those which correspond to nonbonded coordinates. We will denote the set of vectors $\mathbf{e}_i$ and f_{ij} of the separated group of atoms by the symbol $\mathbf{e}_\alpha$, and the set of the internal coordinates by the symbol q_α.

We will assume that in the transition to another molecule the mutual orientation of $\mathbf{e}_\alpha$ and the coordinates q_α are maintained and all coordinates, except q_α, in the characteristic normal vibrations equal zero. The transition to another molecule can be considered as an introduction of a new coordinate system, in which some of the coordinates ($\mathbf{e}_\alpha$ and q_α) are maintained, and all remaining coordinates are replaced.

Let's look at what happens to the vector $\Delta\mu_m$ if, as formerly, the form of the vibration is such that only $q_\alpha \neq 0$. We will focus our attention on the term

$$(\mathbf{e}_1, \ldots, \mathbf{e}_{N-1})\cdot\Big\|\Big(\frac{\partial\mu}{\partial q}\Big),\ \Big(\frac{\partial\mu}{\partial\gamma}\Big)\Big\|\cdot\left\|\begin{matrix} q \\ \gamma \end{matrix}\right\|.$$

On transition to a new system of coordinates, in the line $\{\mathbf{e}_1, \ldots, \mathbf{e}_{N-1}\}$ the vector $\mathbf{e}_\alpha$ will remain unchanged, and in the matrix

$$\Big\|\Big(\frac{\partial\mu}{\partial q}\Big),\ \Big(\frac{\partial\mu}{\partial\gamma}\Big)\Big\|$$

only those elements which are derivatives of the dipole moments of the bonds of the characteristic group of atoms with respect to the coordinates of the set q_α are unchanged.

On multiplication of

$$\Big\|\Big(\frac{\partial\mu}{\partial q}\Big),\ \Big(\frac{\partial\mu}{\partial\gamma}\Big)\Big\| \text{ by } \left\|\begin{matrix} q_\alpha \\ 0 \end{matrix}\right\|$$

in the matrix of the electro-optical parameters only the columns corresponding to the coordinates q_α will remain. It is easy to see that in the zero approximation the term under examination is unchanged on substitution of variables, i.e., the characteristic nature of the valence part of the change of $\Delta\mu_m$ will be present.

In the first approximation of the valence-optical scheme all of the $\mathbf{e}_i$ of the molecule enter the final expression, i.e., already it will not be invariant relative to the set of coordinates of the molecule, and accordingly, the characteristic nature of $\Delta\mu_m$ is violated. However, the smaller the magnitudes of the derivatives of the dipole moments of the bonds not participating in the characteristic group of atoms, with respect to the coordinates q_α, i.e., the weaker the "electrical" bond separating the group of atoms from the remaining portion of the molecule, the smaller will be the change of $\Delta\mu_m$ on transition to other molecules.

Let us examine the term

$$(\mu_1, \ldots, \mu_{\Lambda-1})\,\sigma\,(\Delta\varepsilon\tilde{B}T - E)\left\|\begin{matrix} q \\ \gamma \end{matrix}\right\|.$$

For this calculation it is necessary to find the matrix T, and it is not invariant[14] relative to the system of coordinates, i.e., on transition to another molecule the elements of T related to the coordinates q_α will change even if these coordinates themselves are preserved. However, if the matrix T^{-1} may be approximately represented in a quasi-diagonal form with a separation of the submatrix T_α^{-1}, then also in the matrix T the submatrix T_α can be separated.

In this case the calculation of $\Delta\mu_m$ is simplified since the order of T is decreased and only the columns corresponding to q_α can remain in the matrix $\tilde{B}$. But even then it is not possible to state that all Δe_i's of the bonds not participating in the characteristic group will equal zero. For this condition, it is required in addition that after the elimination in the matrix $\tilde{B}$ of the undesired columns all lines, except those which define the displacements of the atoms of the characteristic group, must be zero.

It should be noted that for both terms the preservation of the normalizing factor, i.e., the quasi-diagonal nature of the matrix U, is necessary.

From all that has been said it is clear that for the appearance of characteristic intensities or polarizations a whole series of conditions must be fulfilled, not always very different from those which can exist in real molecules. Such characteristic behavior is generally encountered far less frequently than the characteristic behavior in frequency and form. Of practical interest is the problem of the calculation of the electro-optical parameters of a molecule from the observed magnitudes of the intensities of the normal vibrations. In the general case, the number of these parameters is greater than the number of vibrational frequencies. However, the presence of symmetry in the molecule and also the fact that the value of the derivatives of the dipole moments of the bonds with respect to the nonbonded coordinates is known to be small, make the problem in many cases completely solvable even for a single molecule. Considerable assistance can also be provided by the investigation of isotopically substituted molecules.

Let us now study an example, clarifying the use of the method and relating to the symmetrical triatomic nonlinear molecule XY_2. The Figure shows the system of unit vectors and the numbering of the atoms of the symmetrical nonlinear triatomic molecule XY_2. The vibrations are described by the coordinates q_1, q_2, and γ. We construct the matrix B by which we express the internal coordinates in terms of the atomic displacements

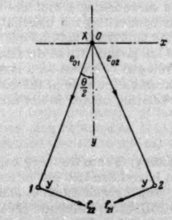

$$\left\|\begin{matrix} q_1 \\ q_2 \\ \gamma \end{matrix}\right\| = \left\|\begin{matrix} e_{01} & 0 & -e_{01} \\ 0 & e_{02} & -e_{02} \\ -\sigma_1 f_{12} & -\sigma_2 f_{21} & F_{12} \end{matrix}\right\| \cdot \left\|\begin{matrix} r_1 \\ r_2 \\ r_0 \end{matrix}\right\| = B\,\|r\|.$$

As a result of formula (5)

$$\Delta\mu_m = \left[(e_1, e_2) \left\|\begin{matrix} \left(\frac{\partial\mu_1}{\partial q_1}\right)_0 & \left(\frac{\partial\mu_1}{\partial q_2}\right)_0 & \left(\frac{\partial\mu_1}{\partial\gamma}\right)_0 \\ \left(\frac{\partial\mu_2}{\partial q_1}\right)_0 & \left(\frac{\partial\mu_2}{\partial q_2}\right)_0 & \left(\frac{\partial\mu_2}{\partial\gamma}\right)_0 \end{matrix}\right\| + (\mu_1, \mu_2)\left\|\begin{matrix} \sigma_1 & 0 \\ 0 & \sigma_2 \end{matrix}\right\| \right.$$

$$\left. \times \left(\left\|\begin{matrix} \varepsilon_1 & 0 & -\varepsilon_0 \\ 0 & \varepsilon_2 & -\varepsilon_0 \end{matrix}\right\| \left\|\begin{matrix} e_{01} & 0 & -\sigma_1 f_{12} \\ 0 & e_{02} & -\sigma_2 f_{21} \\ -e_{01} & -e_{02} & F_{12} \end{matrix}\right\| T - \left\|\begin{matrix} e_{01} & 0 \\ 0 & e_{02} \end{matrix}\right\| \right) \right] \cdot \left\|\begin{matrix} q_1 \\ q_2 \\ \gamma \end{matrix}\right\|_m ,$$

where m = 1, 2, 3.

Here and below we consider the columns of the forms to be normalized. Since the molecule is symmetric, then

$$\mu_1 = \mu_2 = \mu,\ \left(\frac{\partial\mu_1}{\partial q_1}\right)_0 = \left(\frac{\partial\mu_2}{\partial q_2}\right)_0 = \left(\frac{\partial\mu}{\partial q}\right)_0,\ \left(\frac{\partial\mu_1}{\partial q_2}\right)_0 = \left(\frac{\partial\mu_2}{\partial q_1}\right)_0 \ \text{и}\ \left(\frac{\partial\mu_1}{\partial\gamma}\right)_0 = \left(\frac{\partial\mu_2}{\partial\gamma}\right)_0.$$

In addition $\varepsilon_1 = \varepsilon_2 = \varepsilon$, $\sigma_1 = \sigma_2 = \sigma$. For a simplification of the calculations we transform to symmetry coordinates

$$\left\|\begin{matrix} q^A \\ \gamma^A \\ q^B \end{matrix}\right\| = \left\|\begin{matrix} \frac{1}{\sqrt{2}} & \frac{1}{\sqrt{2}} & 0 \\ 0 & 0 & 1 \\ \frac{1}{\sqrt{2}} & -\frac{1}{\sqrt{2}} & 0 \end{matrix}\right\|$$

$$\cdot\, B\,\|r\| = \left\|\begin{matrix} \frac{1}{\sqrt{2}} e_{01} & \frac{1}{\sqrt{2}} e_{02} & -\frac{1}{\sqrt{2}}(e_{01} + e_{02}) \\ -\sigma f_{12} & -\sigma f_{21} & F_{12} \\ \frac{1}{\sqrt{2}} e_{01} & -\frac{1}{\sqrt{2}} e_{02} & -\frac{1}{\sqrt{2}}(e_{01} - e_{02}) \end{matrix}\right\| \cdot \|r\|.$$

We will find $\Delta\mu$ for the completely symmetric vibrations. From consideration of the symmetry of the vibration it is clear that $\Pi P_x \Delta\mu^A = 0$. Accordingly, it is necessary to calculate only $\Pi P_y \Delta\mu^A$. We have

$$\Delta\mu_y^A = \left\{\cos\frac{\theta}{2},\ \cos\frac{\theta}{2}\right\} \left\|\begin{matrix} \left(\frac{\partial\mu}{\partial q}\right)_0 & \left(\frac{\partial\mu_1}{\partial q_2}\right)_0 & \left(\frac{\partial\mu}{\partial\gamma}\right)_0 \\ \left(\frac{\partial\mu_2}{\partial q_1}\right)_0 & \left(\frac{\partial\mu}{\partial q}\right)_0 & \left(\frac{\partial\mu}{\partial\gamma}\right)_0 \end{matrix}\right\| \cdot \left\|\begin{matrix} \frac{1}{\sqrt{2}} q^A \\ \frac{1}{\sqrt{2}} q^A \\ \gamma^A \end{matrix}\right\|$$

$$+ (\mu, \mu)\left\|\begin{matrix} \sigma & 0 \\ 0 & \sigma \end{matrix}\right\| \left(\left\|\begin{matrix} \varepsilon & 0 & -\varepsilon_0 \\ 0 & \varepsilon & -\varepsilon_0 \end{matrix}\right\| \cdot \left\|\begin{matrix} \frac{1}{\sqrt{2}}\cos\frac{\theta}{2} & -\sigma\sin\frac{\theta}{2} \\ \frac{1}{\sqrt{2}}\cos\frac{\theta}{2} & -\sigma\sin\frac{\theta}{2} \\ -\frac{2}{\sqrt{2}}\cos\frac{\theta}{2} & 2\sigma\sin\frac{\theta}{2} \end{matrix}\right\| T^A \left\|\begin{matrix} q^A \\ \gamma^A \end{matrix}\right\|_n \right.$$

$$\left. - \left\|\begin{matrix} \cos\frac{\theta}{2} & 0 \\ 0 & \cos\frac{\theta}{2} \end{matrix}\right\| \cdot \left\|\begin{matrix} \frac{1}{\sqrt{2}} q^A \\ \frac{1}{\sqrt{2}} q^A \end{matrix}\right\| \right),$$

where n = 1, 2.

The matrix is

$$T^A = \left\|\begin{matrix} \frac{2\sigma^2[\varepsilon + \varepsilon_0(1 - \cos\theta)]}{2\sigma^2(\varepsilon^2 + 2\varepsilon_0\varepsilon)} & \frac{\sqrt{2}\,\varepsilon_0\sigma\sin\theta}{2\sigma^2(\varepsilon^2 + 2\varepsilon\varepsilon_0)} \\ \frac{\sqrt{2}\,\varepsilon_0\sigma\sin\theta}{2\sigma^2(\varepsilon^2 + 2\varepsilon_0\varepsilon)} & \frac{[\varepsilon + \varepsilon_0(1 + \cos\theta)]}{2\sigma^2(\varepsilon^2 + 2\varepsilon\varepsilon_0)} \end{matrix}\right\|.$$

Carrying out a cross-multiplication we obtain

$$\Delta\mu_y^A=\left[\sqrt{2}\left(\frac{\partial\mu}{\partial q}\right)_0+\sqrt{2}\left(\frac{\partial\mu_1}{\partial q_2}\right)_0\right]\cos\frac{\theta}{2}\,q^A$$

$$+\left[2\left(\frac{\partial\mu}{\partial\gamma}\right)_0\cos\frac{\theta}{2}-\mu\sin\frac{\theta}{2}\right]\gamma^A.$$

Now it remains only to establish the values of q^A and γ^A, taken from the solution of the mechanical problem, in order to determine $\Delta\mu^A$ corresponding to both completely symmetric vibrations of the molecule.

The molecule being examined will have only one antisymmetric vibration. It is easy to see that only $\Pi P_x \Delta\mu^B$ will be different from zero. Applying the symmetry coordinates we find

$$\Delta\mu_x^B=\left\{-\sin\frac{\theta}{2},\ \sin\frac{\theta}{2}\right\}\left\|\begin{matrix}\left(\frac{\partial\mu}{\partial q}\right)_0 & \left(\frac{\partial\mu_1}{\partial q_2}\right)_0 & \left(\frac{\partial\mu}{\partial\gamma}\right)_0\\ \left(\frac{\partial\mu_2}{\partial q_1}\right)_0 & \left(\frac{\partial\mu}{\partial q}\right)_0 & \left(\frac{\partial\mu}{\partial\gamma}\right)_0\end{matrix}\right\|\cdot\left\|\begin{matrix}\frac{1}{\sqrt{2}}q^B\\ -\frac{1}{\sqrt{2}}q^B\\ 0\end{matrix}\right\|$$

$$+(\mu,\mu)\left\|\begin{matrix}\sigma & 0\\ 0 & \sigma\end{matrix}\right\|\left(\left\|\begin{matrix}\varepsilon & 0 & -\varepsilon_0\\ 0 & \varepsilon & -\varepsilon_0\end{matrix}\right\|\cdot\left\|\begin{matrix}-\frac{1}{\sqrt{2}}\sin\frac{\theta}{2}\\ -\frac{1}{\sqrt{2}}\sin\frac{\theta}{2}\\ \frac{1}{\sqrt{2}}2\sin\frac{\theta}{2}\end{matrix}\right\|T^Bq^B\right.$$

$$\left.-\left\|\begin{matrix}-\sin\frac{\theta}{2} & 0\\ 0 & \sin\frac{\theta}{2}\end{matrix}\right\|\cdot\left\|\begin{matrix}\frac{1}{\sqrt{2}}q^B\\ -\frac{1}{\sqrt{2}}q^B\end{matrix}\right\|\right).$$

where

$$T^B=\frac{1}{[\varepsilon+\varepsilon_0(1-\cos\theta)]}.$$

From this

$$\Delta\mu_x^B=\sqrt{2}\left[\left(\frac{\partial\mu}{\partial q}\right)_0-\left(\frac{\partial\mu_1}{\partial q_2}\right)_0+\mu\,\frac{2\varepsilon_0\cos^2\frac{\theta}{2}}{\varepsilon+2\varepsilon_0\sin^2\frac{\theta}{2}}\right]\sin\frac{\theta}{2}\,q^B.$$

It is interesting to note that, despite the fact that in the antisymmetric vibrations the angle between the bonds does not change and the corresponding coordinate γ equals zero, in the final expression for $\Delta\mu^B$ a term containing the bond dipole moment is present. This is a result of the fact, of which one is easily convinced, that the molecule rocks slightly in the XY plane during the vibration, without changing the angle between the bonds.

REFERENCES

1. M. V. Vol'kenshtein. Doklady Akad. Nauk SSSR 30, 784 (1941).
2. M. V. Vol'kenshtein. Zhur. Eksptl. i Teoret. Fiz. 11, 642 (1941).
3. M. A. El'yashevich and M. V. Vol'kenshtein. J. Phys. SSSR 9, 101 (1944).
4. M. V. Vol'kenshtein and M. A. El'yashevich. Zhur. Eksptl. i Teoret. Fiz. 15, 124 (1945).
5. M. V. Vol'kenshtein, M. A. El'yashevich, and B. I. Stepanov. "Kokebaniya Molekul" (Molecular Vibrations), Vol. 2, Moscow, Leningrad, 1949.
6. L. M. Sverdlov. Opt. i Spektr. 4, 697 (1958).
7. L. M. Sverdlov. Opt. i Spektr. 6, 729 (1959), Optics and Spectroscopy 6, 477 (1959).
8. L. M. Sverdlov. Opt. i Spektr. 7, 152 (1959), Optics and Spectroscopy 7, 97 (1959).
9. B. L. Crawford and W. H. Fletcher. J. Chem. Phys. 19, 141 (1951).
10. D. A. Long. Proc. Roy. Soc. A217, 203 (1953).
11. S. M. Ferigle and A. Weber. Can. J. Phys. 32, 799 (1954).
12. L. A. Gribov. Doklady Akad. Nauk SSSR 127, 788 (1959).
13. L. S. Mayants. Zhur. Eksptl. i Teoret. Fiz. 19, 627 (1949).
14. L. S. Mayants. Trudy Fiz. Inst. Akad. Nauk SSSR, 5, 63 (1951).
15. L. S. Mayants. Opt. i Spektr. 5, 378 (1958).

ON THE ROLE OF UNIVERSAL AND SPECIFIC INTERMOLECULAR INTERACTIONS IN THE INFLUENCE OF THE SOLVENT ON THE ELECTRONIC SPECTRA OF MOLECULES

B. S. Neporent and N. G. Bakhshiev

Received 17 October 1959

A subdivision of the intermolecular interactions in solutions into two fundamental types has been carried out: universal, associated with the collective influence on a dissolved molecule of the entire set of solvent molecules surrounding it, and specific, produced by the individual interactions of the molecule being studied with one or a few of the particles surrounding it and associated with the peculiarities of their structure. On the basis of ideas concerning the internal field in solution, a method is proposed for calculating and separating the universal actions out of the over-all effects observed experimentally, a method which opens the possibility of detailed study of the specific interactions. The applicability of the methods developed is shown on a large and varied body of experimental data. A criticism is given of works in which the role of the collective influence of the molecules of the medium on the absorbing or radiating center is not taken into account.

A large number of works, beginning in the middle of the last century, have been devoted to the question of the influence of the solvent on spectra. Nevertheless, up to the present time, the problem cannot be regarded as solved, and the results of the numerous investigations are in part contradictory. From the very beginning, two fundamental courses have been laid out in the field which we are considering. The first of these is associated with consideration of the collective influence of the particles of the medium on the spectra of the dissolved molecule, and the second with its description by introducing the macroscopic characteristics of the solvent (dielectric constant, refractive index, dispersion, etc.). In works referring to the second course, the object is to set up connections between the action of the solvent on the spectra of the dissolved substance and the microscopic characteristics (physical, physico-chemical, and chemical) of the molecules of the solvent and of the dissolved substance. Here the action of the medium is considered as the consequence of the interaction of the dissolved molecule with one or a few of the particles surrounding it.

We propose that a sufficiently complete description of real systems can be attained only through calculation of both the collective (macroscopic description) and the individual (microscopic description) action of the molecules of the surrounding medium on the spectrum of the dissolved molecule. In accordance with established terminology, we shall call the first of the above-mentioned actions universal, the second specific. This terminology makes sense, since the types of action considered are evidently not of the same rank: systems can be imagined in which specific interactions are absent, while the collective action must take place in all cases. In real systems, specific interactions of one degree or another apparently always exist. A molecule of the dissolved substance which is linked by specific interactions to a solvent molecule or a third particle should be considered as a new absorbing or emitting center, subject in turn to the universal action of the set of surrounding particles, which is described by the internal field in the solution. A separation of the over-all effects may be achieved by means of a comparison of the properties of solution spectra with the predictions of the theory which describes the universal action of the solvent. Then, from the discrepancy between experiment and theory, one may judge the existence, strength, and nature of the specific interactions. We note that in works concerned with the study of specific interactions, no separation of effects of a universal character has been carried out up to now. In certain cases this circumstance may play a small role on account of the great predominance of a specific interaction (strong hydrogen bonds, acid-base interactions, etc.); in other cases, however, misconceptions are possible, associated with the interpretation of predominantly universal interactions as specific.

Theoretical consideration of the influence of the collective actions is associated with the necessity of summing the action of the surrounding particles on the molecule of the dissolved substance, and is inevitably coupled, at the present time at least, with the introduction of models representing the system studied. Agreement of theory with a sufficiently broad and varied body of experimental data is evidently a reliable criterion of the applicability of one model or another.

Voigt[1] and Kravets[2] in their works have already used two models in which the molecule was considered as a dipole placed in a dielectric medium, either "opposing" it or only surrounding it. In the second case, the internal field in the solution was evaluated according to Lorentz's theory. In recent years, certain progress has been achieved in the question under consideration, in connection with the transfer into molecular spectroscopy of model-representations of the structure of liquids and solutions derived from the theory of the polarization of liquid dielectrics (see references 3-11). In all these works it is assumed that some optical and electrical properties of the molecule remain unchanged when it goes over into the dissolved state.

With respect to intensities, the solvent appears as a continuous dielectric medium which changes the magnitude of the light field acting on the molecule, and this determines the change in the measured absorption integral and duration of the excited state, the values of the transition probabilities being unchanged. An investigation of the intensities of vapor and solution spectra carried out by us[8] has shown that, with respect to a series of aromatic compounds, the theory based on the Onsager model agrees satisfactorily with experiment. Figure 1, taken from reference 8, may characterize the results obtained. The separate deviations of the experimental results from the predictions of theory are to be considered as the result of specific actions on the dissolved molecules, leading to some change of the transition probabilities within them.

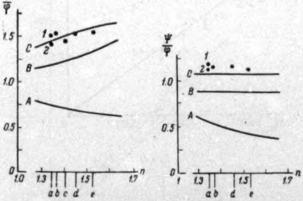

Fig. 1. Experimental (points) and theoretical (lines) values of the corrections which take into account the universal influence of the solvent on the values of the absorption integrals ($1/\varphi$) and the duration of the excited state (ψ/φ) as a function of the refractive index of the medium n for 3-acetamidophthalimide (according to reference 8). Method of calculating the internal field in the solution: curve A—Maxwell's theory; curve B—Lorentz's theory; curve C—Onsager's theory. Code for the solvents, designated by letters on the horizontal axis: a(1)—methyl alcohol; a(2)—water; b—diethyl ether; c—n-heptane; d—dioxane; e—benzene.

Let us turn to consideration of the influence of the solvent on the position of the spectra of solutions. In the above-mentioned model representations, the molecule is depicted, as before, in the form of a dipole (representing the sum of the permanent moment of the molecule and the moment induced by the light wave) which undergoes the influence of the internal field of the solvent. The difference between the values of this dipole in the ground and the excited states of the molecule determines the different change in the position of the levels and, consequently, the spectral shift.

We recall the expression for the spectral shift obtained in references 10 and 11 on the basis of Onsager's theory:

$$\Delta\nu = \frac{1}{r^3}\left[C_1 \frac{2\varepsilon - 2}{2\varepsilon + 1} + (C_2 + fC_3)\frac{2n^2 - 2}{2n^2 + 1} \right]. \qquad (1)$$

Here $\Delta\nu$ is the shift in the frequency of the electronic transition, r is the Onsager cavity radius, which is practically equal to the radius of the molecule, ε and n are respectively the dielectric constant and the refractive index of the solvent, and f is the oscillator strength of the particular transition in the molecule under study. The constants C_1 and C_2 are functions of the permanent dipole moments of the molecule in the lower and the upper electronic states, C_3 depends on the frequency of the electronic transition. Regardless of the extremely schematic character of the model, this expression describes the spectral shift for all possible combinations from the case of dipolar molecules in polar solvents to nondipolar molecules in nonpolar media. In the latter case, although $C_1 = C_2 = 0$, the very existence of spectra ($f \neq 0$) anticipates the necessity of a shift in them.

The applicability of the model representations here considered is illustrated by the data of Fig. 2, taken from reference 11, where the shifts of solution spectra relative to vapor spectra for a nondipolar molecule—anthracene—and for dipolar ones—two substituted phthalimides—are presented in a form corresponding to expression (1), showing their dependence on the corresponding function of ε and n. Since his purpose was to check the theory under consideration, the author[10, 11] excluded from consideration those solvents in which strong specific interactions were a priori to be expected. From Fig. 2 it is easy to see that the linear dependence (1) is entirely satisfactorily fulfilled. The constants C_1 and $(C_2 + fC_3)$ are determined from the characteristics of the straight lines drawn through the set of experimental points. The assumption is made here that specific interactions may equally probably bring about spectral shifts on both sides of the shifts described by the straight lines of Fig. 2. This viewpoint is confirmed by the data of Fig. 5, which includes information on solvents known to show strong specific actions.

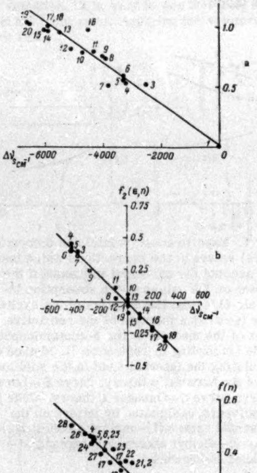

Fig. 2. Dependence of the frequency shift $\Delta\nu_S$ in the spectra of 4-aminophthalimide (a), 3,6-diacetamidophthalimide (b), and anthracene[19-21] (c) on the dielectric constant ε and the refractive index n of the solvent (according to reference 11). $f_1(\varepsilon, n) = (2\varepsilon - 2)/(2\varepsilon + 1) + p_1[(2n^2 - 2)/(2n^2 + 1)]$; $f_2(\varepsilon, n) = -(2\varepsilon - 2)/(2\varepsilon + 1) + p_2[(2n^2 - 2)/(2n^2 + 1)]$; $f(n) = (2n^2 - 2)/(2n^2 + 1)$ (for the values of p_1 and p_2, see reference 11). Solvent code: 1—vapor, 2—n-heptane, 3—CCl_4 4—benzene, 5—toluene, 6—xylene, 7—dioxane, 8—diethyl ether, 9—anisole, 10—butyl acetate, 11—chloroform, 12—ethyl acetate, 13—pyridine, 14—isoamyl alcohol, 15—isobutyl alcohol, 16—acetone, 17—ethyl alcohol, 18—methyl alcohol, 19—glycerin, 20—water, 21—n-pentane, 22—n-hexane, 23—cyclohexane (110°C), 24—CCl_4 (110°C), 25—mesitylene, 26—chlorobenzene, 27—amyl alcohol, 28—naphthalene (90°C).

We note that, for the nondipolar anthracene molecules, there appears a dependence on the refractive index only. For the dipolar 3,6-diacetamidophthalimide molecules, there also appears a dependence on the dielectric constant of the medium, the different directions of shift in the spectra of solutions in different solvents being determined by the ratios of the magnitudes of the permanent and induced dipole moments in the normal and excited states of the molecule.

The considerable quantity of data already obtained for a wide variety of compounds enables us to suppose that the model representations here considered may serve as a basis for systematic analysis of the results of numerous experiments.

Before mentioning examples of the simultaneous influence of universal and specific interactions, we must pause to consider some works whose authors, trying to give a general treatment of the action of solvents, hold points of view which differ in principle from that set forth above. Under this heading, in particular, come the works of Zelinskii and his collaborators[12-14] and of Kosower,[15, 16] who showed that, for large groups of substances which they investigated, the different solvents may be arranged in a single sequence according to their influence on the position of the spectra, and furthermore, that the relative strength of the action of the solvent maintains approximately the same value for certain substances. To describe the varying action, these authors introduce an empirical universal "solvent scale"[12, 14] or an empirical quantity "Z,"[15] which represent the position of the spectra for standard substances.

The results of the works of Zelinskii and Kosower may serve as empirical rules for predicting the position of spectra, but the limits of applicability of these rules must be determined experimentally. Besides, the approach of these authors to a solution of the problem cannot be fruitful for clarifying the nature of the intermolecular interactions under consideration and, furthermore, it would be difficult to recognize this approach as systematic. Actually, on the one hand, it is stated in references 12, 14, and 15 that the shift in the spectra of solutions is associated exclusively with the microscopic interactions and cannot be associated with the macroscopic parameters of the system, while on the other hand the same works contain statements of the applicability of a universal scale or quantity "Z" to the spectra of solutions of compounds of various classes in solvents of varied chemical nature. Thus the works under consideration contain an internal contradiction, since the universal action of a solvent may be governed only by its general physical characteristics.

The considerations presented here may easily be confirmed by consideration of the experimental data obtained in studies 12-14 and 15, 16.

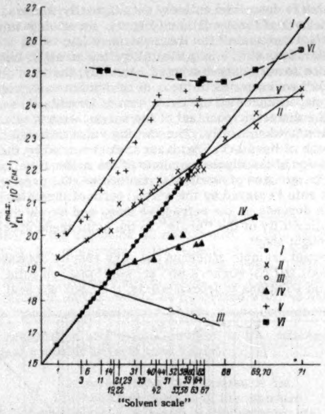

Fig. 3. Dependence of the position of the maxima of the fluorescence spectra ($\nu_{\Pi.}^{max}$) of phthalimide derivatives and anthracene on Zelinskii's empirical "solvent scale" (according to references 12-14). I—4-amino-N-methylphthalimide (standard substance); II—3-amino-N-methylphthalimide; III—3-hydroxy-N-methylphthalimide; IV—3-acetamido-6-amino-N-methylphthalimide; V—4-acetamido-N-methylphthalimide; VI—anthracene (according to references 18-21). Solvent code: 1—water, 2—chloroacetic acid, 3—glycerin, 4—glycol, 5—phenol, 6—acetic acid, 7—benzyl alcohol, 8—formamide, 9—tertiary butyl alcohol, 10—butyric acid, 11—methyl alcohol, 12—isobutyl alcohol, 13—ethylene glycol monomethyl ether, 14—ethyl alcohol, 15—nonylic acid, 16—stearic acid, 17—isopropyl alcohol, 18—glycerin dichlorohydrin, 19—butyl alcohol, 20—cyclohexanol, 21—secondary octyl alcohol, 22—menthol, 23—benzaldehyde, 24—dimethyl oxalate, 25—diethyl oxalate, 26—isobutyraldehyde, 27—thymol, 28—acetic anhydride, 29—methyl formate, 30—propyl formate, 31—ethyl acetate, 32—ethyl orthoformate, 30—propyl formate, 31—ethyl acetate, 32—ethyl orthoformate, 33—α-bromonaphthalene, 34—dibutyl sebacate, 35—quinoline, 36—cyclohexanone, 37—methyl butyl ketone, 38—pinacolone, 39—benzyl acetate, 40—pyridine, 41—ethyl malonate, 42—acetone, 43—nitromethane, 44—propyl acetate, 45—acetal, 46—isoamyl acetate, 47—diethyl maleate, 48—tributyl phosphate, 49—butyl acetate, 50—crystalline state, 51—triethylamine, 52—chloroform, 53—dimethyl phthalate, 54—dibutyl phthalate, 55—α-chloronaphthalene, 56—propyl chloride, 57—methyl benzoate, 58—dioxane, 59—anisole, 60—diethyl ether, 61—diisopropyl ether, 62—bromobenzene, 63—diisoamyl ether, 64—propyl bromide, 65—chlorobenzene, 66—benzene, 67—toluene, 68—CCl_4, 69—n-hexane, 70—n-octane, 71—vapor.

In Fig. 3 are presented the dependences of the position of the maxima of the fluorescence spectra of substituted phthalimides on Zelinskii's "solvent scale,"[12-14] 4-amino-N-methylphthalimide being taken as standard substance. In Fig. 4 is presented the analogous dependence on the quantity "Z," constructed according to Kosower's data[15, 16] for the complexes of iodine with aromatic compounds (1-ethyl-4-carbomethoxy-pyridine-iodine was taken as standard substance). Comparing the linear dependence of the position of the spectra of 4-aminophthalimide on the "solvent scale" in Fig. 3 and on function (1) in Fig. 2a,* one can easily conclude that the "solvent scale" is linearly related to function (1). Actually, juxtaposition of the data obtained in references 10, 11, and 12-14 does lead, as shown in Fig. 5, to a linear dependence of the "solvent scale" on the function determined by expression (1). An analogous result obtained from Kosower's data for his standard substance is represented in Fig. 6. The results presented testify that the "solvent scale" and the quantity "Z" reflect the dependence of the spectra on universal interactions, which may be described with the help of the macroscopic parameters.

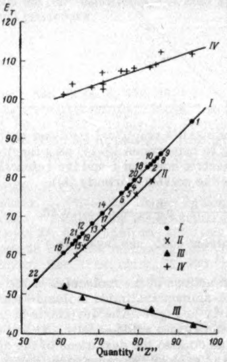

Fig. 4. Dependence of the position of the maxima of the absorption spectra ($E_T \sim \nu_{abs.}^{max}$) of various organic compounds on Kosower's empirical quantity "Z" (according to references 15, 16). I—1-ethyl-carbomethoxypyridine-iodine (standard substance); II—1-ethyl-4-cyanopyridine-iodine; III—phenol blue; IV—pyridine 1-oxide. Solvent code: 1—water, 2—methyl alcohol, 3—ethyl alcohol, 4—propyl alcohol, 5—butyl alcohol, 6—isopropyl alcohol, 7—tertiary butyl alcohol, 8—glycol, 9—tetrafluoropropanol, 10—octafluoropropanol, 11—chloroform, 12—acetone, 13—dimethylformamide, 14—acetonitrile, 15—pyridine, 16—isooctane (extrapolated), 17—dimethyl sulfoxide, 18—formamide, 19—methyl cyclopropyl ketone, 20—acetic acid, 21—methylene chloride, 22—vapor.

---

*From the data of references 12-14, it is easy to construct a graph of the type of Fig. 2 for the maxima of the fluorescence spectra. This graph is practically analogous with Fig. 2.

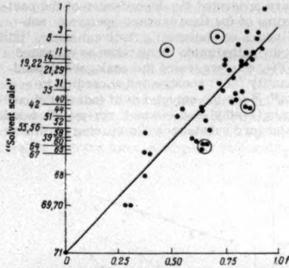

Fig. 5. Zelinskii's empirical "solvent scale" (according to references 12-14) as a function of the dielectric constant ε and the refractive index n of the solvent (formula (1)).

$$f(\varepsilon, n) = \frac{2\varepsilon - 2}{2\varepsilon + 1} + p\frac{2n^2 - 2}{2n^2 + 1};\ p = -0{,}20.$$

For the solvent code, see legend to Fig. 4.

The specific actions of the molecules of the separate solvents on the 4-aminophthalimide molecule manifest themselves clearly in Fig. 5. The deviations of the spectra of solutions in organic acids—acetic and butyric—leap to the eye, as do also the deviations of the opposite sign in solutions in acetone, nitromethane, and in some halogenated derivatives of aromatic hydrocarbons. We note that the presence of a hydrogen bond with amines has been shown for acetone solutions,[11] and the characteristic influence of acids or halogenated derivatives has been the object of a large number of studies. These specific interactions are masked in Fig. 3 by virtue of the very principle on which the universal scale is constructed. Furthermore, the scatter of the points for other substances (2-6, Fig. 4) is still not a measure of specific interactions but expresses complex regularities which yield with difficulty to analysis.

The fruitfulness of the procedure proposed in references 8-11 for describing the universal interactions may be illustrated by a series of examples.

Let us consider the simplest case—the action of solvents on the spectra of the nondipolar anthracene molecule, which is described entirely satisfactorily within the framework of theory (1) (see Fig. 1). An attempt to use the "solvent scale" for this substance (curve VI, Fig. 3) shows its entire inapplicability: the straight-line dependence is seriously disrupted. Actually, the "solvent scale" corresponds to the case of dipolar molecules, in which dependences on the first term of formula (1)—i.e., on the dielectric constant of the solvent—manifest themselves predominantly. The varying value and sign of the slope of lines I-V, Fig. 3 are then governed by the relationships of the dipole moments of the molecules studied. In the case of nondipolar molecules, the predominant role is played by the second term of formula (1), which depends on the refractive index and by which the inapplicability of the "scale" to the anthracene spectra is brought about.

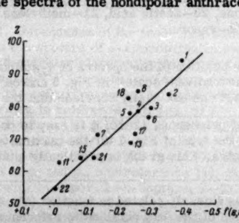

Fig. 6. Kosower's empirical quantity "Z" (according to references 15-16) as a function of the dielectric constant ε and refractive index n of the solvent (formula (1)).

$$f(\varepsilon, n) = -\frac{2\varepsilon - 2}{2\varepsilon + 1} + p\frac{2n^2 - 2}{2n^2 + 1};\ p = +\,1.75.$$

For the solvent code, see legend to Fig. 4.

A second example concerns the very results obtained by Zelinskii and co-workers who showed[17] that, on going from liquid solutions to frozen solids, the "solvent scale"

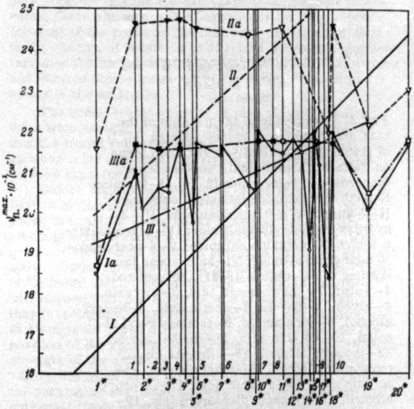

Fig. 7. Dependence of the position of the maxima of the fluorescence spectra ($\nu_{\text{fl.}}^{\text{max}}$) of phthalimide derivatives in liquid (I), (II), (III) and frozen solid (Ia, IIa, IIIa) solutions on Zelinskii's empirical "solvent scale" according to reference 17). I—4-amino-N-methylphthalimide (standard substance); II—4-acetamido-N-methylphthalimide; III—3-amino-N-methylphthalimide. Open symbols—"snowy;" solid symbols—glassy media. Solvent code, glassy media: 1—glycerine, 2—tertiary butyl alcohol, 3—methyl alcohol containing 10% water, 4—ethyl alcohol, 5—acetic anhydride, 6—ethyl orthoformate, 7—propyl acetate, 8—triethylamine, 9—diisoamyl ether, 10—toluene. "Snowy" media: 1*—water, 2*—acetic acid, 3*—methyl alcohol, 4*—benzaldehyde, 5*—menthol, 6*—thymol, 7*—ethyl acetate, 8*—pyridine, 9*—acetone, 10*—nitromethane, 11*—chloroform, 12*—α-chloronaphthalene, 13*—dioxane, 14*—anisole, 15*—diethyl ether, 16*—propyl bromide, 17*—chlorobenzene, 18*—benzene, 19*—carbon tetrachloride, 20*—n-hexane.

is seriously disrupted, it being characteristic that solvents of different chemical and physico-chemical nature, when in the glassy state, show influences on the spectra which differ only slightly (see Fig. 7). This phenomenon, which was not explained in reference 17, is fully accommodated within the framework of the model representations considered above. Actually, the transition to the glassy state is accompanied, in the general case, by a sharp diminution in the dielectric constant of the solvents, on account of its orientation component. The spectral shift, which is determined under these circumstances fundamentally by the refractive index, is not greatly different for different solvents.* Furthermore, this shift, in accordance with theory, is close to that attained in a liquid nonpolar solvent (see Table).

Frequencies of the Maxima of the Fluorescence Spectra of the Standard Substance (4-amino-N-methylphthalimide) in Liquid and Glassy-Solid Solutions According to the Data of Reference 17

Solvent	Liquid		Glass	
	ε	$\nu_{\text{fl.}}^{\text{max.}}$ (cm^{-1})	ε	$\nu_{\text{fl.}}^{\text{max.}}$ (cm^{-1})
Benzene	2.25	22400	—	—
Toluene	2.35	22500	2.5	22000
Propyl acetate	5.6	20650	2.42	22000
Ethyl orthoformate	(4.5)	19750	(2.5)	21600
Ethyl alcohol	26.3	18700	2.7	21700
Glycerine	44.0	17600	3.3	21000

From what has been said, the expediency of introducing the concept of universal interactions is clear, all the more so since the attempts[12-16] at describing the phenomena under consideration (for the sake of analyzing them) not only suffer from internal contradictions, but also cannot be applied to a wide range of systems.

We call attention once again to the fact that the subdivision of the influences undergone by molecules in solutions into universal and specific is associated with the introduction of model representations. In real systems, a continuous transition takes place from pair-interactions of molecules to an over-all action of the totality of surrounding particles on a dissolved molecule which retains a number of its properties unchanged. It would probably be difficult to assign certain real interactions beforehand to one type or the other. Furthermore, it is very probable that the variant of the theory considered by us also describes, even though only formally, those systems in which specific actions also manifest themselves in part. The form of the theory which takes account of the universal interactions may and should be perfected. Nevertheless, it appears to us that the proposed subdivision of the actions undergone by a molecule in solution into universal and specific (macro- and microscopic) is at the present time not only a justified, but also a necessary investigational procedure.

REFERENCES

1. W. Voigt. Ann. phys. 6, 459 (1901).
2. T. P. Kravets. Izvest. imp. Mosk. Inzh. Uchilishcha, Ser. II, No. 6 (1912); Trudy Fiz. (Works on Physics), Izd. Akad. Nauk SSSR, Moscow, Leningrad, 1959.
3. N. Bayliss and E. McRae. J. Phys. Chem. 58, 1002 (1954);
   E. McRae. J. Phys. Chem. 61, 562 (1957).
4. Y. Ooshika. J. Phys. Soc. Japan 9, 594 (1954).
5. N. Mataga, Y. Kaifu, and M. Koizumi. Bull. Chem. Soc. Japan 28, 690 (1955); 29, 465 (1956).
6. E. Lippert. Z. Electrochem. 61, 962 (1957).
7. J. Schuyer. Rec. trav. chim. 72, 933 (1953).
8. B. S. Neporent and N. G. Bakhshiev. Opt. i Spektr. 5, 634 (1958).
9. N. G. Bakhshiev. Opt. i Spektr. 5, 646 (1958).
10. N. G. Bakhshiev. Izv. Akad. Nauk SSSR, Ser. Fiz. 22, 1387 (1958).
11. N. G. Bakhshiev. Opt. i Spektr. 7, 52 (1959), Optics and Spectroscopy 7, 29 (1959).
12. V. V. Zelinskii, V. P. Kolobkov, and L. G. Pikulik. Opt. i Spektr. 2, 402 (1957).
13. V. V. Zelinskii, V. P. Kolobkov, and I. I. Reznikova. Tr. soveshch. po termodinamike i stroeniyu rastvorov (Proceedings of the Conference on Thermodynamics and the Structure of Solutions), p. 262, Moscow, 1958.
14. I. A. Zhmyreva, V. V. Zelinskii, and V. P. Kolbkov. Doklady Akad. Nauk SSSR 129, 1089 (1959).
15. E. Kosower. J. Am. Chem. Soc. 80, 3253, 3261, 3267 (1958).
16. E. Kosower and B. Ramsey. J. Am. Chem. Soc. 81, 856 (1959).
17. V. V. Zelinskii and V. P. Kolobkov. Opt. i Spektr. 5, 423 (1958).
18. S. Sambursky and G. Wolfsohn. Trans. Faraday Soc. 36, 427 (1940).
19. S. Sambursky and G. Wolfsohn. Phys. Rev. 62, 357 (1942).
20. A. S. Cherkasov. Zhur. Fiz. Khim. 29, 2209 (1955).
21. S. Veljkovic. Trans. Faraday Soc. 53, 1181 (1957).

---

*Solutions in "snowy"—polycrystalline—media do not fit either of the dependences considered. In this case, evidently, the molecules of the dissolved substance are subject to the action of the fields of the crystal lattices, with a unique anisotropy and magnitude for each solvent. Such systems naturally cannot be described with the help of the model representations which we are considering.

SPECTROSCOPIC STUDY OF THE PROCESSES OF VIBRATIONAL ENERGY TRANSFORMATION IN COMPLEX MOLECULES IN COLLISIONS

II. Effect of Foreign Gases on the Fluorescence Yield of 3-Dimethylamino-6-Aminophthalimide

S. O. Mirumyants and B. S. Neporent

Received 22 July 1959

The effect of a large group of foreign gases (monatomic He, Ne, Ar, Kr, Xe, diatomic H_2, D_2, N_2, CO, and polyatomic H_2O, D_2O, NH_3, C_5H_{12}) on the fluorescence yield of 3-dimethylamino-6-aminophthalimide vapor was investigated with excitation by four wavelengths covering a wide spectral region. The data obtained on the enhancement and weakening of the fluorescence by each gas were used to determine the amount of vibrational energy transformed in a single collision of the excited 3-dimethylamino-6-aminophthalimide molecule with a foreign gas molecule, as a function of the supply of vibrational energy of the former molecule. Values of the accommodation coefficient, which specifies the efficiency of the collision with respect to energy exchange, were determined for all the cases. It was shown that the efficiency of a collision in energy exchange depends basically on the Van der Waals interaction constant, that is, apparently, on the duration of the collision. It was established experimentally that transformation of the energy of the foreign gas molecules into vibrational energy of the molecule under study takes place with much lower efficiency than the reverse transformation.

The effect of foreign gases on the yield, i.e., the enhancement or weakening of the fluorescence of vapors of aromatic compounds was observed and studied in references 1-3; it has been the object of further investigations[4-8] and has also been discussed in review articles.[9-12] Already in the first communications it was proposed that these effects be used to study the processes of vibrational energy transfer in molecular collisions, and a method was developed for determining from experimental data the amount of energy ΔE transferred in a collision; it was also suggested that the efficiency of the collision be specified by an accommodation coefficient α which characterizes the degree of approach of the system of colliding particles to equilibrium. The first part of the present investigation[13] included a short discussion of the above-mentioned papers and an analysis of the method of determining ΔE, the amount of energy transferred, and α, the accommodation coefficient, along with a more precise definition of this coefficient. In this study[13] it was shown that, although the dependence of the quantities ΔE and α on the supply of vibrational energy E^* of the excited molecule and on the type of foreign gas molecule can be found, the experimental data do not permit a direct determination of the extent of the participation of the various degrees of freedom of the collision partners in the processes of vibrational energy conversion. An estimate of this participation could be made by studying the transformation of the vibrational energy of the complex molecule in collisions with a series of very different types of foreign gas molecules. It is in this connection that we have undertaken the present investigation, in which the effect of monatomic (He, Ne, Ar, Kr, Xe), diatomic (H_2, D_2, N_2, CO) and polyatomic (H_2O, D_2O, NH_3, C_5H_{12}) gases on the fluorescence yield of 3-dimethylamino-6-aminophthalimide vapor was studied. This substance was chosen for investigation because of the fact that the complex absorption spectrum, and also the fluorescence spectra and fluorescence yield of its vapor have already been studied in our laboratory.[14-16] Spectra of the vapor, with areas normalized as in reference 17, and a graph of the fluorescence yield as a function of the frequency of the exciting light are presented in Fig. 1; the structure formula of the substance is also given.

A photoelectric arrangement, similar to that described in reference 2, was set up for the measurements.

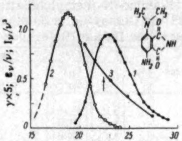

Fig. 1. Curve 1—absorption spectrum, curve 2—fluorescence spectrum, and curve 3—quantum fluorescence yield of 3-dimethylamino-6-aminophthalimide vapor at T = 528°K.

The integrated fluorescence intensity was measured, since special experiments carried out with the photoelectric spectrometer described in reference 18 showed, in agreement with a number of earlier investigations, that the fluorescence spectrum of this substance does not change even with isopentane (the most strongly stabilizing gas) at a pressure of 300 mm Hg. Measuring the integrated emission intensity allowed the vapor pressure of the substance to be greatly decreased as compared with previous investigations; in our experiments the vapor pressure was $P_N = 5.4 \times 10^{-3}$ mm Hg.*

The experimental temperature was T_0 = 528°K in all cases. The fluorescence was excited with an SVDSH mercury lamp, the individual lines of which were isolated by a monochromator.

Figure 2 shows a typical family of experimental curves giving the variation of the fluorescence intensity of 3-dimethylamino-6-aminophthalimide vapor with the pressure of the foreign gas (carbon monoxide) for excitation with light of various wavelengths. The upper abscissa scale gives the pressure of carbon monoxide, the lower abscissa scale the corresponding number of collisions per second, Z, of a molecule of the substance studied with molecules of carbon monoxide. The value of Z was calculated from the well-known formulas of kinetic theory; the values assumed for the gas kinetic molecular radii are given in the Table below. The value

---

*The variation of P_N with the temperature of the solid was measured earlier by Klochkov.[19]

Values of the Accommodation Coefficient α and of the Average Amount of Vibrational Energy ΔE Transferred in a Collision of an Excited 3-dimethylamino-6-aminophthalimide Molecule with Foreign Gas Molecules

Van der Waals interaction constant, a[34] $\left(\frac{l^2 \times atm}{(moles)^2}\right)$	Temperature coefficient of the specific heat, β (cal/mole/°C)	Specific heat C (cal/mole/°C) for the temperature in °C given in brackets	Molecular radius (A)	Foreign gas or vapor \ λ_e (mμ) ν_e (cm^{-1}) E* (cm^{-1})	492 20300 −1950		436 22950 700		405 24700 2450		365 27400 5150	
					ΔE (cm^{-1})	α	ΔE (cm^{-1})	α	ΔE (cm^{-1})	α	ΔE (cm^{-1})	α
0.034	0	3 (15)	0.98 [2,25]	He	− 6	0.03	5.7	0.07	13.3	0.07	45	0.07
0.21	0	3 (15)	1.40 [26]	Ne	−11	0.05	11.3	0.17	49.7	0.18	94.5	0.18
1.35	0	3 (15)	1.83 [27]	Ar	−13.1	0.06	16.2	0.25	71.5	0.26	138	0.26
2.32	0	3 (15)	2.15 [26]	Kr	−14.1	0.06	16.1	0.32	86	0.33	180	0.34
4.19	0	3 (15)	2.45 [27]	Xe	−17.7	0.08	25	0.35	93	0.36	216	0.38
0.24	0.0008 [33]	4.84 (15) [32]	1.23 [28]	H_2	− 1.6	0.01	14.7	0.088	27.3	0.089	63	0.093
0.24(d)	0.0005(b)	4.98 (25) [33]	1.23 [5]	D_2	− 2.5	0.01	18.8	0.22	74.4	0.22	150	0.23
1.39	0.001 [33]	4.94 (15) [32]	1.59 [28]	N_2	−16.7	0.06	32.4	0.34(?)	81.5	0.25	194	0.29
1.49	0.001 [33]	4.94 (15) [32]	1.88 [29]	CO	− 2.6	0.09	28.3	0.29	108.5	0.33	240	0.36
5.46	0.004 [33]	5.99 (0) [33]	1.3 [30]	H_2O	−14.6	0.05	24	0.23	106	0.29	430	0.59
5.46(d)	0.004(e)	6.96 (255)(a)	1.3 (e)	D_2O	−12.2	0.04	34	0.31	132	0.35	460	0.61
4.17	0.006 [33]	6.8 (15) [32]	1.43 [28]	NH_3	−36	0.11	56.5	0.48	244	0.59	735	0.86
18.1	0.04(c)	32.3 (58) [34]	2.4 (f)	iso-C_5H_{12}	−137	0.18	50.5	0.18	278	0.28	990	0.47
—	0.04(g)	690(g)	4.5 [16]	3-dimethylamino-6-aminophthalimide ($C_{10}H_{11}N_3O_2$)	—	—	—	—	—	—	—	—

Comments: (a) Calculated from the known vibrational and rotational frequencies; (b) interpolation of data in reference 33; (c) extrapolation of data in reference 34; (d) approximate values, assumed equal to those for H_2 and H_2O, respectively; (e) assumed equal to the value for H_2O; (f) mean value from the data in references 2 and 31; (g) calculated values of the vibrational specific heat, C'_{vib}, and β for t = 255° C from experimental data.[16]

of the relative fluorescence intensity, F_z/F_0, is plotted along the ordinate axis, the intensity F_0 for Z = 0 being assumed equal to unity in all cases. It is easily seen that the first small additions of the foreign gas (P ~ 1 mm Hg) give rise to a sharp decrease in the fluorescence intensity; as shown by our investigations,[20-22] this is due to an effect on the unexcited molecules of the substance under study, that is, on the absorption coefficient of the vapor. Preliminary results of a study of this effect for our case are given in reference 23; more detailed data will be published later. We note here only that, in agreement with reference 20, the decrease in the absorption coefficient does not depend on the wavelength of the incident light and that the effect comes to saturation at low gas pressures. Using this fact it is easy to take into account the effect of the change in the absorption coefficient of the vapor being studied by a method similar to that used in reference 2. The result of this revision is given in Fig. 3.

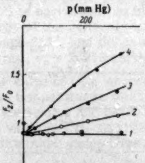

Fig. 2

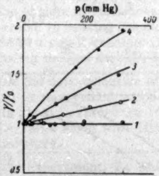

Fig. 3

Fig. 2. Effect of carbon monoxide on the fluorescence intensity of 3-dimethylamino-6-aminophthalimide vapor for excitation by various wavelengths λ_e. λ_e(mμ): curve 1—492; curve 2—436; curve 3—405; curve 4—365.

Fig. 3. Enhancement and weakening of the fluorescence of 3-dimethylamino-6-aminophthalimide vapor on addition of carbon monoxide. Designations as in Fig. 2.

The data obtained in the study of the effect of all the foreign gases used are given in Figs. 4-6 in somewhat different form: along the ordinate axis are plotted values

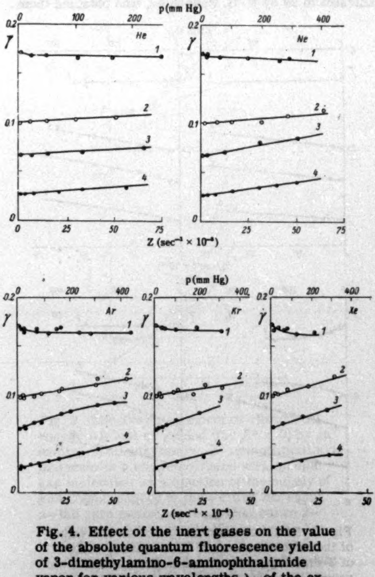

Fig. 4. Effect of the inert gases on the value of the absolute quantum fluorescence yield of 3-dimethylamino-6-aminophthalimide vapor for various wavelengths λ_e of the exciting light. λ_e(mμ): curve 1—492; curve 2—436; curve 3—405; curve 4—365.

of the quantum yield of the fluorescence of the vapor.*

Necessary data for this representation of the value of the fluorescence yield of the vapor for exciting light of various wavelengths were obtained for the temperature of the experiment from the results of measurements by Borisevich[16] (cf. Fig. 1) by interpolation.

For a detailed analysis of the data in Figs. 4-6, which agree qualitatively with all the results obtained in previous investigations, it is necessary to characterize the process of energy transfer by values of the amount of vibrational energy ΔE lost (or gained) by the excited molecule in the collision, and also by values of the accommodation coefficient α. A method of determining these quantities was discussed in detail in the first part of the present investigation.[13]

The results of the determination of the value of ΔE as a function of E* for stabilization (or labilization) of excited 3-dimethylamino-6-aminophthalimide molecules by the foreign gases enumerated above are given in the Table. Necessary data for the calculation of values of the duration τ of the excited state for λ_e = 365, 405, and 436 mμ were obtained by interpolation using data communicated to us by N. G. Bakhshiev, who obtained them by direct fluorometric measurements at various temperatures on the fluorometer of Bonch-Bruevich et al.[24] The value of τ for λ_e = 492 mμ was obtained from the known value of γ, assuming that quenching of the second kind occurs according to Vavilov, that is,

$$\tau_{\lambda_1} = \tau_{\lambda_2} \frac{\gamma_{\lambda_1}}{\gamma_{\lambda_2}} .$$

The values of τ used are given in Fig. 7.

From the data in the Table it follows, in agreement with previous investigations, that the average amount of energy transferred in a collision increases with increasing supply of vibrational energy of the excited molecule and with increasing mass and complexity of the foreign gas molecule. The transition to excitation in the region $\nu_e < \nu_1$ is accompanied, as in reference 3, by a change in the direction of the energy transfer (ν_1 is the inversion frequency). On absorption of a quantum of frequency ν_1 the vibrational energy supply of the excited molecule, as shown in reference 3, does not change. Absorption of light with frequencies $\nu_e < \nu_1$ is accompanied by a decrease in the vibrational energy of the excited molecules. We note here that in most cases the total supply of thermal energy of the foreign gas molecule is less than the vibrational energy deficit of the 3-dimethylamino-6-aminophthalimide molecule formed by excitation by λ_e = 492 mμ, which is equal to 1950 cm^{-1}.

For clarity the values of ΔE = f(E*) for E* = 5150 cm^{-1} are given for all the gases studied in Fig. 8. The foreign gas molecules are arranged according to increasing values of their mass M, by the convenient method of plotting the value of $\sqrt{M}$ along the abscissa axis. It is immediately evident that in a collision with a rare gas molecule the excited 3-dimethylamino-6-aminophthalimide molecule loses an amount of energy which increases in

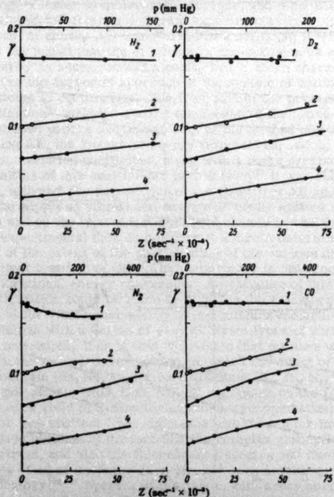

Fig. 5. Effect of diatomic gases on the value of the absolute quantum fluorescence yield of 3-dimethylamino-6-aminophthalimide vapor for various wavelengths λ_e of the exciting light. Designations as in Fig. 4.

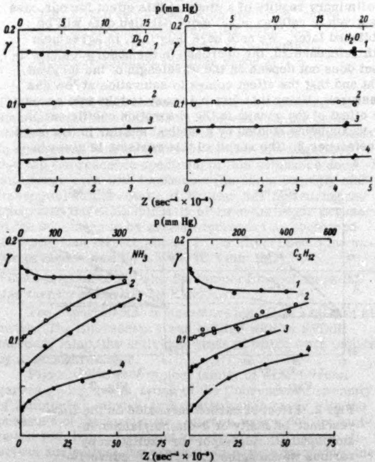

Fig. 6. Effect of polyatomic gases on the value of the absolute quantum fluorescence yield of 3-dimethylamino-6-aminophthalimide vapor for various wavelengths λ_e of the exciting light. Designations as in Fig. 4.

---

*We note that data given in reference 3 on the enhancement of the fluorescence of 3-dimethylamino-6-aminophthalimide vapor under of the action of pentane differ somewhat from ours. It is possible that this is due to the great difference in the vapor pressures in the experiments in reference 3 and those described by us; this, in particular, impelled us to eliminate the effect of the gases on the absorption of the vapor. The effect was small in reference 3.

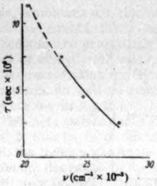

Fig. 7

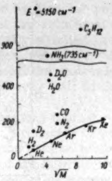

Fig. 8

Fig. 7. Variation of the duration of the excited state of the 3-dimethylamino-6-aminophthalimide molecule with the frequency ν_e of the exciting light ($T_{vapor} = 528°K$).

Fig. 8. The average amount of vibrational energy ΔE lost in a single collision by an excited 3-dimethylamino-6-aminophthalimide molecule as a function of the mass of the foreign gas molecule ($\lambda_e = 365\ m\mu$).

going from helium to xenon, in spite of the fact that the specific heats of these gases, which possess only translational degrees of freedom, are the same. The corresponding increase in efficiency must be ascribed to a change in the mechanism or in the duration of the collision of the rare gas atoms with the excited molecule. The points corresponding to all the remaining gases are located higher in Fig. 8 than those for the rare gases. This indicates to a first approximation that, in addition to the translational degrees of freedom, the other degrees of freedom—rotational and vibrational—of the foreign gas molecules also take part in the process of energy transfer. For a more definite pronouncement in this matter it is necessary to find values of the accommodation coefficients, in which the efficiency of energy transfer is defined taking into consideration all degrees of freedom of the partner molecules in the collision.

The dependence of ΔE on E^*, which is necessary for the calculation of α, is given in Fig. 9 for all the gases used; here, values of the frequency ν_e of the excited light and also the excess (or deficit) in the vibrational energy, $E^* = \nu_e - \nu_1$, acquired by the 3-dimethylamino-6-aminophthalimide molecule are plotted along the abscissa axis. The absorption of large quanta ($\lambda_e = 365\ m\mu$, $\nu_e = 27400\ cm^{-1}$) is equivalent, as far as the change in vibrational energy of the molecule is concerned, to heating the gas through 215°, and the absorption of a small quantum ($\lambda_e = 492\ m\mu$, $\nu_e = 20350\ cm^{-1}$) to cooling the gas through 82° * relative to the temperature of the experiment, T_0, which was equal to 528°K. As is evident from the data given, the inversion frequency is located near $\nu_1 = 22250\ cm^{-1}$ for all the gases studied; this differs a little from the estimate given in reference 3. The position of the inversion frequency relative to the spectra is shown by the arrow in Fig. 1.

A consideration of the data in Fig. 9 shows that for the rare gases and the H_2 and D_2 molecules the dependence of ΔE on E^* in the region for $E^* > 0$ is practically linear, whereas in the other cases, from N_2 to C_5H_{12}, the nonlinearity observed is greater the more complex the foreign gas molecule. This circumstance is evidently related to the fact that the specific heat of these gases rises with the increase of the amount of energy available for redistribution, which results from the increase in the "temperature" of the complex, the inclusion in the process of transfer of the energy of new vibrational degrees of freedom and the increase in the heat capacity of the foreign gas molecules.

In calculating values of the accommodation coefficient we used values of the specific heat of the molecule being studied and of the foreign gases (cf. the Table), which correspond to the calculated values of the equilibrium "temperature" θ (cf. reference 13). The values obtained for the accommodation coefficient for all the cases studied are also given in the Table, along with other initial data and results of the investigation.

An analysis of the data obtained shows that for the rare gases the values of the accommodation coefficient, while practically independent of E^* for $E^* > 0$, increase rapidly in going from helium to xenon. This increase in

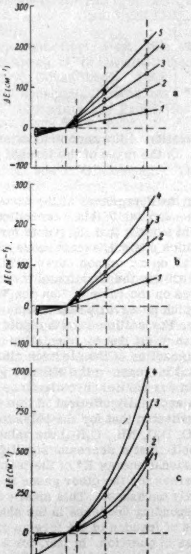

Fig. 9. The average amount of vibrational energy ΔE lost or gained (for $E^* < 0$) by an excited 3-dimethylamino-6-aminophthalimide molecule in a single collision with foreign gas molecules as a function of the supply of vibrational energy of the excited molecule. a—the rare gases: curve 1—He, curve 2—Ne, curve 3—Ar, curve 4—Kr, curve 5—Xe; b—diatomic gases: curve 1—H_2, curve 2—D_2, curve 3—N_2, curve 4—CO; c—polyatomic gases: curve 1—H_2O, curve 2—D_2O, curve 3—NH_3, curve 4—C_5H_{12}.

---

*The value of $C'_{vib.}$ necessary for the determination of these temperatures was obtained by the method proposed in reference 2 and based on data given in reference 16. The value of $C'_{vib.}$ is given in the Table along with data for the other gases from the literature.

efficiency must be ascribed to the increase in the duration of a collision of the atoms in question with the excited molecule. It can hardly be expected that the rules governing the process of energy transfer would be the same as the well-known rules for the collision of hard spheres. In fact, if the values of α (for example, for $E^* = 5150\ \mathrm{cm}^{-1}$) are arranged in order of increasing mass of the foreign gas molecule (Fig. 10, where for convenience values of $\sqrt{M}$ are plotted along the abscissa axis), only the points for the rare gases fall on a single curve. It is difficult moreover to believe that the linear variation of the initial slope of the stabilization curve of perylene with the mass of the foreign gas molecules (nitrogen, paracymene, hexamethylbenzene), which was established in reference 6, substantiates that the mass of these molecules plays a definite role, since the magnitude of the initial slope of the stabilization curves is not a property which shows directly the efficiency of the energy transfer.

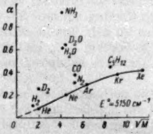

Fig. 10. Variation of the accommodation coefficient α with the mass of the foreign gas molecules.

If we consider the dependence of the accommodation coefficient α on the Van der Waals interaction constant (Fig. 11), it is quite evident that the points for all the foreign gas molecules studied, except those which have dipole moments, fall on a common curve. This result shows that it is precisely the duration of the collision, depending as it does on the value of Van der Waals interaction constant, which apparently determines the efficiency of energy transfer. For collisions with dipole molecules there is probably an effect due to orientation or to an increased mutual interaction of the electron clouds which causes an additional increase in the efficiency of the collision. As shown in our earlier investigations, the ammonia molecule is especially efficient in this respect.

It is clearly indicated that for the polyatomic foreign gas molecules (H_2O, D_2O, NH_3, C_5H_{12}) the values of the accommodation coefficient α decrease significantly as the supply of vibrational energy E^* of the molecule studied decreases, whereas for the other gases the values of α remain practically unchanged. This must evidently be related to a corresponding decrease in the share of the vibrational degrees of freedon of the foreign gas molecules in the process in question. In fact, for a relatively high frequency vibration, the probability of excitation in a single collision in the case of a small excess of transferable energy can be considerably less than the probability of excitation of this vibration in conditions of steady equilibrium, which determines the magnitude of the specific heat of the gas.

For relatively large values of $E^* = 5150\ \mathrm{cm}^{-1}$ (cf. Fig. 11(a)) the magnitude of α for the nondipole pentane molecule reaches values which are characteristic of simple molecules with large values of the Van der Waals constant. Thus the efficiency of the participation of the vibrational degrees of freedom of the pentane molecule apparently matches the degree of their excitation in equilibrium conditions. With further increase of the value of E^* the possibility is not excluded that there would be a further increase in α, due also to the increased probability of a quantum energy transfer to the high frequency vibrations of the pentane molecule. This transfer is naturally not taken into account in our expressions which are based on the assumption of the conservation of classical statistical equilibrium, in which for low frequency vibrations all quantum limitations are removed, and the high frequency vibrations take only an extremely limited part in the process in question.

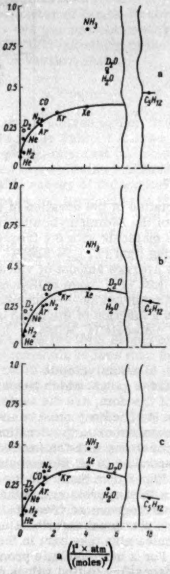

Fig. 11. Variation of the accommodation coefficient α with the Van der Waals interaction coefficient a of the foreign gases. $\lambda_e(\mathrm{m}\mu)$ and E^* (cm^{-1}, in brackets): a—365 (5150); b—405 (2450); c—436 (700).

In the cases studied by us the vibrational degrees of freedom of diatomic molecules evidently do not take part in the processes of energy transfer. These vibrations are not taken into account in the assumed values of the specific heat. Also the relatively high frequency rotational states of the hydrogen molecule are apparently only weakly excited, since values of α for hydrogen calculated with the assumption of a full share of the rotations in the process do not fall on the curves in Fig. 11. For deuterium the transfer takes places considerably more easily, in contrast to the results obtained[8] for the stabilization of β-naphthylamine (it should be noted in this connection that the values which we have assumed for the Van der Waals constants of D_2 and D_2O are equal to the values for H_2 and H_2O, respectively). Thus, in the phenomena under consideration one does not observe for hydrogen and deuterium the enhanced activity which has been postulated from a study of reaction kinetics, for example, in references 9 and 12. For all the other molecules, which are not characterized by high values of the rotational quanta, the translational and rotational degrees of freedom are practically identically efficient in processes of vibrational energy transfer, since the values of the accommodation coefficient for all the molecules, monatomic as well as diatomic, fit very well on the general curves in Fig. 11.

We note particularly that in passing from $E^* > 0$ to $E^* < 0$, that is, to cases involving a transfer of energy from the foreign gas molecule to the excited molecule, an abrupt decrease in the values of the accommodation coefficient occurs. This effect is especially pronounced for H_2 and D_2 and is considerably weaker for the polyatomic NH_3 and C_5H_{12} molecules, which possess relatively large supplies of thermal energy. Similar results were obtained[3] for another substance, where it was also found that the value of α for $E^* < 0$ is not very dependent on the value of E^*. These facts, which disagree in a certain sense with the other results, merit additional analysis and experimental study.

L. I. Shpiller, a student of the Leningrad State University, took part in the measurements.

REFERENCES

1. B. S. Neporent. Zhur. Fiz. Khim. 13, 965 (1939).
2. B. S. Neporent. Zhur. Fiz. Khim. 24, 1219 (1950).
3. N. A. Borisevich and B. S. Neporent. Opt. i Spektr. 1, 536 (1956).
4. H. G. Curme and G. K. Rollefson. J. Am. Chem. Soc. 74, 28 (1952).
5. M. Boudart and J. T. Dubois. J. Chem. Phys. 23, 223 (1955).
6. E. J. Bowen and S. Veljkovic. Proc. Roy. Soc. (London), A236, 1 (1956).
7. H. Okabe and E. W. R. Steacie. Can. J. Chem. 36, 137 (1958).
8. G. Giacometti, H. Okabe, and E. W. R. Steacie. Proc. Roy. Soc. (London), A250, 287 (1959).
9. G. Porter. Ann. Rev. Phys. Chem. 7, 207 (1956).
10. B. Stevens and M. Boudart. Proc. Natl. Acad. Sci. 67, 570 (1957).
11. B. Stevens. Chem. Revs. 57, 439 (1957).
12. J. C. McCoubrey and W. D. McGrath. Quart. Revs. (London) 11, 87 (1957).
13. B. S. Neporent and S. O. Mirumyants. Opt. i Spektr. 8, 635 (1960), Optics and Spectroscopy 8, 336 (1960).
14. B. S. Neporent. Zhur. Ekspt. i Teoret. Fiz. 21, 172 (1951).
15. B. S. Neporent and N. A. Borisevich. Opt. i Spektr. 1, 143 (1956).
16. N. A. Borisevich. Kand. diss., Leningrad, 1954.
17. B. S. Neporent. Doklady Akad. Nauk SSSR 119, 682 (1958); Izvest. Akad. Nauk SSSR, Ser. Fiz. 22, 1372 (1958).
18. B. S. Neporent and V. P. Klochkov. Izvest. Akad. Nauk SSSR, Ser. Fiz. 20, 641 (1956).
19. V. P. Klochkov. Zhur. Fiz. Khim. 30, 2823 (1956).
20. B. S. Neporent. Doklady Akad. Nauk SSSR 72, 35 (1950).
21. B. S. Neporent and A. A. Solodovnikov. Opt. i Spektr. 1, 951 (1956).
22. B. S. Neporent and V. P. Klochkov. Opt. i Spektr. 3, 529 (1957).
23. S. O. Mirumyants. Opt. i Spektr. 7, 276 (1959), Optics and Spectroscopy 7, 175 (1959).
24. A. M. Bonch-Bruevich, V. A. Molchanov, and V. I. Shirokov. Izvest. Akad. Nauk SSSR, Ser. Fiz. 20, 596 (1956).
25. B. S. Neporent. Doct. diss., Moscow, 1945.
26. "Kratkii spravochnik khimika" (Short Handbook of Chemistry), Goskhimizdat, 1951.
27. M. V. Vol'kenshtein. "Struktura i fizicheskie svoistva molekul" (Structure and Properties of Molecules), Izd. Akad. Nauk SSSR, 1955.
28. H. A. Stuart. "Structure of Molecules." Springer, Berlin, 1934.
29. S. Chapman and T. G. Cowling. "The Mathematical Theory of Non-uniform Gases." Cambridge, 1939.
30. M. Born. "Optik." Springer, Berlin, 1933.
31. J. C. McCoudrey, J. B. Parke, and A. R. Ubbelohde. Proc. Roy. Soc. (London) A223, 155 (1954).
32. Landolt-Börnstein. "Tabellen," 2 Erg., Vol. II, p. 1227, 1931.
33. Landolt-Börnstein. "Tabellen," 3 Erg., Vol. III, p. 2324, 1936.
34. "Tekhnicheskaya entsiklopediya. Spravochnik fizicheskikh, klimicheskikh i tekhnologicheskikh velichin" (Technical Engyclopaedia. Handbook of Physical, Chemical, and Technological Quantities), Vol. 7, p. 269. OGIZ, RSFSR, Moscow, 1931.
35. H. M. Spencer. J. Chem. Phys. 25, 357 (1956).
36. "Handbook of Chemistry and Physics," Vol. II, p. 2124, 1955-1956.

THE pH DEPENDENCE OF ELECTRONIC SPECTRA OF THE SIMPLEST DERIVATIVES OF BENZENE

I. Absorption Spectra of Hydroxybenzenes

L. V. Smirnov and A. I. Suprunenko

Received 6 October 1959

The pH dependence of the electronic absorption spectra of a number of benzene derivatives was investigated and the bands correlated with the ^1L_b and ^1L_a bands in the spectrum of benzene.

INTRODUCTION

Similarity between the absorption spectrum of benzene and the spectra of its monosubstituted derivatives is to be expected if the substituent is a group which interacts only weakly with the π-electron system of the ring (for example, the CH_3 group). Considerable similarity is retained also when the substituents are the groups NO_2, OH, or NH_2, since the order of the bond between the benzene ring and the heteroatom apparently never exceeds 1.3.[1] The presence of N and O atoms in the molecules of benzene derivatives leads one to expect the appearance of a weak $n - \pi$ transition in the long wavelength part of the spectrum. The influence of a second substituent on the shape of the spectrum is of substantial interest, particularly in the case of substituents such as the OH group, whose presence makes the spectrum immediately dependent on the pH of the medium.

The introduction of substituents into the molecule and the use of polar solvents leads to a washing-out of the vibrational structure of the long wavelength band, thus excluding from consideration an important characteristic of the spectrum. However, it is not this circumstance that impedes the study of the spectra of hydroxy derivatives of benzene. The general aspect of the spectra of aqueous solutions of dihydroxybenzenes is so different from that of the benzene spectrum that, at first glance, any identification of bands in those spectra becomes very uncertain. To this, it must be added that aqueous solutions of dihydroxybenzenes are, as is generally known, unstable and hence experimental results in this case are always more or less dependent on the conditions of preparation of the solutions and on the experimental procedure of measurements. The latter circumstance is one of the reasons for the contradiction between the experimental results published at present in the literature (see, for example, reference 2) concerning the spectra of hydroxybenzenes.

The present work is devoted to an investigation of the electronic absorption spectra of solutions of a number of hydroxy derivatives of benzene, as a function of the pH of the medium, and to the identification of bands in the above spectra.

For the sake of convenience, from now on, in discussing the experimental results, we will use the letters A, B, and C to designate the absorption bands, starting from the short wavelength side. In the spectrum of benzene, the A-band corresponds to the band ^1B_b (allowed transition $^1A_{1g} - {}^1E_{1u}$), the B-band to the band ^1L_a (forbidden transition $^1A_{1g} - {}^1B_{2u}$) and the C-band to the band ^1L_b (forbidden transition $^1A_{1g} - {}^1B_{2u}$).[3]

EXPERIMENTAL RESULTS

Introduction of a substituent into the benzene ring must cause a bathochromic shift of the A-band; but, as shown by comparison of the spectra of benzene, phenol, and dihydroxy-derivatives the A-band is never shifted into the region $\lambda > 200$ mμ. Figure 1 shows the results concerning the position and intensities of the absorption bands of all the compounds investigated. The full lines correspond to the aqueous solutions and the dotted lines to the alkaline solutions. Addition of hydrochloric acid to the aqueous solutions does not change the aspect of the absorption spectra (even at very low pH values). Hence it can be assumed, with sufficient justification, that the bands shown in Fig. 1 by full lines correspond to the undissociated molecules.

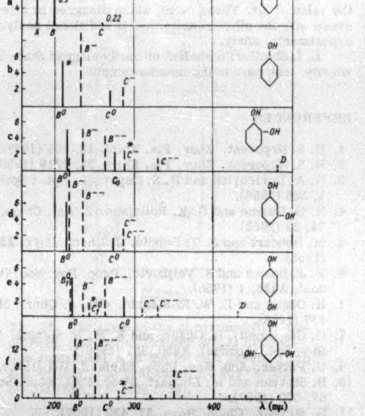

Fig. 1. Position and intensities of bands in the absorption spectra of solutions of hydroxybenzenes.

A number of conclusions can be drawn from an analysis of the results presented here. We assigned all bands lying in the region 200-230 mμ to the B-band, and the bands in the region 260-290 mμ to the C-band, i.e., assuming the two types of bands to originate from the ^1L_a and the ^1L_b bands of benzene, respectively. The bands assigned to the undissociated molecules were labeled B^0 and C^0. Addition of alkali to a solution of a dihydroxybenzene leads initially to the formation of a certain concentration of monovalent ions. With an increase in the pH of the solution, divalent ions can also appear, and at sufficiently high pH they must become the preponderant species.

The B-band of benzene (^1L_a) does not change its intensity on introduction of one or two hydroxyl groups into the molecule. Its position in the ortho- and meta-hydroxybenzenes is the same, while in the para-hydroxybenzene (hydroquinone) it is shifted towards the long wavelength region by only 6 mμ.

The introduction of one OH group into the molecule shifts the weak C-band of benzene (^1L_b, $\varepsilon = 220$) by 12 mμ and increases the extinction coefficient at the band maximum by about eight times (fifteen times in the case of hydroquinone). This band is quite sensitive to a change in the position of the second hydroxyl group, and can be used as an indicator in the analysis of mixtures of ortho- and para-isomers (see Fig. 1, the position of the C^0-bands for pyrocatechol and hydroquinone). There are indications in the literature concerning the sensitivity of the C-band of benzene and some of its derivatives of the formation of associated molecules, in particular through intermolecular hydrogen bonds.[4] We did not investigate this problem, even though in many cases we used concentrated solutions. It must be noted that in none of the compounds we investigated did we detect the presence of a side-band in the long wavelength absorption band, characteristic of the formation of associated molecules, even though association was undoubtedly present in our solutions.[5]

DISCUSSION OF RESULTS

Phenol (see Fig. 1b and Fig. 2). In pure aqueous solution (without addition of acid or alkali), the B^0-band appears at about 212 mμ (at 222 mμ in ethyl alcohol) and the C^0-band at 270 mμ (at 272 mμ in ethyl alcohol). These bands correspond to undissociated molecules of phenol, since the number of phenoxide ions present under these conditions is too small to be detected spectroscopically. This is also supported by the fact that addition of hydrochloric acid does not influence the spectrum.

The degree of dissociation of phenol (relatively small in aqueous solution where $k = 10^{-10}$) increases sharply even with small additions of alkali. The concomitant formation of sodium phenolate leads to the appearance of two new bands in the spectrum—B^- at 234 mμ and C^- at 286 mμ.

Curve 1 in Fig. 2 is obtained at a phenol concentration of 17.2×10^{-5} moles/liter in 0.004 N NaOH solution. In a recently published article,[6] the aim of which was the development of a spectroscopic method of quantitative analysis for phenol content of industrial wastes, it was pointed out that complete transition from phenol to sodium phenolate in ethyl alcohol solution occurs at 10% alkali content.

Dihydroxyderivatives. Divalent as well as monovalent ions can be present in alkaline solutions of these compounds, and at higher pH the divalent ions can be preponderant. It is possible, sometimes, to detect four to five bands in the spectra of these solutions, and their assignment to a particular molecular species in solution is quite difficult, even though it is known in general that the bands in the spectra of divalent ions are shifted more towards the red part of the spectrum than those of the monovalent ions. Removal of a proton in a molecule of a dihydroxybenzene does not in itself lead to the appearance of a new electronic transition, but the process of oxidation related to the removal of the proton leads to the rearrangement of the π-electron system (formation of ortho-paraquinones). In this case, as well as bands B and C, it is possible to expect the appearance of a weak band in the long wavelength region which does not appear in the benzene spectrum (in Fig. 1 this band is denoted by D).

The most specific characteristic of the spectra of alkaline solutions of dihydroxybenzenes is their change with time, caused by the presence of oxidation-reduction processes (occurring at varying rates). Experiments show that in this case some bands in the spectrum of a solution completely vanish with time while the intensity of other bands in the spectrum increases. It is evident that the bands which behave in the same way should be assigned to the same species in the solution. In Fig. 1 the bands due to the divalent ions are designated B^{--} and C^{--}.

In many cases, the bands overlap each other considerably and hence their position in Fig. 1 is only approximate. An asterisk is used to indicate these bands. Reliable determination of the molar extinction coefficients ε is impossible in such rapidly changing multicomponent systems as the alkaline solutions of dihydroxybenzenes (in particular, solutions of pyrocatechol and hydroquinone). In Fig. 1 the dotted lines show the relative intensities of bands for a solution at a definite pH.

Pyrocatechol (see Fig. 1c and Fig. 3). At high pH the freshly prepared solution has a slight pinkish tinge due to the weak band in the region $\lambda \approx 480$ mμ (D-band). On standing (1.5-2 hr or more, depending on the initial value of the pH), the tinge becomes an indeterminate brownish one. At the same time, the D-band disappears completely and the C^{--} band at 330 mμ and the B^{--} band at 264 mμ increase considerably. A simultaneous decrease also occurs in the intensities of the B^- and the C^- bands. It must be noted that the positions of the B^- and C^- bands corresponding to the undissociated molecules of pyrocatechol and to its mono- and divalent anions, given in Fig. 1c, agree with the results of other authors.[5]

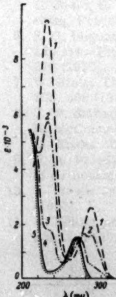

Fig. 2

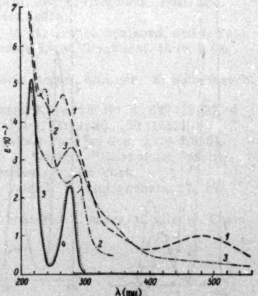

Fig. 3

Fig. 2. Absorption spectra of aqueous solutions of phenol ($c = 17.5 \times 10^{-5}$ moles/liter). Curve 1—pH = 12.3 (freshly-prepared); curve 2—pH = 10.7 (40 hr after preparation); curve 3—pH = 10.0 (after 27 hr); curve 4—pH = 6.5 (without alkali); curve 5—pH = 2.5.
Fig. 3. Absorption spectra of aqueous solutions of pyrocatechol ($c = 29.1 \times 10^{-5}$ moles/liter). Curve 1—freshly prepared in 0.006 N NaOH solution; curve 2—freshly prepared in 0.002 N NaOH solution; curve 3—0.002 N solution after 2 hr; curve 4—pH = 6.0 (without alkali); curve 5—pH = 1.8.

In general, the following four species can be present in a basic solution of pyrocatechol:

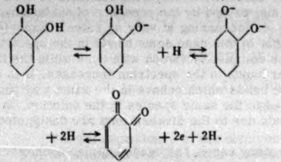

The D-band present at relatively high alkalinity (0.004 N NaOH) corresponds to the orthoquinone. In a nonpolar solvent such as CCl_4, this band is at 600 mμ,[7] thus satisfying the three requirements for an n → π transition:[8] low intensity, appearance in the long wavelength part of the spectrum, and a "blue" shift in going from a polar to a nonpolar solvent.

Resorcinol (see Fig. 1d and Fig. 4). The aqueous solution remains colorless on addition of alkali, and the D-band is absent (due to the impossibility of formation of a metaquinone structure). Of the three easily detectable bands, two exhibit a rather rapid decrease in intensity with time: the B^{--} band at 236 mμ and the C^{--} band at 286 mμ. The B^- band at 218 mμ also decreases in intensity but at a slower rate. At low pH and in the absence of alkali the band at 286 mμ exhibits a slight shoulder. We tentatively identified the latter as a C^- band. On standing, the first to disappear are the B^{--} and the C^{--} bands corresponding to the divalent ions.

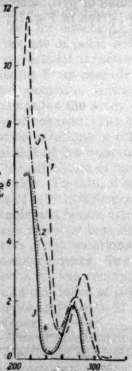

Fig. 4

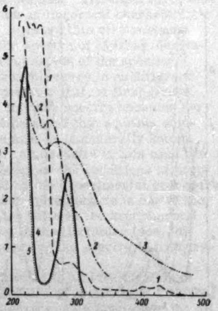

Fig. 5

Fig. 4. Absorption spectra of aqueous solutions of resorcinol (c = 18.2×10^{-5}) moles/liter). Curve 1—pH = 11.3 (freshly prepared in 0.001 N NaOH); curve 2—pH = 9.7 (after 26 hr); curve 3—pH = 6.0 (without alkali); curve 4—pH = 2.0.

Fig. 5. Absorption spectra of aqueous solutions of hydroquinone (c = 36.4×10^{-5} moles/liter). Curve 1—pH = 8.9 (freshly prepared in 10^{-4} N NaOH solution); curve 2—same solution after 30 min; curve 3—pH = 11.1 (in 0.002 N NaOH solution after 3 hr); curve 4—pH = 6.2 (without alkali); curve 5—pH = 1.7.

Hydroquinone (see Fig. 1e and Fig. 5). In pure aqueous solutions the B^0 and C^0 bands are very evident, and their intensities and positions (222 and 288 mμ, respectively) remain unchanged even in very acid solutions. In the case of small additions of NaOH, the solution acquires a yellowish tinge which then rapidly changes into an indeterminate brownish tinge. A rapid measurement of a freshly prepared alkaline solution of hydroquinone allows the detection of a weak ($\varepsilon < 200$) wide band in the region 400-440 mμ, with characteristic weak maxima at 405 mμ and 430 mμ which are more clearly resolved in nonpolar solvents. In the case of a CCl_4 solution these maxima occur at 430 mμ and 450 mμ,[7] and in the case of a hexane solution, at 435 mμ and 455 mμ, respectively.[9] Thus, the D-band of hydroquinone in alkaline solutions satisfies the three requirements for the n → π transitions mentioned above, similar to the D-band of pyrocatechol.

The high rates of oxidation-reduction processes in alkaline solutions of hydroquinone forced us to perform the measurements on the SF-4 spectrophotometer in two or three steps. In each step it was necessary to reproduce identically the conditions of preparation of the solutions and the duration of measurements. Only then did it become possible to detect all the bands and find out about their behavior as a function of time.

The position of the C-band in alkaline solutions of hydroquinone has been investigated by other authors[10] who proposed a method of quantitative evaluation of the relative concentrations of the three components—undissociated molecules, monovalent, and divalent ions. In Fig. 1e the bands at 310 mμ and 330 mμ are designated C^- and C^{--} respectively. The B^- band at 236 mμ decreases rapidly in intensity, while the B^{--} band at 264 mμ increases in intensity as a function of time. The similarity in position and behavior of these bands with the B^- and B^{--} bands of pyrocatechol is noteworthy. The D-band present in the spectrum of alkaline solutions of hydroquinone is assigned to the paraquinone, which also exhibits an intense B-band and a weak C-band. The bands designated B_1^0 and C_1^0 in Fig. 1e become evident at high alkalinity. It is possible that they too should be assigned to a paraquinone.

Phloroglucinol (see Fig. 1f and Fig. 6). The spectra of phloroglucinol (symmetrical trihydroxybenzene) solutions are given here for comparison with the spectra of the mono- and dihydroxy derivatives. The specific differences between the phloroglucinol spectra and the spectra of the dihydroxybenzenes consist in the shift of the C^0 band towards the short wavelength region, a sharp decrease in the intensities of B^0 and C^0 bands, and high band intensities in alkaline solutions. The following keto-enol transformations can exist in alkaline solution of phloroglucinol:

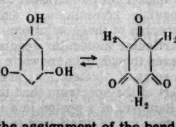

However, the assignment of the band at 350 mμ (C^{--}) to the keto form (see discussion on this subject in the literature[3, 11]) is not well-founded. This band, because of its position and high intensity, is a typical π → π transition.

The behavior of bands in the spectra of alkaline solutions of phloroglucinol, as a function of time, is analogous to the behavior of the corresponding bands in the spectrum of resorcinol.

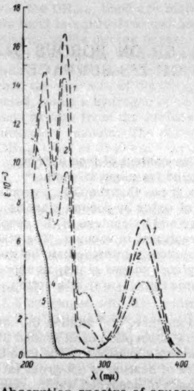

Fig. 6. Absorption spectra of aqueous solutions of phloroglucinol ($c = 11.9 \times 10^{-5}$ moles/liter). Curve 1—pH = 11.5 (freshly prepared); curve 2—pH = 10.2 (after 15 hr); curve 3—pH = 9.7 (after 64 hr); curve 4—pH = 6.1 (without alkali); curve 5—pH = 2.2.

CONCLUSIONS

1. The A-band in the spectra of the compounds investigated lies in the region $\lambda < 200$ mμ.
2. The B-band of phenol, dihydroxy-, and symmetrical trihydroxybenzene in the region 210-228 mμ is the analogue of the ^1L_a band of benzene.
3. The C-band of the above-mentioned compounds is more mobile than the B-band, lies in the region 265-290 mμ, and originates from the ^1L_b band of benzene. Being very weak in benzene, it becomes much more intense in the hydroxybenzenes, but remains always weaker than the B-band.
4. The D-band detected in the spectra of alkaline solutions of pyrocatechol and hydroquinone does not have an analogue in the spectrum of benzene and is an $n \to \pi$ transition of ortho- and paraquinones.
5. The spectra of alkaline solutions show the presence of B^- and C^- bands due to the monovalent anions and the B^{--} and C^{--} bands due to the divalent anions, shifted as a rule towards the red region relative to the B^0 and C^0 bands of the undissociated molecules. A knowledge of the pH of the solution and the behavior of bands as a function of time is indispensable in order to interpret the spectra of alkaline solutions of hydroxybenzenes and to assign the bands to one or another component species. Bands exhibiting similar behavior as a function of time were assigned to the same species (anion).

REFERENCES

1. H. B. Klevens and J. R. Platt. J. Am. Chem. Soc. 71, 1714 (1949).
2. U. Nens and H. Staude. Z. wiss. Phot. 48, 7, 163 (1953);
   N. A. Valyashko and M. M. Shcherbak. Zhur. Obshchei Khim., Ser. A 8 (70), 1597 (1939);
   A. Saint-Maxens. J. chim. phys. 32, 161, 273, 410 (1935).
3. P. G. Wilkinson. Can. J. Phys. 34, 596 (1956);
   V. J. Hammond and W. C. Price. Trans. Faraday Soc. 51, 605 (1955);
   L. Pickett, M. Muntz and E. M. McPherson. J. Am. Chem. Soc. 73, 4862 (1951);
   H. B. Klevens and J. R. Platt. J. Chem. Phys. 17, 470 (1949);
   A. L. Sklar. Revs. Modern Phys. 14, 232 (1942).
4. V. M. Chulanovskii, T. G. Meister, and E. N. Struzhanskaya. Vestnik Leningrad. Gosudarst. Univ., No. 2, 143 (1955);
   V. Keussler. Z. Elektrochem. 58, 136 (1954).
5. W. Lüttke and R. Mecke. Z. physik. Chem. 196, 56 (1950);
   L. Joule, G. Carpeni, and Y. Hammann. Bull. Soc. chim. France 3, 448 (1956).
6. S. G. Bogomolov, M. N. Grebenshchikova, and L. Ya. Liplavk. Fiz. Sbornik Lvov. Gosudarst. Univ. 3 (8), 270 (1957).
7. W. Flaig, Th. Ploetz, and A. Küllmer. Z. Naturforsch. 10b, 668 (1955).
8. J. W. Sidman. Chem. Revs. 58, No. 4, 689 (1958);
   H. McConnel. J. Chem. Phys. 20, 700 (1952);
   M. Kasha. Discussions Faraday Soc. 9, 14 (1950).
9. R. A. Friedel and M. Orchin. "Ultraviolet Spectra of Aromatic Compounds," New York.
10. H. Staude and M. Teupel. Z. Elektrochem. 61, 181 (1957).
11. H. Köhler and G. Scheibe. Z. anorg. u. allgem. Chem. 285, 221 (1956).

SPECTRAL INVESTIGATION OF THE ADSORPTION OF WATER ON POROUS GLASS AS A FUNCTION OF THE DEGREE OF HYDRATION OF ITS SURFACE

A. N. Sidorov

Received 17 October 1959

The infrared absorption spectra of porous glass with a varying content of free hydroxyl groups (OH_{free}) and of hydroxyl groups perturbed by a hydrogen bond from one to another ($OH_{pert.}$) on its surface have been investigated. The conclusion is drawn that the OH_{free} groups are not adsorption centers for water molecules. The adsorption of water by porous glass is determined by the $OH_{pert.}$ groups in the case of a hydrated surface and by centers of the second kind in the case of a surface dehydrated as a result of thermal treatment in vacuum. The state of the water molecules bonded to centers of the second kind is apparently intermediate between the physisorbed and chemisorbed states. On the surface of methylated porous glass, as opposed to ordinary porous glass, the $OH_{pert.}$ groups take no part in the process of water adsorption.

In recent years, the idea of the nonuniformity of the surface of a silicate adsorbent toward the adsorbed molecules has spread through works concerned with the study of adsorption. This nonuniformity consists first of all in the existence, on a silicate surface, of at least two types of adsorption centers: hydroxyl groups and centers of the second kind—supposedly silicon or oxygen atoms.[1-4] The hydroxylic covering of the surface of the adsorbent is nonuniform in its turn: it consists of free OH groups and of OH groups linked together by a hydrogen bond.[3, 5, 6] The question of the nature of the adsorption centers of the second kind and of the behavior of the free and bonded hydroxyl groups during their interaction with the adsorbed molecules still remains unsolved. The article here offered to the reader's attention has as its goal the clarification of this question on the occasion of an investigation, with the help of infrared absorption spectra, of the adsorption of water on porous glass.

EXPERIMENTAL PROCEDURE

The samples of porous glass were prepared from discs of DV-1 sodium borosilicate glass 0.1-1.0 mm in thickness by treating them in 3N hydrochloric acid at 20°C followed by washing in distilled water. The samples obtained had a specific surface of about 200 $meter^2/gm$ and pore diameters of the order of 25 A. The vacuum treatment, the procedures for adsorption and methylation of the porous glass, and the taking of the spectra were carried out in the previously-described[2] glass vacuum cell.

The spectra were taken on a UR-10 spectrophotometer of the firm of Carl Zeiss, Jena, with a lithium fluoride prism. During measurement of the intensity of the narrow absorption band of free OH groups at 3749 cm^{-1}, the spectral slit width was 4 cm^{-1}. The width of the absorption band at 3749 cm^{-1}, which varied with the temperature to which the porous glass was heated in vacuum, was not less than 8 cm^{-1}.

RESULTS AND DISCUSSION

Adsorption of water on ordinary porous glass. Let us consider the influence of the temperature of dehydration of the porous glass on the properties of its surface. In Fig. 1 are depicted the spectra of porous glass heated in vacuum at various temperatures. In these spectra, a broad absorption band which is associated with the vibrations of surface $OH_{pert.}$ groups, perturbed by a hydrogen bond from one to another,[3, 5, 6] adjoins the low-frequency wing of the narrow absorption band around 3749 cm^{-1}, which corresponds to vibrations of the free OH_{free} groups.[2] If the temperature of heating is not great (around 100°C), the absorption bands of adsorbed water around 3665 and 3450 cm^{-1} overlap the $OH_{pert.}$ band (curve 1, Fig. 1). After heating at 300°C, practically no adsorbed water remains on the surface of silicate adsorbents,[7] and we may consider that curve 2, Fig. 1 represents the superposition of only two absorption bands: the OH_{free} band at 3749 cm^{-1} and the $OH_{pert.}$ band which overlaps it on the low-frequency side. We note that the $OH_{pert.}$ band is not resolved, in consequence of which it is difficult to determine its position in the spectrum with sufficient accuracy. Furthermore, it is asymmetric; it has a steep high-frequency slope but a gradual low-frequency one. The asymmetry of the $OH_{pert.}$ band may be explained by the fact that different $OH_{pert.}$ groups are perturbed to different degrees by the interaction among them, as a result of the different distances of one from another. The greater the distance between the $OH_{pert.}$ groups, the less the width of the corresponding absorption band and the greater the frequency of its maximum. The existence of a definite distribution of the OH groups with respect to their distance one from another also produces asymmetry of the $OH_{pert.}$ absorption band.

The intensity of the corresponding absorption bands may serve as a criterion of the quantity of hydroxyl groups on the surface of the adsorbent. Measurements

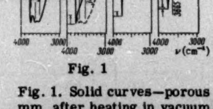

Fig. 1

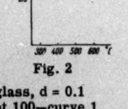

Fig. 2

Fig. 1. Solid curves—porous glass, d = 0.1 mm, after heating in vacuum at 100—curve 1, 300—curve 2, 540—curve 3, and 650°C—curve 4; dashed curves—the same after 30 min standing in water vapor at p = 16 mm Hg and sample temperature 25-30°C. The vertical arrows show the diminution in the intensity of the OH_{free} band on adsorption of water.

Fig. 2. Dependence of the peak intensity of the 3749 cm^{-1} band on the temperature of vacuum heating of the porous glass.

of the intensity of the $OH_{pert.}$ band are made difficult by the fact that this band is unresolved and asymmetric. However, by comparing the curves presented in Fig. 1, it may be asserted that, as the temperature of heating rises, the intensity of the $OH_{pert.}$ band falls considerably more rapidly than the intensity of the OH_{free} band. This was to be expected, since a hydrogen bond favors the removal of hydroxyl groups from the surface of the adsorbent when it is heated in vacuum. The change in the intensity of the OH_{free} band at 3749 cm^{-1} on thermal dehydration of porous glass is characterized by the curve depicted in Fig. 2. This curve shows that after heating porous glass to 600°C about 70% of the maximum quantity of OH_{free} groups (the maximum is found at 200-300°C) still remains on its surface. Together with this, it is well known that the adsorption of water on porous glass at low pressures of its vapor is significantly lowered as the temperature of heating is raised. At 600°C, the adsorption of water at a relative pressure of 0.1 is lowered by a factor of 5.5 compared with its maximum value (at 200°C).[7] Hence it follows that the free hydroxyl groups to which the narrow absorption band at 3749 cm^{-1} corresponds are not the centers which determine the adsorption of water at low relative pressures of its vapor. Either centers of the second kind or $OH_{pert.}$ groups, to which the relatively broad absorption band which overlaps the band of the OH_{free} groups corresponds, are the adsorption centers in this case. Which of these centers plays the determining role in water adsorption depends on the degree of hydration of the porous glass surface (see below).

It has been shown in the work of Zhdanov that pairs of hydroxyls are the adsorption centers for water molecules on the surface of porous glass.[7] Such pairs evidently consist of $OH_{pert.}$ groups. The adsorbing power of an OH_{free} group toward a water molecule is not independent and manifests itself only when another hydroxyl or adsorbed water molecule is located nearby, forming a pair with the OH_{free} group. This may take place either at high pressures of water vapor or during adsorption on an unheated sample of porous glass. In the light of what has been said, the low sensitivity of the OH_{free} absorption band toward the adsorption of water (see references 1, 2 and also Fig. 1) becomes understandable.

The adsorption of water on porous glass leads to the appearance in its spectrum of absorption bands at 3450 cm^{-1} (water molecules adsorbed on hydroxyl groups) and at 3665 cm^{-1} (water molecules on centers of the second king).[1,2] The intensity of these bands, and consequently the distribution of the water molecules between the corresponding adsorption centers, depends on the relative pressure of water vapor in the cell with the sample and on the degree of hydration of the porous glass. The dependence of the adsorption of water on partially dehydrated porous glass on the pressure of the vapor has previously been investigated qualitatively.[1,2] Figure 1 enables us to decide how the adsorption of water on porous glass depends on the degree of hydration of its surface at a relative pressure of water vapor of the order of 0.5-0.7. It can be seen from the figure that the intensity of the absorption band at 3450 cm^{-1} diminishes with the dehydration of the surface. This is evidently explained by the diminution in the quantity of $OH_{pert.}$ groups and the proportional diminution in the quantity of water molecules adsorbed on them. The intensity of the band at 3665 cm^{-1}, within the limits of error of the measurements, does not change with the dehydration of the surface. These facts confirm the interpretation given by us for the absorption bands at 3450 and 3665 cm^{-1}. The intensity ratio of these bands shows that, in the case of hydrated porous glass, the quantity of adsorbed water is determined by the quantity of $OH_{pert.}$ groups. Although in this case the water molecules also attach themselves to centers of the second kind, the quantity of these centers is small in comparison with the quantity of $OH_{pert.}$ groups. As the dehydration of the surface increases, the quantity of centers of the second kind, at an approximate estimate, remains constant, but their fraction increases in consequence of the decrease in the quantity of $OH_{pert.}$ groups, and after heating of porous glass at temperatures above 550°C, the adsorption of water takes place predominantly on centers of the second kind.

It is curious to note that as the dehydration of porous glass increases the power of the OH_{free} groups to interact with water molecules diminishes (in Fig. 1, see the change in the intensity of the band at 3749 cm^{-1} on adsorption of water, as a function of the temperature of heating). This confirms the conclusion drawn above concerning the nonindependent character of the adsorbing power of the OH_{free} groups.

What is the state of the water molecules adsorbed on centers of the second kind in porous glass? These molecules must not be identified with the $OH_{pert.}$ groups (see curves 2 and 4 in Fig. 1: the band at 3665 cm^{-1} in curve 4 is clearly separated from the 3749 cm^{-1} band, while the $OH_{pert.}$ band in curve 2 is not resolved). These molecules, furthermore, do not undergo the chemical changes associated with the rupture of bonds and transformation into some kind of hydroxyl groups. Two facts serve as evidence of this: first, the relatively easy removal of these molecules on pumping, and secondly, the difference in the frequencies of the absorption bands of D_2O and HDO adsorbed on centers of the second kind.[2] It is possible that water molecules which are bonded to centers of the second kind by stronger forces than the forces of interaction between water molecules and $OH_{pert.}$ groups are in a state intermediate between the physisorbed and chemisorbed states. Under certain conditions (prolonged standing in liquid water), such molecules may possibly go over into the chemisorbed state, being transformed into hydroxyl groups, which leads to rehydration of the surface of the adsorbent.

Adsorption of water on methylated porous glass. It is known that on heating porous glass in methanol vapor the OH_{free} groups are replaced by methoxyl groups, OCH_3—methylation of the surface of the adsorbent takes place.[1,2] In the spectrum of methylated porous glass, there remains a broad absorption band at 3680 cm^{-1} in the region of the characteristic vibrations of OH groups: The intensity of this band diminishes as the temperature of methylation and subsequent vacuum treatment of the sample is increased, and, on adsorption of heavy water on methylated porous glass, the band shifts into the region of the characteristic vibrations of OD bonds. This enables us to draw the conclusion that the absorption band at 3680 cm^{-1} corresponds to vibrations of the surface $OH_{pert.}$ groups, which, in contradistinction to the OH_{free} groups, either do not enter into reaction with the methanol molecules at all, or else react with them at a higher temperature than the OH_{free} groups.*

In Fig. 3 are presented the spectra of two samples of porous glass, one of which was methylated at 430°C and the other at 550°C. After methylation, the samples were subjected to vacuum treatment for one hour at the same temperature as the one at which methylation took place. In the spectrum of the sample methylated at 550°C, the absorption band of the $OH_{pert.}$ groups is absent. In the spectrum of the sample methylated at 430°C, it is fairly intense. Let us compare the adsorbing power of the two samples toward water vapor. As can be seen from Fig. 3 (curves 2 and 3), this power, if we allow for the superposition of the absorption bands of $OH_{pert.}$ and of adsorbed water, differs only slightly for the two samples. In both cases, an intense absorption band at 3660 cm^{-1} is observed (at a pressure of 15 mm Hg of water vapor, the maximum of this band shifts to 3640 cm^{-1}), and on the slope of this band there is a relatively weak shoulder at approximately 3500 cm^{-1}, the origin of which may be explained either by the interaction of adsorbed water molecules with one another or by the activity, in the infrared spectrum, of various types of vibrations of these molecules. The similarity in the adsorbing power of samples of methylated porous glass which did or did not contain $OH_{pert.}$ groups enables us to assert that these groups on a methylated porous glass surface do not take part in the process of adsorption of water molecules. This conclusion is corroborated by the fact that in the spectrum of methylated porous glass with adsorbed water at high relative pressures of its vapor the intense absorption band at 3450 cm^{-1}, which corresponds to H_2O molecules adsorbed on $OH_{pert.}$ groups, is absent. The absorption band at 3660 cm^{-1} in the spectrum of methylated porous glass with adsorbed water, just like the 3665 cm^{-1} band in the spectrum of ordinary porous glass, belongs to H_2O molecules adsorbed on centers of the second kind. In order to verify that $OH_{pert.}$ groups were not formed in the process of adsorption of water on the surface of a sample of methylated porous glass which had no hydroxyl groups up to the time of adsorption, both samples of methylated porous glass were subjected to vacuum treatment at 400°C after the water-adsorption experiments. Subsequent spectral measurements (curve 4, Fig. 3) showed that $OH_{pert.}$ groups did not arise in the process of adsorption of water. Only an insignificant replacement of OCH_3 groups by OH_{free} groups (weak bands at 3749 cm^{-1} appeared in the spectra of both samples) took place, which could not substantially influence the results of the experiment.

---

*In reference 1, an incorrect interpretation was given to the absorption band at 3680 cm^{-1} in the spectrum of methylated porous glass; it was assigned not to vibrations of OH groups, but to vibrations of other bonds. An admixture of H_2O in the heavy water when its vapors were adsorbed on the sample under study was apparently the cause of the error.

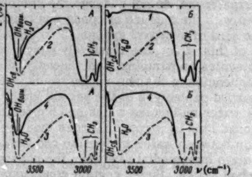

Fig. 3. Spectra of methylated porous glasses, d = 1.0 mm. A—sample methylated at 430°C; B—sample methylated at 550°C. Curve 1—before adsorption of water; curve 2—after 15 min standing in water vapor at p = 4 mm Hg; curve 3—after 17 hr standing in water vapor at p = 4 mm Hg; curve 4—after vacuum treatment of the samples for 2 hr at 400°C.

The author expresses his deep gratitude to A. N. Terenin, under whose direction the work was done, and to I. P. Kotlyar for his help in carrying out the experiments.

REFERENCES

1. A. N. Sidorov. Zhur. Fiz. Khim. 30, 995 (1956).
2. A. N. Terenin and A. N. Sidorov. Opt.-Mekh. Promyshl. No. 1, 1 (1959)?
3. M. Folman and D. J. C. Yates. Proc. Roy. Soc. **A246**, 32 (1958); Trans. Faraday Soc. 54, 1684 (1958); J. Phys. Chem. 63, 183 (1959).
4. N. Sheppard. Conf. Molecular Spectroscopy, London, 1958, p. 277. Pergamon Press, London, 1959; Spectrochimica Acta 14, 249 (1959).
5. A. V. Kiselev and V. I. Lygin. Proc. Second Intern. Congr. of Surface Activity, Vol. 2, p. 204, Butterworths, London, 1957;
V. I. Lygin. Vestnik Moskov. Gosudarst. Univ., Ser. Mat., Mekh., Astron., Fiz., Khim. No. 1, 223 (1958).
6. R. S. McDonald. J. Phys. Chem. 62, 1168 (1958).
7. S. P. Zhdanov. Zhur. Fiz. Khim. 32, 669 (1958).

PARAMAGNETIC RESONANCE SPECTRA OF FLUOROALKYL AND NITROSEFLUOROALKYL RADICALS IN IRRADIATED TEFLON

Ya. S. Lebedev, Iu. D. Tsvetkov, and V. V. Voevodskii

Received 21 September 1959

Paramagnetic resonance spectra of fluoroalkyl and nitrosofluoroalkyl radicals in irradiated Teflon have been obtained at high temperature. The hyperfine structure has been analyzed and the dependence of line width on temperature studied. The results of the measurements are compared with theoretical and experimental data from the literature.

The paramagnetic resonance (EPR) spectra of fluoroalkyl radicals

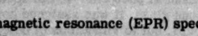

$$\underset{(\gamma)}{\sim CF_2}-\underset{(\beta)}{CF_2}-\underset{(\alpha)}{\dot{C}F}-\underset{(\beta)}{CF_2}-\underset{(\gamma)}{CF_2\sim},$$

obtained by irradiating Teflon in vacuo are now well known. In previous investigations spectra have been observed consisting of ten hyperfine structure components, arising from interaction of the unpaired electron with the fluorine atoms in the α- and β-positions. The magnitude of the splitting arising from the fluorine atom in the α-position relative to the free valence amounts to 93 oe, and that arising from the β-fluorine atom is 31 oe. A partial superposition of hyperfine components occurs at the middle of the spectrum. The great stability of fluoroalkyl radicals has likewise been noted earlier. (Kinetic data on their reactions with oxygen have been obtained up to 300°C.[3])

Results of a high temperature investigation of the EPR spectra of fluoroalkyl and nitrosofluoroalkyl radi-

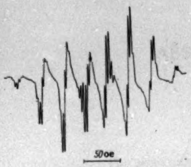

Fig. 1

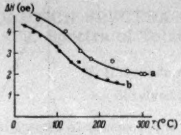

Fig. 2

Fig. 1. EPR spectrum of fluoroalkyl radical at 250°C. Experimental conditions: amplitude of the high frequency modulation 1 oe; magnetic field scanning rate 0.35 oe/sec; time constant 0.5 sec.

Fig. 2. Dependence of the half width of the EPR line on temperature for fluoroalkyl (curve a) and nitrosofluoroalkyl (curve b) radicals.

cals are presented in the present communication. A spectrometer with high frequency (300 kc) field modulation, similar to one described earlier,[4] was used for the measurements. The temperature of the sample was maintained by means of a stream of heated air.

At high temperatures the spectra of fluoroalkyl radicals exhibit an additional hyperfine splitting, arising from interaction of the unpaired electron with the fluorine atoms in the γ-positions (Fig. 1). Analysis of the spectrum shown in Fig. 1 shows that each of the 10 components is split in turn into 5 lines, consistent with an interaction with the four equivalent γ-fluorine atoms. It is difficult to check the agreement of the intensities with this picture, since the lines are incompletely resolved. The central part of the spectrum is complicated by a partial masking by the β-components. The γ-splitting is 3.5 oe.

The widths of the various γ-components were measured in this work at a number of temperatures. It was found that the lines become broader with decreasing temperature (Fig. 2), so that at room temperature the γ-components cannot be resolved. It is clear from Fig. 3 that further lowering of the temperature in the region 16°-22°C likewise results in a broadening of the β-components, so that below 0°C the hyperfine splitting from the α- and β-fluorine atoms vanishes completely.

Gordy[2] noticed that the reaction of NO with fluoroalkyl radicals resulted in the disappearance of the EPR spectrum. We have established that simultaneous with the disappearance of the primary fluoroalkyl radical spectrum there appears a complicated spectrum of a new radical (Fig. 4). This spectrum can be satisfactorily resolved only at high temperatures (100°-200°C), and is not seen at room temperature on account of the broadening of its components (Fig. 2). Inasmuch as it is asymmetric and incompletely resolved even at high temperatures, its interpretation is difficult. We propose that this spectrum belongs to a nitrosofluoroalkyl radical

$$\sim CF_2-CF_2-\dot{C}(NO)-CF_2-CF_2\sim$$

and consists of a quintet of 14.5 oe splitting from the four β-fluorine atoms, each line of which is in turn split into 3 components of equal intensity by interaction with the nitrogen atom (nuclear spin I = 1). If we adopt such a model, the EPR lines must fall into 7 groups, whose integrated intensities are in the ratios 1 : 5 : 11 : 14 : 11 : 5 : 1. Such a relationship is in satisfactory agreement with the experimental facts, as is shown in Fig. 4.

The asymmetry of the EPR spectrum may be explained by saying that the components with different Δg are broadened to different extents, as occurs, for example, in solutions of $CuCl_2$.[5] It is interesting to note that the theory worked out by McConnell[5] to explain this phenomenon predicts a temperature dependence of the line width as well.

The mechanism by which the radical $\sim CF_2-\dot{C}(NO)-CF_2\sim$ is produced may be described as follows: In the first stop, an NO radical unites with the free valence of a fluoroalkyl radical, forming a neutral molecule. Because of a redistribution of electron density the bond $C-F^{(\alpha)}$ is weakened, and another NO radical can abstract a fluorine atom from the α-position to create a nitrosofluoroalkyl radical. This mechanism explains not only the structure of the spectrum but also the fact that, according to the preliminary data, the growth in concentration of the nitrosofluoroalkyl radical lags behind the decrease in concentration of the fluoroalkyl radical. Of course the concentration of the nitrosofluoroalkyl radical is smaller than that of its precursor and depends on the temperature at which the reaction occurs.

It should be remarked that the new radical is remarkably stable, and does not react with O_2 or H_2 (even at temperatures as high at 200°C). However, the EPR spectrum gradually disappears at temperatures higher than 200°C, possibly because the radical reacts with dissolved NO.

The data presented above on the EPR splittings of fluoroalkyl and nitrosofluoroalkyl radicals show that the unpaired electron in the latter has an appreciable density at the nitrogen atom. Actually the β-fluorine splitting in the nitrosofluoroalkyl radical (14.5 oe) is half as large as that in the fluoroalkyl radical, whereas the nitrogen splitting (12.3 oe) has the same value that is found in radicals of similar structure, where the unpaired electron is mainly localized on the nitrogen atom (for example, di-

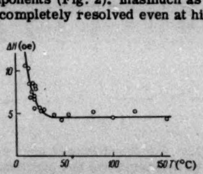

Fig. 3. Dependence on temperature of the half width of the β-component in the EPR spectrum of the fluoroalkyl radical.

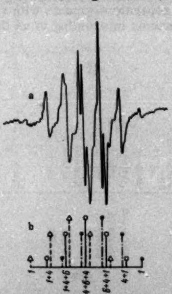

Fig. 4. EPR spectrum of the nitrosofluoroalkyl radical at 150°C (a) and comparison with theoretical intensities (b).

phenylnitrile oxide,[6] and nitrobenzene negative ion[7]). The small reactivity of the nitrosofluoroalkyl radical confirms its similarity to the stable radicals just mentioned.

Gordy[2] has examined possible mechanisms of interaction of the unpaired electron with the α- and β-fluorine atoms in the fluoroalkyl radical. The interaction with the γ-fluorine atoms evidently arises through a superposition of the mechanisms responsible for the α- and β-splittings. The hyperfine splittings in the nitrosofluoroalkyl radical can be explained in the same manner.

Broadening of the lines with decreasing temperature (Fig. 2) is usually explained as the influence of an anisotropic dipole-dipole interaction.[8] At high temperatures, the thermal motions of the surrounding atoms (that is, rotations of groups of atoms about chemical bonds, vibrations, and motions of other sorts) averages out the anisotropic interaction and removes the line broadening. In such a case, if the frequency of the motion is smaller than the splitting (in frequency units), the spectrum will not be resolved. Proceeding thus, it is possible to explain why curves a and b in Fig. 2 are perfectly parallel. Actually the temperature dependence of the line width is caused by motions of more or less distant atoms, whose properties are not changed by substituting NO for F. The temperature of the transition (the abscissa of the inflection point of the curve) is the same in both cases and lies at about 135°C. From the line width at this point one can say that the frequency of the averaging motion is about 8 Mc. Similar transitions have been observed earlier in Teflon in the line width of the nuclear magnetic resonance (NMR) and in the absorption of sound of various frequencies.[9, 10] In those investigations, it was proposed that the transitions mentioned are caused by the same internal motions, in which case the dependence of transition frequency on temperature may be written in the conventional manner:

$$\nu = \nu_0 e^{-\frac{\varepsilon}{RT}}. \qquad (1)$$

In reference 10, a straight line on a log ν vs 1/T plot was drawn through the three points obtained, and an activation energy ε of 7.7 kcal/mole determined. The points mentioned are represented by the various circles in Fig. 5, and the dots show our data, obtained from the investigation of EPR line broadening. It is evident from the figure that the depencence (1) is confirmed. The wide temperature interval permits an accurate determination of the activation energy, which is 8.6 ± 0.5 kcal/mole. It is reasonable that this value represents the potential barrier to rotation of separate segments with respect to the polymer chain. It seems interesting to us that (1) is fulfilled over such a wide range of temperature and frequency.

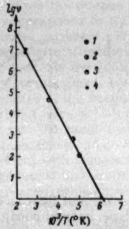

Fig. 5. Dependence of the transition frequency on temperature. 1—sound absorption at 115 cps; 2—sound absorption at 683 cps; 3—NMR line broadening; 4—EPR line broadening.

Broadening of the β-component of the spectrum occurs in the interval 16°-22°C, and is evidently not connected with the above mechanism. It is possible that this broadening is connected with a first order phase transition which occurs in Teflon at these temperatures.[11]

REFERENCES

1. Iu. D. Tsvetkov and N. N. Bubnov et al. Doklady Akad. Nauk SSSR **122**, 1053 (1958).
2. H. N. Rexroad and W. Gordy. J. Chem. Phys. **30**, 399 (1959).
3. Iu. D. Tsvetkov, Ya. S. Lebedev, and V. V. Voevodskii. High Molecular Weight Compounds **1**, 1519 (1959).
4. A. G. Semenov, N. N. Bubnov. Apparatus and Technique of Experiment, **1**, 92 (1959).
5. H. M. McConnell. J. Chem. Phys. **25**, 709 (1956).
6. R. Hoskins. J. Chem. Phys. **25**, 788 (1956).
7. R. L. Ward and M. P. Klein. J. Chem. Phys. **28**, 518 (1958).
8. D. J. E. Ingram. "Free Radicals as Studied by Electron Spin Resonance," London, 1958.
9. J. A. S. Smith. Discussions Faraday Soc. **19**, 207 (1955).
10. J. G. Powles and J. A. E. Kail. J. Polymer Sci. **31**, 183 (1958).
11. N. G. McCrum. J. Polymer Sci. **34**, 355 (1959).

ABSORPTION SPECTRA OF BENZENE HOMOLOGUES

V. Spectra of Toluene Crystals at 20°K

V. L. Broude and M. I. Onoprienko

Received 21 October 1959

The absorption spectra of toluene in the amorphous and crystalline states at 20°K were obtained and interpreted. From a comparison of the spectra of benzene and toluene the nonequivalence of the aromatic bonds C—C in the toluene molecule was proposed. By comparing the absorption spectra of two crystalline modifications of toluene, it was concluded that the broad and diffuse appearance of the spectral bands in the low temperature modification are related to imperfections of these crystals and to their mechanical deformation on cooling.

In this work the analysis of the absorption spectra of toluene in amorphous and crystalline states is presented. The conclusions reached in a previous article[1] have made it possible to make a more thorough interpretation of several special characteristics of these spectra.

Earlier[2] we made an analysis of the absorption spectra of crystalline toluene at 77°K. This temperature, however, was not sufficiently low for the analysis of vibrational structure of the spectrum. The present investigation, conducted at 20°K, was undertaken for a study of the fine structure in the toluene spectra.

The main physical constants of the toluene reagent which was at our disposal are as follows: M.Pt. = −95.00°C, B. Pt. = 110°C, $d_4^{20} = 0.86694$, $n_D^{20} = 1.4970$, purity 99.6%. The reagent was prepared and purified in the laboratory of A. L. Liberman (Institute of Organic Chemistry, Academy of Sciences of the USSR). Data on the crystallization of toluene and the characteristics of its crystalline modifications were described elsewhere.[2]

The spectra of single crystals using polarized light were obtained with the aid of an ISP-22 spectroscope. The samples were prepared and cooled in a metallic cryostat with special adapters.[3]

1. The absorption spectrum of amorphous toluene consists of a small number of smeared out bands whose widths attain 150 cm⁻¹ (Fig. 1). The whole spectrum is easily brought into one to one correspondence with the spectrum of the vapor phase if the center of the first intense band at 37130 cm⁻¹ is taken to be that of the pure electronic transition, which corresponds to a bathochromic shift of 350 cm⁻¹ with respect to the vapor phase. It must be noted that the lowering of temperature from 77° to 20°K does not affect the position or shape of the spectrum, within the accuracy of measurement.

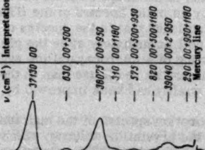

Fig. 1

The three most intense bands are related to the pure electronic transition, and are separated by a period of about 950 cm⁻¹, which is caused by the superposition of two close totally symmetric frequencies of the molecule (934 and 964 cm⁻¹). About 500 cm⁻¹ away from the pure electronic transition there is a weak diffuse band, with a similar period of about 950 cm⁻¹. These bands correspond to combinations with the vibration frequencies 455 and 530 cm⁻¹ (see below).

2. The absorption spectrum of the low temperature crystalline modification of toluene (LTM) also consists of broad bands, which render a similar interpretation quite difficult.

We have succeeded in growing LTM crystals, whose developed surfaces belong to two different planes of the lattice. The birefringence of these samples differs by a factor of two to three for the same thickness. The spectra of these samples are shown in Fig. 2. The practically complete coincidence of one of the components of the sample I spectrum with one of the components of the sample II spectrum points to the fact that the investigated planes of the lattice apparently possess one edge in common.

In the second component of the sample II spectrum a series of characteristic features is observed. The pure

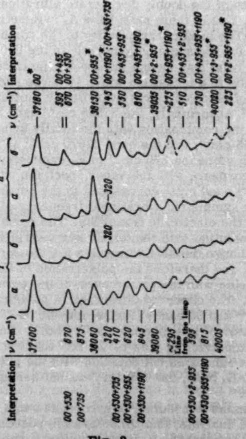

Fig. 2

The asterisk designates vibrations of split bands, the frequencies for which were calculated from their center of gravity.

electronic transition band in this spectrum is shifted by 80 cm^{-1} towards the short wavelength region. Analogous shifts are observed for all the bands periodically connected with it by the vibration 950 cm^{-1}. The remaining bands of this component are not shifted. One's attention is drawn to the pronounced weakening of the band 37875 cm^{-1}, which in this component may be observed only in very thick samples (more than 5 μ).

The position of the pure electronic transition in both components of sample I and of one of the components of sample II correspond to the frequency 37100 cm^{-1}, whereas in the second component of sample II it corresponds to the frequency 37180 cm^{-1} (Fig. 2). Thus, in the first case, all vibrational intervals are shifted higher with respect to the spectrum of toluene in the vapor phase and in the second case, lower.[4] This, generally speaking, may serve as an argument in favor of the fact that the bands 37100 and 37180 cm^{-1} are components of the exciton splitting of the pure electronic transition of the molecule in the field of the crystal. If, for the theoretical position of the pure electronic transition, one takes the center between the two bands of the doublet (37140 cm^{-1}), then one obtains for the vibrations of molecules magnitudes which are close to those obtained from the spectral analysis of the vapor phase. As for the relatively wide and strongly polarized bands 38060 and 38130 cm^{-1}, they correspond to the combination of the pure electronic transition with the two molecular frequencies 934 and 964 cm^{-1} which are superimposed.

The splitting is observed only for the pure electronic transition and for its combination with vibration 955 cm^{-1}. The remaining bands, although they originate from the combination with other totally symmetric vibrations, do not show any observable splitting.

The 37595 and 37670 cm^{-1} bands of the crystal spectrum must be related to the 37932 and 38005 cm^{-1} bands of the vapor spectrum. They correspond[4] to the combination of the pure electronic transition with the split components of the doubly degenerate vibration of benzene, E_{2g}. One of them must have A_1 symmetry and the other B_1. The band corresponding to the combination with A_1 must have the same polarization as the 0-0 transition. The other band may have a different polarization, since it corresponds to a transition which is perpendicular to the direction of electronic transition dipole moment in the molecule.[2] Accordingly, the 37595 cm^{-1} band is interpreted as the combination with the totally symmetric vibration 455 cm^{-1}, and the band 37670 cm^{-1} as the combination with vibration 530 cm^{-1} of B_1 symmetry.

In accordance with the vapor spectrum analysis the 37875 cm^{-1} band must correspond to the combination of the totally symmetric vibrational frequency of about 750 cm^{-1} with the electronic transition. The combination of the 0-0 transition with the totally symmetric vibration does not change the selection rules for the corresponding transition, and therefore the polarization of this band must coincide with the polarization of the pure electronic transition. The observed difference in polarization of the 37875 cm^{-1} and 00 bands (Fig. 2) may be used as an argument in favor of interpreting the 735 cm^{-1} vibration as non-totally symmetric. In view of the fact that the polarization of this band does not coincide with the polarization of the 00 + B_1 band, the 735 cm^{-1} cannot belong to B_1 type symmetry.

It remains to assume, in accordance with group theoretical analysis, that this vibration possesses A_2 symmetry and that the corresponding absorption band is polarized in the direction which is normal to the plane of the molecule. In this case a difficulty arises in the interpretation of 38410 cm^{-1} band (Fig. 2), since a consistent analysis leads to the fact that the corresponding transition (00 + 530 + 735) must be forbidden.

The comparison of the absorption spectrum of the LTM toluene crystal with the spectra of crystals in which the interaction between electronic transitions and phonons is large (cf. classification in §3, reference 1) points to several significant differences. Thus, in the spectra of the latter the fundamental absorption bands are broad at all, even very low temperatures. At the same time, however, these bands are definitely not diffuse and possess very sharply defined borders; besides, together with these broad bands there are always present several weaker bands, whose width and sharpness differ but little from the bands observed in the crystals exhibiting small forces of interaction with phonons. These two characteristics are not observed in the spectrum of the LTM toluene crystal, in which all the bands, including the very weak ones, are diffuse and equally broad.

On the other hand the general appearance of the absorption spectrum of the LTM toluene crystal is very similar to those observed in crystals that have been subjected to mechanical deformation.[1] Such a comparison is not in any way inconsistent, since it may be assumed that the peculiar characteristics of the spectrum of the LTM toluene crystal may be related to internal stresses of the crystalline sample. These stresses may be caused by imperfections in the LTM crystals, which were grown directly from a glassy mass, and which in contrast to the HTM crystals could not be improved by recrystallization in the vicinity of the melting point.[2]

One of the characteristic differences in the spectrum of the LTM crystal compared to that of the high temperature modification (HTM) crystal consists also of a very significant splitting of the 00 band (Fig. 2). This splitting amounts to 80 cm^{-1}. In view of the above discussion, however, it may be erroneous to explain this splitting as having exciton origin. If the assumption regarding the deformation of LTM crystals is correct, then this splitting is analogous to the splitting of diffuse bands of the previously investigated stressed crystals of anthracene and naphthalene,[5] whose nature and relation with exciton absorption have not still been clarified.

To some extent, an additional argument in favor of the assumption that the LTM crystals of toluene are under stressed condition at 20°K is afforded by the relatively large shift observed in the LTM spectrum which takes place when the temperature is lowered from 77° to 20°K. This shift amounts to 70 cm^{-1} and surpasses in magnitude all other temperature shifts in crystals previously observed in this temperature interval. If the crystal is in the deformed state, then according to our observations,[5] in parallel with the broadening of absorption bands there may be observed a shift which, for example in naphthalene, may attain 100 cm^{-1}.

The variation in the shape of absorption bands was also observed by us in the spectra of the HTM crystals. Thus it was established that in the spectra of crystals obtained in the cell immediately after the phase transition, and consisting of a microcrystalline aggregate, the absorption bands are more diffuse than in the spectra of samples whose quality had been improved by recrystallization.

3. The absorption spectra of the high temperature modification of the crystalline toluene, which were obtained with polarized light at 20°K, are reproduced in Fig. 3. The spectral shift of the crystal with respect to the vapor phase amounts to 327 cm^{-1}. The shift between the two modifications is of the order of 10 cm^{-1}. The shift of the HTM crystal associated with cooling from 77° to 20°K amounts to a few cm^{-1}. The pure electronic transition and also certain electronic-vibrational bands of the HTM are split to a small extent (Fig. 4). The

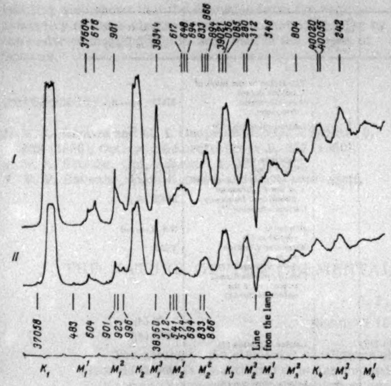

Fig. 3

amount of splitting does not exceed 10 cm⁻¹. The intensity of absorption in one component (I) is somewhat greater (this difference is not noted in the Table).

The molecular vibrations 454, 526, 751, 940, 969, and 1197 cm⁻¹ which are combined with the pure electronic transition singly or in combinations be identified from the spectrum (refer to the Table). Also the spectrum shows low intensity bands 333, 425, and 652 cm⁻¹ away from the 00 band. The difference of the polarization of the 37676 cm⁻¹ band from the polarization of the remaining bands agrees with the interpretation which assigns it as a combination with the non-totally symmetric vibration B_1, equal to 526 cm⁻¹.

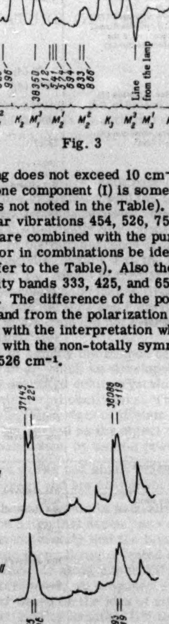

Fig. 4

If, in accordance with the analysis of the LTM crystal spectrum, the vibration 751 cm⁻¹ is assumed to be of A_2 symmetry, then the selection rules do not permit the interpretation of the 38429 cm⁻¹ band as being a combination of 526 and 751 cm⁻¹ vibrations. On the other hand, this vibration in the HTM has the same appearance as the other totally symmetric frequencies, and if we did not possess data on the LTM, it would have to be assigned to A_1 and not A_2 symmetry type. Besides, it must be noted, that this vibration practically coincides with the frequency found in the spectrum of the vapor phase, which is not true in the case of the LTM crystal.

At 20°K, some bands, whose origin is probably due to the lattice vibrations (refer to the Table), may be found in the spectrum of the HTM crystal. The weak and strongly polarized band at 37058 cm⁻¹ is apparently related either to impurities or to deformed portions of the crystal and corresponds to the electronic transition of the toluene molecule in the vicinity of such a defect. The 37996 cm⁻¹ band which has the same polarization corresponds to the combination of this transition with the totally symmetric molecular vibration with the 940 cm⁻¹ frequency.

All the remaining absorption bands of the HTM crystal are in good agreement with transitions in the molecule, which to a large extent preserves its individuality in the molecular crystal of toluene. In the spectra of thick samples (5-50 μ) there appear additional narrow bands in the intervals between the bands that have already been analyzed. The interpretation of these bands is difficult at present, although some of them undoubtedly belong to the lattice vibrations.

4. The crystalline structure of toluene has not been investigated to any great extent,[6] and the information on the structure and symmetry of the molecule within the crystal are unknown. Therefore, it seems to be in order to make some qualitative conclusions about the structure of the molecule from the spectra of the crystals.

As was previously shown in the case of benzene,[1] from the relative intensities of the bands corresponding to the pure electronic transition and combinations with the non-totally symmetric vibrations, it is possible to estimate the extent of deviation of the electron cloud of the six π-electrons from the hexagonal symmetry. In the toluene spectrum* the 00 + B_1 band has a notable intensity in comparison with the intensity of the 00 band. This shows that the symmetry of the π-electronic cloud is still close to the regular one. Therefore, it is possible, in the first order approximation, to take the relative intensity of the 00 and 00 + B_1 bands as being proportional to the deviation from regular symmetry, if this deviation is expressed in terms of the difference in the previously equivalent linear dimensions of the molecule.

In the spectrum of crystalline benzene the ratio of the intensities of the bands in which we are interested is 1:3 and results from a change in the linear dimensions of the molecule in the crystal by 0.4% compared to the free molecule.[1] In the toluene spectrum this ratio is ~5:1 and must correspond* to a change in the linear dimensions of the ring of the order of 6%. For the C—C bond, which is about 1.4 A, this corresponds to a change of 0.08 A. Such a deformation of the carbon skeleton of the benzene ring is caused by the perturbing action of the methyl radical and may already be observed in the free toluene molecule (vapor phase). This is not in contradiction with the electron diffraction investigations of the toluene vapor,[7] according to which a small difference in length may exist between the separate C—C linkages in the ring.

On the other hand, another magnitude characterizing the deviation of the six π-electrons from the regular symmetry is provided by the extent of splitting of the degenerate E_{2g} vibration of benzene.[1] In the spectrum of crystalline benzene this splitting amounts to 9 cm⁻¹.[8] In the toluene spectrum it attains 72 cm⁻¹. This variation in the

---

*In view of the fact that the LTM spectrum of toluene is affected by the deformation of the sample, here, and in what follows, the discussion will be limited to the spectrum of HTM.

*Assuming that the amplitudes of vibration in the benzene and toluene crystals are practically identical.

Identification	Band frequencies (cm^{-1})	Intensity*	Polarization**		Distance*** from 00 (cm^{-1})	Interpretation	Error in interpretation (cm^{-1})	Observations	Analogous bands in the vapor spectra (cm^{-1})
			Along the spectral components	Along the axes of the molecule					
K_1	37058	3	II	—	−92	$(00)_d$ (?)	—	Transition to the level of lattice defect	—
	145	10	I	x	0	00	—	Pure electronic transition	37477 ($A_1 \rightarrow B_1$)
	155	10	II						
	206	8	II	—	51	00 + 51	—	Lattice vibrations (?)	—
	221	10	I	—	76	00 + 76			
M_1^1	483	0	I = II	x	333	00 + 333	—	Molecular vibration (?)	37823 (?)
	575	1	I = II	x	425	00 + 425 (?)	—	Diffuse band	37913 (?)
	604	4	I = II	x	454	00 + 454	—	The splitting components of the E_{2g} benzene vibrational frequency	37934 (A_1)
	676	5	I > II	y	526	00 + 526			38005 (B_1)
	730	0	I > II	y	580	00 + 526 + 54	—	Lattice vibration (?)	
M_1^2	802	1	I = II	x	652	00 + 652	—	Molecular vibration (?)	Not observed
	901	7	I = II	x, z (?)	751	00 + 751	—	Molecular vibration A_1 or A_2 (?)	38228
	923	2	I = II	—	773	00 + 751 + 22	—	Lattice vibration (?)	—
	996	2	II > I	—	846	$(00)_{II}$ + 940 (?)	—	Electronic-vibrational transition in the defect center (?)	—
K_2	38088	10	I	x	943	00 + 940	—	—	38409 (A_1)
	093	9	II		938				
	119	10	I = II	x	969	00 + 969	—	—	38441 (A_1)
	148	6	I = II	—	998	00 + 940 + 58(?) 00 + 969 + 29(?)	—	Lattice vibration (?)	—
M_1^3	344	8	I	x	1199	00 + 1197	—	—	38666 (A_1)
	350	8	II		1195				
	370	5	I = II	—	1220	00 + 1197 + 20	—	Lattice vibration (?) (see text)	—
	429	3	I > II	?	1279	00 + 526 + 751 (?)	2		38757
M_2^1	512	2	I = II	x	1362	00 + 425 + 940	3	—	38840 (?)
	541	2	I = II	x	1391	00 + 454 + 940	3	—	38870
	574	2	I = II	x	1424	00 + 454 + 969	1	—	Not observed
	617	2	I > II	y	1467	00 + 526 + 940	1	—	38942
	648	2	I > II	y	1498	00 + 526 + 969	3	—	38972
	694	2	I = II	x	1544	00 + 1544 (?)	—	Molecular vibration (?)	Not observed
M_2^2	795	0	I = II	x	1645	00 + 454 + 1197	6	—	39124
	833	4	I = II	x	1683	00 + 940 + 751	8	—	39162
	866	4	I = II	x	1716	00 + 969 + 751	4	—	39204
	894	4	I = II	—	1744	00 + 969 + 751 + 28	—	Lattice vibration (?)	—
K_3	39021	4	I = II	x	1871	00 + 2.940	9	—	39341
	056	9	I = II	x	1906	00 + 940 + 969	3	—	39375
	085	9	I = II	x	1935	00 + 2.969	3	—	39406
	178	1	I > II	y	2028	00 + 526 + 2.751	0	Diffuse band	39513
M_3^2	280	7	I = II	x	2130	00 + 1197 + 940	7	—	36602
	312	8	I = II	x	2162	00 + 1197 + 969	1	—	36936
	362	1	I = II	?	2212	00 + 526 + 751 + 940?	5	—	36993
M_3^1	546	2	I = II	x	2396	00 + 2.1197	2	—	38953
	621	1	I > II	y	2471	00 + 526 + 2.969	7	—	39930
M_3^3	767	1	I = II	x	2617	00 + 2.940 + 751	14	—	Not observed
	804	2	I = II	x	2654	00 + 969 + 751 + 940	6	—	40135
K_4	960	1	I = II	x	2810	00 + 3.940	10	—	Not observed
	989	3	I = II	x	2839	00 + 2.940 + 969	10	—	40306
	40020	2	I = II	x	2870	00 + 940 + 2.969	8	—	40337
	055	1	I = II	x	2905	00 + 3.969; 751 + 969 + 1197	2/12	Diffuse band	40384
M_4^2	209	1	I = II	x	3059	00 + 1197 + 2.940	18	—	Not observed
	242	3	I = II	x	3092	00 + 1197 + 940 + 969	14	Diffuse band	40565
	271	2	I = II	x	3121	00 + 1197 + 2.969	14	Same	Not observed
M_4^1	495	1	I = II	x	3345	00 + 2.1197 + 940	11	"	40816
	530	1	I = II	y	3380	00 + 526 + 3.940/969	—	"	40859
M_4^3	750	1	I = II	x	3600	00 + 3.940/969 + 751	—	"	Not observed
K_5	980	1	I = II	x	3830	00 + 4.940/969	—	"	Same
M_5^2	41250	0	I = II	x	4100	00 + 1197 + 3.940/969	—	"	"
M_5^1	430	0	I = II	x	4280	00 + 2.1197 + 2.940/969	—	"	"
M_5^3	700	0	I = II	x	4550	00 + 4.940/969 + 751; 00 + 3.1197	—	"	"
K_6	930	0	I = II	x	4780	00 + 5.940/969	—	"	"
M_6^2	42120	0	I = II	x	4970	00 + 1197 + 4.940/969	—	"	"
M_6^1	330	0	I = II	x	5180	00 + 2.1197 + 3.940/969	—	"	"

Notes

*Visual estimate based on the ten unit scale. The intensity is referred to component I, except when mentioned otherwise.

**The x-axis lies in the plane of the molecule and is perpendicular to the bond connecting the methyl group to the ring, as well as perpendicular to the y-axis.

***For the weakly polarized bands the interval is measured from the center of the 00 doublet, which is equal to 37150 cm^{-1}. For the strongly polarized bands the intervals are measured from the 00 bands of the corresponding spectral components.

splitting also shows that the deviation from the regular symmetry of the π-electrons is approximately greater by one order of magnitude in toluene than in the crystal of benzene.

REFERENCES

1. V. L. Broude and M. I. Onoprienko. Opt. i Spektr. 8, 629 (1960), Optics and Spectroscopy 8, 332 (1960).
2. V. L. Broude. Opt. i Spektr. 1, 387 (1956).
3. V. P. Babenko, V. L. Broude, and V. S. Medvedeff. Pribory i Tekh. Ekspt. No. 3, 99 (1956).
4. Ginsburg. J. Chem. Phys. 14, 511 (1946).
5. V. L. Broude, O. S. Pahomova, and A. F. Prihotko. Opt. i Spektr. 2, 323 (1957); Ukrain. Fiz. Zhur. 2, 96 (1957).
6. S. G. Biswas and S. C. Sirkar. Indian J. Phys. 31, 141 (1957).
7. F. A. Keidel and S. H. Baner. J. Chem. Phys. 25, 1218 (1956).
8. V. L. Broude, V. S. Medvedeff, and A. F. Prihotko. Opt. i Spektr. 2, 317 (1957).

THE NATURE OF THE ELEMENTAL OSCILLATORS OF THE URANIUM ION

P. P. Feofilov

Received 10 November 1959

The nature of the elemental oscillators of hexavalent uranium ions introduced into lithium fluoride crystals as activators, is determined with the aid of luminescence polarization diagrams. It is shown that magnetic dipole radiators are observed, as well as electric dipole radiators.

The question of the nature (multipole type) of the elemental oscillators associated with the luminescence of hexavalent uranium compounds was raised by Vavilov[1] in connection with the necessity of reconciling the spontaneous character of the luminescence of uranyl salts in cases of a prolonged afterglow with the dipole character of the radiation. The dipole character was determined from luminescence polarization diagrams of uranium glasses.[2] The interference and polarization experiments performed in his time did not give a definite answer to this question.[3]

We attempted to employ the method of luminescence polarization diagrams,[4] which we developed for application to the case of activated cubic crystals,[5] to investigate the nature of the elemental oscillators. The intense green luminescence of single crystals of lithium fluoride activated with uranium served as the object of the investigation.* As was pointed out by us in a previous note,[6] the luminescence of these crystals is partially polarized. An investigation of the azimuthal dependence of this polarization indicates unequivocally that the luminescent centers are anisotropic formations, oriented in the crystal lattice of lithium fluoride along a fourfold axis of symmetry (C_4). In reference 6, we proposed a model of the luminescent center based on the idea of an isomorphic replacement of Li^+ ions by uranium U^{+6} ions and the principle of local compensation of excess charges. In this work, the observations were made on spectrally unresolved luminescent light at room temperature. Further investigation showed that on cooling the crystals to liquid air temperature, the degree of polarization of the over-all radiation changes substantially. As a result of the appearance of a spectral line structure, the possibility arose of determining the sign and degree of polarization of the individual lines in the emission spectrum. This permitted the determination of the multipole type of the individual transitions, by employing the methods developed in reference 5.

As in reference 5 (the case of centers oriented along C_4), the samples investigated were parallelepipeds cleaved from crystals along the (100) cleavage planes; observations were made in a direction perpendicular to the direction of excitation. For excitation, the light of a SVDSh-250 mercury lamp was passed through a light filter which isolated the 405, 365, and 313 mμ radiation. This light was polarized by a Glan prism with an air gap and directed on the sample. A slit and a crystal of Iceland spar were placed in front of the sample, giving a double image of the region of the crystal outlined by the slit. This image was projected onto the slit of a grating spectrograph having a dispersion of about 6.5 A/mm. The high dispersion of the apparatus made it possible to carry out determinations for a large number of closely neighboring lines.

The spectra were photographed at two orientations of the plane of polarization of the exciting light ($\eta = 0$ and $\pi/2$), using the same exposure conditions. The spectrograms obtained made it possible to judge the effect of changing η on both the intensity of luminescence and the sign of polarization. It is not difficult to see that here one can restrict oneself to qualitative observations. Figure 1, plotted on the basis of data from reference 5, demonstrates the theoretically possible cases. Consideration of this figure shows first of all that the character (electric or magnetic) of the absorbing system can be determined immediately from the value of η ($\pi/2$ or 0) at which polarization of the emitted radiation is absent. In our case,

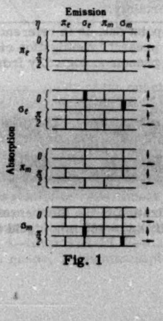

Fig. 1

---

[*] The crystals were grown and kindly placed at our disposal by L. M. Belyaev and his co-workers.

unpolarized radiation was observed at $\eta = \pi/2$ for all lines in the luminescence spectrum, for all wavelengths of the exciting light used. Thus it seems certain that the absorbing systems of the luminescent centers in LiF-U are electrical in nature.

To identify the type of absorption and radiation oscillators more precisely required a determination of the sign of polarization at $\eta = 0$ and the sign of the quantity $(I_0/I_{\pi/2}) - 1$. In most cases, the spectrograms were clear enough to make this determination unambiguous. This, however, does not imply the possibility of a unique determination of the type of emitter, since reference 5 demonstrated the impossibility of distinguishing between certain pairs of oscillator types.

Before discussing the results, it is necessary to dwell briefly on the characteristics of the luminescent spectra of LiF-U crystals. The crystals at our disposal differed with regard to the nature and concentration of the initial uranium compound used for activation. These, or some other uncontrolled circumstances, caused substantial differences among the spectra of the various samples. Roughly speaking, it was found that at low temperatures the spectra consisted of two groups of lines located at 490-520 and 520-560 mμ. The relative intensity of these groups differs significantly in different samples and depends on the wavelength of the exciting light. Evidently this permits one to speak about several types of radiation centers in crystals of LiF-U. It should be noted that investigation of the angular dependence shows that at least the centers responsible for these two groups of lines have the same orientation: along a fourfold axis.

The principal results, given below, were obtained with an intensely luminescent crystal of LiF activated with 0.2% uranyl nitrate. Both groups are clearly defined in the spectrum of this crystal, although the short wavelength group is relatively weaker than in certain other samples.

Light with a wavelength of 405 mμ excites practically only the long wavelength group of lines in the luminescent spectrum, and a distinct polarization of the radiation is observed, varying in magnitude and sign for the various lines. On excitation by 365 mμ light, both groups are observed in the emission spectrum; however, only the short wavelength group is definitely polarized (Fig. 2). The lines of the long wavelength group are practically unpolarized for $\lambda_{exc} = 365$ mμ. For $\lambda_{exc} = 313$ mμ, a substantial change of the relative intensity of the individual luminescent lines is observed; the luminescence spectrum is not polarized.

Comparison of observation with theory (Fig. 1) makes it appear very probable that 365 mμ light is absorbed by circular electrical oscillators σ_e. The emitting oscillators also turn out to be circular; however, they are partly electric and partly magnetic* (Table 1). This can be stated with some certainty.

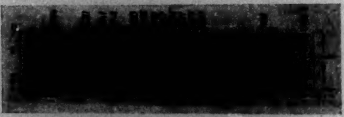

Fig. 2. Polarization in the luminescent spectrum of LiF-U; $\lambda_{exc} = 365$ mμ; liquid air temperature.

Table 1. Nature of the Elementary Emitters in the Short Wavelength Group of the Luminescent Spectrum of LiF-U (−183°C; $\lambda_{exc} = 365$ mμ)

λ (A)	Intensity*	Type of emitter	λ (A)	Intensity*	Type of emitter
4828	3	σ_e	5012	3	σ_e
4884	5	σ_e	5017	8	σ_m
4920	5	σ_e	5024	3	σ_m
4941	10	σ_e	5051	5*R*	σ_m
4948	5	σ_m	5057	3	σ_e
4993	3	σ_m	5067	3	σ_m
5002	3	σ_m	5136	5	σ_e?

*Visual estimate.

The results of the identification are given in Table 2.

Table 2. Nature of the Elementary Oscillators in the Long Wavelength Group of the Luminescent Spectra LiF-U (−183°C; $\lambda_{exc} = 405$ mμ)

λ (A)	Intensity*	Types of oscillators
5186	5*R*	$\sigma_e \to \pi_e$ or $\pi_e \to \sigma_e$
5195	5	$\sigma_e \to \pi_m$ » $\pi_e \to \sigma_m$?
5210	5	$\sigma_e \to \pi_e$ » $\pi_e \to \sigma_e$
5240	3	$\sigma_e \to \pi_m$ » $\pi_e \to \sigma_m$
5245	3	$\sigma_e \to \pi_e$ » $\pi_e \to \sigma_e$
5280	10	$\sigma_e \to \pi_m$ » $\pi_e \to \sigma_m$
5285	3	$\sigma_e \to \pi_e$ » $\pi_e \to \sigma_e$
5409	8	$\sigma_e \to \pi_e$ » $\pi_e \to \sigma_e$
5511	5	$\sigma_e \to \pi_m$ » $\pi_e \to \sigma_m$

*Visual estimate.

The situation is not so clear when we come to the nature of the emitters in the long wavelength group. As we noted, a well-defined polarization of the lines of this group is observed only for $\lambda_{exc} = 405$ mμ. It turns out that all the lines of this group can be considered either as $\sigma_e - \pi_e$ and $\sigma_e - \pi_m$ or as $\pi_e - \sigma_e$ and $\pi_e - \sigma_m$ transitions. In reference 5 we noted the impossibility of distinguishing between these combinations by means of the method of polarization diagrams.

It is necessary to note that the degree of certainty with which one determines the nature of the elementary emitters of the U^{+6} ion is somewhat less than in the case of the europium ion.[7] This is a consequence of the rather substantial deviation of the values for the degree of polarization of the different lines from the theoretical limiting values.

From the data of Tables 1 and 2 one can see that in the luminescence of uranium ions, as in the luminescence of rare earth ions,[7] we find both electric and magnetic dipole emitters. The intensities of the lines corresponding to magnetic and electric dipoles are comparable. This indicates that transitions accompanied by emission of electric dipoles are forbidden, and that we are dealing with induced dipole emission.

Thus, in spite of a certain indefiniteness of the results, the luminescence of a hexavalent uranium ion should be regarded as a superposition of induced electric and magnetic dipole emission.

O. V. Sokolova, to whom the author expresses sincere thanks, was of great assistance in the experimental part of the work.

---

*It is necessary to point out, as in reference 5, that for the purposes of the present investigation circular oscillators do not differ phenomenologically from linear oscillators, which are perpendicular to the orientation axis. The question of which model to prefer reduces to a question of the coherence of the oscillations in the plane under consideration, and requires a special investigation.

REFERENCES

1. S. I. Vavilov. Vestnik Leningrad. Gosudarst. Univ. No. 1, 5 (1946); Sobr. Soch. (Collected Works) **2**, 252 (1952); Trudy Gosudarst. Opt. Inst. **20**, No. 132, 4 (1950); Sobr. Soch. **2**, 260 (1952).
2. A. N. Sevchenko. Doklady Akad. Nauk SSSR **42**, 349 (1944).
3. P. P. Feofilov. Doklady Akad. Nauk SSSR **55**, 407 (1947).
4. S. I. Vavilov. Zhur. Eksptl. i Teoret. Fiz. **10**, 1363 (1940); Sobr. Soch. **2**, 58 (1952).
5. P. P. Feofilov. Opt. i Spektr. **1**, 131 (1956); "Polarized Luminescence of Atoms, Molecules, and Crystals," Gosudarst. Izd. Fiz.-Mat. Lit., Moscow, 1959.
6. P. P. Feofilov. Opt. i Spektr. **7**, 842 (1959), Optics and Spectroscopy **7**, 493 (1959).
7. P. P. Feofilov. Doklady Akad. Nauk SSSR **99**, 975 (1954).

FLUORESCENCE QUANTUM YIELD OF CERTAIN SUBSTANCES IN POLYSTYRENE

E. A. Andreeshchev and I. M. Rozman

Received 12 October 1959

A procedure for measuring the quantum yields of eight organic compounds in polystyrene is described, and the results are presented.

The luminous efficiency of plastic scintillators is proportional to the fluorescence quantum yield of the luminescent additives. The quantum yields of several substances in polystyrene scintillators have been reported previously.[1, 2] Measurements were made by means of a comparison with the quantum yield of 1,3,5-triphenyl-Δ^2-pyrazoline. The quantum yield of triphenylpyrazoline was in turn measured relative to the yield of the aqueous fluorescein solution using Alentsev's data.[3] As a result of the large number of conversions, the accuracy of the values obtained was low, particularly for substances which have luminescence spectra in the ultraviolet (n-terphenyl, diphenyloxodiazole, etc.). In view of this, a direct determination of the quantum yield of 2,5-dipheyl-1,3-oxazole (2PO) in polystyrene was undertaken. The yield of other substances was determined relative to 2PO. All samples were prepared* by a thermal polymerization method.[1, 2]

THE QUANTUM YIELD OF DIPHENYLOXAZOLE

Measurements of the fluxes of exciting and luminescent photons were made using the following "quantum meters": (1) a solution of 1,5-dipheyl-3 (4-phenylbutadienyl)-Δ^2-pyrazoline in dioxane (5×10^{-3} gm/ml), and (2) a plastic scintillator with 1,5-diphenyl-3-styryl-Δ^2-pyrazoline (1.8×10^{-2} gm/ml).

The spectral yields of the meters, measured by Solomin method,[4] are presented in Fig. 1. A reduction in yield of the second meter at $\lambda < 360$ mμ is attributed to competing absorption in polystyrene. At $\lambda > 460$ mμ light starts to pass through both meters (thickness of layer—15 mm).

A diagram of the experimental apparatus is shown in Fig. 2. The 313 mμ line was isolated from the spectrum of a mercury vapor lamp by a monochromator (SF-4). The exciting light was incident on the sample at an angle of 14° to the normal. The plastic scintillation samples, in the form of cylinders (diameter 16 mm and height 1 mm) with a polished surface, were placed in a special multiposition holder. The back surface of the samples was optically coated with smoked ebonite to eliminate light reflection. The fluorescent light was recorded in a small solid angle Ω. Disregarding secondary effects, the photomultiplier current can be written in the form

$$I_{\text{fl.}} = N_0 \cdot (1 - R)\, \eta\, \frac{\Omega}{n^2_{\text{eff.}}}\, (1 - r)\, I_0, \tag{1}$$

where N_0 is the flux of exciting photons; R is the coefficient of reflection of exciting light from the front surface of the sample; η is the fluorescence quantum yield of 2PO; $\eta_{\text{eff.}}$ is the coefficient allowing for refraction of light upon leaving the sample; r is the coefficient of reflection from the front surface of the quantum meter; I_0 is the current of the FEU corresponding to absorption in the quantum meter of 1 photon per second. In order to determine N_0 the quantum meter (Fig. 2: 6 and 7) was set in place of the sample. In this instance, the current of the FEU is obviously equal to

$$I_{\text{exc.}} = N_0 (1 - R_0)\, I_0, \tag{2}$$

where R_0 is the coefficient of reflection of exciting light from the front surface of the quantum meter. For the second quantum meter, a coefficient of 0.76 (Fig. 1, curve 2) should be inserted in Eq. (2).

Within sufficient accuracy for our work, the refractive index of polystyrene plastic scintillators does not

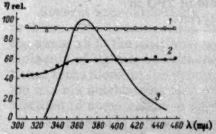

Fig. 1

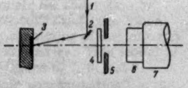

Fig. 2

Fig. 1. Spectral yields of the quantum meters. Curve 1—solution of 1,5-diphenyl-3(4-phenylbutadienyl)-Δ^2-pyrazoline in dioxane (5 gm/liter); curve 2—plastic scintillator with 1,5-diphenyl-3-styryl-Δ^2-pyrazoline (18 gm/liter); curve 3—fluorescence spectra of 2,5-diphenyl-1,3-oxazole.

Fig. 2. Diagram of the instrument for measuring quantum yields. 1—monochromatic beam of exciting light, 2—aluminum mirror, 3—sample, 4—filter SZS-17, 5—diaphragm, 6—quantum meter, 7—photomultiplier FEU-29.

---

*The authors are grateful to V. M. Shoniya for preparation of the scintillators.

depend on the presence of luminescent additives and is equal to 1.59.[5] Therefore for the second meter r ≈ R ≈ R_0 ≈ 0.05. For the first meter (quartz) R_0 ≈ r ≈ 0.04. The solid angle Ω was determined from the geometrical conditions and was 2.11 × 10^{-3}.

For a perfectly plane sample surface, the coefficient $n_{\text{eff.}}$ in (1) is obviously equal to the refractive index of polystyrene (n = 1.59). Actually, the surface is not a perfect plane and $n_{\text{eff.}} < n$. In order to determine $n_{\text{eff.}}$ experimentally, another instrument was used and the intensity of luminescence of samples, prepared by a standard procedure, was measured with and without a flat layer (~1 mm) of α -chloronaphthalene (n = 1.63) above them. Thus, we obtained:

$$\frac{n_1^2}{n_{\text{eff.}}^2} = 1.10 \pm 0.02, \text{ т. е. } n_{\text{eff.}}^2 = 2.42 \pm 0.05.$$

Incomplete absorption of fluorescence in the quantum meter and scattered excitation light are possible sources of error. The first effect was controlled by placing a filter Zh.S-17 between the "meter" and the FEU. The scattered light, which was determined by replacing the sample with a cylinder of Plexiglass of similar size, constituted approximately 20% in the absence of the filter SZS-17 (Fig. 2: 4) and approximately 2% in its presence (the filter reduced the intensity of fluorescence of 2PO by a factor of 1.16).

Thus, from (1) and (2) the following formula for the determination of the quantum yield of 2PO is obtained.

$$\eta = \frac{I_{\text{fl.}}}{I_{\text{exc.}}} \times \left.\begin{matrix} 1.40 \cdot 10^3 \text{ (для 1-го счетчика)} \\ 1.07 \cdot 10^3 \text{ (для 2-го счетчика).} \end{matrix}\right\} \qquad (3)$$

Measurements were made, using both quantum meters, for a series of scintillators with a relative concentration of 2PO from 3 × 10^{-4} to 3 × 10^{-2} gm/gm. The measured currents attained values of $I_{\text{fl.}}$ = 5 × 10^{-9} A and I = 9 × 10^{-6} A. The photomultiplier FEU-29 was selected for having good linearity in this range of currents. The mean values of η from eleven series of experiments are presented in Table 1. It is evident that the results of different experiments are in good agreement (the standard deviation does not exceed 5%). At small concentrations of 2PO, $\eta_{\text{expt.}}$ is lowered as a result of partial absorption of the exciting light by polystyrene (corrections were introduced in accordance with the values of absorption coefficients, Table 1, column 3). A certain increase in the value of $\eta_{\text{corr.}}$ with increase of 2PO concentration is connected with an increase in the amount of secondary fluorescence. Reference 6 shows that for a concentration of 5 × 10^{-3} gm/gm the secondary fluorescence increases the quantum yield by 3-4%. A reduction of $\eta_{\text{corr.}}$ observed at higher concentrations is apparently connected with quenching of the fluorescence. Thus, the quantum yield of 2PO in polystyrene is equal to 0.80 ± 0.05.

Table 1. The Fluorescence Quantum Yield of 2PO in Polystyrene

Concentration of 2PO (10^{-4} gm/gm)	$\eta_{\text{exp.}}$	$\eta_{\text{corr.}}$
3	0.73 ± 0.03	0.80
6	0.77 ± 0.03	0.80
10	0.78 ± 0.03	0.80
20	0.80 ± 0.03	0.81
50	0.82 ± 0.04	0.82
75	0.80 ± 0.03	0.80
200	0.79 ± 0.02	0.79
300	0.78 ± 0.02	0.78

THE QUANTUM YIELDS OF CERTAIN LUMINESCENT ADDITIVES IN POLYSTYRENE

The fluorescence quantum yields of several luminescent additives in polystyrene were measured by a comparison with 2PO.

For this, samples with concentrations of 2PO of 2.5 and 7.5 × 10^{-3} gm/gm were used. The fluorescence was excited according to the diagram in Fig. 2. Measurement of the intensity of luminescence was made either by a quantum meter (no. 1) or directly with a photomultiplier. In the second instance the current of the photomultiplier, I, is related to the flux of fluorescent photons, N, by

$$I = I_0 N \bar{s},$$

where $\bar{s}$ is the mean quantum sensitivity of the photomultiplier for a given luminescence spectrum:

$$s = \frac{\int f(\nu) \cdot s(\nu) \cdot d\nu}{\int f(\nu) \cdot d\nu}.$$

The numerical values of the spectral corrections are presented in Table 2. For 2PO, the value s = 1 was taken. Both methods of measurement were in agreement for n-terphenyl.

Table 2. External Quantum Yields of Luminescent Additives in Polystyrene

Luminescent additive	Concentration (10^{-4} gm/gm)	Sample thickness (mm)	Spectral correction of method of measurement	External quantum yield (%)	Correction for secondary fluorescence
1	2	3	4	5	6
2,5-diphenyl-1,3-oxazole	2—7.5	1	1	81	—
2,5-diphenyl-1,3,4-oxodiazole	10	1	quantum meter	69	—
	20	1		72	—
	30	1	•	66	—
Acenaphthene	10	1	•	42	—
	20	1	•	41	—
	30	1	•	43	—
n-terphenyl	3	1	•	78	—
	10	1	•	80	—
	20	1	•	81	—
n-terphenyl	3	1	0.98	77	—
	10	1	—	81	—
1,1,4,4-tetraphenyl-1,3 butadiene	2	10	0.90	78	0.95
	5	10	—	77	0.94
	7.5	10	—	77	0.94
1,3,5-triphenyl-Δ^2-pyrazoline	1	10	0.92	83	0.88
	3	10	—	87	0.85
	10	10	—	86	0.89
1,3,4-triphenyl-Δ^2-pyrazoline	10	10	0.89	84	—
	20	10		86	—
4-styrylstilbene	5	1	0.95	95	0.90
	10	1	—	96	0.88
	15	1	—	94	0.88

The concentration dependence of the external quantum yield is determined by secondary fluorescence and by concentration quenching. The molecular quantum yield may be obtained, in general, by extrapolation to zero concentration. However, the results presented in Table 2 do not permit reliable extrapolation. The intensity of luminescence was measured (according to the diagram in Fig. 2) for tetraphenylbutadiene and 1,3,5-triphenylpyrazoline at concentrations from 1 × 10^{-4} to 3 × 10^{-2} gm/gm which permitted the role of secondary fluorescence to be considered. The lowest concentration of 4-styrylstilbene was 1 × 10^{-3} gm/gm, which proved to be sufficient for extrapolation. The results obtained by this method are presented in column 6 of Table 2 (the error is ±3%). Measurements at low concentrations of acenaphthene, n-terphenyl, and diphenyloxodiazole are not strictly accurate since there is a competing absorption in polystyrene. Therefore, the results of column 5 were used to calculate the molecular quantum yield and this led to an increase in error. Owing to a lack of samples with a low

Table 3. Quantum Yields of Luminescent Substances in Polystyrene

Luminescent substance	Quantum yield
2,5-diphenyl-1,3-oxazole	0.80 ± 0.05
2,5-diphenyl-1,3,4-oxodiazole . . .	0.66 ± 0.08
Acenaphthene	0.42 ± 0.06
n-terphenyl	0.75 ± 0.08
1,1,4,4-tetraphenyl-1,3-butadiene .	0.73 ± 0.07
1,3,5-triphenyl-Δ^2-pyrazoline . . .	0.74 ± 0.07
1,3,4-triphenyl-Δ^2-pyrazoline . . .	0.76 ± 0.10
4-styrylstilbene	0.84 ± 0.08

concentration of 1,3,4-triphenylpyrazoline, the correction was determined by another method[6] and was found to be equal to 0.9. The obtained results are presented in Table 3.

REFERENCES

1. E. A. Andreeshchev, E. E. Baroni, K. A. Kovyrzina, I. E. Pani, I. M. Rozman, and V. M. Shoniya. Pribory i Tekhn. Eksp. No. 1, 32 (1956).
2. E. A. Andreeshchev, E. E. Baroni, K. A. Kovyrzina, I. E. Pani, I. M. Rozman, and V. M. Shoniya. Izvest. Akad. Nauk SSSR, Ser. Fiz. 22, 67 (1958).
3. M. N. Alentsev. Zhur. Eksptl. i Teoret. Fiz. 21, 133 (1951).
4. S. S. Solomin. Doklady Akad. Nauk SSSR 31, 741 (1941).
5. E. E. Baroni. Zhur. Fiz. Khim. (in print).
6. M. D. Galanin. Trudy Fiz. Inst., Akad. Nauk SSSR 5, 339 (1950).

THE THEORY OF THE LUMINESCENCE OF ACTIVATED CRYSTAL PHOSPHORS

N. D. Potekhina

Received 6 October 1959

The Williams method for calculating the spectra of crystal phosphors is analyzed quantum-mechanically, and it is shown that the "repulsion energy" determined by the Williams method for the excited state corresponds to the sum of the S-energy and the exchange energy, and in contradistinction to the ground state, does not include the energy of the Coulomb overlap. Thus it is shown that the Williams method correctly accounts for the shift of the excited level of the impurity ion in the crystal field. The calculations carried out also prove that the $4d^{10}$-$4d^9 5p$ transition in the silver ion is responsible for the luminescence bands in the phosphor NaCl : Ag.

INTRODUCTION

In 1951 Williams[1] suggested a method for calculating the luminescence bands in alkali halide crystal phosphors. The merit of this method consists in the relative simplicity of calculation and the agreement of the theoretical results with experimental data, at least for the crystal KCl:Tl calculated by Williams. The shortcomings of the method are connected with the fact that the energy calculation of the impurity center in the excited state has no physical basis.[2, 3] According to Born and Mayer,[4] the energy of interaction of ions in a crystal in the ground state is the sum of the electrostatic energy of interaction of point (zero radius) ions, the repulsion energy of the type $be^{-r/\rho}$, and the van der Waals attraction. The latter energy appears in the second approximation of the perturbation theory. In the first approximation, however, all the corrections for the overlap of the nonpoint (finite radius) ions in the crystal are included in the repulsion forces. This is confirmed by the quantum mechanical calculations made by Löwdin.[5] However Williams, in determining the energy of the impurity center in the excited state, suggests the introduction of one more term in the energy of interaction in addition to the repulsion energy; namely, a correction for Coulomb overlap of the electron clouds. The introduction of this term in addition to the repulsion energy appears to be inconsistent. But since Williams has calculated the repulsion energy in the excited state on the basis of a certain empirical rule found for the ground state, it remains unclear whether the repulsion energy found in this manner actually takes into account the complete interaction between ions in the excited state.

To evaluate the Williams method, we calculated the spectra of the crystal phosphor NaCl:Ag, first by the abovementioned method, and then by the quantum mechanical method. The results of the first calculation were given in reference 2, in which two possible transitions in the silver ion were considered: $4d^{10}$-$4d^9 5s$ and $4d^{10}$-$4d^9 5p$, because there are disagreements among different authors in the interpretation of the emission and absorption bands caused by impurities in this crystal phosphor. The present paper gives the results of the quantum mechanical calculations for the abovementioned crystal phosphor, and compares the results obtained by the two methods of calculation with experimental data. It is evident that such a comparison should reveal whether the Williams method correctly describes the behavior of an excited impurity center and which transition in the silver ion is responsible for the luminescence.

STATEMENT OF THE PROBLEM

Several approximations were used for solving the problem. The luminescence center was assumed to be the same as in the Williams model: the absorption or emission of light were connected with electronic-vibrational transitions in the system consisting of the impurity ion and six neighboring ions of the lattice. This model is justified to some extent in references 6, 7, 8, and 9.

We made use of the harmonic approximation[10] in the quantum mechanical treatment of a crystal with an impurity. In this method, the electron energy can be presented by a quadratic parabola with respect to the displacement of the nuclei, and the harmonic vibrations of the nuclei are completely determined by this parabola. The total energy of the crystal is taken to be the sum of the energy eigenvalue of electron motion in the equilibrium state of the crystal and the energy of the harmonic oscillators. The luminescence spectrum is found by calculating the probability of transition between the ground and excited states of this system. In order to make a choice between two possible transitions, it is sufficient to apply classical statistics.[11, 12] Thus the problem of determining the spectra is reduced to a calculation of the energy of impurity electrons as a function of displacement of the nuclei.

ONE-ELECTRON WAVE FUNCTIONS FOR THE CRYSTAL

The Hartree-Fock equations for the one-electron functions of the crystal were the basis for our calculations. Assuming that the electrons are strongly localized around the corresponding ions (including those of the impurity), this equation can be approximately solved by considering only the field of the ion itself and the field of the point charges of the crystal. We take account of the finite radii of the neighboring ions and the exchange interaction with the lattice only in the calculation of the total energy of the crystal. We obtain the following equations for the outer electron of the impurity ion Ag$^+$ in the ground and excited states:

$$\left.\begin{aligned} -f''_{4d}+2\left[-\frac{3}{r^2}+V_1^{4d}(r)+V_0(r)+V_4(r)\right]f_{4d}(r)&=2E_{4d}f_{4d}(r),\\ -f''_{5s}+2\left[V_1^{5s}(r)+V_0(r)\right]f_{5s}(r)&=E_{5s}f_{5s}(r),\end{aligned}\right\} \quad (1)$$

where V$_1$(r) is the total potential with respect to the central ion (including exchange), V$_0$(r) is the spherically symmetric part of the potential of the point lattice, and V$_4$(r) is the contribution to the lattice potential made by a cubic harmonic of the fourth order. A semiempirical approximation method proposed by Petrashin'[13] was used for the solution of these equations. In this method, the asymptotic behavior of the function is determined by the electron energy, which in the crystal field is approximately equal to $\varepsilon_{nl} \pm A_M/a$. Here ε_{nl} is the eigenvalue of the electron energy in the free ion (the sign ± refers to the electron at the positive or negative nodes, respectively). Since $\varepsilon_{nl} < 0$, the absolute value of the electron energy is increasing at the negative nodes, and decreasing at the positive ones. Correspondingly, the wave functions of the negative ions in the crystal become compressed in comparison with free ions, and those of the positive ions are expanded. This fact is confirmed by the change of the polarizability of ions in the crystal in comparison with the free ions.[14] Nevertheless, it is interesting to see how well the above-mentioned method of calculation takes account of the actual change of the functions. For this purpose, we calculate the polarizabilities of the ions Ag$^+$ and Cl$^-$ in the free state and in the crystal, and compare the results of calculations with the experimental data (Table 1).

Table 1. Polarizabilities of Ag$^+$ and Cl$^-$ Ions (in A^3)

Ion	Experimental values		Theoretical values	
	Free ion	Ion in crystal	Free ion	Ion in crystal
Ag$^+$ . .	1.72	2.37—2.45	1.61—1.80	2.44
Cl$^-$ . . .	3.66	2.96	6.9 5.65 [13]	3.39

The theoretical values were calculated according to the Kirkwood's formula taking account of exchange.[15] Consideration of the inner shells has essentially no effect on polarizability values.

The wave functions for the free silver ion were calculated by a method suggested by Petrashen',[16] which is based on the utilization in the Hartree equation of the ionization potentials, instead of the energy parameters, of the respective states. The wave functions in the crystal were determined by means of these semiempirical functions for the free Ag$^+$ ion, and the exact functions with exchange for the free Cl$^-$ ion.[17]

CALCULATION OF THE INTERACTION ENERGY BETWEEN THE IMPURITY ION AND THE SURROUNDING LATTICE

Repulsion energy: Our wave functions, like the functions of different free ions, are not mutually orthogonal. We used the results of Löwdin[5] for calculating the interaction energy of the impurity ion with its surroundings. Löwdin took a determinant consisting of one-electron functions of the free ions as the wave function of the crystal. It follows from Table 1 that the semiempirical functions are more appropriate for our crystal than the free ion functions, and we shall therefore calculate the bond energy with the new functions. Löwdin breaks up the total bond energy E$_{bd}$ corresponding to a given ion pair into several terms: (1) the energy of Coulomb interaction between ions, (2) the exchange energy, and (3) the so-called S-energy (E$_S$) which appears in the expression for the total energy because of the nonorthogonality of the wave functions, i.e.

$$E_{bd}=E_{\text{elect.}}+E_{\text{exch.}}+E_S,$$

where

$$\left.\begin{aligned} E_{\text{elect.}}&=\frac{1}{R}+\sum_{\mu_{Ag}}\sum_{\nu_{Cl}}\left(\mu\nu\left|\frac{1}{r_{12}}-\frac{1}{R}\right|\mu\nu\right)\\ &-\sum_{\mu_{Ag}}z_{Cl}\left(\mu\left|\frac{1}{r}-\frac{1}{R}\right|\mu\right)-\sum_{\nu_{Cl}}Z_{Ag}\left(\nu\left|\frac{1}{r}-\frac{1}{R}\right|\nu\right);\\ E_{\text{exch.}}&=-\sum_{\mu_{Ag}}\sum_{\nu_{Cl}}\left(\mu\nu\left|\frac{1}{r_{12}}\right|\nu\mu\right);\\ E_S&=-\sum_{\mu_{Ag}}\sum_{\varkappa_{Cl}}S_{\mu\varkappa}\left\{\left[\sum_{\nu}{}'\left(\varkappa\nu\left|\frac{1}{r_{12}}-\frac{1}{R}\right|\mu\nu\right)-\left(\varkappa\mu\left|\frac{1}{r_{12}}\right|\varkappa\mu\right)-\right.\right.\\ &\left.\left.S_{\varkappa\mu}\left[\sum_{\nu}{}'\left(\mu\nu\left|\frac{1}{r_{12}}-\frac{1}{R}\right|\mu\nu\right)-\left(\varkappa\mu\left|\frac{1}{r_{12}}\right|\varkappa\mu\right)\right]\right\}+\text{the same } c\mu_{Cl}\nu_{Ag}.\end{aligned}\right\} (2)$$

The prime indicates summation over all ions not "belonging to" the ion μ.

If the interaction energy between point ions is separated from E$_{bd}$, then the remaining part corresponds to the repulsion energy of classical theory. Thus we obtain the quantum mechanical expression for the repulsion energy per ion pair

$$W_{\text{rep.}}=\left(E_{\text{elect.}}-\frac{1}{R}\right)+E_{\text{exch.}}+E_S. \quad (3)$$

By using this expression for the repulsion energy, one can calculate the energy of the impurity center in the excited state and the configurational curves for the excited state.

All two-center integrals are calculated by series expansion in terms of spherical functions around one center. The series is infinite only for exchange; for the Coulomb overlap and the S-energy, the series is reduced to one term in each integral. We have calculated the repulsion energy for five values of R: 4.8, 5.0, 5.2, 5.4, and 5.6 a.u. (atomic units) (in the exchange series, only terms of the orders 0, 1, 2, and 3 were calculated; the rest was estimated). As an example, in Table 2 the results are given of the calculation of the electron-ion interaction energy.

Table 2. Overlap Integrals and S-Energy

R	$S_{5s,\,3p}$	$S_{5s,\,3s}$	$S_{5s,\,2s}$	$S_{5s,\,2p}$	$E_S(5s,\,3s)$	$E_S(5s,\,3p)$	$E_S(5s,\,2s)$	$R_S(5s,\,2p)$
4.8	0.1706	0.2081	0.0385	0.0072	0.04241	0.02842	0.00148	0.00005
5.2	0.1544	0.1760	0.0318	0.0056	0.02814	0.02088	0.00101	0.00003
5.6	0.1415	0.1501	0.0274	0.0046	0.01928	0.01595	0.00075	0.00002

The repulsion energy between the silver ion in the ground state ($1s^2 \ldots 4d^{10}$) and the surrounding chloride ions is known from the classical theory of the solid state. If one assumes that the excitation of one electron has little effect on the wave functions of the rest of electrons, then the repulsion energy of the core ($1s^2 \ldots 4d^9$) can be determined. This determination was possible because the part contributed by the shells 4p and 4s was known. Table 3 gives the final results of the repulsion energy calculation in the excited state.

Table 3. Repulsion Energy Values in the Ground and Excited States

R	$W_{\text{rep.}}^{'S_0}$	$W_{\text{rep.}}^{\text{core}}$	$E_S(5s)$	$E_{\text{exch.}}(5s)$	$E_{\text{coul.}}(5s)$	$W_{\text{rep.}}^{3D}$
4.8	0.2097	0.1944	0.64302	−0.2791	−0.2112	0.1343
5.0	0.1366	0.1254	0.3579	−0.2333	−0.1796	0.0704
5.2	0.08904	0.0821	0.2979	−0.1948	−0.1500	0.0352
5.4	0.05800	0.0533	0.2479	−0.1627	−0.1266	0.0119
5.6	0.03765	0.0345	0.2062	−0.1359	−0.1063	−0.0015

It can be seen from Table 3 that the repulsion energy of the excited state, determined according to Löwdin ($W^{3D}_{\text{rep.}}$), is lower than that of the ground state. This decrease is accompanied by a very sharp increase in the energy of the Coulomb overlap, whose contribution is negative. The rapid change of the Coulomb overlap is due to the very steep slope of the potential near the neighboring ions (see Figure). The increase of electron density in the well on excitation has a strong effect on the Coulomb energy (Table 4). One can see from this table that, in the ground state, the Coulomb overlap is only a small fraction of the total repulsion energy (~10%), whereas in the excited state all the energy components are of the same order of magnitude. Thus, the repulsion energy in the ground state is determined mainly by S-energy, which is proportional to the square of the overlap integrals $S_{\mu\nu}$ of the wave functions of the neighboring ions. This is the reason why the Williams procedure proved valid for a number of ions in the ground state. In the excited state, however, this procedure deals only with the sum of the S-energy and the exchange energy, which increase approximately 1.5 to 2 times. In this case the Coulomb overlap plays a quite special role, a fact that was correctly guessed by Williams without any substantiation. It is interesting that the sum of the S-energy and the exchange energy (like the Coulomb overlap by itself) change with R exponentially, whereas one cannot find an exponential function for the total sum.

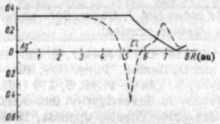

Potential of a point lattice in the node of a positive ion ignoring (full line), and considering (dashed line) the finite radii of the six nearest ions of Cl⁻.

Table 4. The Energy Values of the Coulomb Interaction in the Ground and Excited States

R	$E^{'S_0}_{\text{coul.}}$	$E^{3D}_{\text{coul.}}$
4.8	−0.0184	−0.2295
5.2	−0.0092	−0.1579
5.6	−0.0049	−0.1120

For the final evaluation of the results by the Williams method, however, it is necessary to compare the spectra obtained by the two methods. We therefore calculate the rest of the energy constituents, i.e., the van der Waals energy, and the ion-dipole interaction. In calculating the van der Waals energy we used the variational method,[15] which seems to us to be more consistent and more convenient for the treatment of the excited state than the perturbation method used previously.[1, 2] The overlapping of the electron clouds was taken into account by integrating the matrix elements

$$(r^k_{\mu\mu}) = \int \psi^*_\mu r^k \psi_\mu d\tau$$

with respect to r from 0 to R, where R is the distance to the nearest ions.

In calculating the interaction energy of the dipoles which are formed in the displaced Cl⁻ ions, we not only considered the field of the surrounding lattice, but also took into account the fact that the effective positive charge of the central Ag⁺ ion acting in the excited state on the Cl⁻ ions is equal to

$$e^* = 2 - \int_0^R f^2_{Ag} dr.$$

The values of all energy constituents and of the total energy of the impurity center in the ground and excited states are given in Table 5. The energy of interaction between the impurity center and the lattice due to radial displacement of Cl⁻ ions is well described by the following parabolas:

For the ground state

$$W_{1S_0} = 0.2012\Delta a^2 + 0.0265\Delta a - 0.0019 \text{ (a.u.)}$$
$$= 5.475\,(\Delta a + 0.066)^2 - 0.079 \text{ (ev)}, \quad \Delta a = a_0 - R,$$

where a_0 is the lattice constant of NaCl.

For the excited state

$$W_{3D} = 0.1641\Delta a^2 - 0.021\Delta a + 0.1227 \text{ (a.u.)}$$
$$= 4.47\,(\Delta a - 0.064)^2 + 3.34 \text{ (ev)}.$$

Table 5. Total Energy of the Impurity Center in the Ground (I) and Excited (II) States

R	$W_{\text{rep.}}$	$W_{\text{v. d. w.}}$	$W_{\text{ion-dip.}}$	$\Delta W_{\text{lat.}}$	$W_{\text{tot.}}$
			I		
4.8	0.2097	−0.1246	−0.0058	+0.00049	+0.0798
5.0	0.1367	−0.0986	−0.0019	−0.00645	0.0297
5.2	0.0890	−0.0794	−0.0002	−0.00512	0.0042
5.4	0.0'80	−0.0639	−0.0001	+0.00324	−0.0027
5.6	0.0376	−0.0520	−0.0009	+0.02177	+0.0065
			II		
4.8	0.1343	−0.1821	−0.00009	+0.0005	−0.0174
5.0	0.0704	−0.1499	−0.00008	−0.0064	−0.0860
5.2	0.0352	−0.1255	−0.00079	−0.0051	−0.0962
5.4	0.0119	−0.1062	−0.00197	+0.0032	−0.0931
5.6	−0.0015	−0.0902	−0.00286	+0.0218	−0.0727

We obtained the curve for the excited state by adding the difference between the ion eigenvalues in the ground and excited states at equilibrium state of the lattice to the interaction energy.

The difference of the eigenvalues: This quantity was obtained in the following manner. We obtain the eigenvalues for the one-electron wave functions from Eq. (1)

$$2E_{4d} = -\int_0^\infty f_{4d} f''_{4d} dr + 2\int_0^\infty \left[\frac{3}{r^2} + V_1^{4d}(r)\right] f^2_{4d} dr + 2\int_0^\infty [V_0 + V_4] f^2_{4d} dr,$$

$$2E_{5s} = -\int_0^\infty f_{5s} f''_{5s} dr + 2\int_0^\infty V_1^{5s}(r) f^2_{5s} dr + 2\int_0^\infty V_0(r) f^2_{5s} dr. \qquad (4)$$

calculated with the new functions, and with the potential used in the equation. The potential from the inner shells $V_1^{4d}(r)$ and $V_1^{5s}(r)$ used in Eq. (1) is the same as for the free ion, as follows from the very method used to obtain a solution for the crystal.

We shall not calculate the energy of the whole ion in the ground and excited states, but shall find only the change of those quantities which, in the semiempirical method, determine the excitation energy of the free ion. As mentioned before, the ionization potential of a given state is being used in the semiempirical method as the energy parameter, and a function is being sought which corresponds to this potential. One can express the ionization potentials through the functions

$$\left.\begin{aligned} -2I_{4d} &= -\int_0^\infty f^0_{4d} f^{0''}_{4d}\,dr + 2\int_0^\infty \left[\frac{3}{r^2} + V_1^{4d}(r)\right] f^{0^2}_{4d}\,dr, \\ -2I_{5s} &= -\int_0^\infty f^0_{5s} f^{0''}_{5s}\,dr + 2\int_0^\infty V_1^{5s}(r)\, f^{0^2}_{5s}\,dr. \end{aligned}\right\} \qquad (5)$$

by using an equation which is analogous to Eq. (1), but which corresponds to a free ion.

Since the energy difference between the ground and the excited states of the free ion is given by the difference of the ionization potentials, Eq. (4), we find for the ion in the crystal, in a similar manner, that the energy difference is determined by the difference of the quantities in Eq. (4).

Calculation of the corresponding integrals yields

$$\begin{aligned} E_{4d} &= -0.8033 + \int_0^\infty \left[V_0(r) + V_4(r)\right] f^2_{4d}\,dr \\ &= -0.8033 + 0.3275 + 0.0028, \qquad (6) \\ E_{5s} &= -0.5813 + \int_0^\infty V_0(r) f^2_{5s}\,dr = -0.5813 + 0.2577. \end{aligned}$$

The second term on the right determines the interaction energy with the point lattice. Since this interaction was already considered (with the exception of the term with V_4), in a more complete manner (with a correction for the finite radius), we will need the difference of the first components only. This difference, $\Delta E = -0.5813 + 0.8033 - 0.0028 = 0.2192$ a.u., must be added to the interaction energy with the lattice in the excited state in order to obtain the separation of the potential curves.

It can be shown that consideration of the polarization of the core caused by excitation of one electron in the crystal does not increase the energy difference.

DISCUSSION OF THE RESULTS OBTAINED

Let us compare the final results of calculation of the spectra for the transition $4d^{10}$-$4d^9 5s$ by the quantum mechanical method and the Williams method:

Spectral characteristics	Williams method	Quantum mechanical method
$W_{^1S_0}$ (ev)	$4.997\,(\Delta a + 0.069)^2 - 0.279$	$5.475\,(\Delta a + 0.066)^2 - 0.079$
$W_{^3D}$ (ev)	$4.478\,(\Delta a - 0.107)^2 + 3.353$	$4.465\,(\Delta a - 0.064)^2 + 3.34$
Absorption maximum (ev)	3.77	3.52
Emission maximum (ev)	3.477	3.32
Stokes shift (ev)	0.29	0.20
Frequencies of local vibrations (sec^{-1})		
$\nu_{^1S_0}$	$3.1 \cdot 10^{12}$	$3.34 \cdot 10^{12}$
$\nu_{^3D}$	$3.02 \cdot 10^{12}$	$3.01 \cdot 10^{12}$

When one considers the great differences in the methods of calculation, functions used, and calculations of the van der Waals energy, the agreement between the results can be considered almost complete. This agreement demonstrates the validity of Williams' method for calculating luminescence spectra in the first approximation.

Neither the unavoidable lack of accuracy in the determination of repulsion forces in the Williams method nor the approximate character of the calculation of the van der Waals forces has much effect on the final results, inasmuch as the energy components partly compensate each other, and their sum turns out to be 5 to 6 times smaller than the energy of the Coulomb overlap. Thus, the latter is the major factor in the energy difference between the ground and excited states, and determines the character of the spectra.

We are of the opinion that these calculations, together with the results of reference 3, can be considered a proof that the transition $4d^{10}$-$4d^9 5p$, and not the transition $4d^{10}$-$4d^9 5s$, is responsible for the luminescence bands in silver-activated crystal phosphors.

In conclusion, I wish to thank M. I. Petrashen' and A. I. Gubanov for the discussion of the results of this work.

REFERENCES

1. F. E. Williams. J. Chem. Phys* **19**, 457 (1951).

---

*Translator's note: Not J. Chem. Soc. as mistakenly quoted in the Russian original.

---

2. N. D. Potekhina. Opt. i Spektr. **2**, 388 (1957).
3. R. Knox and D. Dexter. Phys. Rev. **104**, 1245 (1956).
4. J. E. Mayer. J. Chem. Phys. **5**, 270 (1933).
5. P. O. Löwdin. An Investigation into Some Properties of Ionic Crystals. Thesis, Uppsala, 1948.
6. E. Montroll and R. Potts. Phys. Rev. **100**, 525 (1955).
7. R. Bjork. Phys. Rev. **105**, 456 (1957).
8. C. Klick. Phys. Rev. **85**, 154 (1952).
9. O. Maeda. J. Phys. Soc. Japan **14** (1959).
10. M. Born and Huang Kun'. "Dinamicheskaya teoriya kristallicheskich reshetok" (Dynamical Theory of Crystal Lattices), Izd. Inostrannoi Lit., Moscow, 1959.
11. F. E. Williams and M. H. Hebb. Phys. Rev. **84**, 1181 (1951).
12. M. Lax. J. Chem. Phys. **20**, 1752 (1952).
13. M. I. Petrashen', A. V. Ivanova, and G. Vol'f. Vestnik Leningrad. Gosudarst. Univ. No 10, 29 (1956).
14. J. Tessman, A. Kahn, and W. Shockley. Phys. Rev. **92**, 890 (1953).
15. R. A. Buckingham. Proc. Roy. Soc. **A160**, 94 (1937); O. Sternheimer. Phys. Rev. **96**, 951 (1954).
16. M. I. Petrashen' and I. V. Abarenkov. Vestnik Leningrad. Gosudarst. Univ. No 5, 141 (1954).
17. D. R. Hartree. Proc. Roy. Soc. **A156**, 59 (1936).

SPECTROSCOPY OF THE LUMINESCENCE CENTERS IN ALKALI HALIDE CRYSTALS ACTIVATED BY HOMOLOGOUS SERIES OF IONS*

*Presented at the Conference on the Physics of Alkali Halide Crystals (Tartu, June, 1959)

A correspondence is established between the spectral characteristics of three series of free ions: Ga^+, Ge^{++}, In^+, Sn^{++}, Tl^+, Pb^{++} (I); Cu^+, Ag^+, Au^+ (II); and Ca^+, Sr^+, Ba^+, Zn^+, Cd^+ (III), and the characteristics of the luminescence centers in alkali halide monocrystals activated by these ions.

The "compression of the energy diagrams" effect is considered in crystalline lattices, along with the possibility of predicting the spectral characteristics of phosphors from the characteristics of the free ion-activators.

The emission of light by solids is usually associated with electron-vibrational transitions in particular defect locations in a crystalline lattice called luminescence centers. The most thoroughly studied activated luminescence centers in crystals have been those deliberately introduced as impurities. It is customary to distinguish two basic types of activation—direct and indirect.[1] In the first case, the electron-vibrational transitions are accompanied by a change in the electronic state of the activator ion. In the second case, the emission arises from electron-vibrational transitions in the basic substance of the phosphor, which has been disturbed in the vicinity of the impurity ions. Currently, we are concerned with indirect activation in phosphors of the ZnS-Cu, ZnS-Ag, and ZnS-Au type.[2] Alkali halide crystals activated by thallium are usually considered as cases of direct activation.[3-5] During our investigation of luminescence centers in activated alkali halide crystals we also proceeded from the latter assumption. In this connection, it seemed that it might be worth while to study a set of alkali halide phosphors activated by a homologous series of ions.[6,7] We have assumed that the energy and probability rules which hold for a homologous series of ions in the case of direct activation will also be observed by the luminescence centers in crystals activated by these ions, even if only qualitatively. This could serve as a proof of direct activation.

In the present work we will consider certain results obtained in an investigation of alkali halide crystals activated by three homologous series of ions: Ga^+, Ge^{++}, In^+, Sn^{++}, Tl^+, Pb^{++} (I); Cu^+, Ag^+, Au^+ (II), and Ca^+, Sr^+, Ba^+, Zn^+, Cd^+ (III).

THE DIRECT ACTIVATION OF ALKALI HALIDE CRYSTALS ACTIVATED BY MERCURY-LIKE IONS

The best prospect seemed to us to be the consideration of the homologous series of ions analogous to the mercury atom—Ga^+, Ge^{++}, In^+, Sn^{++}, Tl^+, Pb^{++} (electronic configuration $1s^2 \ldots np^6nd^{10}(n+1)s^2$, n = 4, 5, 6).[6,7] The characteristics of the free mercury-like ions are well known. We prepared and thoroughly studied NaCl, KCl, KBr, and KI phosphors activated by all six of the ions just enumerated.[7-14]*

As an example, Fig. 1 shows absorption, excitation, and emission spectra for monocrystals of KBr activated by gallium, germanium, indium, tin, thallium, and lead, measured at 298°K with the help of photoelectric equipment. These figures also show the absorption lines of the free ions of the activator according to data in the literature. A detailed comparison of the energy and probability

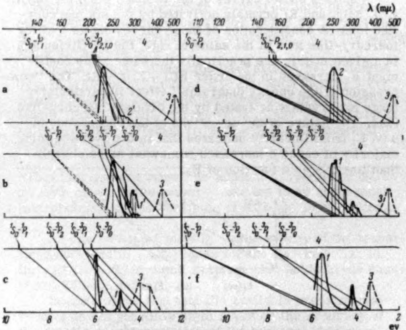

Fig. 1. Spectral characteristics of KBr phosphors activated by mercury-like ions Ga^+ (a), In^+ (b), Tl^+ (c), Ge^{++} (d), Sn^{++} (e), Pb^{++} (f). Curves 1, 1′—absorption spectra; curves 2, 2′—excitation; curve 3—emission; curve 4—absorption spectra of the free activator ions.

rules for the various mercury-like ions and their homologous series on the one hand, with the various luminescence centers in crystals and their homologous series on the one hand, with the various luminescence centers in crystals and their homologous series on the other, is found in references 7-9, 12, 13. Figure 1 shows that the luminescence centers in the phosphors investigated certainly preserve the patterns characteristic of the free mercury-like ions. On the basis of the evidence we have obtained, we consider it to have been spectroscopically demonstrated that the "nuclei" of the luminescence centers in alkali halide crystals activated by gallium, germanium, indium, tin, thallium, and lead, are the Ga^+, Ge^{++}, In^+, Sn^{++}, Tl^+, and Pb^{++} ions. Upon excitation of the centers the electron state of the mercury-like ions changes. As can be seen in Fig. 1, the intense absorption (excitation) band corresponds to the allowed transition $^1S_0 - {^1P_1}$, and the weak one to the intercombination transition $^1S_0 - {^3P_{0,1,2}}$. The primary emission bands for the phosphors activated by Ga^+, In^+, Ge^{++}, and Sn^{++} correspond to the transition from the lowest excited level to the ground state—$^3P_0 - {^1S_0}$; for phosphors activated by Tl^+ and Pb^{++} the transition is $^3P_1 - {^1S_0}$. Under favorable conditions, it is possible to observe both transitions in emission: $^3P_0 - {^1S_0}$ and $^3P_0 - {^1S_0}$.

In the phosphors investigated we have a well-defined case of direct activation. In spite of this, the spectral characteristics of the luminescence centers in the crystals differ considerably from the characteristics of the free ions. As a result of the interaction between the activator ion and the surrounding lattice, which differs for the normal and excited states, the energy intervals between the levels of the luminescence centers are considerably smaller than those in the free ion (see Fig. 1). A quantitative analysis shows that the "compression" coefficient ρ (the ratio of the energy of a transition in the free ion E_f to the energy of the maximum of the corresponding absorption band of the luminescence center in the crystal E_c) increases linearly with E_f[7, 8]

---

*Some of these phosphors had also been studied previously (for references see reference 7).

$$\rho = \frac{E_f}{E_{c.}} = 1 + aE_f\,. \qquad (1)$$

Figure 2 shows curves of the function $\rho(E_f)$ for NaCl, KCl, KBr, and KI crystals activated by the six mercury-like ions. A consideration of these curves shows that for mercury-like ions of the same charge, the coefficients a in a given matrix are practically the same. The coefficient a increases in the order KCl → KBr → KI. The "compression of the energy diagrams" effect is particularly large for crystals activated by the divalent mercury-like ions. The nature of the deviations of the dependence of ρ on E_f from linearity indicates that in the overwhelming majority of cases ρ increases somewhat more sharply than linearly as a function of E_f.

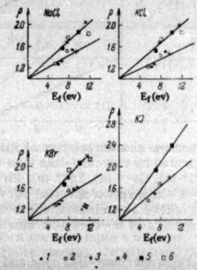

Fig. 2. Relation between the transition energies in the free activator ions and the luminescence centers for NaCl, KCl, KBr, and KI phosphor crystals with mercury-like activators Ga^+ (1), In^+ (2), Tl^+ (3), Ge^{++} (4), Sn^{++} (5), and Pb^{++} (6).

We do not attribute any deep physical significance to the linear dependence of ρ on E_f, but we do point out that the establishment of the above-mentioned approximate relationship between E_c and E_f uncovers several possibilities for prediction of the spectral characteristics of previously unknown phosphors in terms of the known spectrum of the free ions of the activator. Utilizing the data of atomic spectroscopy and Eq. (1), we estimated the location of the primary absorption bands for the previously unknown phosphors KCl-Ga and KCl-Ge.[7] Experiment subsequently confirmed the accuracy of the estimate.[11]

DIRECT ACTIVATION OF ALKALI HALIDE CRYSTALS BY NOBLE METAL IONS

As a second series of ions activating alkali halide crystals, we chose the ions Cu^+, Ag^+, and Au^+, with the electronic configuration $1s^2 \ldots np^6nd^{10}$ (n = 3, 4, 5). The characteristics of the free "noble" ions are well known. We prepared and investigated NaCl and KCl phosphors activated by copper, silver, and gold. The copper- and silver-activated phosphors have also been the subjects of earlier studies (see, for example, references 15 and 20).

The absorption, excitation, and emission spectra of the KCl phosphors which we investigated at 298°K are presented in Fig. 3. This figure also shows literature values for lines of the free ions.* We have concluded from a detailed analysis of the experimental results that in these phosphors, just as in the phosphors activated by mercury-like ions, there is direct activation. The luminescence centers preserve features similar to the free Cu^+, Ag^+, and Au^+ ions which are thus the "nuclei" of the luminescence centers. Unfortunately, it is considerably more difficult to make a detailed comparison between the spectra of the luminescence centers and the free activator ions for phosphors activated by "noble" ions than it is for the mercury-like ions.

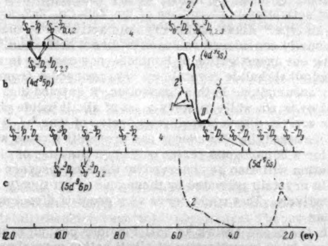

Fig. 3. Spectral characteristics of KCl-phosphors activated by the "noble" ions Cu^+ (a), Ag^+ (b), and Au^+ (c). Curve 1—absorption spectra; curve 2—excitation; curve 3—emission; curve 4—absorption spectra of the free activator ions.

Because of the nature of the electron configurations of "noble" ions, their spectra are far more complicated than those of the mercury-like ions. Transitions from the ground level to the first four excited D-levels are forbidden by Laporte's rule. The next electron configuration—$nd^9(n+1)n$—has twelve levels concentrated within a narrow energy range. It is significant that the coupling in free Au^+ and Ag^+ ions is very close to j,j coupling, a fact which further complicates the interpretation of the data. The coupling in free Cu^+ is intermediate between the (L,S) and (j,j) types. However, as we showed in the case of the mercury-like ions,[7] a weakening of the L,S coupling takes place when these ions are introduced into a crystalline lattice. One might think that this effect would also be observed for Cu^+ ions.

According to the selection rules for j,j coupling, in addition to the transitions to P-levels which we considered for the mercury-like ions, other transitions will also be permitted (e.g., ${}^1S_0 - {}^3D_1$) in the case of the "noble" ions.

---

*The levels ${}^3F_{4,3,2}$ and ${}^1F_3$ are not shown in the scheme, for simplicity.

When these ions are introduced into a crystalline lattice, the degeneracy of several energy states is removed and still another series of permitted transitions appears. Thus each kind of luminescence center in alkali halide phosphors activated by Cu^+, Ag^+, and Au^+ ions should show complicated absorption and excitation spectra, consisting of a series of closely-spaced overlapping bands. An inspection of Fig. 3 shows that this actually occurs.

In comparing the spectral characteristics of the phosphors and the free Cu^+, Ag^+, and Au^+ ions, it is necessary to take account of the above-mentioned compression of the energy diagrams of cation impurities which are incorporated into a crystalline lattice. The existence of this effect is confirmed by all of the experimental data known to us on phosphors with direct activation, and also by theoretical calculations.[12-24] Since the transitions $nd^{10} \to nd^9(n+1)s$ require the expenditure of less energy in the case of the free "noble" ions than for the excitation of the luminescence centers in the corresponding phosphors, it must follow that the absorption (excitation) bands in Series I centers do not represent such transitions. Potekhina had already concluded as much after a detailed theoretical treatment of the luminescence centers in the phosphor NaCl-Ag.[22] It is necessary to compare the absorption (excitation) bands which are observed in the phosphors KCl-Cu, KCl-Ag, and KCl-Au with the transitions $nd^{10} \to nd^9(n+1)p$ of the free "noble" ions.

In the Cu^+ ion the energy levels of the electronic configuration $3d^94p$ are close together (twelve levels within a range of 1 ev). In view of the usual width of elementary absorption bands in alkali halide phosphors (0.2-0.3 ev at 300°K) the absorption bands corresponding to these transitions in the phosphor KCl-Cu can hardly be resolved. In the absorption and excitation spectra of the phosphor KCl-Cu, three bands can be resolved at 5.25, 4.70, and 4.30 ev. The principal emission band (3.12 ev) shown in Fig. 3 is effectively excited by the first two of these. A yellow glow is excited in the band 4.30 ev, marked with a II in Fig. 3. In our opinion, this band corresponds to a second kind of luminescence center in KCl-Cu.* Most of the absorption in KCl-Cu in the vicinity of 4.7 ev is due, apparently, to the $^1S_0 \to {}^1P_1$ transition in Cu^+ ions, which is allowed by all of the selection rules. Its probability should not depend on temperature. In accordance with this, we did not observe any marked decrease in the intensity of the 4.7 ev absorption band in the phosphor KCl-Cu upon cooling the phosphor from 300 to 100°K.

In the Ag^+ ion, the energy levels of the electron configuration $4d^95p$ are less closely grouped than in the Cu^+ ion. In the phosphor KCl-Ag one can expect partial resolution of the three absorption bands corresponding to the transitions in Ag^+ ions: $^1S_0 \to {}^3P_2$ (1); $^1S_0 \to {}^3P_1$, $^1S_0 \to {}^3P_0$, etc. (2); $^1S_0 \to {}^3D_1$, $^1S_0 \to {}^1P_1$, etc. (3). As can be seen in Fig. 3, one actually observes three bands at 5.6, 5.65, and 5.9 ev in the absorption and excitation spectra of KCl-Ag, which can be attributed to one kind of center. The existence of the shortest wavelength band is inferred from the excitation spectrum which we obtained. This probably corresponds to the transition $^1S_0 \to {}^1P_1$. Just as in the alkali halide crystals activated by mercury-like ions,[25] activated phosphorescence is well excited in this band.

The absorption band at 5.45 ev probably corresponds to the transition $^1S_0 \to {}^3P_2$. It is known that in phosphors activated by thallium the integrated absorption of the $^1S_0 \to {}^3P_2$ band depends on the temperature, a fact which is associated with the decreasing probability of a transition forbidden according to ΔJ with decreasing temperature.[26] It is natural to expect an analogous behavior for the 5.45 ev band in KCl-Ag. Our experiments have shown that at 100°K the absorption in the region of the two long wavelength absorption bands of KCl-Ag (just as for the $^1S_0 \to {}^3P_2$ transitions in thallium phosphors) is diminished by one-half. In reference 18, the oscillator strength for the 5.65 ev band in KCl-Ag was measured and found to be equal to several hundred. This value for the oscillator strength also agrees with the proposed interpretation of the absorption band in question.

The middle absorption band (5.65 ev) is probably nonelementary. It may be due to an overlapping of the $^1S_0 \to {}^3P_1$, $^1S_0 \to {}^3P_0$, etc. bands. The decrease of its intensity when the temperature is lowered must be connected with the diminishing probability of the transitions $^1S_0 \to {}^3P_0$ and a lessening of the overlapping with the strong short wavelength band.

In the KCl-Ag absorption band at 5.05 ev, indicated by a II, it is not the fundamental emission band (4.5 ev) which is excited, but a luminescence at a longer wavelength. It undoubtedly corresponds to Ag^+ ions that have an environment different from that of the fundamental emission centers.*

As can be seen from Fig. 3, the energy of the transitions $nd^{10} \to nd^9(n+1)p$ is less for the Cu^+ ions than for the Ag^+ ions. This same relation also holds in the phosphors KCl-Cu and KCl-Ag.

In spite of the fact that the available experimental results do not yet allow us to insist on the accuracy of the details of interpretation of the spectral characteristics of the copper- and silver-activated phosphors, a comparison of the general spectral regularities in these phosphors with the regularities observed in the free ions Cu^+ and Ag^+ permits us to conclude that direct activation also occurs in these phosphors.

In crystals activated by copper and silver, the coefficient of compression a (see Eq. 1) is somewhat larger than for the univalent mercury-like ions, and somewhat smaller than in the divalent mercury-like ions.

In Au^+, the energy levels of the electronic configuration $5d^96p$ are widely separated. Hence one might expect to succeed in completely resolving at least some of the absorption bands in the phosphor KCl-Au. It was for this reason that we undertook the synthesis of gold-activated alkali halide phosphors as early as 1956.[7] "Gold" phosphors were successfully synthesized;* however their spectra proved to be more complicated than had been anticipated. (See Fig. 3.)

Au^+ ions are larger than K^+ ions. According to considerations of "volume compensation" it is energetically advantageous for them to be associated with lattice defects such as vacancies and discharged regions of dislocations. Therefore, in our opinion, different types of complicated luminescence centers arise in gold phosphors, even at very low activator concentrations. In such centers, as was shown in references 9 and 14, there exist conditions for the occurrence of large Stokes losses, such as are also observed in phosphor KCl-Au.

---

*Analogous centers are also observed in alkali halide phosphors with mercury-like ions at high concentrations of the activator or of defects in the crystal lattice.[9]

*This fact was not taken into account in reference 20, as a result of which the authors were led to an erroneous interpretation of the spectrum of KCl-Ag, in our opinion.

*The method of preparation and spectral characteristics will be completely described in a special paper.

DIRECT ACTIVATION OF ALKALI HALIDE CRYSTALS BY Ca^+, Sr^+, Ba^+, Zn^+, and Cd^+ IONS

Analysis of the energy diagrams for the series of free ions Ca^+, Sr^+, and Ba^+ with electronic configurations $1s^2 \ldots np^6$ and a rough calculation of energy diagram compression in the lattice of alkali halide crystals show that the absorption and possibly also the emission of these ions will lie in the vicinity of the fundamental absorption of the matrix. The direct activation of alkali halide salts by these ions is not very likely.

It is well known, however, that after x-ray irradiation of crystals containing Ca^{++}, Sr^{++}, and Ba^{++} ions, so-called Z_1 centers are formed in them. According to Seitz Z_1 centers can be considered as electrons which have been trapped by the Ca^{++}, Sr^{++}, and Ba^{++} ions distributed in the cation sites of the crystal.[27] It is natural to compare the spectral characteristics of Z_1 centers with the electronic transitions in free Ca^+, Sr^+, and Ba^+ ions. Such a comparison was made, upon our suggestion, by Zaitov.[28] For a long time it has not been clear why bands analogous to the Z_1 bands are not formed on the long wavelength side of the F band upon x-irradiation of alkali halide crystals containing ions of the second subgroup of column II of Mendeleev's Table—Zn^{++} and Cd^{++}. A simple answer to this question can be given by comparing the energy diagrams of Ca^+, Sr^+, Ba^+, Zn^+, and Cd^+ presented in Fig. 4. It follows from Fig. 4 that the absorption bands analogous to Z_1 bands in Zn- and Cd-activated NaCl, KCl, and KBr crystals must be sought in the near ultraviolet, and not in the red. We have actually detected these bands in x-irradiated crystals of KCl-Cd and NaCl-Cd.[28, 29] It is interesting to note that a visible luminescence is excited in the region of these absorption bands. Ca^+ and Sr^+ ions in alkali halide crystals (Z_1 centers), as it later appeared, luminesce in the infrared region of the spectrum.[30] It is probably necessary to compare the electronic transitions occurring in absorption and emission of alkali halide crystals containing the ions Ca^+, Sr^+, Ba^+, Zn^+, and Cd^+ with the transitions $^2S_{1/2} - {}^2P_{1/2,\,3/2}$ in the free ions. The energy compression effect for these ions has approximately the same magnitude as for Ge^+, In^+, and Tl^+ ions.

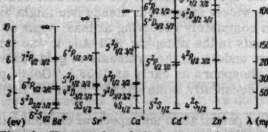

Fig. 4. Energy level diagrams of the ions Ba^+, Sr^+, Ca^+, Cd^+, and Zn^+.

We thus see that the assumption of direct activation of alkali halide crystals appears to be fruitful also in the study of so-called color centers.

CONCLUSION

In conclusion it should be noted that alkali halide crystals which are transparent up to the vacuum ultraviolet region are favorable material for direct activation by various impurities (the possibilities of ZnS phosphors in this regard are considerably more limited).

In alkali halide crystals activated by mercury-like ions we undoubtedly have a case of direct activation. In this class of phosphors, the retention of many of the characteristic features of the free ions by the luminescence centers can be considered as spectroscopically demonstrated. The data on the two other homologous series of activating impurities considered above has also led us to conclude that direct activation was present. An important argument in favor of this view is the fact that a consideration of the free ions led to a prediction of the possibility of the existence of a series of new crystal phosphors activated by indium, gallium, germanium, gold, and cadmium, the subsequent synthesis of which confirmed the correctness of the prediction. The values we obtained from Eq. (1) show that, in principle, direct activation of alkali halide crystals is possible by still other homologous series of ions. In particular, it would be enlightening to try direct activation of alkali halide crystals by Sc^+, Ti^{++}, V^+, Zr^{++}, La^{++}, and Hf^{++} ions, which differ from the mercury-like ions in lacking filled d shells.

REFERENCES

1. F. Kröger. "Some Aspects of the Luminescence of Solids." New York, 1948.
2. H. Klassens. J. Electrochem. Soc. 100, 72 (1953).
3. F. Seitz. J. Chem. Phys. 1, 150 (1938).
4. F. D. Klement. Kand. diss Leningrad. Gosudarst. Univ. (Candidate's Dissertation, Leningrad State Univ.), 1942.
5. K. V. Shalimova. Dokt. diss., Moskva, 1953.
6. Ch. B. Lushchik. Trudy Inst. Fiz. i Astron., Akad. Nauk Eston.SSR No. 3, 3 (1955).
7. N. E. Lushchik and Ch. B. Lushchik. Trudy Inst. Fiz. i Astron., Akad. Nauk Eston.SSR No. 6, 5 (1957).
8. N. E. Lushchik. Trudy Inst. Fiz. i Astron., Akad. Nauk Eston.SSR No. 7, 119 (1958).
9. N. E. Lushchik. Trudy Inst. Fiz. i Astron., Akad. Nauk Eston.SSR No. 10, 68 (1959).
10. N. E. Lushchik. Izvest. Akad. Nauk SSSR, Ser. Fiz. 21, 754 (1957); Trudy Inst. Fiz. i Astron., Akad. Nauk Eston.SSR No. 6, 149 (1957).
11. N. E. Lushchik. Trudy Inst. Fiz. i Astron., Akad. Nauk Eston.SSR No. 7, 134 (1958).
12. Ch. B. Lushchik and N. E. Lushchik. Izvest Akad. Nauk SSSR, Ser. Fiz. 22, 1351 (1958).
13. N. E. Lushchik. Kand. diss., Tartu, 1959.
14. Ch. B. Lushchik, N. E. Lushchik, and K. K. Shvarts. Trudy Inst. Fiz. i Astron., Akad. Nauk Eston.SSR No. 8, 3 (1958).
15. M. McMahon. Z. Physik 52, 336 (1929).
16. M. Forro. Z. Physik 56, 534 (1929).
17. M. Kato. Sci. Papers Inst. Phys. Chem. Research (Tokyo) 41, 113 (1943).
18. H. Etzel and J. Shulman. J. Chem. Phys. 22, 1549 (1954).
19. I. A. Parfianovich. Dokt. diss., Moskov. Gosudarst. Univ., 1958.
20. M. L. Kats and V. K. Nikol'skii. Materialy V. Soveshch. po liuminests. (Proc. 5th Conf. on Luminescence), p. 63, Tartu, 1957.
21. F. Williams. J. Chem. Phys. 19, 457 (1951).
22. N. D. Potekhina. Opt. i Spektr. 2, 388 (1957).
23. N. N. Kristofel'. Kand. Diss., Tartu, 1959.
24. M. I. Petrashen', T. L. Gutman, and M. Balarin. Vestnik Leningrad. Gosudarst. Univ. 22, 28 (1958).
25. I. V. Yaek. Trudy Inst. Fiz. i Astron., Akad. Nauk Eston.SSR No. 10, 166 (1959).

26. P. Yuster and C. Delbecq. J. Chem. Phys. 21, 802 (1953).
27. F. Seitz. Phys. Rev. 83, 134 (1951).
28. F. N. Zeitov and V. Ya. Kark. Trudy Inst. Fiz. i Astron., Akad. Nauk Eston.SSR 6, 82 (1957).
29. Ch. B. Lushchik, F. N. Zaitov, V. Ya. Kark, and L. A. Teiss. Materialy V Soveshch. po liuminests. (Proc. 5th Conf. on Luminescence), p. 75, Tartu, 1957.
30. E. West and W. Compton. Phys. Rev. 108, 576 (1957).

TEMPERATURE EFFECT ON THE PHOTOLUMINESCENCE OF THE EVAPORATED ZnS:Mn PHOSPHOR

N. A. Vlasenko

Received 19 October 1959

A study was made of the effect of temperature on the absorption and emission spectra of an evaporated ZnS:Mn phosphor between 100 and 550°K. The temperature dependence of the relative quantum yield of luminescence for samples with different activator concentrations was also studied. On the basis of these data, certain conclusions were drawn regarding the excitation mechanism of the luminescence center, the character of luminescent and the nonradiative transitions, and the nature of concentration extinction in the phosphor studied.

A study of the temperature dependence of basic phosphor properties gives valuable information on luminescence and the processes accompanying it. Thus, for example, data concerning the effect of temperature on the position and width of absorption and emission bands of the luminor make it possible to draw certain conclusions concerning the nature of the centers which absorb and emit luminous energy and their interaction with lattice vibrations.[1] The nature of the nonradiative processes in the phosphor may be determined from the temperature variation of the luminescence yield and the decay constant,[2] while the nature of processes involving the capture and liberation of charge carriers may be determined from thermoluminescent and electrical properties.

So far, most investigations of ZnS phosphors have been carried out on powdered samples, and have been limited to a study of the temperature dependence of luminescence intensity and thermal stimulation. The strong scattering of light in powders interferes with quantitative determination of their absorption spectrum, while the lack of precise data concerning the temperature variation of the absorptivity of a phosphor introduces a considerable error into the temperature dependence of the luminescence yield.

Studies have recently begun to appear on the effect of temperature on the properties of single crystals of zinc sulfide containing various activators.[3] However, the methods of growing these crystals are complicated, and do not produce homogeneous samples of sufficient size.

Evaporated phosphors, which are characterized by the absence of scattered light, homogeneity of sample, and the possibility of thickness control, are particularly convenient for temperature and other physical measurements. Furthermore, the method which we developed for preparing evaporated ZnS-base phosphors allows us to regulate and determine the phosphor composition. The evaporated ZnS:Mn phosphor obtained by this method without fluxes or co-activators has only one orange emission band, as opposed to the corresponding powdered phosphors, in which an additional blue band is observed, which is characteristic of self-activated ZnS. This simplifies the study of the effect of temperature on phosphor properties, since there is no longer any need to take into account the overlapping of spectra corresponding to different activators. In this article we made a study of the effect of temperature on the absorption and emission spectra of the evaporated ZnS:Mn phosphor, and on the temperature extinction of luminescence for different manganese concentrations.

The effect of temperature on the absorption spectrum was studied first in order to ascertain the nature of the absorption, and secondly, to obtain the temperature dependence of the luminescence yield. The introduction of manganese into ZnS causes the appearance of additional absorption,[4] which adjoins the edge of the fundamental band of pure zinc sulfide and (at room temperature) has a maximum in the region of 340 mμ. The magnitude of this absorption is proportional to activator concentration and decreases monotonically as the wavelength increases. The region of maximum efficiency of phosphor excitation coincides with the region of the maximum of additional absorption. A temperature rise* causes a displacement of this absorption maximum towards longer wavelengths (Fig. 1a). The magnitude of the temperature coefficient of the displacement was found to be the same as for the edge of the fundamental absorption band of pure ZnS ($-4.5 \cdot 10^{-4}$ ev/deg). The wavelength dependence of the difference between the absorption coefficients of ZnS:Mn and ZnS has a maximum. As the temperature increases, this maximum broadens, decreases in magnitude, and is displaced towards longer wavelengths with the same temperature coefficient. (See Fig. 1a, curves I, II, III.) Thus the additional absorption in ZnS:Mn and the long wavelength maximum of the fundamental band of pure ZnS[5] show the same temperature dependence. This indicates that the additional absorption is connected with the zinc sulfide lattice, which is distorted by the presence of manganese. Simultaneously with the appearance of this absorption, we observed a certain decrease in the coefficient of absorption in the region of the maximum (325 mμ) of the fundamental ZnS band. (See Fig. 1b.) Taking into account the fact that this maximum is apparently caused by transitions into excited lattice states,[5] rather than into the conduction band, we may assume the following: The additional absorption in ZnS:Mn which we are considering is due to excited states of sulfur ions located in the immediate vicinity of the manganese ion. (These excited states must have a somewhat lower energy than in the case of the ideal lattice, since the polarizability of the manganese ion is higher than that of Zn^{2+}.) We may then

---

*The procedure for studying the absorption spectrum at different temperatures has been described previously.[5]

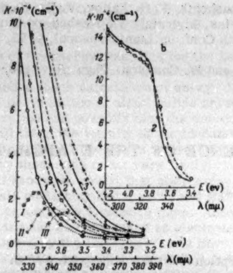

Fig. 1. Absorption spectra of ZnS phosphors (solid lines) and ZnS:Mn (2%) (dashed lines) at different temperatures. Temperature (in °K); curve 1—115; curve 2—293; curve 3—510. Curves I, II, III represent the difference of the absorption coefficients of ZnS:Mn and ZnS phosphors at the same temperatures, respectively.

draw the following picture of the excitation of the activator center by light of a wavelength corresponding to the region of additional absorption, and the emission process: The absorption of a light quantum causes the excitation of the sulfur ion adjoining Mn, i.e., the transfer of an electron from the sulfur ion to one of the three remaining nearest zinc ions. The return of this electron to the normal state liberates energy which may be absorbed by a nearby manganese ion and cause its excitation. Luminescence is thus the result of the transition of an excited activator ion to the normal state. With this mechanism, the energy used to excite the manganese ion is liberated in its own vicinity. Excitation in this case must be more efficient than when the light quantum is absorbed by the undistorted lattice, since in the latter case the energy must be transferred an appreciable distance in order to give rise to luminescence. This agrees with the experimentally observed excitation spectrum.[4]

In evaporated ZnS:Mn films, we could not find the absorption caused by electron transitions in the manganese ions even when the thickness was considerable 3-5μ) and the activator concentration high (~5%). According to the data of Kröger[6] and Bube[7] this absorption consists of a series of bands in the 380-500 mμ region. This is apparently connected with the fact that although these transitions are forbidden in the free ion, the extent to which this rule may be broken for an ion placed in some medium depends on the symmetry of the crystalline lattice field.[1] Field asymmetry is much higher in the wurtzite lattice than in the sphalerite lattice. Therefore, in the evaporated ZnS:Mn phosphor, which has a cubic lattice, the absorption connected with the "forbidden" transitions may be much weaker than in the hexagonal samples used in references 6 and 7.

A temperature change also affects the emissive capacity of a phosphor. Starting with a certain definite temperature, we observe a sharp decrease in the total number of quanta emitted, due to an increase in the probability of nonradiative transitions. Furthermore, an increase in temperature causes a change in the emission spectrum. A study of the emission spectrum of an evaporated ZnS:Mn phosphor was carried out over the 100-550°K range for different activator concentrations. The spectra were measured by a photoelectric procedure.

Figure 2 shows the results of measurements* for two cases: (a) Low activator concentration; concentration quenching absent; (b) Mn concentration = 5%, which corresponds to the region of strong concentration quenching.[4] In the first case, the position of the emission maximum (583 mμ) does not vary with temperature. The half-width of the band is practically invariant for temperatures below 150°K, but increases as the square root of the temperature for high temperatures. This characteristic of the variation of the emission spectrum with temperature confirms the assumption that luminescence in ZnS:Mn phosphors is due to the transition of the activator ion from an excited to the normal state. In this case the emission process may be described by means of a system of potential curves in configuration coordinates.[8] The finite width of the emission bands of crystalline phosphors, which in most cases reaches several hundred angstroms,[9] and the dependence of their half-width on temperature is explained by the interaction of activator electrons with the vibrations of surrounding ions.[10] A quantum mechanical computation[11] results in the following relation between the half-width H of the spectrum, the temperature T, and the vibration frequency ν in the initial state

$$H = A\left[h\nu \coth\left(\frac{h\nu}{2kT}\right)\right]^{1/2}. \tag{1}$$

where A is a constant, h the Planck constant, and k the Boltzmann constant. By comparing the experimental temperature dependence of the half-width of the emission spectrum with the theoretical value computed from Eq. (1), we may obtain the vibration frequency of lattice ions surrounding the excited activator center. A simple expression for ν is obtained if we know the half-width H_0 at sufficiently low temperatures (in the range where the half-width is independent of T) and the half-width H_T at sufficiently high temperatures where it is proportional to $\sqrt{T}$; this expression is

$$\nu \simeq \frac{2kT}{h} \cdot \left[\frac{H_0}{H_T}\right]^2. \tag{2}$$

By substituting the experimental values $H_0 = 0.168$ ev, $H_T = 0.245$ ev, and T = 510°K into Eq. (2), we obtain $\nu = 9.8 \cdot 10^{12}$ sec^{-1}. This value is very close to the frequency of optical lattice vibrations of pure ZnS deter-

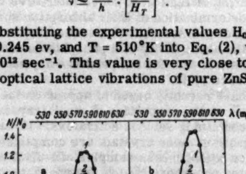

Fig. 2. Emission spectra of evaporated ZnS:Mn phosphor for different temperatures and activator concentrations (sample thickness—7μ). a, C = 0.5%; T (in °K): curve 1—110; curve 2—293; curve 3—370; curve 4—455; curve 5—510. b, C = 5%; T (in °K); curve 1—110; curve 2—293; curve 3—360; curve 4—450; curve 5—535.

---

*To represent the emission spectra, the relative number of quanta emitted is given as a function of the quantum energy.

mined by the method of residual rays[13] ($9.1 \cdot 10^{12}$ sec^{-1}). The solid curve in Fig. 3 represents the theoretical values of the half-width H of the spectrum computed from Eq. (1) using the value of ν just obtained. The circles represent the experimental values. Thus there is good agreement between theory and experiment. Hence the model used in deriving Eq. (1) represents the true luminescence process in ZnS:Mn at low activator concentrations.

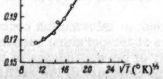

Fig. 3. Temperature dependence of the half-width of the emission spectrum of the evaporated phosphor ZnS:Mn (0.05). The line gives the theoretical values, the circles the experimental values.

The emission spectrum and its temperature dependence change in the case of high concentrations, when concentration quenching is severe and the interaction of activator centers begins to play an appreciable role. It has been shown previously[4] that when the Mn concentration increases beyond 0.1%, the emission spectrum begins to be displaced monotonically towards longer wavelengths. (When the concentration changes from 0.1 to 5%, the maximum of the spectrum is, at room temperature, displaced by 70 A.) At the same time, its half-width remains practically unchanged. Figure 2b shows that at high concentrations, a temperature increase causes not only a broadening of the band but also a displacement of its maximum towards shorter wavelengths. This displacement stops when the position of the maximum coincides with that for samples with low activator concentration. To explain these phenomena, it was originally[4] assumed that the spectrum of an evaporated ZnS:Mn phosphor contains two bands whose relative intensities vary with activator concentration and temperature. However, measurements at low temperatures did not support this assumption: there is no indication of a two-band structure in the spectrum taken at 110°K. A possible explanation of the temperature displacement of the spectrum for samples with high Mn concentration will be given below, after we discuss the results of studying the temperature dependence of the luminescence yield at different activator concentrations.

The temperature dependence of the luminescence yield of the evaporated ZnS:Mn phosphor was studied from 100 to 550°K, with excitation by the 365 mμ mercury line. The relative quantum yield was determined by means of the formula

$$\eta = \frac{N}{A} = \frac{N}{1 - e^{-kt}}, \tag{3}$$

where N is the relative number of quanta emitted under the given conditions of excitation, $A = 1 - e^{-kt}$ is the fraction of the exciting radiation absorbed by the phosphor,* k is the absorption coefficient of the phosphor for λ = 365 mμ, and t is the thickness of the sample. The thickness of the samples was determined by an interferometric method, and N by a graphical integration of the emission spectrum.

Experiments show that the luminescence yield and intensity depend differently on temperature. (See Fig. 4.) When the temperature is raised, the relative quantum yield at first remains unchanged and then starts decreasing, while the number of quanta emitted, and hence the intensity of luminescence, goes through a maximum. A similar maximum in the temperature dependence of the luminescence intensity of powdered ZnS:Mn phosphor was found in a series of articles.[7, 14] It was ascribed either to the saturation of manganese centers at low temperatures[14] or to a "freezing" of phosphorescence. It seems to us, however, that this maximum is connected with a change in the absorptive capacity of the phosphor with temperature, since it disappears for samples with high (≥2) optical density over the entire temperature range studied, i.e., when the fraction of the exciting radiation absorbed by the phosphor does not vary with temperature. (See, for example, Fig. 2.) The shapes of the $\eta(T)$ and N(T) curves also differ in the region of temperature quenching. We must therefore be very careful in using data on the temperature dependence of the intensity of luminescence in determining the characteristics of this process.

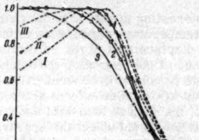

Fig. 4. Temperature dependence of the relative quantum yield of luminescence η (solid lines) and the relative number N/N_0 of emitted quanta (dashed lines) for different manganese concentrations. 1, I—0.05%; 2, II—0.5%; 3, III—5%. Sample thickness—1 μ.

Figure 4 shows the temperature dependence of the luminescence yield of samples with different manganese concentrations. At low Mn concentrations (< 0.1%) the yield remains constant up to 320°K. The decrease in the yield in the region of higher temperatures is well described by[15] the formula

$$\frac{\eta}{\eta_0} = \frac{1}{1 + Ce^{-\frac{E}{kT}}}, \tag{4}$$

where η_0 is the luminescence yield in the absence of temperature quenching, η is the yield at the temperature T, E = 0.36 ev is the activation energy of the quenching process, K is the Boltzmann constant, and C is a constant equal to $1.2 \cdot 10^4$.

When the Mn content exceeds 0.1%, an increase in concentration causes a monotonic decrease in the temperature at which temperature quenching begins. (For example, for a concentration of 5%, quenching begins at 140°K.) Equation (4) is inapplicable in the low temperature range, while the high temperature portions of the yield curve are well described by this formula for the same values of E and C. This is seen particularly clearly in Fig. 5, which shows $\log(\eta_0/\eta - 1)$ as a function of 1/T for samples with different manganese concentrations. A similar change in the behavior of the temperature dependence of the luminescence yield with increased activator concentration was found by Shvarts in alkali halide phosphors.[16] We should note, however, that for ZnS:Mn the low temperature portions of the $\log(\eta_0/\eta - 1)$ versus 1/T curve are not straight lines as they were in Shvarts' case. Thus in this case we may not speak of the appearance of a second activation energy.

---

*One more factor should be taken into account in the expression for A, namely (1 − R), where R is the reflection coefficient. We ignored it since it depends only weakly on temperature. (For an absorption coefficient ≤ $5 \cdot 10^4$ cm^{-1}, the reflective capacity is determined by the index of refraction, which varies only insignificantly with temperature.[13]

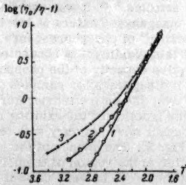

Fig. 5. The dependence of $\log(\eta_0/\eta - 1)$ on 1/T for samples with different manganese concentrations. Curve 1—0.05%; curve 2—0.5%; curve 3—5%.

It is also interesting to note that the change in the behavior of the temperature dependence of the luminescence yield, the displacement of the emission spectrum, and the appearance of concentration quenching all appear in the same range of activator concentration (above 0.1%). This suggests that all of these effects are connected with the interaction of manganese ions with each other.

This interaction should affect the appearance of the potential curves of the normal and excited states of the ion. (The effect on the excited state curve will be more pronounced.) Consequently, the emission spectrum and other characteristics of the luminescence center (e.g., the activation energy of temperature quenching) will change. We may explain the experimentally observed monotonic displacement of the emission spectrum towards longer wavelengths with increasing manganese concentration by the use of a system of potential curves in configurational coordinates, if we make the following assumption: We must assume that the interaction of activator centers causes an additional displacement of the minimum of the excited state curve relative to the minimum of the normal state curve. A decrease in the activation energy of the temperature extinction will cause a decrease in the luminescence yield at that temperature, i.e., a concentration quenching.[17] We can also explain the peculiarities of temperature extinction and the displacement of the emission spectrum with temperature at high activator concentrations. For that we must assume that the activator ions begin to interact at distances smaller than some definite length R_0 (according to data on concentration quenching, R_0 amounts to 30 A for ZnS:Mn) and take into account the fact that the distribution of impurity ions in the lattice is statistical. When the Mn content exceeds C_0 (C_0 is the concentration which corresponds to the average inter-ionic distance R_0), the characteristics of the majority of luminescence centers will be changed more or less as compared with the characteristics of "isolated" centers. In addition to this there is also a certain number of centers at distances greater than R_0. At low temperatures, when the probability of nonradiative transitions is small even for centers with a lowered activation energy, the emission spectrum and other characteristics will be determined primarily by the properties of interacting activator ions. When the temperature rises, the quenching of luminescence will be stronger for those centers which are closer to each other, i.e., the properties of the phosphors should approach those of isolated centers as the temperature increases. This is observed experimentally. This general picture is consistent with the lowering of the temperature extinction "threshold" with increase in activator concentration, with the absence of a definite slope in the low temperature portion of the plot of $\log(\eta_0/\eta - 1)$ versus 1/T at high manganese concentrations, and finally with the invariance of the temperature extinction constants in the high temperature region for samples with different concentration.

A certain amount of information concerning the nature of the process of temperature quenching can be obtained from a study of the dependence of the intensity of luminescence on the intensity of the exciting light in the region of temperature quenching.[18] For an evaporated ZnS:Mn phosphor excited by $\lambda = 365$ mμ and for temperatures $T \geq 290$°K, this dependence remains practically linear for all activator concentrations. This indicates that the extinction which we observed in ZnS:Mn is internal.

In conclusion I take this opportunity to thank K. D. Sinel'nikov for his interest in this work and I. N. Shklyarevskii and V. K. Miloslavskii for discussion of the results.

REFERENCES

1. F. Seitz. Revs. Modern Phys. 23, 328 (1951);
   C. C. Klick and J. H. Schulman. Solid State Phys. 5, 97 (1957).
2. F. A. Kröger et al. Physica 14, 81, 425 (1948); 15, 557 (1949).
3. F. A. Kröger. Physica 22, 6, 37 (1956);
   J. Broser and R. Broser-Warminsky. Z. Electrochem. 61, 209 (1957);
   A. Lempicki. J. Opt. Soc. Am. 48, 67 (1958);
   A. Halperin and H. Arbell. Phys. Rev. 113, 1216 (1959).
4. N. Vlasenko. Dokl. na VII Soveshch. po lyuminests. (Rept. VII Conf. on Luminescence), Moscow, 1958.
5. N. A. Vlasenko. Opt. i Spektr. 7, 511 (1959); 8, 414 (1960), Optics and Spectroscopy, 7, 320 (1959); 8, 215 (1960).
6. F. A. Kröger. Physica 6, 369, 779 (1939).
7. R. H. Bube. Phys. Rev. 90, 70 (1953).
8. Seitz. Trans. Faraday Soc. 35, 79 (1939).
9. C. C. Klick. J. Opt. Soc. Am. 41, 816 (1951).
10. M. Schön. Ann. Physik 3, 343 (1948).
11. F. E. Williams and M. A. Hebb. Phys. Rev. 84, 1181 (1951);
    M. Lax. J. Chem. Phys. 20, 1752 (1952).
12. M. Born and Khuan Kun'. "Dinamicheskaya teoriya kristallicheskikh reshetok" (Dynamic Theory of Crystalline Lattices), Izd. Inostrannoi Lit., Moscow, 1958.
13. C. K. Coogan. Proc. Phys. Soc. B7, 453, 845 (1957).
14. V. L. Levshin. "Fotolyuminestsentsiya zhidkikh i tverdykh veshchestv" (Photoluminescence of Liquid and Solid Substances), Gosudarst. Izd. Tekh.-Teoret. Lit., Moscow (1951).
15. R. Gurney and N. Mott. Trans. Faraday Soc. 35, 69 (1939).
16. K. K. Shvarts. Trudy Inst. Fiz. i Astron., Akad. Nauk Eston.SSR 7, 153 (1958).
17. P. D. Johnson and F. E. Williams. J. Chem. Phys. 18, 1477 (1950).
18. M. Schön. Z. Physik 119, 470 (1942);
    W. Hoogenstraaten and F. A. Kröger. Physica, 15, 541 (1949).

POLARIZATION PHENOMENA IN ELECTROLUMINORS

A. M. Bonch-Bruevich and O. S. Marenkov

Received 19 October 1959

Results of studies of rapid polarization processes and luminescence peaks that occur on pulsed excitation of the electroluminor ZnS-CuAl are presented. It is shown that the polarization field is established in 10-20 μsec; i.e., in a time several orders of magnitude less than the luminescence decay time. A conclusion is drawn concerning the quenching of electroluminescence by a field opposite to the exciting one, based on an analysis of the kinetics of the luminescence decay associated with pulsed excitation.

1. It is known that in electroluminors, polarization phenomena, which determine the actual value of the field in individual grains of the phosphor, play an essential role in the mechanism of electroluminescence.[1-4] In this connection one must distinguish between long-lasting "frozen" polarization, which arises and remains in the sample for hundreds of seconds,[1] and the polarization which is established and dissipated in immeasurably less time. The development of polarization of the first type determines the kinetics of the establishment of a constant amplitude of luminescence in the face of periodically varying signals.[1] Polarization of the second type leads, in the final analysis, to a decrease in luminescence while the voltage pulse is still acting (a single pulse, or each of a periodic succession of them). In addition to this, an effect in the form of an electric field associated with rapid polarization leads to a flash of luminescence when the external field is removed ("switching off" luminescence). Some authors connect the kinetics of luminescence decay with the kinetics of the establishment of a space charge and estimate that the time required to establish the polarization field is of the order of 700 μsec.[4] Our previous observations[5] were not successful in detecting a correspondence between the polarization processes and the luminescence decay time in an electroluminescent condenser. This paper is a further study by way of a comparison of optical processes and rapidly developing polarization processes in electroluminors.

2. Direct studies of polarization processes can be made by observing the form of the current pulse in the charging circuit of the electroluminescent condenser when the electric field is switched on and off. Following the usual presentation,[6, 7] an equivalent circuit (Fig. 1,a) is substituted for the electroluminescent condenser. Here C_1 is the capacity of those regions of the sample in which polarization processes develop, and the capacities C_2 and C_3 are the capacities of the dielectric and the inactive zones of the luminor. The polarization processes in the sample correspond to a transition from the initial capacity of the sample

$$C' = C_3 + \frac{C_1 C_2}{C_1 + C_2}$$

to the capacity $C'' = C_3 + C_2$. The rate of these processes in the equivalent circuit is essentially determined by the value of the resistance R_1. It is easy to show that, if the time constant of the growth of polarization τ_p is significantly larger than the time constant for charging the original capacity of the sample ($\tau = RC'$), then the drop of the voltage across the resistor R, which is included in the circuit through which the current flows, can be represented as the sum of two exponential components corresponding to the time constants τ and τ_p (Fig. 1,b). In this case, the initial value of the polarization exponent is determined by the expression

$$U_2 = \frac{C_2^2 R}{C_1 + C_2} \frac{V_1}{\tau_p},$$

where V_1 is the amplitude of the sudden voltage change at the input.

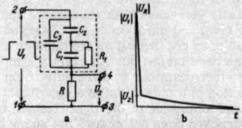

Fig. 1. The equivalent circuit of the electroluminescent condenser with the resistor R connected in its charging circuit (a) and the shape of the voltage in this resistor associated with the action of a step voltage at the output (b).

As a test sample we used a plane condenser with a gap of about 200μ between the electrodes, one of which was transparent. The condenser was filled with a suspension of the electroluminor ZnS-CuAl in cable oil. A resistance R ~ 5 kohm was connected in series with the electroluminescent condenser. The values of the capacities C_1, C_2, and C_3 are estimated on the assumption that the rapid polarization phenomena evolve in electroluminescently active regions of the luminophor grains. The assumption that the volume of these regions comprises 7-10% of the volume of the grains[8] leads to the conclusion that $U_2 \sim 10^{-5} U_1$ (if the duration of the polarization processes is of the same order as the duration of the luminescence decay).

In order to be able to observe the shape of a signal having a level of about 1 mv, which is immediately preceded by a signal of the order of 100 volts, we used an amplifier specially constructed for this purpose with multiple plate circuit signal-limiting, adjusted so that a strong signal does not go through the amplifier or overload its individual stages. The input of the amplifier is connected to the resistor R; its output signal is fed to an oscillagraph (EIO-1 or SI-1). Standard pulse generators (GIP-1, GIS-2, 26I), to which special output stages operating as fast-acting electronic switches had been added, were used for charging the electroluminescent condenser. The electroluminescent condenser with the resistor R is connected in parallel with the plate load of the output tube, as a consequence of which the condenser plates remain shorted through a fairly low resistance when the voltage is removed from the condenser. The durations of the leading and trailing edges of the pulses were of the order of 1 μsec. The amplitude of the pulses could be varied from 0 to 360 volts, and the pulse duration and repetition rate could be varied over wide limits. Control experiments on the setup of the apparatus were conducted with an equivalent circuit constructed according to the schematic of Fig. 1,a. The circuit used air condensers and condensers filled with cable oil in place of the electroluminescent condenser.

The observation of the flashes occurring on the application and removal of the voltage from the test sample was not difficult. In our setup, this was accomplished with the aid of an FEU-19 photomultiplier and a cathode ray oscillograph. The results cited below pertain to observations in the region of the green radiation band of the electroluminor with a maximum near 500 mμ (isolated with ZhS18 and SZS-8 spectrofilters). The blue band in the spectrum was comparatively weak in the electroluminor that we used.

3. Use of the amplifier-limiter made it possible to observe a component decaying in 10^{-3}-10^{-2} sec (Fig. 2,a) in the current flowing in the sample charging circuit. When the electroluminor has been previously exposed to red light, the first application of voltage is not accompanied by a flash of light, and the intensity of the following flashes gradually increases with subsequent applications. However, the level and duration of the observed polarization process does not depend on the number of times the voltage has been turned on. An exactly similar exposure of the electroluminor to ultraviolet light at the time of the action of a pulsed voltage significantly affects the duration and amplitude of the light flashes, but to all intents and purposes does not change the shape of the current curves. Finally, control experiments showed that the processes with durations of the order of 10^{-3} to 10^{-2} sec are also observed on replacing the electroluminor in the condenser by the photoluminor ZnS-Cu, cadmium selenide powder, Aquadag,* powdered quartz, and polyethylene, on installation of a thin layer of mica or cellophane in the condenser and on substitution of a ceramic condenser for the electroluminescent one. For this reason we think that the polarization processes observed in the electroluminescent condenser, although they also agree in duration with the luminescence decay, are not specific to electroluminors and are not directly related to electroluminescent phenomena. It should be noted that the initial value of the voltage component under consideration has a magnitude on the order of a hundred mv; i.e., turns out to be significantly larger than the expected value of U_2 (even if it is assumed that the polarization processes essential to the mechanism of electroluminescence occur throughout the entire volume of the electroluminor, and not only in those regions where the luminescence is localized). That is why it is not possible to achieve direct observation of polarization processes which could be compared with light pulses.

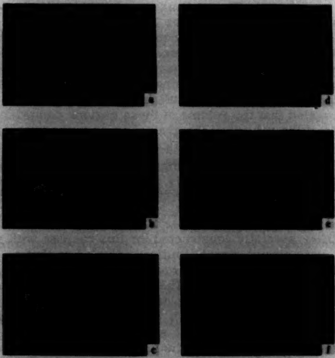

Fig. 2. Oscillogram of the voltage at the resistor R (a) and oscillograms of the luminescence associated with different voltage pulse durations (b-f) (the time markers are 20 μsec apart).

4. It turns out to be possible to estimate the duration of the polarization processes connected with electroluminescent phenomena by observing the luminescence associated with different voltage pulse durations (t′). Oscillograms originating from these pulses of luminescence are shown in Fig. 2. As a result of processing a number of such oscillograms, graphs were obtained which give an idea of the decay mechanism of the luminescence associated with "switching on" and "switching off" the voltage (Fig. 3). One's attention is attracted to the fact that the kinetics of the decay of the luminescence associated with removing the voltage are practically independent of the value of t′ to t′ ~ 30 sec. (Actually, there is some dependence, since generally speaking the experimental points in the graph of $I_2/I_{m2} = f(t)$ lie lower the shorter the time t′; however this displacement is small and does not alter the conclusions drawn below). In other words, the "switching off" luminescence does not depend on the phase of the "switching on" luminescence at which the voltage is taken off the test sample. In connection with this, it is natural to assume that the removal of the field is accompanied not only by the excitation of luminescence but also by quenching of the "switching on" luminescence. It is known that during electroluminescence, the luminescence of each grain of the phosphor is concentrated in limited regions, always facing an electrode whose potential is changing in a particular direction.[9] That is why the luminescence accompanying the application of the field and the luminescence associated with its removal are spatially separated, and it may be that the processes of quenching and stimulation of radiation by a field occur simultaneously but are to a marked degree independent.

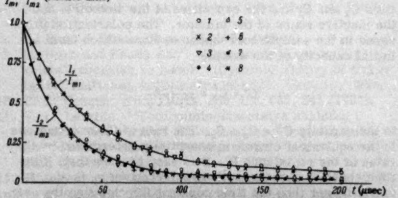

Fig. 3. Graphs of the decay of the "switching on" (I_{m1}) and "switching off" (I_{m2}) luminescence with different exciting pulse durations t′. The values of t′ (in μsec): 1—500, 2—400, 3—300, 4—200, 5—140, 6—90, 7—50, 8—30.

---

*Editor's note: Aquadag is the trade-name of a suspension of colloidal graphite.

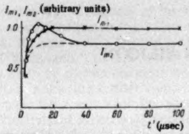

Fig. 4. The dependence of the amplitude of the luminescence peak associated with application (I_{m1}) and removal (I_{m2}) on the duration (t′) of the exciting pulses. The dashed line is a possible shape of the curve $I_2/I_{m2} = f(t')$, uncomplicated by the residual luminescence associated with switching on.

Figure 4 shows the amplitude of the flash excited by application and removal of the field (I_{m1} and I_{m2}) as a function of the duration of the voltage pulses. The rise of the $I_{m2} = f(t')$ curve in the range of $t' \sim 10$-20 μsec can be explained by the superposition of the "switching on" luminescence (Fig. 5) on the "switching off" luminescence. At the same time, the general shape of the $I_{m2} = f(t')$ curve indicates that a 10-20 μsec pulse is sufficiently long, for practical purposes, to fully establish the polarization field. An approximately similar or somewhat longer time is required to extinguish the luminescence.

5. We think that the results of the experiments with pulse excitation of electroluminescence presented above permit one to conclude that fast polarization processes in the electroluminor ZnS-CuAl occur within a time of the order of 10^{-5} sec. After that time, the field accelerating the electrons in the electroluminor is removed and growth of the "switching on" luminescence terminates. The kinetics of the subsequent luminescence decay are apparently not complicated in practice by the influence of the electric field on recombination processes in the phosphor, if the external voltage remains unchanged.

This is perhaps too general a statement since the information available at present is insufficient to determine the mechanism of polarization processes in electroluminors and the configuration of the polarization field. In this connection, our attention is attracted to the differences between the kinetics of the decay of "switching on" luminescence (related to the action of the external field) and the kinetics of the decay of "switching off" luminescence (associated with the action of the polarization field). These differences can serve as an indication of the nonequivalence of these fields. It should be added that the function $U_2 = f(t)$ (Fig. 2,a) is not exponential, and consequently the electrical equivalent of the electroluminescent sample is more complicated than is usually assumed.[7]

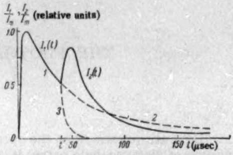

Fig. 5. Graphs of the luminescence associated with switching on (I_1) and off (I_2) as a function of time. Curve 1—oscillogram of the electroluminescence excited by application of voltage pulses of duration t′; curve 2—the decay curve of the "switching on" luminescence with pulses of longer duration t′; curve 3—approximate behavior of the "switching on" luminescence when the external voltage is turned off at the instant t = t′.

As to the quenching of electroluminescence by a field counter to the exciting one, possibly this effect can be compared to the known quenching of photoluminescence by an electric field. In both cases, the basic question is the effect of the field on the excited luminescence centers, and the difference between these effects lies only in the way the centers are excited. A more extensive study of quenching by fields may prove to be essential for refining our understanding of the mechanism of electroluminescence. In addition to this, the quenching of electroluminescence by an electric field should be taken into consideration in evaluating the luminescence yield at various frequencies of the applied voltage.

REFERENCES

1. J. Waymouth and F. Bitter. Phys. Rev. **95**, 941 (1954).
2. S. Nudelman and F. Matossi. J. Electrochem. Soc. **101**, 546 (1954).
3. F. Matossi and S. Nudelman. Phys. Rev. **99**, 1100 (1955).
4. I. Orlov and I. Lyamichev. Trudy Nauch.-Issledovatel. Inst. Min. Radiotekh. Prom. **9**, 3 (1957).
5. A. M. Bonch-Bruevich. Opt. i Spektr. **6**, 256 (1959), Optics and Spectroscopy **6**, 165 (1959).
6. H. Kallman, B. Kramer, and A. Perlmuter. Phys. Rev. **89**, 700 (1953).
7. A. Ince and Z. Oatley. Phil. Mag. **46**, 1081 (1955).
8. V. E. Oranovskii and Z. A. Trapeznikova. Opt. i Spektr. **5**, 302 (1958).
9. P. Zalm, T. Dimer, and H. Klasens. Philips Research Repts. **9**, 81 (1954).

THE PHOTOIONIZATION PROCESS IN SILICON

K. I. Britsyn and V. S. Vavilov

Received 19 October 1959

Data are presented on the spectral and temperature dependence of the quantum yield (generation of electron-hole pairs) in silicon during absorption of photons with energies up to 4.9 ev. A method was used which excluded the effects of capture centers. The temperature dependence of the quantum yield was observed in the region of collision ionization effected by carriers liberated in the absorption of photons. As the temperature increased, the boundary of this region shifted toward lower photon energies, partially because of a narrowing of the energy gap in silicon.

INTRODUCTION

The quantum yield of the photoionization process, (i.e., the primary formation of charge carriers accompanying the absorption of photons in crystals) which has been under investigation for several decades, has recently gained particular importance in connection with the possibility of investigating high-purity crystals of such semiconductors as germanium and silicon. In studying the internal photoelectric effect in these semiconductors, it is possible in many cases to make quantitative studies of those volume and surface properties whose determination is extremely difficult, for example, in the typical case of crystalline phosphors or polycrystalline layers of semiconductors. Thus, in 1950[1] it was established that absorption of photons in the fundamental absorption band of germanium leads to the generation of pairs of carriers with a quantum yield Q = 1. In subsequent studies it was shown that for sufficiently energetic photons (⩾ 2.2 ev, according to reference 2 and ⩾ 2.9 ev, according to our data[3]) the region of constant quantum yield moves into a region in which the yield increases with photon energy. The increase in quantum yield is explained by collision ionization, i.e., the formation of secondary pairs at the expense of the excess kinetic energy of photoelectrons and holes. An analogous dependence of quantum yield on photon energy was observed by us in silicon[4] and also by Tauc in indium antimonide.[5] The approximate theory of the phenomenon worked out by Antončik does not predict a temperature dependence of the quantum yield. Nevertheless, one might expect that such a dependence exists.

The results presented below confirm the existence in silicon of a temperature dependence of the quantum yield in the region of collision ionization.

METHOD AND TECHNIQUE OF MEASUREMENT

Measurement of the steady-state photoconductivity[1, 6] is the method most frequently used in determining the quantum yield Q, which is given by the number of current-carrying pairs* per absorbed photon. However, in a majority of semiconductors, particularly in CdS and PbS crystals, and also in silicon, the changes in conductivity observed during absorption of light are connected not only with the process of ionization but also with the capture of one of the types of carriers by the trapping centers. As a result of this, there can be a substantial increase in the lifetime of the other type of carrier. The effect of capture centers can be excluded by making use of semiconductors with p-n junctions for the determination of the number of carrier pairs produced. Crystals of germanium and silicon with p-n junctions are frequently used as phototube elements. The principle of these photoelements is based on the separation of electron-hole pairs in the strong field of the space-charge region at the p-n junction. This principle is considered in detail in papers concerned with the conversion of solar energy.[7, 8] In an actual crystal with p-n junctions, the short circuit current I in the external circuit between regions of electron (n) and hole (p) conduction which arises during excitation in the fundamental absorption band is proportional, for small intensities, to the number N of electron-hole pairs produced, i.e., I = αqN, where q is the electron charge. The coefficient α, which has values less than unity, is a function of the crystal geometry, the diffusion length of carriers, the rate of surface recombination, the mobility, and the absorption coefficient of light. A general expression for α in the one-dimensional case is derived in reference 9.

Another important advantage in the use of crystals with p-n junctions is their very low noise level. This is due chiefly to the absence of external sources of supply (batteries): the measuring circuit consists only of the object being studied, leads, and a sensitive low-resistance galvanometer.

In the present work we used single p-type crystals of silicon with p-n junctions, prepared by thermal diffusion of phosphorus from the gaseous phase (see Fig. 1).

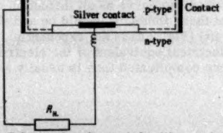

Fig. 1. Schematic of crystal with p-n junction and nonrectifying contacts.

The final formula for calculation of the quantum yield from experimentally determined values and from α has the form

$$Q = \frac{I}{q \alpha N_{h\nu} (1 - R_\nu)}$$

where R_ν is the reflectivity of silicon. The method we chose for measuring R_ν (use of an integrating sphere[10]) was dictated by the dependence of results on correct evaluation of the reflectivity of silicon and on the fact that surface and thermal treatment of the crystals to be studied can noticeably influence the value of R_ν. On the suggestion of M. N. Alentsev, a film of luminor with constant yield ("liumogen," or 2,2′-dioxy-1,1′-naphthaldiazine) and an FEU-25 photomultiplier were used as a radiation detector in the ultraviolet region.

---

*Ion pairs arise during absorption of light in the fundamental band (band-to-band transition); in photoionization of impurities (in the case of deep levels) either electrons or holes arise in the conduction band.

Average measured results for the spectral dependence of the reflectivity of an etched "matte" surface of silicon are given in Fig. 2.

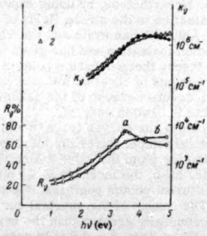

Fig. 2. Average experimental values for spectral dependence of reflectivity R_ν of etched silicon surface and for absorption coefficient k_ν. Curve a—type-II specimens; curve b—type-I specimens. 1—curve from reference 12; 2—experimental curve.

Evaluation of the absorption coefficient from the expression

$$R_\nu = \frac{(n-1)^2 + \chi^2}{(n+1)^2 + \chi^2},$$

where $\chi = 2\pi k/\lambda$ (where k is the absorption coefficient and n the index of refraction[11]) gives good agreement with data obtained by other methods.[12] For several of the crystals studied, secondary maxima, apparently resulting from interference of light in oxide films on the surface, were observed in the curves of $R_\nu = R(h\nu)$.

The general arrangement of apparatus for investigating the spectral and temperature dependences of photoionization in silicon is pictured in Fig. 3. The basic parts are the mirror monochromator with LiF prism and incandescent lamp; PRK-4 mercury lamp and SVDSh-500 lamp, used in different regions of the spectrum; and the cryostat, in which the crystal specimen is placed. The incident flux ($N_{h\nu}$) was measured with a calibrated thermopile.

RESULTS AND INTERPRETATION

The dependence of the product Qα on the photon energy hν was plotted on the basis of data on the incident flux, the reflection coefficient, and the short circuit current.

The curves obtained can be classified according to two types. In curves of the first type, which refer to p-n junctions at shallow depths and to a "clean" (etched) crystal surface, a "plateau" is observed; i.e., a region of constant Qα, which subsequently increases with increasing hν (see Fig. 4). Curves of this type can be interpreted using the expression for the collection coefficient α. Actually, in the case of sufficiently strong absorption, i.e., when $1/k \ll d$, where d is the depth of the p-n junction, the formula for α becomes

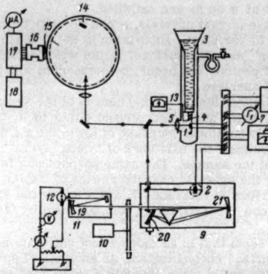

Fig. 3. Schematic diagram of experimental setup. 1—specimen of silicon with p-n junction; 2—thermopile; 3—cryostat; 4—electric heater; 5—quartz lens (f = 5 cm); 6—type PPTN-1 potentiometer; 7—G_1 and G_2, type M-21/4 low-resistance galvanometer; 8—type 28-I narrow band amplifier; 9—mirror monochromator; 10—light interrupter; 11—mirror condenser; 12—radiation source; 13—thermocouple with controlling apparatus; 14—integrating sphere containing MgO surface or silicon specimen; 15—plate with luminor; 16 to 18—photomultiplier with stabilized supply (1500 volts); 19 to 21—aluminized spherical mirrors.

$$\alpha = \frac{2}{\left(1 + \frac{SL}{D}\right) e^{\frac{d}{L}} + \left(1 - \frac{SL}{D}\right) e^{-\frac{d}{L}}}.$$

Here S is the rate of surface recombination, L is the diffusion length for carriers in the n-type layer, and D is the coefficient of bipolar diffusion. It is seen from this expression that the collection coefficient α does not depend on the absorption coefficient. In agreement with the data of reference 12 and also with the evaluation of k from the reflectivity as given above, for photon energies greater than 2.5 ev, $1/k < 10^{-5}$ cm, and for hν = 4.9 ev, $1/k < 10^{-6}$ cm, i.e., even in the visible region (and to a still greater degree in the ultraviolet) the conditions for

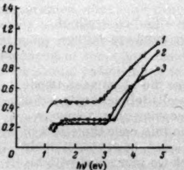

Fig. 4

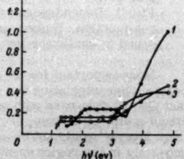

Fig. 5

Fig. 4. Spectral dependence Qα = f(hν) for "thin" p-n junctions. Type-I curves. Temperatures: curve 1—400°K; curve 2—100°K; curve 3—300°K.

Fig. 5. Effect of "dead" surface layer on function Qα = f(hν). Type-II curves. Temperatures: curve 1—100°K; curve 2—300°K; curve 3—400°K.

independence of α on $h\nu$ are satisfied.

In the case of real crystals, α can actually be independent of $h\nu$ for strong absorption in the absence of a "dead layer" near the surface, within which an inactive absorption of photons can occur, not connected with the generation of carriers.

In our opinion, the $Q\alpha = f(h\nu)$ curves of the second type (Fig. 5), which are characterized either by a "dip" or by a sharply nonlinear increase of $Q\alpha$ to the right of the plateau, indicate the existence of "dead layers" at the surface of the sample. The same phenomenon is responsible for the spectral characteristics of "solar batteries" described in reference 7, and also for the ionization of silicon observed under bombardment by fast electrons.[13]

It would seem that in an independent calculation of the rate of surface recombination, an analysis of spectral characteristics would make possible a more precise judgment of the thickness of the "dead layer," which is of wide interest in connection with increasing the efficiency of photoelements.

Control measurements were carried out, since the recombination rate of carriers, and consequently also the value of α, can in general depend on the excitation intensity. These measurements showed that in the specimens investigated, α remained constant for incident radiation fluxes from 2×10^{11} to 4×10^{13} cm^{-2} sec^{-1} (see Fig. 6).

When the depth of the p-n junction was decreased by etching the front surface of the crystal, the value of $Q\alpha$ increased for all photon energies. This was to be expected from the expression for the collection coefficient α. In this case, the boundary of the region of collision ionization did not shift (Fig. 7).

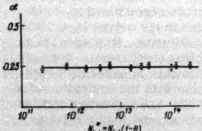

Fig. 6

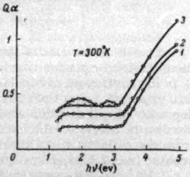

Fig. 7

Fig. 6. Dependence of α on excitation intensity. $N^*_{h\nu}$ is the number of absorbed photons; $h\nu$ = 2.25 ev.

Fig. 7. Dependence of $Q\alpha = f(h\nu)$ on depth of p-n junction. Higher curve numbers correspond to shallower levels.

Most important for us were the specimens whose spectral characteristics had a well-defined region of constant $Q\alpha$ and then rose with increasing photon energy, without a dip. Of course, even in this case the effect of "dead layers" could not be excluded; however, it could occur only in the region in which $Q\alpha$ increased with $h\nu$, leading to a decrease in the value of $Q\alpha$, since the presence of a "dead layer" can only decrease the coefficient α.

Proceeding from the usual assumptions about pair formation in the absorption of photons, we can calculate that within the photon energy range $E_g < h\nu < 2E_g$, where E_g is the width of the energy gap, the quantum yield must equal unity. The existence of a "plateau" serves as additional verification of this. Extrapolating the constant value of α into the region of increasing $Q\alpha$, we obtain the curve $Q = f(h\nu, \alpha)$, i.e., the spectral dependence of the absolute value of the quantum yield.

Curves of this type are shown in Figs. 8 and 9 for three temperatures, 100, 295, and 400°K. In Fig. 8 the $Q = f(h\nu)$ curves refer to the first type and in Fig. 9, to the second type.

The approximate theory of Antončik does not consider the effect of lattice vibrations on the absorption of light, i.e., the dependence of the residual kinetic energy of electrons on the type of primary transition.[14] Moreover, it assumes the simplest structure of valence bands, which, apparently, does not correspond to reality in the case of silicon. Nevertheless, by using experimental data on collision ionization in the strong fields of the p-n junction in silicon, Antončik has evaluated the "limiting" energy of collision ionization and has given it a value of 3.4 ev. In this theory there occurs a point of inflection separating the regions of constant and increasing quantum yield which occurs because of the assumption of a fixed value of the ionization energy.

As is seen from our curves (Figs. 8 and 9), for all three experimental temperatures the increase of Q with $h\nu$ begins not too far from the value indicated by Antončik. On the other hand, the increase in $Q\alpha$ and Q begins at considerably different photon energies, depending on the temperature. The change of the spectral curve with temperature is substantially greater than the errors of measurement. From Figs. 8 and 9 it is seen that at a high temperature (400°K) the rise of the quantum yield begins at a considerably lower energy (2.95 ev) than at 100°K (3.4 ev). The shift can be partially explained by a narrowing of the energy gap with increasing temperature. At 100°K, E_g = 1.17 ev; at 400°K, E_g = 1.04 ev. In view of the fact that each creation of a primary and secondary pair of carriers takes an energy $E \geqslant E_g$, the indicated circumstance can only explain a shift of about 2(1.17-1.04) = 0.26 ev. The remaining unaccounted shift, which amounts to about 0.2 ev, is not explained by existing theories. It may be that this shift occurs as a result of an increase in the relative number of indirect electron transitions involving photons as the temperature increases.

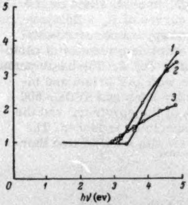

Fig. 8

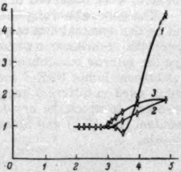

Fig. 9

Fig. 8. Spectral dependence of quantum yield Q in type-I specimens of silicon for different temperatures: curve 1—100°K; curve 2—300°K; curve 3—400°K.

Fig. 9. Spectral dependence of quantum yield Q in type-II specimens of silicon for different temperatures: curve 1—100°K; curve 2—300°K; curve 3—400°K.

Let us note that the slope of Q as a function of $h\nu$ increases sharply at lower temperatures. We assume that an accurate determination of the quantum yield in the region of collision ionization, and of the effect of lattice vibrations on the value of Q can give other information on the motion of "very hot" electrons and holes.

However, the data obtained for values of Q in the region of 4 ev photons must not be considered accurate since the absorption coefficient is very large and the smallest variation of the properties at the surface can bring about a reduction in the calculated experimental values of the quantum yield.

The authors express sincere thanks to B. M. Vul, S. G. Kalashnikov, M. N. Alentsev, and V. A. Chuenkov for their interest in this work and for many valuable comments.

REFERENCES

1. F. S. Goucher. Phys. Rev. 78, 816 (1950).
2. S. Koc. Czechoslov. J. Phys. 6, 668 (1956).
3. V. S. Vavilov and K. I. Britsyn. Zhur. Eksptl. i Teoret. Fiz. 34, 521 (1958).
4. V. S. Vavilov and K. I. Britsyn. Zhur. Eksptl. i Teoret. Fiz. 34, 1354 (1958).
5. J. Tauc and E. Abraham. Czechoslov. J. Phys. 9, 95 (1959).
6. R. W. Pohl and B. F. Gudden. "Lichtelektrische Erscheinungen." Berlin, 1928.
7. V. S. Vavilov, G. N. Galkin, and V. M. Malovetskaya. Atomnaya Energ. 4, 571 (1958).
8. V. K. Subashiev. "Poluprovodnikovye preobrazovateli solnechnoi energii." (Semiconductor Converters of Solar Energy), Leningrad, 1958.
9. W. G. Pfann and W. van Roosbroeck. J. Appl. Phys. 25, 1422 (1954).
10. Meier and Zeitts. "Ul'trafioletovoe izluchenie" (Ultraviolet Radiation), Izd. Inostrannoi Lit., Moscow, 1952.
11. "Elektrofizicheskie svoistva germaniya i kremniya" (Electrophysical Properties of Germanium and Silicon), Izd. Inostrannoi Lit., Moscow, 1958.
12. E. Burstein and J. Egli. Advances in Electronics and Electron Physics 7 (1955).
13. V. S. Vavilov, L. S. Smirnov, and V. M. Patskevich. Doklady Akad. Nauk SSSR 112, 1020 (1957).
14. E. Antončik. Czechoslov. J. Phys. 7, 651 (1957).

OPTICAL AND ELECTRICAL PROPERTIES OF THIN FILMS OF TIN DIOXIDE

V. K. Miloslavskii and S. P. Lyashenko

Received 9 November 1959

An investigation was made of the temperature dependence of the electrical conductivity and Hall constant of thin layers of SnO$_2$ between 20° and 300°C. The transmission and reflection coefficients of these layers were also measured in the 0.35-2.5 μ and 1.5-6 μ regions. The data obtained on the optical and electrical properties of this semiconductor permitted quantitative comparison with theory and also with the results of other authors.

INTRODUCTION

It is well known that thin layers of tin dioxide which result from the pyrolytic decomposition of the chlorides of tin[1, 2] possess two interesting properties: high conductivity and high transparency in the visible part of the spectrum. These properties, along with thermal stability and high mechanical strength, allow these layers to be used as heaters, transparent electrodes, and electrostatic screens in all kinds of technical apparatus.

In spite of this, the physical properties of such films have not been studied very extensively. In particular, there is very little information about the effects of various impurities on the electrical and optical properties of the layers, nor has the behavior of current carriers in this semiconductor been explained. In a previous paper,[3] we showed that the infrared absorption spectrum of thin layers of SnO$_2$ which have relatively low conductivity ($\sigma \sim 10$ ohm^{-1} cm^{-1}) can be ascribed to neutral impurity atoms. On this basis, we estimated the location of impurity levels in the forbidden energy gap of semiconducting SnO$_2$. In addition, it was observed[3, 4] that the introduction of antimony into SnO$_2$ not only reduced the resistance of the samples, but also caused a considerable increase in the infrared absorption of the material. By varying the impurity content of the samples over a wide range, it was possible to change both the electrical and optical properties of the SnO$_2$. Because of the large value of the forbidden energy gap of the semiconductor (~3.5 ev) it is possible to separate the impurity spectra from the fundamental absorption spectrum; tin dioxide thus turns out to be a very convenient material for studying the optical behavior of free carriers in a semiconductor. This paper is devoted to an investigation of the electrical and optical properties of thin layers of SnO$_2$.

ELECTRICAL PROPERTIES OF SnO$_2$

Thin layers of SnO$_2$ with antimony as additive were prepared by evaporating SnCl$_4$ containing a small amount of SbCl$_3$ onto a glass substrate which was heated to a high temperature. Since the ionic radius of Sn^{4+} (0.71 A) is nearly equal to that of Sb^{5+} (0.65 A), the introduction of antimony into the crystal lattice of SnO$_2$ leads to the replacement of some Sn^{+4} ions by Sb^{5+} ions. Such a substitution should result in the formation of new donor levels in the forbidden band, i.e., to an increase of electronic conductivity of the semiconductor. It should be noted that a layer of SnO$_2$ obtained by evaporating pure chlorides has high conductivity and a high concentration of carriers ($N \sim 10^{19}$ cm^{-3}). The introduction of antimony leads to a further increase of conductivity and carrier concentration (up to 10^{21} cm^{-3}). Our investigation was principally concerned with electrical and optical properties of samples with carrier concentrations between 2×10^{19} and 1×10^{21} cm^{-3}.

The temperature dependence of electrical conductivity and the Hall constant between 20 and 300°C were studied in samples prepared in various ways. The Hall emf was determined by a null method. In order to determine the temperature dependence of the Hall constant R, the sample was clamped to the flat copper face of a slab heater covered with a thin layer of mica. In this way a very uniform temperature distribution over the sample was achieved. The sample was thermally isolated by glass and asbestos and the temperature of the sample measured by a copper-constantan thermocouple. Platinum wires were used both as current electrodes and Hall electrodes. A good electrical contact was provided by a liquid indium-gallium paste. The Hall emf and resistance of the samples were measured when an equilibrium electrical state was attained at a given temperature. The measurements were considered satisfactory if the temperature dependence was found to be reversible when the temperature was raised or lowered. Raising the temperature to very high values (> 350°C) led to a loss of reversibility which was obviously related to changes in sample composition.

The thickness of the samples was determined by studying the spectral dependence of the transmission in the transparent region (400-1100 mμ) with the help of an SF-4 spectrophotometer. In this region, the variation is caused principally by interference effects. It is well known that it is possible to determine the index of refraction of the layers n from the minimum values of the transmission coefficient by using the expression

$$T_{\min} = \frac{4n^2 n_1}{(n^2 + n_1)^2}, \tag{1}$$

where n_1 is the refractive index of the substrate. One can readily determine the order of the interference m from neighboring minima if one takes into account the dispersion of the refractive index n. By utilizing the condition of an interference minimum

$$(2m+1)\frac{\lambda}{4} = nt,$$

one can easily obtain the layer thickness t. By means of this method, it is possible to attain an accuracy of about 2% in the determination of n and t.

The investigation of the temperature dependence of the Hall constant R and specific conductivity σ was made on samples with various impurity center concentrations (Figs. 1 and 2). Samples I and II (σ = 46 and 14 ohm^{-1} cm^{-1}; N = 2.9 and 4.4 × 10^{19} cm^{-3} at 20°C respectively) were obtained by sputtering pure $SnCl_4$; samples III and IV (σ = 261 and 480 ohm^{-1} cm^{-1}; N = 2.75 and 3.77 × 10^{20} cm^{-3} respectively) were obtained by adding about 1% $SbCl_3$. Preliminary observations showed that the introduction of antimony did not change the sign of the Hall emf, i.e., all the samples were n-type.

From these data it is clear that none of the samples showed any marked change of Hall constant with temperature. This indicates that for large concentrations (N > 10^{19} cm^{-3}) an impurity band is formed in the semiconductor, and the conductivity becomes metallic in character.*

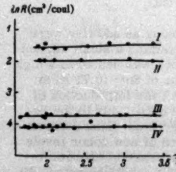

Fig. 1

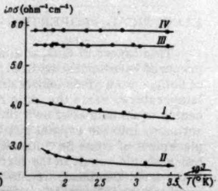

Fig. 2

Fig. 1. Temperature dependence of the Hall constant of thin layers of SnO_2 for samples containing various amounts of impurities. Conductivity (in ohm^{-1} cm^{-1}) and carrier concentration (in cm^{-3}) at 20°C. Curve I—46 and 2.9 × 10^{19}; curve II—14 and 4.4 × 10^{19}; curve III—261 and 2.75 × 10^{20}; curve IV—480 and 3.77 × 10^{20}.

Fig. 2. Temperature dependence of the specific conductivity of thin layers of SnO_2 for samples with various impurity center concentrations. The significance of the roman numerals on the curves is given in the caption of Fig. 1.

It is interesting to note that for samples with a small carrier concentration, an increase in σ was observed with increasing temperature even though R was almost constant. This phenomenon is well known in other semiconductors (PbS, Si) and is related to the increase of mobility of charge carriers with increasing temperature. The theory of this phenomenon has not been worked out as yet.[5] It is possible that the apparent increase in mobility is brought about by the existence of two conduction bands in the semiconductor[6]—the fundamental band and an impurity band. As the temperature increases, electrons make a transition into the fundamental band, which leads to an increase in σ for the same value of R.

The temperature dependence of σ disappears in samples containing antimony, indicating that in this case the impurity and fundamental conduction bands overlap. The weak temperature dependence also indicates that the mobility is due principally to the scattering of electrons by ionic impurities and discontinuities in the crystal lattice. The electrical properties of some of the samples are given in the Table. The Table does not show any clear-cut regularities in the changes of mobility v from sample to sample. The average value v ≈ 10 cm²/volt sec is approximately equal to the mobility of an ordinary metal.

Electrical and Geometrical Characteristics of some of the SnO_2 Samples Investigated

Sample No.	t (μ)	σ (ohm^{-1}cm^{-1})	N × 10^{-20} (cm^{-3})	v $\left(\frac{cm^2}{volt\ sec}\right)$
1	0.928	25.5	0.269	8.0
2	0.550	293	0.855	14.35
3	0.472	214	0.89	15.05
4	0.273	311	2.15	8.9
5	0.590	540	2.21	14.9
6	0.450	261	2.75	5.93
7	0.420	480	3.77	7.94

OPTICAL PROPERTIES OF SnO_2

The absorption of samples with various carrier concentrations was determined by measuring the transmission of layers deposited onto a glass substrate with the help of SF-4 and IKS-2 spectrophotometers between 0.35 and 2.5 μ. Since pronounced interference effects occur in the visible part of the spectrum, the samples were set up so that the incident light beam fell on them at Brewster's angle.[7] The measurements were made with polarized light; the polarization plane coincided with the plane of incidence; because of this, interference effects were almost completely eliminated. The infrared transmission was measured in the usual way.

The electrical characteristics of the samples under investigation are shown in the Table (in Figs. 3 and 4,

---

*The absence of a temperature dependence of R can be explained only by a degeneracy in the electron gas, since the impurity ionization energy ε_i is larger than kT ($\varepsilon_i \approx 0.15$ ev).[3]

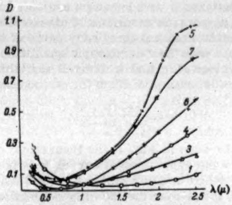

Fig. 3. Optical density of thin layers of SnO_2 in the 0.35 to 2.5 μ region. The numbers beside the curves refer to sample numbers in the Table.

the numbers beside the curves correspond to the sample numbers in the Table).

The results of measuring the optical density D of some samples are shown in Fig. 3. As is evident from the drawings, the following rules governing the optical behavior were observed: (1) The optical density, as a rule, increases with increasing conductivity and decreasing Hall constant (assuming that the thickness of the samples does not change much); (2) the absorption increases with increasing wavelength (for most of the samples, a transparent region is found to lie in the range of 0.5 to 1.0 μ); and (3) the absorption increases with decreasing wavelength in the region $\lambda < 0.5$ μ, as preliminary investigations had shown in the case of layers deposited on a rock salt substrate; in that case, the absorption in the ultraviolet region increased monotonically with decreasing λ in the region 0.5 to 0.23 μ; D attained a value greater than 1 for $\lambda < 0.3$ μ and $t = 0.2$ μ. Thus, absorption in the violet part of the spectrum corresponds to the long wavelength edge of the fundamental absorption band of SnO_2.

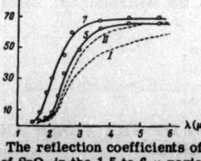

Fig. 4. The reflection coefficients of thin layers of SnO_2 in the 1.5 to 6 μ region. Solid lines—experimental curves (the numbers beside the curves refer to sample numbers in the Table); dashed lines—calculated from Eq. (4); curve I—v = 14.9 cm²/volt sec; curve II—v = 21 cm²/volt sec.

The introduction of a large amount (> 1%) of antimony into SnO_2 leads to a marked decrease of transparency in the visible. Samples acquire a black color and show additional absorption bands whose origin has not been explained. At the same time, there is no marked increase of absorption in the infrared (up to 2.5 μ) over the absorption of ordinary samples.

For some samples, the value of the reflection coefficient r was also determined between 1.5 and 6 μ with the aid of an IKS-2 spectrophotometer with glass and LiF prisms. An aluminized mirror was used as a sample of known reflection coefficient. The reflection coefficient was measured on samples which had low transmission at 2 to 2.5 μ. In this case the incident radiation was reflected principally at the air-layer interface, i.e., one could assume that the calculated reflection coefficient was approximately equal to the reflection coefficient of a bulk sample. The results of the measurements (Fig. 4) indicate that in the 3-6 μ region, a high r value (65-70%) is observed for samples with high electron concentrations. Thus, by choosing samples with optimum characteristics, it is possible to make reflection filters for the near infrared from SnO_2 containing Sb. As the wavelength decreases, the reflection coefficient of such filters drops rapidly to very low values.

DISCUSSION OF THE RESULTS

Since for the majority of samples optical measurements and determinations of the conductivity and Hall constant were made simultaneously, it is possible to make quantitative comparisons of the results.

Figure 5 shows the specific optical density (the optical density per unit thickness of sample) as a function of the electron concentration N on a log-log plot ($\lambda = 2.5$ μ). From this graph, it is evident that the experimental points fall very close to a straight line whose slope is close to unity. The scatter of the points is random and is caused by errors in determining the thickness, Hall emf, and transmission of the samples. The slope of this line indicates a linear dependence of the absorption coefficient on the electron concentration. This fact shows that the absorption in the near infrared is caused by conduction electrons.

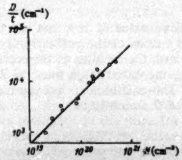

Fig. 5. Specific optical density of thin layers of SnO_2 plotted against electron concentration.

Frequencies ω which lie in the range defined by the inequality

$$\omega' \ll \omega \ll \omega_1, \tag{2}$$

where ω' is the collision frequency and ω_1 is the red limit of the fundamental absorption band, are very important for studying the optical properties of the carriers. In this frequency interval, a simple relation exists between the real part of the complex dielectric constant and the frequency, namely

$$\varepsilon = n^2 - k^2 = \varepsilon_0 - \frac{4\pi N e^2}{m^* \omega^2} \tag{3}$$

Here ε_0 is the optical dielectric constant of the host material and m^* is the effective mass of the carriers, which must be determined.

From Eqs. (2) and (3), it follows that evaluating ε depends on finding the values of the optical constants n and k near the short wavelength edge of the infrared absorption band for samples in which the charge carriers have a rather high mobility. The optical constants were evaluated for sample No. 5 (see the Table). The index of refraction in the visible region was determined from Eq. (1). The optical constants in the absorption edge region (1.7 to 2.5 μ) were determined from the experimental values of r and T for the known sample thickness. In calculating the values of the optical constants, the cumbersome Airy equations for a thin absorbing layer on a transparent substrate were used.[8] The accuracy in determining the optical constants was not very great (~10 to 20%) since for $\lambda = 1.5\ \mu$ the reflection coefficient was very small (< 3%). The results of determining n and k are shown in Fig. 6. Figure 7 shows that a linear dependence of ε on λ^2 is observed in the region under investigation. The intercept of this line with the ordinate axis gives $\varepsilon_0 = 3.6$, which is somewhat lower than the value for the pure material ($\varepsilon_0 = 4$). The slope of the line allows one to calculate m^* for a known value of N. From these calculations, it is found that $m^* = (0.25 \pm 0.03)m_e$. This value is close to the effective mass value $0.2\ m_e$ obtained in reference 9 for thin layers of SnO_2 made without any Sb impurity. Similar values of m^* were obtained from calculations on other samples.

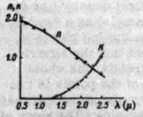

Fig. 6

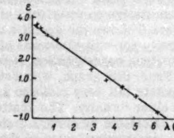

Fig. 7

Fig. 6. Optical constants n and k for thin layers of SnO_2 in the 0.5-2.5 μ region.
Fig. 7. The function $\varepsilon = f(\lambda^2)$ for thin layers of SnO_2.

Using the above value of m^*, one can try to compare the experimental values of the reflection coefficient between 2 and 6 μ with the results of theoretical calculations. In the given case, the calculation must be made by taking ω' into account. The collision frequency can be found from the known value of the mobility

$$\omega' = \frac{e}{m^* v}.$$

The constants n and k can be evaluated from the well-known dispersion equations of classical theory, which relate the real and imaginary parts of the dielectric constants with the microscopic quantities N, ω', and m^*.[10] The values of n and k arrived at in this manner were used to determine r from the well-known relation

$$r = \frac{(n-1)^2 + k^2}{(n+1)^2 + k^2}. \tag{4}$$

As can be seen in Fig. 4, the theoretical curve (curve I) falls below the experimental curve. It is possible that the mobility found in static fields (v = 14.9 cm²/volt sec) is somewhat lower than the mobility determined in high frequency electric fields since in the latter case scattering at crystal grain boundaries does not play an important role. Better agreement between theory and experiment is obtained at v = 21 cm²/volt sec, but complete agreement between the curves is still not observed (curve II).

In conclusion, the authors wish to thank I. N. Shklyarevskii and N. A. Vlasenko for discussion of the results.

REFERENCES

1. B. A. Ryabov, O. V. Borob'eva, and A. S. Egorova. Steklo, Inform. Byull. VNIIS **1**, (1957).
2. A. Ya. Kuznetsov, A. V. Kruglova, and B. P. Kryzhanovskii. Zavodskaya Lab. **22**, No. 3 (1956).
3. V. K. Miloslavskii. Opt. i Spektr. **7**, 246 (1959), Optics and Spectroscopy **7**, 154 (1959).
4. A. Fisher. Z. Naturforsch. **9**, 508 (1954).
5. A. F. Ioffe. Fiz. Tverd. Tela **1**, 157 (1959).
6. C. Hung and J. Gliesmann. Phys. Rev. **96**, 1226 (1954).
7. N. A. Vlasenko. Uchenye Zapiski Kharkovsk. Univ., Trudy Fiz. Otd. **7**, 321 (1958).
8. H. Murmann. Z. Physik **80**, 161 (1933).
9. O. Ischiguro, O. Sasaki, P. Arai, and O. Imai. J. Phys. Soc. Japan **13**, 755 (1958).
10. H. Fan and M. Becker. Sb. "Poluprovodnikovye Materialy" ("Semiconductor Materials" Russian Translation), Izd. Inostrannoi Lit., Moscow, 1954.

SHORT COMMUNICATIONS

INVESTIGATION OF ENERGY OF THERMAL ACTIVATION OF THE FLASH AND OF TRAPPING LEVELS IN CaS PHOSPHORS

V. L. Levshin and N. Kh. Faizi

Received 11 November 1959

INTRODUCTION

Many phosphors with deep electron trapping levels, once excited, will flash under the action of infrared, even after the decay of their natural phosphorescence. This phenomenon is caused by the liberation of electrons remaining on deep levels by the infrared radiation. Sufficient cooling of the phosphor freezes the flash.[1] This indicates that in order to absorb infrared, electrons must first shift under the action of heat from deeper to shallower trapping levels. The electron must acquire a certain "thermal flash activation" energy. Thus, in flash-exhibiting phosphors, we must apparently assume the existence of an additional flash level above the deep level. Analogous phenomena have been described by Tolstoi, Feofilov, et al.[2, 3] and by Parfianovich.[4]

In a recent paper, Orlov and one of the authors[5] studied the thermal activation energy of the flash in ZnS:Cu, Pb phosphors. This type has a highly inertial flash, so that the authors had to estimate the thermal activation energy from the development of secondary phosphorescence. Our purpose here is to study the phenomenon for another class of phosphors, with relatively low flash inertia. We used CaS-base phosphors. They were prepared from $CaCO_3$ purified with hydrorubeanic acid. The $CaCO_3$ was ignited at 1000° to give CaO. For activation we used Eu_2O_3, $Ce(NO_3)_3$, Sm_2O_3, Pr_2O_3, $Bi(NO_3)_3$, and $Cu(NO_3)_2$. The oxides were transformed into nitrates.

The absence of chlorine was checked. Four percent of Na_2SO_4 flux was introduced. The water of crystallization was taken into account. The temperature and duration of ignition were 1050° and 25 min, respectively.

We thus obtained the following 11 luminors:

1. CaS; CaS:Sm 3×10^{-5}; CaS:Cu 2.3×10^{-4}.
2. CaS:Bi 3×10^{-5}; Ce 1.4×10^{-4}; CaS:Bi 3×10^{-5}; Eu 1.3×10^{-4}; CaS:Bi 3×10^{-5}; Pr 1.4×10^{-4}.
3. CaS:Sm 3×10^{-5}; Cu 2.3×10^{-4}; CaS:Sm 3×10^{-5}; Ce 10^{-4}.

Investigations of the flash and of thermal stimulation were carried out with the arrangement described in reference 5. To determine the depth of local levels, we used the formula

$$E = \frac{kT'_m T''_m}{T''_m - T'_m}\left(\ln\frac{\beta_2}{\beta_1} + 2\ln\frac{T'_m}{T''_m}\right), \quad (1)$$

which holds when the probability of repeated capture of thermal electrons is small as compared with the probability of recombination.

The quantities T'_m and T''_m represent the temperature of the peaks corresponding to heating rates β_1 and β_2, respectively.

GLOW CURVES OF CaS PHOSPHORS, THEIR TRAPPING LEVELS AND THE INERTIA OF FLASH PROCESSES

The glow curves are shown in the Figure.

The effect of the activators and of their interaction on the formation of localization levels is shown fairly clearly in the Figure. We should note, however, that in Sm-activated phosphors, the effect of Cu and Ce on the shape of the glow curves is within the limits of experimental error; it is essential for the development of the flash. The position of the system of levels in the phosphors investigated is shown (in ev) at the top of the Figure.

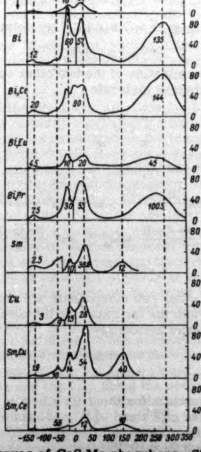

Glow curves of CaS:Mn phosphors. Stimulation rate 11°/min. Activators are indicated at the left. The numbers on the curves represent light sums (relative) corresponding to the temperature intervals bounded by the thin vertical solid lines.

All the phosphors listed were studied with regard to flash inertia. It was found that the flash for CaS:Sm, CaS:Cu, and CaS:Bi:Ce phosphors is very long-lasting. Its rise proceeds almost as slowly as the further decrease in luminescence after infrared action is stopped. In order to study flash activation, we chose CaS:Sm, Cu and CaS:Sm, Ce phosphors with low flash inertia and insignificant secondary phosphorescence.

DETERMINATION OF THE THERMAL ACTIVATION ENERGY OF THE FLASH IN CaS:Sm, Cu AND CaS:Sm, Ce PHOSPHORS

The phosphors listed have five trapping levels, the +30° and +150° levels being the principal ones. In order to determine the thermal activation of electrons of any system, we must select the temperature of the experiment so that there is no liberation of electrons from other nearby levels. There was no difficulty in distinguishing the deep level at 150°. We were also successful in investigating the level at 30°. In carrying out the experiments, we proceeded from the formula

$$\lg\frac{I_0}{I_b} = 0.43\,\frac{\Delta E}{kT}, \quad (2)$$

where I_b/I_0 is the relative flash brightness at temperature T and ΔE is the thermal activation energy.

The slope of the straight line (2), which defines the proportionality between log (I_0/I) and $1/T$, is numerically equal to $0.43 \cdot \Delta E/k$, thus giving us the magnitude of ΔE.

To study the magnitude ΔE of the +150°C level of the CaS:Sm, Cu phosphor, the phosphor was excited at +80° for 10 min. It was then kept in the dark for 15 min, after which it was subjected to an infrared pulse and the flash brightness measured. The phosphor was then cooled several degrees and the flash brightness measured again. The temperature of the sample was kept low until the flash brightness was reduced to 1/10th of its initial value. The experiments were repeated with the phosphor temperature being raised. The values of the brightness of corresponding flashes were the same for both sequences of experiments. The linear relationship (2) between the logarithm of the intensity and the inverse temperature was well satisfied. The measurements were carried out for infrared wavelengths of 0.8, 0.9, 1, 1.1, and 1.2 μ.

Analogous measurements were performed for the +30°C level. In this case the phosphor was excited at 7°C. The levels at +30° as well as those at 150°C were filled at excitation. According to reference 5, however, it is evident that at 7° the infrared has practically no effect on the deep levels, and stimulates only the 30° levels. Finally, we investigated the +30° levels for the CaS:Sm,

	CaS-Sm, Cu		CaS-Sm, Ce
λ_{IR} (mμ)	I Level $T_m = +30°$	II Level $T_m = +150°$	$T_m = +30°$
0.8	0.16	0.32	0.25
0.9	0.20	0.35	0.25
1.0	0.17	0.39	0.27
1.1	0.20	0.36	0.27
1.2	0.18	0.33	0.22
ΔE_{av}	0.18	0.35	0.25

Ce phosphor. In this case the phosphor was excited at +10°.

The results of all the determinations of ΔE (in ev) are listed in the Table.

It is evident from our experiments that electrons from different levels may be used in producing the flash. The activation of the flash from deeper levels requires the addition of much larger amounts of thermal energy than that from the shallower ones. This agrees with the results of reference 5 with ZnS:Cu, Pb phosphors.

The Table shows that the values of the thermal activation energy obtained when the flash is initiated by infrared radiation of different wavelengths are approximately the same for electrons of a given level. The marked deviations of individual measurements from the average value are random in character and are apparently caused by experimental inaccuracies. The error in the average values of the activation energy is ~6%.

REFERENCES

1. V. V. Antonov-Romanovskii, V. L. Levshin, Z. L. Morgenshtern, and Z. A. Trapeznikova. Izvest. Akad. Nauk SSSR 13, 75 (1949).
2. N. A. Tolstoi and P. P. Feofilov. Doklady Akad. Nauk SSSR 68, 285 (1949).
3. N. A. Tolstoi, N. N. Tkachuk, M. Ya. Tsenter, Z. S. Mansurova, and A. V. Burlakov. Opt. i Spektr. 1, 719 (1956).
4. I. A. Parfianovich. Zhur. Eksptl. i Teoret. Fiz. 21, 314 (1951); Opt. i Spektr. 2, 391 (1957).
5. V. L. Levshin and B. M. Orlov. Opt. i Spektr. 7, 530 (1959), Optics and Spectroscopy 7, 330 (1959).

THE POLARIZABILITY TENSOR COMPONENTS OF THE DOUBLE BONDS C=C AND C=O

M. F. Vuks

Received 3 November 1959

Despite the fact that the polarizability tensor of double bonds does not possess axial symmetry, in all calculations it has been taken as being axially symmetric; this, of course, introduces a certain error into the results of the calculation. In this communication I want to show the possibility of finding all three polarizability tensor components of the C=C and C=O bonds.

We will begin with the C=O bond. Since in the scheme proposed by me for the determination of the principal polarizabilities of the C—H and C—C bonds[1] the acetone molecule is not involved, it is possible to take it for the determination of the three polarizability tensor components of the C=O double bond, which we will designate by α_σ in the direction of the axis of the σ-electrons, α_π in the direction of the axis of the π-electrons, and α_Ω in the direction of the perpendicular to the plane defined by the axes of the σ- and π-electrons.

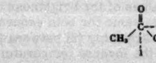

If we take for the mean polarizability the quantity[2] 63.86×10^{-25} and make use of the data from light scattering and the Kerr effect,[3] then for the polarizability tensor components of the acetone molecule we obtain the following numbers: $\alpha_1 = 71.3$, $\alpha_2 = 71.5$, $\alpha_3 = 48.7 \times 10^{-25}$. Knowing further the polarizability of the CH_3 group: $\alpha_{\parallel}^{CH_3} = 18.9$, $\alpha_{\perp}^{CH_3} = 19.8 \times 10^{-25}$ and of the C—C bond[1]: $\alpha_{\parallel}^{C-C} = 16.1$, $\alpha_{\perp}^{C-C} = 0.65 \times 10^{-25}$, and also the angle C—C—C = 114°,[4] we obtain without difficulty

$$\alpha_\sigma^{C=O} = 21.8,\ \alpha_\pi^{C=O} = 7.8,\ \alpha_\Omega^{C=O} = 10.1 \cdot 10^{-25}\ \text{cm}^3.$$

Let us now consider the C=C bond. For the determination of $\alpha_\pi^{C=C}$ we will use the benzene molecule. The objections against such a choice (i.e., that this molecule is nonadditive) are not well founded in this case. This is a result of the fact that the conjugation of the double bonds occurring in benzene leads to a delocalization of the π-electrons only in the plane of the ring. In the perpendicular direction no significant changes take place. Therefore, it is possible to consider that, perpendicular to the ring, the molecule is additive.

Having designated the polarizability perpendicular to the ring (i.e., parallel to the sixfold axis) by $\alpha_{\parallel}^{\text{benz}}$, we can write

$$\alpha_{\parallel}^{\text{benz.}} = 6\alpha_{\perp}^{C-H} + 3\alpha_{\perp}^{C-C} + 3\alpha_{\pi}^{C=C} = 64.3 \cdot 10^{-25}.$$

Since $\alpha_{\perp}^{C-H} = 6.2$, $\alpha_{\perp}^{C-C} = 0.6 \times 10^{-25}$ we obtain

$$\alpha_{\pi}^{C=C} = 8.5 \cdot 10^{-23}.$$

For the determination of the two other components we utilize the ethylene molecule

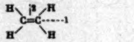

For this case we can write

$$\alpha_1 = 4\alpha_{\parallel}^{C-H} \cos^2 \frac{H-C-H}{2} + 4\alpha_{\perp}^{C-H} \sin^2 \frac{H-C-H}{2} + \alpha_\sigma^{C=C},$$

$$\alpha_2 = 4\alpha_{\parallel}^{C-H} \sin^2 \frac{H-C-H}{2} + 4\alpha_{\perp}^{C-H} \cos^2 \frac{H-C-H}{2} + \alpha_\Omega^{C=C},$$

$$\alpha_3 = 4\alpha_{\perp}^{C-H} + \alpha_\pi^{C=C}.$$

Since these other two components are unknown to us, by putting them into the formulas for the mean polarizability and the optical anisotropy

$$3\alpha = \alpha_1 + \alpha_2 + \alpha_3,$$

$$2\gamma^2 = (\alpha_1 - \alpha_2)^2 + (\alpha_1 - \alpha_3)^2 + (\alpha_2 - \alpha_3)^2,$$

we obtain two equations for the determination of the two unknown quantities $\alpha_\sigma^{C=C}$ and $\alpha_\Omega^{C=C}$. All of the remaining quantities are known to us: $\alpha_{\parallel}^{C-H} = 7.1$, $\alpha_{\perp}^{C-H} = 6.2$, $\alpha = 42.4 \times 10^{-25}$, $\gamma^2 = 3.28 \times 10^{-48}$.[1]

As the result of all these computations we obtain

$$\alpha_\sigma^{C=C} = 27.9,\ \alpha_\pi^{C=C} = 8.5,\ \alpha_\Omega^{C=C} = 12,8 \cdot 10^{-25}\ \text{cm}^3.$$

Comparing the principal polarizabilities of the C=C and C=O bonds, we see that the two tensors have similar forms. In both cases α_σ has by far the greatest, and α_π by far the smallest magnitude. The numbers obtained also show that the polarizability of the double bonds examined does not differ very strongly from axial symmetry.

REFERENCES

1. M. F. Vuks. Opt. i Spektr. 2, 494 (1957).
2. J. R. Partington. "An Advanced Treatise of Physical Chemistry," Vol. 4, London, 1951.
3. H. A. Stuart. "Die Struktur die freien Moleküls," Berlin, 1952.
4. P. W. Allen, L. E. Sutton. Acta Cryst. 3, 46 (1950).

SOME CRITERIA FOR THE APPLICABILITY OF THEORETICAL INTENSITIES TO THE SPECTRA OF COMPLEX ATOMS IN THE PRESENCE OF LS-COUPLING

P. F. Gruzdev and G. P. Startsev

Received 29 May 1959

In the absence of experimental data, the theoretical relative intensities calculated on the assumption of normal LS-coupling and tabulated by Goldberg, White, Eliason, and Russell[1] are often used in practice. However, the indicated assumption is only approximately fulfilled for complex atoms, and as a result it is desirable to have some sort of indication to check the degree of divergence of the theoretical intensities from the experimental.

Analysis of the available experimental material shows that divergences of the measured values of the Landé g-factors from the theoretical ones (for LS-coupling) and deviations from the interval rule may serve as such indications. Divergence of the observed g-factors from the theoretical ones indicates a deviation from normal coupling, if this divergence is not produced by the presence of a perturbed level.[2]

Comparison of experimental[3-6] and theoretical data for the intensities on the one hand, and of observed and calculated (for LS-coupling) values of the g-factors[7] on the other, shows that there are three cases to be considered:

1. $\Delta g = g_{\text{obs.}} - g_{\text{theor.}}$ does not exceed 0.010 for any level (except the level with smallest J). In this case the experimental intensity ratios for the multiplet agree well with the intensities calculated on the basis of LS-coupling.
2. $\Delta g = 0.010$-0.030. Here some deviation of the observed intensities from the theoretical is observed.
3. $\Delta g > 0.030$; a great discrepancy between the experimental and theoretical intensities is observed.

All of this applies to Δg for any level consisting of two terms forming a multiplet, except for the level with the smallest value of J. For the level with smallest J, the agreement of the observed and theoretical intensities is satisfactory at $\Delta g = 0.010$-0.020. At Δg values of 0.020-0.050, the first three or four most intense lines agree well with theory, but the rest diverge from it. At $\Delta g > 0.05$, a great discrepancy is observed.

In Figs. 1 and 2, which are presented to illustrate what has been said above, graphs have been constructed for two Fe I multiplets; $\log I_{\text{theor.}}$ values are along the abscissa axis and $\log I_{\text{exp.}}$ along the ordinate axis. (I is the relative intensity of the line of the multiplet.) The experimental data are taken from King's work.[4] The straight line drawn at an angle of 45° on these graphs corresponds to agreement of the experimental values of the relative intensities with the theoretical. Fig. 1, for the a^5D-z^5D multiplet, illustrates the case when Δg for the levels does not exceed 0.010 and the theoretical intensities agree well with the experimental. The points on the graph in this case are located close to the 45° line.

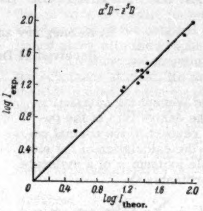

Fig. 1

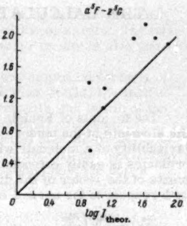

Fig. 2

Figure 2, for the a^5F-z^5G multiplet, illustrates the case when $\Delta g > 0.030$ (in the z^5G term for levels with J equal to 5, 4, and 3, Δg equals respectively 0.049, 0.047, and 0.030), and the theoretical intensities differ greatly from the experimental. There is a large scatter of the points on the graph.

Comparison of the theoretical and experimental relative intensities when there is a deviation from the interval rule shows that some regularity is observed here also. If, for the terms which form the multiplet, the deviation from the interval rule does not exceed ~20%, then the theoretical intensities are fundamentally in satisfactory agreement with the experimental ones. At deviations of 20% to 100% from the interval rule, the theoretical intensity values usually likewise differ sharply from the experimental ones. Multiplets are encountered, however (although rarely), for which the experimental intensities agree well with the theoretical, and the observed and theoretical g-factors also almost coincide ($\Delta g < 0.010$), but the interval rule is to a significant degree not fulfilled (even if for only one of the terms which form the multiplet). For example, for the Cr I a^5D-z^5D multiplet, the experimental intensities agree very well with the theoretical (the maximum Δg for the levels of both terms does not exceed 0.005), but the maximum deviation from the interval rule for the z^5D term amounts to ~45%. It must be supposed that the spin-orbital interaction in such terms is small in comparison with the orbital interaction. If the deviation from the interval rule exceeds 100%, then the theoretical intensities always differ greatly from the experimental.

Thus if experimental values of the relative line intensities are lacking for atoms or ions, but the values of the observed g-factors are known, then, from the deviation of the observed g-factors from the theoretical, one can determine for which multiplets the theoretical intensities may reliably be used, for which ones only approximately, and for which multiplets such intensities may not be used at all. If the g-factors are unknown, then such an estimate, although less exact than in the preceding case, may be made on the basis of deviation from the interval rule.

REFERENCES

1. L. Goldberg. Astrophys. J. 82, 1 (1935); 85, 11 (1936); H. E. White and A. V. Eliason. Phys. Rev. 44, 753 (1933); H. N. Russell. Astrophys. J. 83, 29 (1936).
2. M. A. El'yashevich. "Spektry redkikh zemel'" (Spectra of the Rare Earths), Gosudarst. Izd. Tekh.-Teoret. Lit., 1953.
3. Frerichs. Ann. Physik 81, 807 (1926).
4. R. B. King and A. S. King. Astrophys. J. 87, 24 (1938).
5. R. B. King and A. S. King. Astrophys. J. 87, 124 (1938); R. B. King. Astrophys. J. 106, 376 (1947); 108, 87 (1948); R. B. King, B. R. Parnes, M. H. Davis, and R. H. Olsen. J. Opt. Soc. Am. 45, 350 (1955).
6. Yu. I. Ostrovskii, G. F. Parchevskii, and N. P. Penkin. Opt. i Spektr. 1, 821 (1956); Yu. I. Ostrovskii and N. P. Penkin. Opt. i Spektr. 5, 345 (1958).
7. C. E. Moore. Atomic Energy Levels, Natl. Bur. Standards Circular 467, Vol. I, 1949; Vol. II, 1952; Vol. III, 1958.

THE CALCULATION OF INTENSITIES IN INFRARED SPECTRA OF MOLECULES

B. N. Snegirev and M. A. Kovner

Received 14 December 1959

The formula of Ferigle and Weber[1] for calculating the elements of the tensor of the derivatives of the polarizability of a molecule with respect to the normal coordinates is easily extended to the calculation of the elements of the vector of the dipole moment μ of a molecule with respect to the normal coordinates **Q**:

$$\left(\frac{\partial\mu_u}{\partial Q^m}\right)_0=\sum_{nr}\left(\frac{\partial\mu_n}{\partial q_n}\right)_0\cos(nu)\,T_r^n L_m^r+\sum_{nl}\mu_n S_n^{-1}\left[\mathbf{e}_u-\mathbf{e}_{ji}\cos(nu)\right]\times\left(\frac{\mathbf{S}_i^l}{m_i}-\frac{\mathbf{S}_j^l}{m_j}\right)(L^{-1})_l^m, \tag{1}$$

where u = x, y, z; $\mathbf{e}_u$ are unit vectors along these axes; n is the number of the bond; μ_n and S_n are the dipole moments and equilibrium lengths of the bonds; m_i and m_j are the masses of the atoms forming the bond ji; r and l are numbers of the independent symmetry coordinates and T_r^n the symmetry coefficients; L_m^r are the normalized form coefficients of the m-th normal vibration; $\mathbf{S}_i^l$, $\mathbf{S}_j^l$ are vectors connecting the l-th symmetry coordinate with the displacements of the atoms i, j.[2]

The formula

$$\Delta\mu_m=\left(\frac{\partial\mu}{\partial Q_m}\right)_0 Q_{0m}=\left[\left\{\left(\frac{\partial\mu_n}{\partial q_n}\right)_0,\ 0\right\}\left\|\begin{matrix}\mathbf{E} & 0\\ 0 & 0\end{matrix}\right\| + (\mu_n)\,S^{-1}(\Delta M^{-1}\tilde{\mathbf{B}}T-\mathbf{E})\right]\left\|\begin{matrix}q\\ \gamma\end{matrix}\right\|_m\sqrt{\frac{h\nu_m}{(q,\gamma)_m\,U\left\|\begin{matrix}q\\ \gamma\end{matrix}\right\|_m}} \tag{2}$$

was recently obtained by Gribov.

Equation (2) is written in the symbols used in reference 3. It is of interest to compare formulas (1) and (2) which, at first glance, are not at all similar to each other. We shall show that (2) follows directly from (1).

For this purpose, we shall imagine formula (1) written in internal vibrational coordinates, considering r and l as the numbers of these coordinates and putting $T_r^n = 1$. Then, evidently, after multiplying the stretching part of (1) by Q_{0m} and transferring to vector notation, the stretching parts of (1) and (2) coincide completely.

In order to derive the deformation part of (2) from (1), we shall represent the second term of formula (1) in matrix form, using Gribov's symbols:

$$\left(\frac{\partial\mu_u}{\partial Q_m}\right)_{0,\,\mathrm{def}}=(\mu_n)\,S^{-1}[\mathbf{e}_u\Delta M^{-1}\tilde{\mathbf{B}}-E_u\mathbf{E}\Delta M^{-1}\tilde{\mathbf{B}}]\,\tilde{L}^{-1}, \tag{1'}$$

where $E_u = \|\cos(nu)\|$ is the diagonal matrix of the cosines of the angles of the bonds with the axis u. With the help of the relations $\tilde{L}^{-1} = TL$ and $\tilde{B}_u = \mathbf{e}_u\tilde{\mathbf{B}}$, we write (1′) in the form

$$\left(\frac{\partial\mu_u}{\partial Q_m}\right)_{0,\,\mathrm{def}}=(\mu_n)\,S^{-1}[\Delta M^{-1}\tilde{B}_uT-E_u\mathbf{E}\Delta M^{-1}\tilde{\mathbf{B}}T]\,L. \tag{1''}$$

Since $\Delta\mathbf{r} = (\Delta M^{-1}\tilde{\mathbf{B}}T)\left\|\begin{matrix}q\\ \gamma\end{matrix}\right\|$ and $(\mathbf{E}\Delta\mathbf{r}) = \|q\|$, then $(\mathbf{E}\Delta M^{-1}\tilde{\mathbf{B}}T)\left\|\begin{matrix}q\\ \gamma\end{matrix}\right\| = \|q\|$, and the matrix $\mathbf{E}\Delta M^{-1}\tilde{\mathbf{B}}T$ is the unit matrix whose order equals the number of bonds. Consequently, (1″) takes the form

$$\left(\frac{\partial\mu_u}{\partial Q_m}\right)_{0,\,\mathrm{def}}=(\mu_n)\,S^{-1}[\Delta M^{-1}\tilde{B}_uT-E_u]\,L, \tag{1'''}$$

which, after multiplying by Q_{0m} and transferring to vector notation, coincides with Gribov's formula (2).

We have still to compare the possibility of practical calculations according to formulas (1) and (2).

1. Formula (1) enables us to carry out the calculation in symmetry coordinates, while formula (2) was obtained in internal vibrational coordinates. In the case of large molecules, the degrees of the secular equations are high even after reduction on the basis of symmetry, while in internal vibrational coordinates the mechanical problem is practically insoluble even on the best electronic computers.

2. In order to carry out a calculation according to formula (2), it is necessary to set up the T matrix, the evaluation of which presumes an additional operation and is practically feasible only in numerical form. The same cause makes it difficult to obtain the explicit general dependence of $\partial\mu/\partial Q$ on the atomic masses and the bond lengths, even in the case of simple molecules.

3. The advantage of formula (2) lies in the fact that for calculation according to this formula it is sufficient to set up the L matrix, which is usually obtained during the solution of the mechanical problem, while the elements of the L and L^{-1} matrices enter into formula (1). However, the L^{-1} matrix is used in determining the electro-optical parameters on the basis of experimental intensity values, as can be seen from Sverdlov's work.[4] Therefore one cannot get along without evaluation of the L^{-1} matrix.

REFERENCES

1. S. M. Ferigle and A. Weber. Can. J. Phys. **32**, 799 (1954).
2. M. V. Vol'kenshtein, M. A. El'yashevich, and B. I. Stepanov. "Kolebaniya molekul" (Molecular Vibrations), Vol. 1, p. 100, Gosudarst. Izd. Tekh.-Teoret. Lit., 1949.
3. L. A. Gribov. Doklady Akad. Nauk SSSR **127**, 788 (1959).
4. L. M. Sverdlov. Opt. i Spektr. **7**, 600 (1959), Optics and Spectroscopy **7**, 368 (1959).

LETTERS TO THE EDITOR

I request that you publish the following note in your journal.

The Academy of Science Press of the Hungarian Peoples Republic, at the request of the Academy of Science of the HPR, has begun regular publication of collections of absorption spectra, photographed in the scientific research institutes of Hungary. These collections appear under the title "Absorption Spectra in the Ultraviolet and Visible Region." An introductory volume containing a theoretical synopsis and volume I of the collection of spectra were published in 1959.

In later volumes we foresee inclusion of material resulting from research in other countries as well as that obtained by Hungarian research. At the present time there are similar collections published in some countries, but spectroscopy is growing at such a rapid rate that it is necessary to continually enlarge such collections. Of course it is impossible to insure the absolute completeness of such collections, but continuously published new data promote the establishment of an international collection of spectra.

In compiling the collection we adhere to the following principles:

1. To publish only data for spectroscopically pure substances; if possible in several solvents.
2. To select points of measurement sufficiently close that all characteristic properties of absorption curves will be made apparent, also taking into consideration the accuracy requirements of the absorption measurements.
3. To publish also bibliographic data pertaining to the spectra submitted.
4. The spectra are plotted in log ε, λ coordinates that provide a graphic picture of the spectrum. The tabulated record of the original measurements is also published along with the graphs.
5. To show the structure and empirical formula of the substance studied, its molecular weight, the instrumentation used for the measurements, the length of the cell and the molarity of the measured solutions.
6. The names of the compound studied are given in the index in conformity with international nomenclature, and also under their natural designations; the use of several nomenclatures is permitted.

Budapest
January 26, 1960

Respectfully yours,
Dr. L. Lang

AUTHOR LIST

VOLUME VIII; JANUARY-JUNE

(Numbers in parentheses refer to pages in Russian original)

Afanas'eva, N. V., (8) 4
Aknmanova, M. V., (498) 264
Akselrod, V. S., (721) 379
Aleksandrov, I. V., (575) 304
Aleksanyan, V. T., (324) 170
Al'perovich, L. I., (259) 132
Alyamovskii, V. N., (152) 80
Andreeshchev, E. A., (828) 435
Anisimova, I. D., (218) 112
Antonov-Romanovskii, V. V., (73) 35
Arkhangel'skaya, V. A., (279) 146
Arkhipov, V. M., (124) 61

Bakhshiev, N. G., (777) 408
Baranov, V. M., (268) 138
Barvinskaya, Z. L., (425) 222
Baturicheva, Z. B., (541) 286
Bazhulin, P. A., (206) 106, (394) 203, (492) 260
Belozerskii, G. N., (554) 292
Berezin, I. A., (408) 211
Biberman, L. M., (294) 155, (433) 230
Blazhevich, A. I., (550) 290
Bobovich, Ya. S., (45) 22
Bogomolny, A. M., (257) 131
Bonch-Bruevich, A. M., (855) 449
Borovinskii, L. A., (191) 99
Bresler, P. I., (733) 387
Britsyn, K. I., (861) 452
Broude, V. L., (629) 332, (815) 429
Bukat, G. M., (285) 151

Chaika, M. P., (13) 6
Cheremisinov, V. P., (505) 267
Chibrikin, V. M., (137) 71
Chikhladze, B. Ya., (452) 239
Chisler, E. V., (359) 187
Chulanovskii, V. M., (57) 28, (126) 63

Daich, A. R., (713) 375
Dmitrievskii, O. D., (117) 58, (120) 59
Dolginov, A. Z., (285) 151
Dontsov, Yu. P., (446) 236, (741) 391
D'yachenko, M. N., (531) 281
D'yachenko, N. G., (398) 205

Efimov, A. P., (128) 64
Efremov, Yu. P., (266) 137
Egorov, V. S., (423) 221
Erkovich, S. P., (303) 160, (307) 162

Faizi, N. Kh., (875) 458
Faizullov, F. S., (585) 311, (761) 400
Favorin, V. N., (218) 112
Feofilov, P. P., (824) 433
Filimonov, V. N., (270) 139
Fodiman, N. M., (243) 124
Fradkin, E. E., (13) 6

Galishev, V. S., (417) 217
Gaponova, N. E., (465) 245
Generalov, N. A., (569) 300
Glikman, T. S., (425) 222
Godnev, I. N., (171) 89
Gomon, G. O., (406) 210, (521) 275
Gribkovskii, V. P., (176) 92, (224) 114
Gribov, L. A., (123) 61, (127) 63, (769) 404
Gribkov, V. I., (275) 143
Gross, E. F., (232) 119, (516) 273
Grum-Grzhimailo, S. V., (342) 179
Gruzdev, P. F., (879) 461

Ioganesen, A. V., (126) 63
Ivanov, A. P., (352) 183, (556) 293

Jamagidze, Sh. Z., (274) 142

Kaliteeskii, N. I., (13) 6
Kanevskii, Yu. P., (266) 137
Kark, V. Ya., (144) 76
Karpinskii, V. N., (401) 207
Kashtan, M. S., (23) 11
Karyakin, A. V., (128) 64
Khachkuruzov, G. A., (40) 19
Khellenurme, P. A., (729) 384
Khlopina, T. N., (23) 11
Khodos, E. B., (556) 293
Khomazuk, V. G., (261) 134
Kishko, S. M., (160) 84
Kitaeva, V. F., (152) 80
Klimusheva, G. V., (342) 179
Kochemirovskii, A. S., (399) 206, (412) 214
Kolobkov, V. P., (412) 214
Kolomiitsov, Yu. V., (702) 370
Kolomiitsova, T. S., (363) 189
Kolt'sov, V. V., (582) 309
Komarovskikh, K. F., (516) 273
Kondilenko, I. I., (471) 249
Kondrat'eva, E. V., (130) 66, (132) 67
Korolev, F. A., (3) 1
Korotkov, P. A., (471) 249
Korst, N. N., (575) 304
Kovalev, I. F., (315) 166
Kovner, M. A., (128) 64, (880) 462
Kozina, G. S., (214) 110, (218) 112
Kozlenkov, A. I., (692) 365
Krasnov, K. S., (403) 208
Kudryavtsev, E. M., (585) 311, (761) 400
Kudryashov, P. I., (651) 344
Kulakova, A. F., (140) 73
Kulikov, O. F., (3) 1
Kurilchikova, G. E., (498) 264
Kurskii, Yu. A., (643) 340
Kusakov, M. M., (27) 13
Kuz'min, M. G., (371) 193

Lang, L., (463) 882
Lavrov, A. V., (550) 290
Lazarev, A. N., (511) 270, (614) 325
Lazarev, Iu. A., (206) 106
Lazeeva, G. S., (132) 67
Lebedev, Ya. S., (811) 426
Levina, R. Ya., (371) 193
Levshin, V. L., (663) 350, (875) 458
Liid'ya, G. G., (142) 74,
Lisitsa, M. P., (465) 245
Loginov, V. A., (382) 197
Losev, S. A., (569) 300
Lukirskii, A. P., (563) 297
Lushchik, Ch. B., (144) 76, (839) 441
Lushchik, N. E., (839) 441
Lyashenko, S. P., (868) 455
Lyubimov, Yu. A., (257) 131

Mak, A. A., (278) 145, (439) 233
Maksimov, A. I., (403) 208
Maleyev, E. N., (277) 144
Mal'tsev, Yu. V., (686) 362
Marenkov, O. S., (855) 449
Markova, S. V., (492) 260
Marupov, R., (259) 132
Mayants, L. S., (199) 102
Mel'nikov, A. A., (324) 170
Miloslavskii, V. K., (868) 455
Mirumyants, S. O., (635) 336, (787) 414
Morgenshtern, Z. L., (672) 355
Morozov, V. A., (741) 391
Muratov, V. P., (439) 233

Nagibina, I. M., (376) 195
Naboikin, Yu. V., (657) 347
Nazimov, N. A., (573) 303
Nemilov, Yu. A., (554) 292
Neporent, B. S., (127) 64, (635) 336, (777) 408, (787) 414
Nikitin, E. E., (157) 82, (264) 135
Nikitin, V. A., (117) 58, (120) 59, (739) 389
Norman, G. E., (149) 79, (433) 230
Novikov, M. M., (752) 396
Novikova, I. V., (363) 189

Obukhov-Denisov, V. V., (505) 267
Oganezov, K. A., (452) 239
Omel'chenko, Yu. A., (563) 297
Onoprienko, M. I., (629) 332, (815) 429
Osipov, B. D., (581) 309
Ovander, L. N., (477) 252
Ovcharenko, I. E., (746) 393

Pacheva, I. Kh., (13) 6
Paderno, Yu. B., (410) 212
Panchenko, Iu. N., (371) 193
Pankratov, N. A., (109) 53
Pargamanik, L. E., (713) 375
Pavlova, E. N., (657) 347
Peisakhson, I. V., (57) 28, (116) 57
Perlin, Yu. E., (386) 199
Personov, R. I., (328) 172
Petrash, G. G., (122) 60, (127) 63
Petrova, G. P., (376) 195

Pikulik, L. G., (338) 180
Pisarevskii, A. N., (554) 292
Pisarevsky, Yu. V., (303) 160
Plate, A. F., (324) 170, (492) 260
Podvigalkin, P. M., (146) 77
Popkov, Iu. A., (81) 39
Poskacheeva, L. P., (214) 110
Potekhina, N. D., (832) 437
Prokof'ev, V. K., (376) 195
Prokof'eva, E. A., (27) 13
Prokhorov, A. M., (419) 218
Propin, R. Kh., (300) 158

Rabotkin, V. L., (276) 144
Rautian, S. G., (126) 63
Razbirin, R. I., (232) 119
Razumova, T. K., (279) 146
Rebane, K. S. K., (545) 288
Rebane, T. K., (268) 138, (458) 242
Reznikova, I. I., (399) 206, (412) 214
Rigina, I. V., (171) 89
Romanyuk, N. A., (736) 389
Rozman, I. M., (525) 277, (828) 435
Rozman, S. M., (140) 73
Rusin, B. N., (733) 387
Ryazanov, A. N., (726) 382
Ryskin, A. I., (272) 141
Ryskin, Ya. I., (606) 320

Sakarinen, E., (545) 288
Sall', A. O., (135) 69, (247) 126, (571) 301, (731) 386
Samson, A. M., (89) 43
Samsonov, G. V., (410) 212
Selivanenko, A. S., (643) 340
Serebryakova, T. I., (410) 212
Shabarov, Iu. S., (371) 193
Sharapov, A. I., (239) 122
Shchepkin, D. N., (57) 28, (118) 58
Sheka, E. F., (66) 32
Shekhmamet'ev, R. I., (232) 119
Sherbaf, I. D., (259) 132
Shipulo, G. P., (419) 218
Shishkina, M. V., (27) 13
Shklyarevskii, I. N., (239) 122
Shpak, M. T., (66) 32
Shpol'skii, E. V., (328) 172
Shukhtin, A. M., (423) 221
Shvangiradze, R. R., (274) 142, (452) 239
Sidorov, A. N., (51) 24, (482) 254, (806) 424
Sivkov, A. A., (735) 388
Slonim, I. Ya., (98) 48, (243) 124, (255) 130
Smirnov, L. V., (799) 420
Snegirev, B. N., (880) 462
Sobolev, N. N., (505) 267, (585) 311, (761) 400
Sobotovich, E. V., (23) 11
Soifer, L. M., (537) 283
Sokolov, N. D., (575) 304
Sokolov, V. A., (276) 144, (573) 303
Sokolovskaya, A. I., (394) 203
Solodovnikov, S. P., (137) 71
Solomakho, M. A., (338) 180
Smirnov, B. A., (579) 307
Stanko, V. I., (492) 260
Startsev, G. P., (879) 461
Startsev, V. I., (537) 283, (541) 286
Stavitskaya, G. P., (606) 320
Stepanova, A. I., (408) 211
Stepanov, B. I., (176) 92, (224) 114
Sterin, Kh. E., (324) 170
Striganov, A. R., (741) 391
Strizhevskii, V. L., (165) 86, (471) 249, (623) 329
Suprunenko, A. I., (799) 420
Suslina, L. G., (516) 273
Sverdlov, L. M., (36) 17, (183) 96, (253) 129, (594) 316
Sveshnikov, B. Ya., (651) 344

Tagirov, R. B., (312) 164
Tarasov, K. I., (723) 380
Terebenina, L. B., (569) 300
Terenin, A. N., (482) 254
Tolstoi, N. A., (272) 141
Treshchova, E. G., (371) 193
Tsenter, M. Ya., (45) 22
Tsirlin, Yu. A., (537) 283, (541) 286, (713) 375
Tsvetkov, Iu. D., (811) 426
Tsyashchenko, Yu. P., (465) 245
Tumakaev, G. K., (423) 221
Tunitskaya, V. F., (663) 350
Tunitskii, L. N., (746) 393, (752) 396

Ustinova, Z. M., (243) 124

Vainberg, B. I., (279) 146
Vainstein, L. A., (149) 79
Vanyukov, M. P., (439) 233
Vasil'ev, N. I., (371) 193
Vatulev, V. N., (727) 383
Vavilov, V. S., (861) 452
Veingerov, M. L., (735) 388
Vereschagin, I. K., (420) 219
Vetchinkin, S. I., (137) 71
Vishnevskii, V. N., (736) 389
Vlasenko, N. A., (81) 39, (414) 215, (847) 445
Voevodskii, V. V., (811) 426
Voronkov, M. G., (614) 325
Vuks, M. F., (877) 460

Yaek, I. V., (142) 74, (144) 76, (577) 305
Yakubov, I. T., (294) 155
Yakutin, V. I., (746) 393
Yamshchikov, E. F., (61) 29
Yungman, V. S., (281) 147

Zadorozhny, B. A., (657) 347
Zavrazhin, A. G., (550) 290
Zelinskii, V. V., (412) 214
Zhevandrov, N. D., (275) 143
Zhitnikov, R. A., (285) 151
Zhivliuk, Yu. N., (421) 220
Zhmyrev, I. A., (412) 214

CONTENTS

VOLUME VIII; JANUARY-JUNE

(Numbers in parentheses refer to pages in Russian original)

No. 1—JANUARY

F. A. Korolev and O. F. Kulikov: An Investigation of the Intensity Ratio of the Polarized Components in the Radiation of the "Luminous" Electron—(3) 1

N. V. Afanas'eva: Ground States of Bound Paramagnetic Rare Earth Ions in an External Magnetic Field—(8) 4

N. I. Kaliteevskii, M. P. Chaika, I. Kh. Pacheva, and E. E. Fradkin: Spectroscopic Determination of the Nuclear Moments of the Odd Isotopes of Gadolinium—(13) 6

M. S. Kashtan, E. V. Sobotovich, and T. N. Khlopina: Enhancement of Sensitivity in the Spectral Isotope Analysis of Lead—(23) 11

M. M. Kusakov, E. A. Prokof'eva, and M. V. Shishkina: Electronic Absorption Spectra of Some Indan Homologs—(27) 13

L. M. Sverdlov: Relation between Vibration Frequencies of Isotopic Molecules (the Sums Rules and the Rules for the Product Sums of the Frequency Square Powers)—(36) 17

G. A. Khachkuruzov: Frequencies of the Fundamental Vibrations of the SO_3 Molecule—(40) 19

Ya. S. Bobovich and M. Ya. Tsenter: On Polarization Relationships in Raman Spectra of Molecules with a High Degree of Conjugation—(45) 22

A. N. Sidorov: Study of the Interaction between Pyridine and Water by Infrared Absorption Spectra—(51) 24

V. M. Chulanovsky, I. V. Peisakhson, and D. N. Shchepkin: Determination of the Absolute Value of Parameters Characterizing Intensity in the Infrared Absorption Spectrum in the Cases of the Absence of Time Distortions II.—(57) 28

E. F. Yamshchikov: The Dispersion Curve of Gaseous n-Pentane—(61) 29

M. T. Shpak and E. F. Sheka: On the Intrinsic Luminescence of Crystalline Naphthalene—(66) 32

V. V. Antonov-Romanovskii: Steady-State Luminescence of Phosphors in the Presence of Several Kinds of Traps—(73) 35

N. A. Vlasenko and Iu. A. Popkov: Study of the Electroluminescence of a Sublimed ZnS-Mn Phosphor—(81) 39

A. M. Samson: The Influence of Secondary Absorption and Emission Processes on the Duration of Luminescence of a Plane-Parallel Layer—(89) 43

I. Ya. Slonim: Determination of the Size of Particles by the Scattering of Light. I. Formulas and Nomograms for Computation of Radius of Particles by the Optical Density and by Intensity of Scattered Light—(98) 48

N. A. Pankratov: Selective Optico-Acoustic Receiver with Electrodynamic Microphone—(109) 53

I. V. Peisakhson: Determination of the Parameters, Characterizing the True Contours of Absorption Bands—(116) 57

O. D. Dmitrievskii and V. A. Nikitin: Measurements of the Apparatus Function of an IKS-11 Spectrometer—(117) 58

D. N. Shchepkin: Experimental Determination of the Parameters of Infrared Absorption Bands in Liquids—(118) 58

O. D. Dmitrievskii and V. A. Nikitin: Distortions in Scanning of Single-Beam Spectrometers—(120) 59

G. G. Petrash: Influence of Scanning and the Choice of the Optimum Conditions of Measurement—(122) 60

L. A. Gribov: On Measurements on Double-Beam Spectrometers—(123) 61

V. M. Arkhipov: On the Method of Interference Modulation—(124) 61

Discussion: V. M. Chulanovskii—(126) 63; A. V. Iogansen—(126) 63; S. G. Rautian—(126) 63; G. G. Petrash—(127) 63; L. A. Gribov—(127) 63; B. S. Neporent—(127) 64

M. A. Kovner, A. V. Karyakin, and A. P. Efimov: The Characteristic Frequencies of the Hydroperoxide Group, C—O—O—H—(128) 64

E. V. Kondrat'eva: Variation in the Duration of Luminescence of Trivalent Gadolinium and Terbium Ions in the System Sulfuric Acid-Water, as a Function of Component Concentration—(130) 66

E. V. Kondrat'eva and G. S. Lazeeva: A Study of the Duration and Intensity of Luminescence of Trivalent Gadolinium and Terbium Ions in Solutions—(132) 67

A. O. Sall': On the Ratio between the Signal from a Component being Determined and the Signal from the Total Radiation Flux for Infrared Gas Analyzer—(135) 69

S. I. Vetchinkin, S. P. Solodovnikov, and V. M. Chibrikin: Distribution of the Spin Density in the Dibenzenechromium Cation—(137) 71

A. F. Kulakova and S. M. Rozman: Temperature Quenching in Certain Organic Scintillators—(140) 73

I. V. Yaek and G. G. Liid'ya: Excitation of Recombination Luminescence in the Fundamental Absorption Bands of Certain Halides—(142) 74

V. Ya. Kark, Ch. B. Lushchik, and I. V. Yaek: The Sensitized Phosphorescence of Crystalline Halide Phosphors—(149) 76

P. M. Podvigalkin: The Relation between Photoelectric Characteristics of an Electrophotographic Layer and the Characteristics of Longitudinal Photoconductivity—(146) 77

No. 2—FEBRUARY

L. A. Vainstein and G. E. Norman: Calculation of Photoionization Cross Sections of Aluminum and Gallium Atoms—(149) 79

V. N. Alyamovskii and V. F. Kitaeva: The Contour of the H_β Hydrogen Line Behind a Shock Wave in Argon—(152) 80

E. E. Nikitin: On a Possible Mechanism of Electronic Excitation in Slow Atomic Collisions—(157) 82

S. M. Kishko: Photoelectric determination of the Excitation Functions of the Bands of the Negative System N_2^+—(160) 84

V. L. Strizhevsky: Effect of Interaction with the Environment on Fermi Resonance in Polyatomic Molecules—(165) 86

I. V. Rigina and L. N. Godnev: On the Theory of the Use of Dependent Coordinates in the Problem of Molecular Vibrations—(171) 89

V. P. Gribovskii and B. I. Stepanov: Polarization of Harmonic Oscillator Luminescence—(176) 92

L. M. Sverdlov: Theory of the Intensities of Infrared Spectra of Molecules, VI. BF_3, NF_3, SiF_4, and SF_6—(183) 96

L. A. Borovinskii: New Variant of the Metallic Model of a Molecule—(191) 99
L. S. Mayants: Calculation of Frequency and Form Derivatives of Normal Vibrations of Molecules Possessing Symmetry—(199) 102
P. A. Bazhulin and Iu. A. Lazarev: Photoelectric Investigation of Raman Spectra of Gases at Low Pressures—(206) 106
G. S. Kozina and L. P. Poskacheeva: Total Luminescence Brightness of ZnS-Cu and ZnS-Cu, Mn Electroluminophors in a Pulsating Field—(214) 110
G. S. Kozina, V. N. Favorin, and I. D. Anisimova: Electroluminescence Light Pulses under the Simultaneous Action of dc and ac Voltage—(218) 112
B. I. Stepanov and V. P. Gribkovskii: Polarization of Luminescence in a System of Particles with Three Energy Levels as a Function of the Exciting Light Intensity—(224) 114
E. F. Gross, B. S. Razbirin, and R. I. Shekhmamet'ev: Investigation of Reflectance and Luminescence Spectra of Copper Halides at Low Temperature—(232) 119
I. N. Shklyarevskii and A. I. Sharapov: A Photographic Method of Measuring the Optical Constants of Metals—(239) 122
I. Ya. Slonim, N. M. Fodiman, and Z. M. Ustinova: The Determination of the Size of Particles by Scattering of Light. II. Determination of the Size of Globules of the Polychloroprene Latex by means of Optical and Electron-Microscope Methods—(243) 124
A. O. Sall: Gas Characteristics of an Optico-Acoustic Gas Analyzer—(247) 126
L. M. Sverdlov: Relations Between the Infrared Band Intensities of Isotopic Molecules—(253) 129
I. Ya. Slonim: A Nomogram for Calculating the Diameter of Particles from Turbidity by Means of the Mie Equation—(255) 130
A. M. Bogomolny and Yu. A. Lyubimov: Infrared Absorption Spectra of a Microporous Glass during Adsorption of Methanol and Phenol from Solutions in Carbon Tetrachloride—(257) 131
L. I. Al'perovich, I. D. Sherbaf, and R. Marupov: On the Causes of the Luminescence of Liquids under the Action of Hard Radiation—(259) 132
V. G. Khomazuk: The Determination of the Order of Interference Bands by Means of a Monoprism and a Plate—(261) 134
E. E. Nikitin: On the Interpretation of Pressure-Induced Infrared Spectra of Gases—(264) 135
Yu. P. Efremov and Yu. P. Kanevskii: On the Correction for the Size of Exit Diaphragm in the Photoelectric Recording of Interference Bands of Equal Inclination—(266) 137
V. M. Baranov and T. K. Rebane: On the Semi-Empirical Calculation of the Ionization Potentials of Aliphatic Compounds—(268) 138
V. N. Filimonov: Change in the Infrared Absorption of Certain Semiconducting Adsorbents under Ultraviolet Illumination—(270) 139
N. A. Tolstoi and A. I. Ryskin: Superlinearity in Luminescence and Photoconductivity Phenomena and the Rose-Bube Theory—(272) 141
R. R. Shvangiradze and Sh. Z. Jamagidze: Isotopic Effect of the Central Atom in the Vibrational Spectrum of Methane—(274) 142
V. I. Gribkov and N. D. Zhevandrov: On the Polarization of the Luminescence of ZnS Single Crystals—(275) 143
V. L. Rabotkin and V. A. Sokolov: "Anisotropy" of the Light Pulse from a Polarized Electroluminescent Cell—(276) 144
E. N. Maleyev: An incandescent Lamp with a Mica Window for the Infrared Region of the Spectrum—(277) 144
A. A. Mak: The Channel Temperature of a Spark Discharge in Air—(278) 145
V. A. Arkhangel'skaya, B. I. Vainberg, and T. K. Razumova: Reflexometer for the Vacuum Ultraviolet Region of the Spectrum with the Use of CaSO$_4$:Mn Phosphor—(279) 146
V. S. Yungman: On the Vibrational Analysis of the $A^3\Pi - X^3\Sigma^-$ Band System of the OH$^+$ Molecule—(281) 147
Conference on the Physics of Alkali-Halide Crystals—(283) 148

No. 3—MARCH

G. M. Bukat, A. Z. Dolginov, and R. A. Zhitnikov: The Hyperfine Structure of Multielectron Atoms—(285) 151
L. M. Biberman and I. T. Yakubov: An Approximate Method for Calculating Franck-Condon Factors—(294) 155
R. Kh. Propin: Calculation of the Probability of Autoionization in Helium and Lithium Atoms—(300) 158
S. P. Erkovich and Yu. V. Pisarevsky: Transition Probabilities in the γ- and β-Band Systems of NO—(303) 160
S. P. Erkovich: Coefficient of Continuous Absorption of Radiation by Quasi Molecules of Hydrogen—(307) 162
R. B. Tagirov: The Importance of H$_2$O in the Combustion of Carbon Monoxide in Oxygen—(312) 164
I. F. Kovalev: Vibrational Spectra and Potential Functions of the Methylsilanes CH$_3$SiH$_3$, (CH$_3$)$_2$SiH$_2$, and (CH$_3$)$_3$SiH—(315) 166
V. T. Aleksanyan, Kh. E. Sterin, A. A. Mel'nikov, and A. F. Plate: The Raman Spectra of the Steroisomers of 1,2-Dialkyl Cyclopentanes—(324) 170
E. V. Shpol'skii and R. I. Personov: Emission and Absorption Spectra of Perylene in Solid Solutions at 77°K—(328) 172
L. G. Pikulik and M. A. Solomakho: On the Influence of Temperature on the Electronic Spectra of Complex Molecules—(338) 176
S. V. Grum-Grzhimailo and G. V. Klimusheva: Temperature Dependence of the Broad Absorption Bands in the Spectra of Crystals of Various Structures Colored by Isomorphous Impurities—(342) 180
A. P. Ivanov: The Effect of Strong Illumination on the Absorptivity of Complex Molecules—(352) 183
E. V. Chisler: On the Influence of the Width of the Monochromator Slits on the Accuracy of Photoelectric Measurements of the Intensity of Raman Lines—(359) 187
T. S. Kolomiitsova and I. V. Novikova: Photoelectric Method of Recording Interference Fringes in White Light—(363) 189
E. G. Treshchova, Iu. N. Panchenko, N. I. Vasil'ev, M. G. Kuz'min, Iu. S. Shabarov, and R. Ya. Levina: The Raman Spectra of Hydrocarbons of Different Classes. VI. The Raman Spectra of Some Arylcyclobutanes—(371) 193
V. K. Prokof'ev, I. M. Nagibina, and G. P. Petrova: Determination of Absolute Oscillator Strengths from Spectral Line Widths—(376) 195
V. A. Loginov: Evaluation of the Error of Interpolation by the Normals of the Spectrum Sections on the Rowland Circle—(382) 197
Yu. E. Perlin: The Energy Spectrum of an F-Center in Continuum Theory—(386) 199
A. I. Sokolovskaya and P. A. Bazhulin: The Temperature Dependence of the Intensity of Stokes and Anti-

Stokes Raman Lines in Liquids—(394) 203
N. G. D'yachenko: High-Speed Photoelectric Spectrometer for the Region 0.4-0.9 μ—(398) 205
A. S. Kochemirovskii and I. I. Reznikova: On the Effect of the Solvent on the Fluorescence Yield—(399) 206
V. N. Karpinskii: On the Compensation of Rowland's "Ghosts" in Spectrographs with Double Diffraction on the Grating—(401) 207
K. S. Krasnov and A. I. Maksimov: Calculation of the Vibrational Frequency of Diatomic Molecules from the Reduced Mass—(403)208
G. O. Gomon: Absorption Spectra of Diamonds—(406) 210
I. A. Berezin and A. I. Stepanova: On the Sensitization of Photographic Plates in the Ultraviolet Region of the Spectrum—(408) 211
T. I. Serebryakova, Yu. B. Paderno, and G. V. Samsonov: Emission Coefficients of Some Powdered High-Melting Compounds—(410) 212
I. A. Zhmyrev, V. V. Zelinskii, V. P. Kolobkov, A. S. Kochemirovskii, and I. I. Reznikova: Effect of Solvents on the Electronic Spectra of Organic Molecules—(412) 214
N. A Vlasenko: The Effect of Temperature on the Electroluminescence of a Sublimed ZnS-Mn Phosphor—(414) 215
V. S. Galishev: A Simple Derivation of the Kramers-Krönig Relations—(417) 217
A. M. Prokhorov and G. P. Shipulo: Microwave Investigation of the Molecules F_3BNH_3 and $F_3BN(CH_3)_3$—(419) 218
I. K. Vereshchagin: Influence of Gas Adsorption on Electroluminescence—(420) 219
Yu. N. Zhivliuk: Calculation of the Polarizability of Molecules within the Limits of the Metallic Model—(421) 220
A. M. Shukhtin, V. S. Egorov, and G. K. Tumakaev: A Continuous Emission Source Giving Short-Lived Single Flashes—(423) 221
T. S. Glikman and Z. L. Barvinskaya: Spectrophotometric Study of the Interaction Between Phthalocyanin and Iron Trichloride—(425) 222
I. A. Akimov and G. A. Korsonovskii: Influence of Some Electronophylic Compounds on the Absorption and Luminescence Spectra of Magnesium Phthalocyanin Solutions—(427) 223
The International Conference on Molecular Spectroscopy at Bologna (Italy)—(429) 225
VIII International Symposium on Spectroscopy—(431) 226

No. 4—APRIL

Ninetieth Anniversary of V. I. Lenin's Birthday—(i) 229
L. M. Biberman and G. E. Norman: On the Calculation of Photoionization Absorption—(433) 230
M. P. Vanyukov, A. A. Mak, and V. P. Muratov: Spark Discharge Emission in Helium—(439) 233
Yu. P. Dontsov: Isotope Shift in the Spectrum of Molybdenum—(446) 236
R. R. Shvangiradze, K. A. Oganezov, and B. Ya. Chikhladze: Isotopic Band Shifts in the Electronic-Vibrational Spectra of Some Diatomic Molecules—(452) 239
T. K. Rebane: Calculation of the Polarizability of Conjugated Molecules taking into Account the Electrostatic Interaction of π-Electrons—(458) 242
N. E. Gaponova, M. P. Lisitsa, and Yu. P. Tsyashchenko: Frequencies and Intensities in the Infrared Spectrum of Bromoform—(465) 245
I. I. Kondilenko, P. A. Korotkov, and V. L. Strizhevskii: The Indicatrix of the Raman Scattering of Light—(471) 249
L. N. Ovander: The Anti-Stokes Component of the Raman Spectrum for Hydrogen-Bonded Compounds—(477) 252
A. N. Sidorov and A. N. Terenin: Infrared Spectra of Chlorophyll and its Analogues—(482) 254
S. V. Markova, P. A. Bazhulin, A. F. Plate, and V. I. Stanko: Study of Infrared Absorption Spectra of Dicyclic Hydrocarbons—(492) 260
M. V. Aknmanova and G. E. Kurilchikova: Infrared Absorption Spectra of Hydroxyfluoroboric Complexes of Potassium and Sodium—(498) 264
V. V. Obukhov-Denisov, N. N. Sobolev, and V. P. Cheremisinov: Vibrational Spectra of the Modifications of Germanium Dioxide—(505) 267
A. N. Lazarev: Vibrational Spectra of Alkoxysilanes and Siloxanes. II. Vibrations of the SiO_4 Groups in the Spectra of Tetraalkoxysilanes—(511) 270
E. F. Gross, L. G. Suslina, and K. F. Komarovskikh: Investigation of the Absorption Spectra of Zinc Sulfide Crystals—(516) 273
G. O. Gomon: The Luminescence Spectra of Diamonds—(521) 275
I. M. Rozman: The Mechanism of Scintillations in Organic Substances—(525) 277
M. N. D'yachenko: Effect of High-Temperature Annealing on the Luminescence and Coloration of X-Rayed Quartz Crystals—(531) 281
Yu. A. Tsirlin, V. I. Startsev, and L. M. Soifer: Luminescence Properties of Cesium Iodide Crystals Grown from a Superheated Melt—(537) 283
V. I. Startsev, Z. B. Baturicheva, and Yu. A. Tsirlin: Temperature Dependence of the Luminescence of NaI(Tl) Crystals at Temperatures between 0° and 270°C—(541) 286
K. S. K. Regane and E. Sakarinen: Temperature Effect on Infrared Quenching—(545) 288
A. I. Blazhevich, A. G. Zavrazhin, and A. V. Lavrov: The Properties of ZnS:Mn, Ni, Cl Phosphors under Cathode Ray Excitation—(550) 290
Yu. A. Nemilov, G. N. Belozerskii and A. N. Pisarevskii: The α/β Ratio in a Liquid Scintillator—(554) 292
A. P. Ivanov and E. B. Khodos: Scattering of Light in Media with Variable Optical Parameters—(556) 293
A. P. Lukirskii and Yu. A. Omel'chenko: Use of the Phenomenon of "Total External Reflection" for Filtering the Continuous Spectrum in the Ultra-Soft X-Ray Region—(563) 297
S. A. Losev, N. A. Generalov, and L. B. Terebenina: On the Absorption of Ultraviolet Radiation Behind a Shockwave in the Air—(569) 300
A. O. Sall': Calculation of the Errors of an Absorption Analyzer of Gaseous or Liquid Mixtures—(571) 301
V. A. Sokolov and N. A. Nazimov: The Structure and Nature of Excitation of the Magnesium Oxidation Spectrum—(573) 303
I. V. Aleksandrov, N. N. Korst, and N. D. Sokolov: The Influence of Proton Mobility on Nuclear Magnetic Resonance Line Width in Crystals—(575) 304
I. V. Yaek: The Step-Shaped Dependence of the Recombination Luminescence Quantum Yield of Alkali Halide Crystal Phosphors on the Frequency of the Exciting Light—(577) 305
B. A. Smirnov: A Method of Structural-Group Analysis by Infrared Spectra. Determination of Mono-Olefinic Structures of the Products of the Gamma-Radiolysis of n-Heptane—(579) 307
B. D. Osipov: I-J Interaction in the CH_3I Molecule—(581) 309
V. V. Kolt'sov: High-Speed Spectrometer with Spectrum Scanning by Means of a Rotating Disk with a Spiral Slot as Exit Slit—(582) 309

Corrections—(584) 310

No. 5—MAY

F. S. Faizullov, N. N. Sobolev, and E. M. Kudryavtsev: Spectroscopic Investigation of the State of the Gas behind a Shock Wave. II—(585) 311
L. M. Sverdlov: Theory of the Infrared Spectral Intensities of Deuteroethylenes. VII—(594) 316
Ya. I. Ryskin and G. P. Stavitskaya: Spectroscopic Investigation of the Hydrogen Bond in Acid Silicates and Phosphates—(606) 320
A. N. Lazarev and M. G. Voronkov: Vibrational Spectra of Alkoxysilanes and Siloxanes III. Vibrations of Silicon-Oxygen Chains in the Spectra of Polyalkoxysiloxanes—(614) 325
V. L. Strizhevskii: The Temperature Dependence of the Dispersion and Absorption of Light in Molecular Crystals I. Theory—(623) 329
V. L. Broude and M. I. Onoprienko: Absorption Spectra of Benzene Homologues IV. Pecularities of Crystal Spectra—(629) 332
B. S. Neporent and S. O. Mirumyants: Spectroscopic Study of the Processes of Vibrational Energy Transformation of Complex Molecules in Collisions I. On the Determination of the Amount of Energy Transferred and the Efficiency of Collisions—(635) 336
Yu. A. Kurskii and A. S. Selivanenko: On the Theory of Luminescence Quenching in Liquid Solutions—(643) 340
P. I. Kudryashov and B. Ya. Sveshnikov: On the Concentration Depolarization of the Phosphorescence of Organoluminophors—(651) 344
Yu. V. Naboikin, B. A. Zadorozhny, and E. N. Pavlova: Pecularities of the Luminescence of Ortho-Disubstituted Aromatic Hydrocarbons III. The Fluorescence and Absorption Spectra of Some Carboxylic Acids—(657) 347
V. L. Levshin and V. F. Tunitskaya: Thermoluminescence and the Localized Levels of ZnS:Mn Phosphors—(663) 350
Z. L. Morgenshtern: Luminescence of Unactivated CsI Crystals. II—(672) 355
P. V. Slobodskaya and E. S. Gasilevich: Development of a Method for Determining Relaxation Time Using a Spectrophone. II. Eliminating the Instrumental Phase Shifts—(678) 358
Yu. V. Mal'tsev: A Comparison of Light Scattering Functions of Spherical Particles—(686) 362
A. I. Kozlenkov: Study of Aberrations of a Concave Grating under Defocusing Conditions—(692) 365
Yu. V. Kolomiitsov: Comparison of the Rayleigh and Jamin Types of Interferometers—(702) 370
A. R. Daich, Yu. A. Tsirlin and L. E. Pargamanik: Passage of Light Through Lightguides—(713) 375
V. S. Akselrod: Pressed Samples for Infrared Spectrometry—(721) 379
K. I. Tarasov: Simple Formulas for the Evaluation of Aberrations of a Mirror Objective—(723) 380
A. N. Ryazanov: On the Possibility of Using Amplitude-Phase Objectives to Resolve Two Nonmonochromatic Light Sources—(726) 382
V. N. Vatulev: The Relation of Electron Transitions in Impurity Molecules to Lattice Vibrations of the Crystalline Solvent—(727) 383
P. A. Khellenurme: Investigation of N- and O-Color Centers in the KCl:Tl Crystalline Phosphor—(729) 384
A. O. Sall': Calculation of the Chamber of a Baro-Optical Source of Radiation—(731) 386
P. I. Bresler and B. N. Ruzin: Optical-Acoustic Effect in Mercury Vapor—(733) 387
M. L. Veingerov and A. A. Sivkov: A Single-Beam Optical-Acoustic Gas Analyzer—(735) 388
V. N. Vishnevskii and N. A. Romanyuk: A Monochromator with an Ammonium Dihydrogen Phosphate Prism—(736) 389
V. Nikitin: Decisions of the International Commission for Molecular Spectroscopy—(739) 389

No. 6—JUNE

Yu. P. Dontsov, V. A. Morozov, and A. R. Striganov: Isotope Shift in the Spectrum of Neodymium—(741) 391
I. E. Ovcharenko, L. N. Tunitskii, and V. I. Yakutin: Analysis of the Fine Structure in the Bands of the SiCl Molecule—(746) 393
M. M. Novikov and L. N. Tunitskii: Vibrational Constants and Dissociation Energy of the BeCl Molecule—(752) 396
F. S. Faizullov, N. N. Sobolev, and E. M. Kudryavtsev: Spectroscopic Investigation of the State of the Gas Behind a Shock Wave. III—(761) 400
L. A. Gribov: Calculation of Intensities and Polarizations in the Infrared Spectra of Polyatomic Molecules. I—(769) 404
B. S. Neporent and N. G. Bakhshiev: On the Role of Universal and Specific Intermolecular Interactions in the Influence of the Solvent on the Electronic Spectra of Molecules—(777) 408
S. O. Mirumyants and B. S. Neporent: Spectroscopic Study of the Processes of Vibrational Energy Transformation in Complex Molecules in Collisions II. Effect of Foreign Gases on the Fluorescence Yield of 3-dimethylamino-6-aminophthalimide—(787) 414
L. V. Smirnov and A. I. Suprunenko: The pH Dependence of Electronic Spectra of the Simplest Derivatives of Benzene. I. Absorption Spectra of Hydroxybenzenes—(799) 420
A. N. Sidorov: Spectral Investigation of the Adsorption of Water on Porous Glass as a Function of the Degree of Hydration of its Surface—(806) 424
Ya. S. Lebedev, Iu. D. Tsvetkov, and V. V. Voevodskii: Paramagnetic Resonance Spectra of Fluoroalkyl and Nitrosofluoroalkyl Radicals in Irradiated Teflon—(811) 426
V. L. Broude and M. I. Onoprienko: Absorption Spectra of Benzene Homologues. V. Spectra of Toluene Crystals at 20°K—(815) 429
P. P. Feofilov: The Nature of the Elemental Oscillators of the Uranium Ion—(824) 433
E. A. Andreeshchev and I. M. Rozman: Fluorescence Quantum Yield of Certain Substances in Polystyrene—(828) 435
N. D. Potekhina: The Theory of the Luminescence of Activated Crystal Phosphors—(832) 437
N. E. Lushchik and Ch. B. Lushchik: Spectroscopy of the Luminescence Centers in Alkali Halide Crystals Activated by Homologous Series of Ions—(839) 441
N. A. Vlasenko: Temperature Effect on the Photoluminescence of the Evaporated ZnS:Mn Phosphor—(847) 445
A. M. Bonch-Bruevich and O. S. Marenkov: Polarization Phenomena in Electroluminors—(855) 449
K. I. Britsyn and V. S. Vavilov: The Photoionization Process in Silicon—(861) 452
V. K. Miloslavskii and S. P. Lyashenko: Optical and Electrical Properties of Thin Films of Tin Dioxide—(868) 455

V. L. Levshin and N. Kh. Faizi: Investigation of the Energy of Thermal Activation of the Flash and of Trapping Levels in CaS Phosphors—(875) 458
M. F. Vuks: The Polarizability Tensor Components of the Double Bonds C=C and C=O—(877) 460
P. F. Gruzdev and G. P. Startsev: Some Criteria for the Applicability of Theoretical Intensities to the Spectra of Complex Atoms in the Presence of LS-Coupling—(879) 461
B. N. Snegirev and M. A. Kovner: The Calculation of Intensities in Infrared Spectra of Molecules—(880) 462
Letters to the Editor—(882) 463
Author List, Vol. VIII—(883) 464
Contents List, Vol. VIII—(891) 466
Errata in Vol. VIII—(904) 470

ERRATA IN VOL. VIII

In the paper by V. K. Prokof'ev, I. M. Nagibina, and G. P. Petrova entitled "Determination of Absolute Oscillator Strengths from Spectral Line Widths" in Vol. VIII, No. 3, pp. 195-197, an error was made during computation and for this reason it is necessary to insert the following errata:

Page	Line	Printed	Should be
197	Table 4 7th Column	0.08	1.1
197	2nd and 3rd lines right-hand column	one third	1/4.5
197	4th line right-hand column	$f_{2863} = 0.08$	$f_{2863} = 1.1$
197	6th line right-hand column	0.08	1.1

The value $f_{2863} = 1.1$ should be compared with the value $f_{2833} = 0.60 \pm 0.10$ for the resonance line of Pb of the same serial transition [see H. D. Engler, Z. Physik 144, 343 (1956)].

TO THE READER

The Russian original of the July issue (Vol. IX, No. 1) has been delayed in transit. Therefore, this issue will not appear for approximately six weeks to two months.

(This is filler material and is not in the Russian original.)

OPTICAL SOCIETY OF AMERICA

OSA proposes to issue a bimonthly publication in the areas of applied optics, infrared and closely related industrial and scientific fields, e.g. physical, electron, space, ion, infrared and ultraviolet optics, lens design, optical engineering and instrumentation, plasma and solid state physics, to meet the growing demands of OSA membership for a medium of publication emphasizing, in addition to research papers, those of topical state-of-the-art interest, news re instruments, people, OSA and other meetings, book reviews and many other features to keep the opticist aware of what is happening in his branch of optics throughout the world, both in industry and on the campus. The new publication will supplement JOSA, which will remain the archival journal of the Society. In the interests of fast publication, OSA is considering producing this bimonthly by the photo offset process (see OPTICS AND SPECTROSCOPY) which should give a publication time of approximately two months from acceptance by the Editor.

OSA dues will continue to provide JOSA and OiS; the purpose of this Questionnaire is to determine membership reaction to the new project. Would all members therefore be good enough to complete the Questionnaire sent them in July and to mail it back to the Executive Office without delay. (The card is already stamped and addressed.) Also, please fill in your name, affiliation and mailing address in the way you would like to see these appear in the new Membership Directory.

QUESTIONNAIRE

Would you subscribe to APPLIED OPTICS (a tentative title) at a cost of approximately $6.00 a year to members? ( ) Yes ( ) No.

Would you contribute to APPLIED OPTICS? ( ) Yes ( ) No.

If invited, would you contribute review articles, meetings, reports or book reviews in your area of competence? ( ) Yes ( ) No.

What is your area of interest?
Are you interested more in: ( ) Basic research ( ) Applied research
( ) A mixture of these two.

Comments:

Name________________________ Membership No.________
Affiliation______________________________
Mailing Address____________________________

(FILLER MATERIAL – NOT IN RUSSIAN ORIGINAL)

EDITOR'S NOTE

Comments on the scientific content of the translated Russian articles published in OPTICS AND SPECTROSCOPY are invited. They should be addressed as a Letter to the Editor of the Journal of the Optical Society of America and forwarded to the Editor of that journal, Dr. W. R. Brode, National Bureau of Standards, Washington 25, D.C.

[redacted]

VOL. VIII, NO. 6 JUNE 1960

Isotope Shift in the Spectrum of Neodymium . . . Yu. P. Dontsov, V. A. Morozov, and A. R. Striganov 391
Analysis of the Fine Structure in the Bands of the SiCl Molecule . . . I. E. Ovcharenko, L. N. Tunitskii, and V. I. Yakutin 393
Vibrational Constants and Dissociation Energy of the BeCl Molecule . . . M. M. Novikov and L. N. Tunitskii 396
Spectroscopic Investigation of the State of the Gas Behind a Shock Wave. III . . . F. S. Faizullov, N. N. Sobolev, and E. M. Kudryavtsev 400
Calculation of Intensities and Polarizations in the Infrared Spectra of Polyatomic Molecules. I . . . L. A. Gribov 404
On the Role of Universal and Specific Intermolecular Interactions in the Influence of the Solvent on the Electronic Spectra of Molecules . . . B. S. Neporent and N. G. Bakhshiev 408
Spectroscopic Study of the Processes of Vibrational Energy Transformation in Complex Molecules in Collisions II. Effect of Foreign Gases on the Fluorescence Yield of 3-dimethylamino-6-aminophthalimide . . . S. O. Mirumyants and B. S. Neporent 414
The pH Dependence of Electronic Spectra of the Simplest Derivatives of Benzene. I. Absorption Spectra of Hydroxybenzenes . . . L. V. Smirnov and A. I. Suprunenko 420
Spectral Investigation of the Adsorption of Water on Porous Glass as a Function of the Degree of Hydration of its Surface . . . A. N. Sidorov 424
Paramagnetic Resonance Spectra of Fluoroalkyl and Nitrosofluoroalkyl Radicals in Irradiated Teflon . . . Ya. S. Lebedev, Iu. D. Tsvetkov, and V. V. Voevodskii 426
Absorption Spectra of Benzene Homologues. V. Spectra of Toluene Crystals at 20°K . . . V. L. Broude and M. I. Onoprienko 429
The Nature of the Elemental Oscillators of the Uranium Ion . . . P. P. Feofilov 433
Fluorescence Quantum Yield of Certain Substances in Polystyrene . . . E. A. Andreeshchev and I. M. Rozman 435
The Theory of the Luminescence of Activated Crystal Phosphors . . . N. D. Potekhina 437
Spectroscopy of the Luminescence Centers in Alkali Halide Crystals Activated by Homologous Series of Ions . . . N. E. Lushchik and Ch. B. Lushchik 441
Temperature Effect on the Photoluminescence of the Evaporated ZnS:Mn Phosphor . . . N. A. Vlasenko 445
Polarization Phenomena in Electroluminors . . . A. M. Bonch-Bruevich and O. S. Marenkov 449
The Photoionization Process in Silicon . . . K. I. Britsyn and V. S. Vavilov 452
Optical and Electrical Properties of Thin Films of Tin Dioxide . . . V. K. Miloslavskii and S. P. Lyashenko 455

SHORT COMMUNICATIONS

Investigation of the Energy of Thermal Activation of the Flash and of Trapping Levels in CaS Phosphors . . . V. L. Levshin and N. Kh. Faizi 458
The Polarizability Tensor Components of the Double Bonds C=C and C=O . . . M. F. Vuks 460
Some Criteria for the Applicability of Theoretical Intensities to the Spectra of Complex Atoms in the Presence of LS-Coupling . . . P. F. Gruzdev and G. P. Startsev 461
The Calculation of Intensities in Infrared Spectra of Molecules . . . B. N. Snegirev and M. A. Kovner 462
Letters to the Editor . . . 463
Author List, Vol. VIII . . . 464
Contents List, Vol. VIII . . . 466
Errata in Vol. VIII . . . 470